



**EUROPEAN SCHOOL OF MOLECULAR MEDICINE**

**NAPLES SITE – *Scientific Coordinator Prof. Francesco Salvatore***

**UNIVERSITA' DEGLI STUDI DI NAPOLI "FEDERICO II"**

**Ph.D. in Molecular Medicine**

***Curriculum Human Genetics***

**XX Ciclo**

*In vitro* and *in vivo* characterization of murine  
bone marrow stromal stem cells: self-renewal,  
differentiation, tumorigenic potential

**Supervisor:**

Prof. Francesco Ramirez

**Internal Supervisor:**

Prof. Lucio Pastore

**External Supervisor:**

Dr Nicole Horwood

**Ph.D. student:**

Dr. Maria Teresa Esposito

## **TABLE OF CONTENTS**

<b>Abbreviations List</b>	<b>7</b>
<b>Figure Index</b>	<b>10</b>
<b>Table Index</b>	<b>13</b>
<b>Abstract</b>	<b>14</b>
<b>Introduction</b>	<b>16</b>
<b>Chaper 1 The Bone Marrow system</b>	<b>16</b>
<i>1.1 In vitro characterization of bone marrow stromal cells (BMSCs)</i>	<i>18</i>
<i>1.2 Definition of BMSCs</i>	<i>19</i>
<i>1.3 BMSC immunophenotype</i>	<i>23</i>
<b>Chapter 2 Reaching a balance between self-renewal and differentiation</b>	<b>26</b>
<i>2.1 Niche-External signals</i>	<i>27</i>
<i>2.1.1 Leukaemia inhibitory factor (LIF)</i>	<i>29</i>
<i>2.1.2 Fibroblast growth factor 2</i>	<i>29</i>
<i>2.1.3 Wnt</i>	<i>30</i>
<i>2.2 Niche-Intrinsic signals</i>	<i>30</i>
<i>2.2.1 Transcription factors</i>	<i>30</i>
<i>2.2.1.1 Oct4</i>	<i>31</i>
<i>2.2.1.2 Sox-2</i>	<i>32</i>
<i>2.2.1.3 Rex-1</i>	<i>32</i>
<i>2.2.1.4 Nanog</i>	<i>33</i>
<i>2.2.2 Telomeres length</i>	<i>34</i>

<i>2.3 Differentiation Potential</i>	34
<i>2.3.1 Osteogenesis</i>	36
<i>2.3.2 Chondrogenesis</i>	37
<i>2.3.3 Adipogenesis</i>	38
<b>Chapter 3 Senescence and transformation</b>	<b>40</b>
<i>3.1 Defining senescence</i>	41
<i>3.1.1 DNA damage</i>	42
<i>3.1.2 Telomere length</i>	43
<i>3.2 Molecular pathways involved in senescence</i>	44
<i>3.2.1 p19ARF/p53 pathway</i>	45
<i>3.2.2 p16/pRB pathway</i>	46
<i>3.3 Overcoming the cell crisis: from senescence to spontaneous transformation</i>	47
<b>Materials and Methods</b>	<b>49</b>
<b>Chapter 4</b>	<b>49</b>
<i>4.1 Mice</i>	49
<i>4.2 Cell cultures</i>	49
<i>4.2.1 mBMSCs isolation and expansion</i>	49
<i>4.2.2 Preparation of bone-marrow conditioned medium</i>	51
<i>4.2.3 Culture of cell lines</i>	51
<i>4.2.4 Culture of murine embryonic stem (mES) cells</i>	52
<i>4.3 Flow cytometry analysis</i>	53
<i>4.4 Cumulative duplication number and doubling time measurement</i>	53

<i>4.5 Cell cycle analysis</i>	54
<i>4.6 Senescence associated Beta Galactosidase (SA-B-Gal) staining</i>	54
<i>4.7 Telomeric Repeat Amplification protocol (TRAP) Assay</i>	54
<i>4.8 In vivo tumorigenicity: transplantation of mBMSCs into nude mice</i>	55
<i>4.9 Immunofluorescence for Nanog detection</i>	55
<i>4.10 Differentiation Assay</i>	56
<i>4.10.1 Osteogenic differentiation</i>	56
<i>4.10.2 Chondrogenic differentiation</i>	56
<i>4.10.3 Adipogenic differentiation</i>	57
<i>4.11 Histochemical analysis</i>	57
<i>4.11.1 Alkaline Phosphatase (ALP) staining and activity assay</i>	57
<i>4.11.2 Alizarin Red S staining</i>	58
<i>4.11.3 Von Kossa</i>	58
<i>4.11.4 Alcian Blue staining</i>	59
<i>4.11.5 Oil Red O staining</i>	59
<i>4.12 Reverse Transcription Polymerase Chain Reaction (RT-PCR)</i>	59
<i>4.13 Quantitative Real time PCR</i>	61
<i>4.14 Cell transfection</i>	62
<i>4.14.1 Transfection with lipofectamine 2000</i>	62
<i>4.14.2 Nucleofection Technology</i>	63
<i>4.14.3 Calcium Phosphate transfection</i>	63
<i>4.15 Analysis of Green fluorescent protein (GFP) expression</i>	63
<i>4.16 Cell proliferation assay</i>	64
<i>4.17 Construction of expression plasmids</i>	64

<i>4.18 Western blot analysis</i>	67
<i>4.19 Migration assay</i>	68
<i>4.20 Soft agar assay</i>	68
<i>4.21 Statistical analysis</i>	68
<b>Results</b>	<b>69</b>
<b>Chapter 5 Establishment of mBMSC long term culture and morphologic characterization</b>	<b>69</b>
<i>5.1 Background</i>	69
<i>5.2 Isolation of mBMSCs from adult mouse bone marrow</i>	70
<i>5.3 Immunophenotypical characterization</i>	72
<i>5.4 Growth kinetic of mBMSCs during 30 passages</i>	74
<i>5.4.1 Cumulative duplication number and doubling measurement</i>	75
<i>5.4.2 Cell cycle analysis</i>	76
<i>5.4.3 Senescence Associated Beta Galactosidase expression</i>	78
<i>5.4.4 Cell cycle analysis at late passages</i>	79
<i>5.4.5 Assesment of telomerase activity</i>	82
<i>5.4.6 Tumorigenicity in vivo</i>	83
<i>5.5 Stemness expression in mBMSCs</i>	85
<i>5.6 Differentiation abilities of BMSCs</i>	87
<i>5.6.1 Osteogenesis</i>	87
<i>5.6.2 Chondrogenesis</i>	92
<i>5.6.3 Adipogenesis</i>	95

<i>5.7 Switching the N BMSC cells into standard growth medium does not rescue their osteogenic potential</i>	97
<i>5.8 Expression of leukaemia inhibitory factor (LIF) in NIH3T3</i>	100
<b>Chapter 6 Efficient non viral transfection of mBMSCs using Nucleofection technology</b>	<b>102</b>
<i>6.1 Background</i>	102
<i>6.2 Testing BMSCs transfection efficiency with Lipofectamine 2000</i>	102
<i>6.3 Testing BMSC transfection efficiency by using nucleofection technology</i>	104
<i>6.4 Time course analysis of GFP expression in nucleofected mBMSCs</i>	106
<i>6.5 Effect of nucleofection on cell proliferation</i>	107
<i>6.6 Effect of nucleofection on cellular senescence</i>	108
<i>6.7 Effect of nucleofection on cell migration</i>	109
<b>Chapter 7 Effect of Nanog over-expression and down-regulation in mBMSCs</b>	<b>110</b>
<i>7.1 Background</i>	110
<i>7.2 Stemness factors expression in B BMSCs</i>	111
<i>7.3 Transient over- expression and down-regulation of Nanog</i>	112
<i>7.3.1 Over-expression of Nanog in 293 cell line</i>	113
<i>7.3.2 Down-regulation of Nanog in 293 cell line</i>	115
<i>7.3.3 Transfection efficiency, cell viability and cell recovery in mBMSCs nucleofected with pCMVNanogIRES-GFP-WPRE and pCMVantiNanogIRES-GFP-WPRE</i>	118
<i>7.3.4 Over-expression of Nanog in mBMSCs</i>	121

<i>7.4 Effect of over-expression and down-regulation of Nanog in mBMSCs</i>	122
<b>Discussion</b>	<b>125</b>
<b>Chapter 8</b>	<b>125</b>
<i>8.1 Culture expansion of mBMSCs from C57bl/6 mouse bone marrow</i>	126
<i>8.2 Culture condition select mBMSCs with different differentiation potential</i>	131
<i>8.3 BMSCs express the homeodomain gene Nanog</i>	133
<i>8.4 Conclusions and Future Perspectives</i>	138
<b>Appendix</b>	<b>140</b>
<b>Chapter 9 Effect of Nanog over-expression on BMSC tumorigenesis</b>	<b>140</b>
<i>9.1 Effect of Nanog over expression on cell proliferation</i>	140
<i>9.2 Effect of Nanog over-expression on cellular senescence</i>	141
<i>9.3 Effect of Nanog over-expression on acquisition of tumorigenic ability</i>	143
<b>Acknowledgments</b>	<b>146</b>
<b>References</b>	<b>147</b>

## **ABBREVIATIONS LIST**

$\alpha$  MEM: Alpha Modified Essential Medium

ALP: alkaline phosphatase

BMSSCs: Bone marrow stromal stem cells

Cbfa1/Runx2: Core binding factor alpha 1/Runt related gene

Chip on Chip: chromatin immunoprecipitation on chromatin immunoprecipitation array

CFU-F: Colony forming unit- fibroblast

CMV: Citomegalovirus

DMEM: Dulbecco Modified Essential Medium

DNP: dinitrophenyl group

DSBs: double-strand DNA breaks

EDTA: Ethylenediamine tetraacetic acid

FABP-4: fatty acid binding protein-4

FACS: fluorescence activated cell sorter

FGF: fibroblast growth factors

FITC: Fluorescein isothiocyanate

GAPDH: Glyceraldehyde 3-phosphate dehydrogenase

GFP: green fluorescent protein

GMEM: Glasgow Modified Essential Medium

HCl: Chloride acid

HSC: haematopoietic stem cells

IRES: internal ribosome entry site

$K_4Fe(CN)_6$ : potassium ferrocyanide

$K_3Fe(CN)_6$ : potassium ferricyanide

LIF: leukemia inhibitory factor

LPL: lipoprotein lipase

MAPCs: Multipotent adult progenitor cells

mES cells: murine embryonic stem cells

MgCl<sub>2</sub>: Magnesium Chloride

MIAMI: Marrow isolated adult multilineage inducible cells

MIF: mean fluorescence intensity

mRNA: messenger RNA

MSCs: Mesenchymal stem cells or Marrow stromal cells

NaCl: Sodium Chloride

NaF: Sodium Fluoride

NGF: nerve growth factor

OD: optical density

ORF: open reading frames

PAGE: polyacrylamide gel electrophoresis

PC: positive control

PD: population doublings

PE: Phycoerythrin

PI: Propidium Iodide

PPAR $\gamma$ : The nuclear hormone receptor peroxisome proliferators activated receptor

$\gamma$

RS-1, RS-2, mMSCs: cycling mature mesenchymal stem cell

RT-PCR: Reverse Transcription-Polymerase Chain Reaction

SA- $\beta$ -Gal: senescence associated beta-galactosidase

SA- SP: senescence-associated secretory phenotype.

SPCs: Stromal precursors cells

SSEA-1: stage-specific embryonic antigen-1

TERT: telomerase reverse transcriptase

TRAP: telomeric repeats onto oligonucleotide primers

USSCs: Pluripotent unrestricted somatic stem cells

VCAM-1: vascular cell adhesion molecule-1

WPRE: Woodchuck hepatitis virus posttranscriptional regulatory element

X-gal: 5-bromo-4-chloro-3-indolyl-b-D-galactopyranoside

## **FIGURE INDEX**

Figure 1 The Bone Marrow system .....	17
Figure 2 Colony forming fibroblastic unit (CFU-F assay). .....	19
Figure 3 “Bone marrow stromal cell” functional definition .....	21
Figure 4 Bone marrow niche.....	27
Figure 5 BMSC self renewal and cytodifferentiation .....	28
Figure 6 The stromal system.....	36
Figure 7 Molecular regulation of BMSC differentiation .....	39
Figure 8 Fates of damaged stem cells .....	41
Figure 9 Roles of p53 and p16RB pathways in senescence response.....	45
Figure 10 Model of spontaneous BMSC transformation.....	48
Figure 11 Morphology of mBMSCs varies according to culture conditions.....	72
Figure 12 FACS analysis of mBMSC populations .....	74
Figure 13 Growth kinetic of mBMSCs .....	75
Figure 14 Cell cycle analysis of mBMSCs .....	77
Figure 15 Senescence Associated Beta Galactosidase (SA-B-Gal) expression in mBMSCs.....	79
Figure 16 Cell cycle analysis of mBMSCs after 30 passages in vitro .....	81
Figure 17 Cell cycle comparison between mBMSCs at early and late passages...	81
Figure 18 Telomerase activity assessment in mBMSCs.....	83
Figure 19 mBMSCs do not transform in tumorigenic cells.....	84
Figure 20 Teratocarcinoma development in mice injected with mES cells.....	84
Figure 21 Stemness factors expression in BMSCs .....	86
Figure 22 mBMSCs express Nanog.....	86
Figure 23 Osteogenic differentiation of mBMSCs. ALP expression .....	89
Figure 24 Osteogenic differentiation of mBMSCs. Bone nodule formation .....	91

Figure 25 Osteogenic differentiation of mBMSCs. Von Kossa staining.....	91
Figure 26 Expression of osteoblast specific markers.....	92
Figure 27 Chondrogenic differentiation of mBMSCs micro-drops.....	94
Figure 28 Chondrogenic differentiation of mBMSCs micro-pellet.....	94
Figure 29 Expression of chondrogenic markers .....	95
Figure 30 Adipogenic differentiation of mBMSCs .....	96
Figure 31 Expression of adipogenic specific markers .....	97
Figure 32 Osteogenic differentiation of N*BMSCs .....	98
Figure 33 Expression of osteogenic specific markers in N and N* BMSCs .....	99
Figure 34 Osteocalcin expression in N and N* BMSCs.....	99
Figure 35 Expression of LIF in NIH3T3 .....	101
Figure 36 NIH3T3 secrete bioactive LIF.....	101
Figure 37 Transfection efficiency with lipofectamine 2000.....	103
Figure 38 Transfection efficiency with nucleofection technology. Fluorescence Microscopy .....	105
Figure 39 Transfection efficiency with nucleofection technology. FACS analysis .....	105
Figure 40 Time course analysis of GFP expression.....	106
Figure 41 Nucleofection does not affect cell proliferation .....	107
Figure 42 Nucleofection does not induce cellular senescence.....	108
Figure 43 Nucleofection does not affect cell migration.....	109
Figure 44 Stemness factor expression in B BMSCs .....	112
Figure 45 GFP expression in 293 transfected with pCMVIRES-GFP-WPRE and pCMVNanogIRES-GFP-WPRE .....	114
Figure 46 Nanog expression in 293 transfected with pCMVNanogIRES-GFP- WPRE .....	114

Figure 47 GFP expression in 293 transfected with pCMVIRES-GFP-WPRE and pCMVantiNanogIRES-GFP-WPRE .....	116
Figure 48 GFP expression in 293 co-transfected with pCMVNanogIRES-GFP-WPRE and pCMVantiNanogIRESGFPWPRE.....	117
Figure 49 Down regulation in Nanog expression in 293 co-transfected with pCMVNanogIRES-GFP-WPRE and pCMVantiNanogIRES-GFP-WPRE.	118
Figure 50 GFP expression in B BMSCs nucleofected with pCMVIRESGFP-WPRE derived vectors. Fluorescence microscopy analysis .....	120
Figure 51 GFP expression in cell nucleofected with pCMVIRESGFP-WPRE derived vectors. FACS analysis .....	120
Figure 52 Nanog expression in BMSCs nucleofected with pCMVNanogIRES-GFP-WPRE. Real time PCR.....	121
Figure 53 Nanog expression in BMSCs nucleofected with pCMVNanogIRES-GFP-WPRE. Western-blot.....	122
Figure 54 Effect of over expression or down regulation of Nanog on cell migration .....	123
Figure 55 CCL5 and CXCL10 expression in BMSCs.....	124
Figure 56 Model of interaction among Nanog, STAT3 and NF-Kb.....	137
Figure 57 "Cancer stem cell hypothesis" for BMSCs.....	138
Figure 58 Growth kinetic of BMSCs over expressing Nanog .....	141
Figure 59 Effect of over expression of Nanog on cellular senescence .....	142
Figure 60 Nanog effect on p53 and pRB expression .....	142
Figure 61 Anchorage independent-growth of BMSCs over-expressing Nanog ..	144
Figure 62 Expression of Sox-2, Oct4, c-myc and TERT in BMSCs .....	145

**TABLE INDEX**

Table 1 Representative examples of denominations used for bone marrow stromal cells	22
Table 2 Specific primers for RT-PCR	60
Table 3 Specific primers for Real Time PCR	62
Table 4 Primers used in molecular cloning	67
Table 5 Variations in culture conditions allow selection of different mesenchymal progenitors	73
Table 6 Percentage of Nanog expressing BMSCs. T-Test results	86
Table 7 Level of ALP activity of BMSCs. Anova results	90

## **ABSTRACT**

The use of adult stem cells for applications such as tissue engineering and gene therapy is one of the major challenge approaches of regenerative medicine. In the field of adult stem cells, bone marrow stromal cells (BMSCs) are very promising candidates.

The ability to move forward the use of these cells in therapy depends on the setting up of mammalian models, necessary to evaluate pre-clinical efficacy and standardize procedures. Precisely, murine BMSCs (mBMSCs) characterization is a major breakthrough that can benefit from numerous established genetic models of human diseases now available in this organism. In particular, C57Bl/6 strain is frequently used to prepare transgenic mice because it produces a large number of high-quality embryos and super-ovulate in response to hormone injections.

However, the BMSC is a cell type better studied and characterized in humans than in mouse and, although in the last few years numerous protocols have been developed to isolate these cells, some problems still remain.

In the present study, I define, for the first time, conditions for optimizing the yields of cultures enriched for specific progenitors of bone marrow. I isolated four different sub-populations of mBMSCs using four distinct culture conditions, supernatants from culture of bone fragments, marrow stroma cell line MS-5, embryonic fibroblast cell line NIH3T3 and a cocktail of epidermal growth factor (EGF) and platelet-derived growth factor (PDGF). These cells show very interesting features in immunophenotype, self-renewal ability and differentiation potency. In particular, using NIH3T3 conditioned medium, we obtained cells that show impairment in osteogenic and chondrogenic differentiation, whereas retaining a very high adipogenic potential during passages. These results indicate

that the choice of the medium used for isolation and expansion of mBMSCs is extremely relevant in order to enrich the culture of desired specific progenitors.

A common characteristic among these sub-populations of mBMSCs was the expression of a well known marker of undifferentiated embryonic stem cells, namely Nanog. Recent studies have demonstrated the expression of Nanog in BMSCs and its effect on proliferation and osteogenic and chondrogenic abilities, however its role in these cells is still unknown.

During a six- month period as visitor in the laboratory coordinated by Dr Nicole Horwood, at Imperial College (London, UK), I have generated vectors expressing Nanog sense and antisense in order to analyze the effect of over-expression and down-regulation of Nanog on migration, senescence, apoptosis and tumorigenesis in BMSCs. Preliminary data suggest that over-expression of Nanog does not seem to efficiently reduce the number of senescent cells; however, Nanog over-expressing cells showed a decrease in the expression of p53, a well known tumor-suppressor gene and acquired the ability to grow in soft agar, an *in vitro* hallmark of tumorigenic cells. On the other hand, down-regulation of Nanog in BMSCs enhances migration ability, and induces an increase in the expression of CCL5 (Rantes) and CXCL10 (IP10, interferon  $\gamma$  inducible protein-10), which have been reported to enhance motility, invasion and metastasis of breast cancer cells and to have a potent thymus-dependent antitumoral effect.

This work suggest that defined levels of Nanog could affect BMSCs properties and indicate a further need of a better understanding of the biology of these cells which are already being used in several clinical trials.

## **INTRODUCTION**

### **Chapter 1**

#### **The bone marrow system**

The bone marrow consists on three main cellular systems, haematopoietic, endothelial and stromal. This organ has traditionally been seen as composed of two main distinct lineages, the haematopoietic one, proper able to give rising to the blood lineage cells and the mesenchymal lineage. This includes the non haematopoietic cells of mesenchymal origin that support haematopoiesis, as well as the mesenchymal stem cell and its progeny, such as osteocytes, chondrocytes and adipocytes (Figure 1).

This chapter describes bone marrow stromal cells (BMSCs) from their discovery to the recent advances in their characterization.

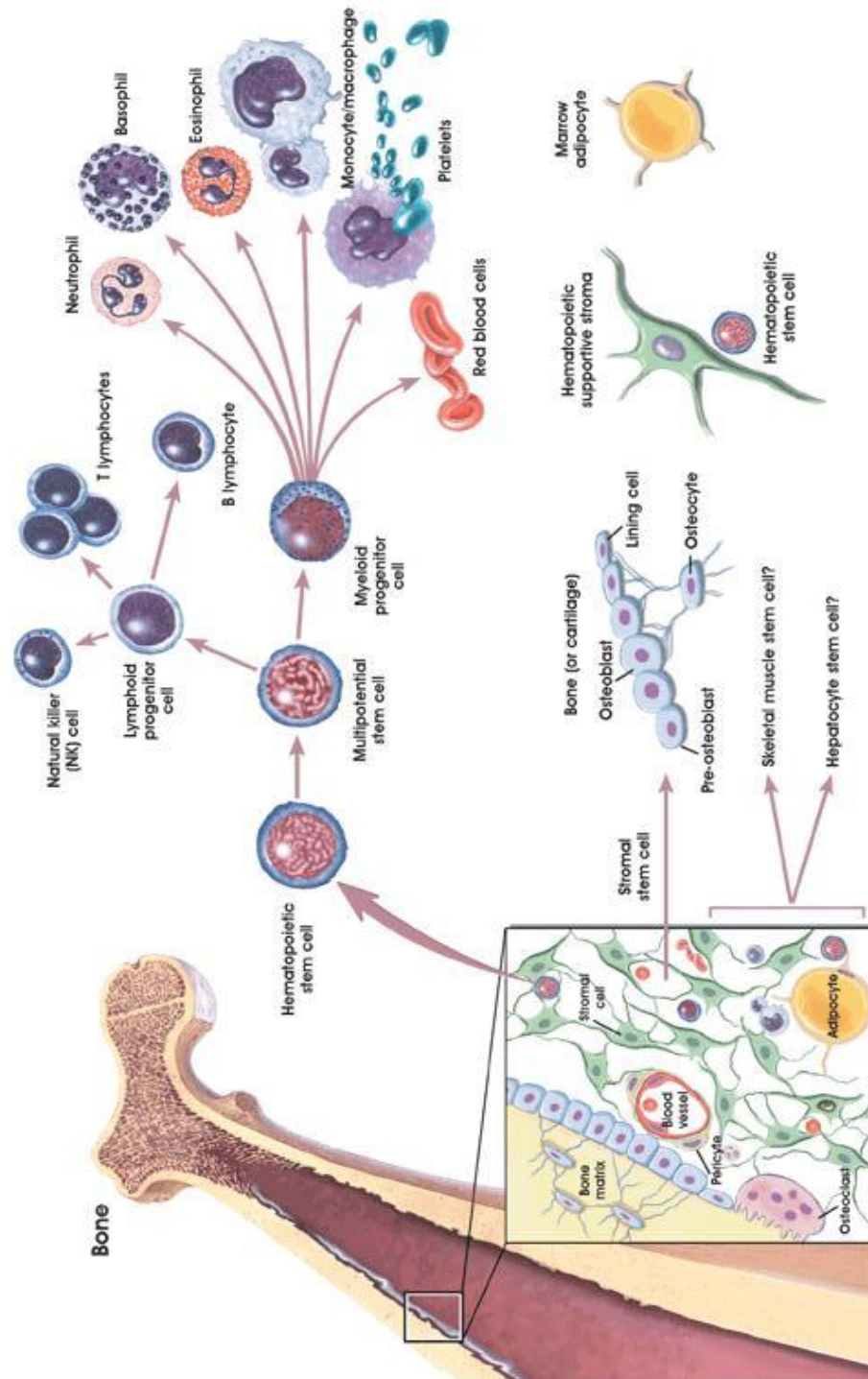


**Figure 1 The Bone Marrow system**

The bone marrow is the source of two distinct lineages, the haematopoietic and the mesenchymal stem cells. From the haematopoietic lineage derive blood cells; from the mesenchymal stem cells derive the supporting stromal cells, osteocytes, chondrocytes and adipocytes. Adapted from <http://stemcells.nih.gov>.

## **1.1 In vitro characterization of bone marrow stromal cells (BMSCs)**

The discovery of the stromal system was one of the major discoveries in the field of stem cells. Alexander Friedenstein, Maureen Owen, and their co-workers were the first to utilize *in vitro* culture and transplantation in laboratory animals, to characterize cells that compose the physical stroma of bone marrow (Friedenstein et al. 1966; Friedenstein et al. 1970; Owen 1988). After mechanical dissociation of the bone marrow, they obtained a single-cell suspension which they plated in culture at low density. In these conditions they were able to observe that little, spindle shaped cells, the bone marrow stromal cells, rapidly adhered to the plastic surface, whereas the non-adherent haematopoietic cells could be removed by repeated washing. With appropriate culture conditions, distinct colonies were formed, each of which was derived from a single precursor cell, the Colony forming fibroblastic unit (CFU-F, Figure 2). Under optimal conditions, these colonies can undergo over 25 passages *in vitro* (more than 50 cell doublings), demonstrating a high capacity for self-replication. Therefore, billions of BMSCs can be generated from a limited amount of starting material, such as 1 ml of a bone marrow aspirate. Thus, these cells were referred as rapidly adherent, clonogenic, and capable of extended proliferation.

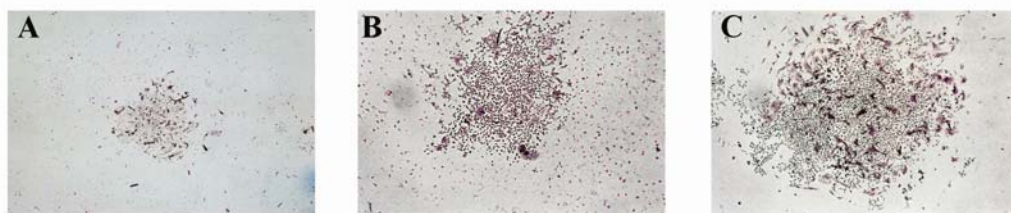


**Figure 2** Colony forming fibroblastic unit (CFU-F assay).

Examples of CFU-F obtained from murine bone marrow stromal cells culture. Original magnification 50X (panel A), 100X (panel B) and 125X (panel C). Adapted from StemCell Technologies.

## 1.2 Definition of BMSCs

Since the identification of the bone marrow stromal stem cell by Friedenstein and co-workers (Friedenstein et al. 1966; Friedenstein et al. 1970; Owen 1988), many researchers have tried to isolate and better characterize this population. The first detailed functional description of the tri-lineage differentiation potential of BMSCs was provided by Pittenger and colleagues in 1999 (Pittenger et al. 1999). They isolated populations of human BMSCs from the bone marrow taken from the iliac crests with a frequency ranging from 1 out of 10.000- 100.000, analyzing their immunophenotype and the *in vitro* differentiation potential. They showed that some of the clones, which they obtained, were able to differentiate in osteoblast, chondroblasts and adipocytes, pointing out a multipotent ability for these clones (Figure 3). Not every clone retained these abilities. Out of six colonies analyzed, all of them were able to differentiate in osteoblasts, five were able to differentiate in chondrocytes and only two were able to differentiate in adipocytes, confirming that these populations were very heterogeneous and made up of multipotent stem cells and progenitors already committed towards a specific cell lineage (Pittenger et al. 1999).

After the publication of this article, these cells have been identified as plastic-adherent multipotent cells, capable of differentiating into bone, cartilage and fat cells (Figure 3) and referred to by different names. The original term “colony forming unit-fibroblast” (CFU-F) or “marrow stromal fibroblasts” (MSF, Castro-Malaspina et al. 1980; Friedenstein et al. 1982; Kuznetsov et al. 1997) has been gradually abandoned and replaced by diverse, still indistinct denominations like “marrow stromal cells” (MSC, Prockop 1997; Digirolamo et al. 1999), “mesenchymal stem cells” (MSC, Caplan 1991; Pittenger et al. 1999; Baddoo et al. 2003; Meirelles Lda et al. 2003; Tropel et al. 2004; Wang et al. 2006), “bone marrow stromal cells” (BMSC, Phinney et al. 1999; Bianco et al. 2001; Short et al. 2001; Sun et al. 2003; Peister et al. 2004), “recycling stem cells” (RS, Colter et al. 2000; Colter et al. 2001), “multipotent adult progenitor cells” (MAPC, Reyes et al. 2001; Jiang et al. 2002) and “marrow isolated adult multilineage inducible cells” (MIAMI, D'Ippolito et al. 2004). Table 1 summarises the definitions used to different populations of cells isolated from human and murine bone marrow.

A lot of new sources of stromal cells have been identified so far. They have been isolated from adipose tissue (Zuk et al. 2001; Schaffler et al. 2007), cord blood (Gang et al. 2004), placenta (Fukuchi et al. 2004) and peripheral blood (Rocheffort et al. 2006; He et al. 2007). However, even if isolated by density-gradient fractionation, they remain a heterogeneous mixture of cells with varying proliferation, differentiation potentials and different denominations that contribute to generate a deep confusion in this field.

Although acceptable for cell-based therapeutic applications, a rigorous understanding of the BMSC requires a better definition of what a BMSC is.

Many laboratories have employed different methods to isolate BMSCs, in both serum and serum deprived conditions, and have developed novel approaches to isolate purified populations of BMSCs.

These advances have furthered our understanding of BMSC biology but have also created differences in terminology and read-out measures (i.e., based on morphology, phenotype, gene expression, and combinations thereof) for describing the fibroblast-like cells derived from bone marrow and adult tissue (Table 1). Although none of these terms can accurately account for both the developmental origin and differentiation capacity of these cells, the term bone marrow stromal cell is often employed, because it applies not only to the stem cell *per se*, but to a vast repertoire of committed progenitors exhibiting at least more than one differentiation potential and described to be present in the bone marrow.

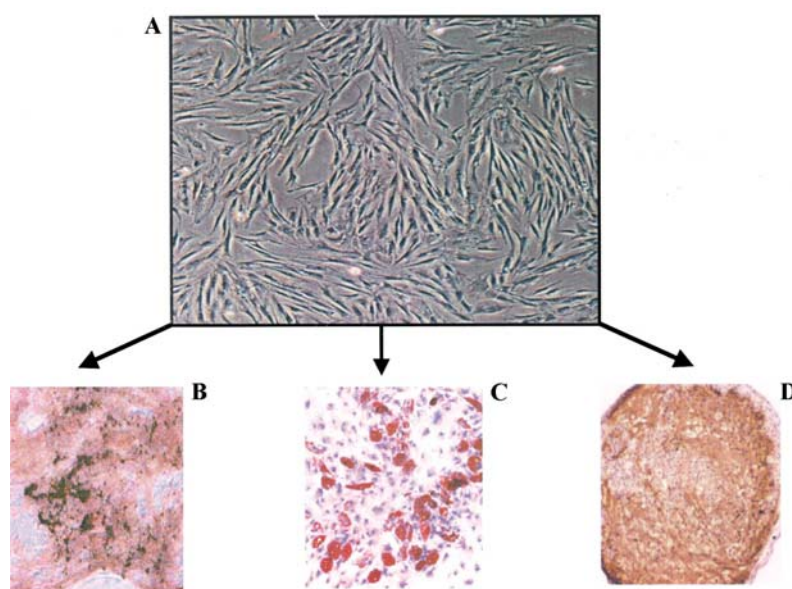


**Figure 3 “Bone marrow stromal cell” functional definition**

*Culture-expanded BMSCs exhibit a spindle-shaped fibroblastic morphology following culture expansion ex vivo (panel A). Under appropriate inducing conditions, the culture will demonstrate osteogenesis as seen by calcium conditions (panel B), adipogenic differentiation evidenced by fat globules (panel c) or chondrogenic differentiation as measured by staining for type II collagen. Adapted from Deans R., Experimental Haematology 2000.*

**Table 1****Representative examples of denominations used for bone marrow stromal cells**

<b>Term</b>	<b>Cell type identified</b>	<b>Animal sources/references</b>
Colony forming unit-fibroblast (CFU-F)	Colonies of fibroblastic cells, with the occasional monocyte/macrophage present	<ul style="list-style-type: none"> <li>• Human (Castro-Malaspina et al. 1980)</li> <li>• Mouse (Friedenstein et al. 1982)</li> </ul>
Mesenchymal stem cells (MSCs)	Cells defined by their selective attachment to a solid surface	<ul style="list-style-type: none"> <li>• Human (Caplan 1991; Pittenger et al. 1999)</li> <li>• Mouse (Baddoo et al. 2003; Meirelles Lda et al. 2003; Tropel et al. 2004; Wang et al. 2006)</li> </ul>
Marrow stromal cells (MSCs)	Adherent cells of bone marrow that include and/or adherent fibroblast-like cells, endothelial cells and colonies monocytes/macrophage	<ul style="list-style-type: none"> <li>• Human (Digirolamo et al. 1999)</li> <li>• Mouse (Prockop 1997)</li> </ul>
Bone marrow stromal stem cells (BMSSCs) and/or Stromal precursors cells (SPCs)	Non-haematopoietic cells of mesenchymal origin, displaying fibroblastic morphology	<ul style="list-style-type: none"> <li>• Human (Bianco et al. 2001)</li> <li>• Mouse (Phinney et al. 1999; Short et al. 2001; Sun et al. 2003; Peister et al. 2004)</li> </ul>
RS-1, RS-2, mMSCs (RS:Recycling stem cell) (m: mature)	RS-1: thin, spindle-shaped cells RS-2: moderately thin, spindle-shaped cells mMSCs: wider, spindle-shaped cells	<ul style="list-style-type: none"> <li>• Human (Colter et al. 2000; Colter et al. 2001)</li> </ul>
Multipotent adult progenitor cells (MAPCs)	Culture-derived bone marrow progenitor cells able to differentiate in neuroectodermic and endodermic derivates	<ul style="list-style-type: none"> <li>• Human (Reyes et al. 2001)</li> <li>• Murine (Jiang et al. 2002)</li> </ul>
Marrow isolated adult multilineage inducible cells (MIAMI)	Culture-derived bone marrow-derived progenitor cells able to differentiate in vitro into mature-like cells from all three germ layers.	<ul style="list-style-type: none"> <li>• Human (D'Ippolito et al. 2004)</li> </ul>
Pluripotent unrestricted somatic stem cells (USSCs)	Culture derived cord blood cells able to differentiate in vitro into osteoblasts, chondrocytes, adipocytes, and neural progenitors.	<ul style="list-style-type: none"> <li>• Human (Kogler et al. 2006)</li> </ul>

### 1.3 BMSC immunophenotype

Several laboratories have developed monoclonal antibodies using BMSCs as immunogen in order to identify one or more markers suitable for identification and sorting of stromal cell preparations. However, to date, the isolation of a “pure” population of multipotent marrow stromal stem cells remains elusive and the immunophenotypical identification of BMSC is still based on a combination of negative and positive markers, rather than on a precise and specific subset of antigens.

There is a consensus that both human and murine BMSCs do not express CD45, marker of all haematopoietic cells, glycophorin-A, an erythroid lineage marker, or CD11b, an immune cell marker (Lai et al. 1998; Deans et al. 2000). CD34, the primitive haematopoietic stem cell (HSC) marker, is rarely expressed in human BMSCs, although can be positive in mice (Peister et al. 2004). CD31, expressed on endothelial and haematopoietic cells, and CD117, a haematopoietic stem/progenitor cell marker, are almost always absent on human BMSCs (Pittenger et al. 1999; Colter et al. 2001), whereas they are present on murine (Baddoo et al. 2003).

In particular, some antigens have had particular relevance and have been used for positive selection of BMSCs, such as Stro-1 (Simmons et al. 1991), CD105 and CD73 (Haynesworth et al. 1992), CD271 (Quirici et al. 2002), SSEA-1 and SSEA-4 (Anjos-Afonso et al. 2007; Gang et al. 2007) and, more recently, CD146, which is the only one identified on BMSCs *in vitro* and *in vivo* (Sacchetti et al. 2007).

Stro-1 is by far the best-known BMSC marker (Simmons et al. 1991). The cell population negative for Stro-1 is not capable of forming colonies, whereas Stro-1-positive cells can become HSC-supporting fibroblasts, smooth muscle cells,

adipocytes, osteoblasts, and chondrocytes (Gronthos et al. 1994), which is consistent with the functional role of BMSCs.

However, Stro-1 is unlikely to be a general BMSC marker, for, at least, three reasons:

- there is no known mouse counterpart of Stro-1
- Stro-1 expression is not exclusive to BMSCs
- Stro-1 expression in BMSCs is gradually lost during culture expansion limiting the use of Stro-1 labelling to the isolation of BMSCs and/or their identification during early passages.

In the 17 years since Stro-1's discovery, no consensus has emerged regarding its use to purify BMSCs. This is due particularly to the fact that other investigators have failed to detect this antigen on BMSCs.

In the laboratory of Caplan some monoclonal antibodies against CD105 (SH-2), or CD73 (SH-3 and SH-4) were developed (Haynesworth et al. 1992). These antibodies react against CD105, endoglin, a 5'-nucleotidase, regulatory component of the TGF-beta receptor complex, or CD73, which is the lymphocyte-vascular adhesion protein 2. Although these antigens were also expressed on many other cell types, these antibodies were developed with specificity for mesenchymal tissue-derived cells, providing a new tool in BMSC isolation (Haynesworth et al. 1992).

Several years later, Thomson et al. identified expression of CD271, the low affinity receptor for nerve growth factor (NGF) on BMSCs (Thomson et al. 1988). Although its function is still unknown, CD271 is highly expressed on directly isolated BMSCs (10% of total bone marrow cells), is maintained in un-stimulated *in vitro* cultures and is rapidly down-regulated upon differentiation. These

characteristics made this antigen a good target for antibodies to be employed in positive selection (Quirici et al. 2002).

Very recently it has been reported the identification, isolation, and detailed characterization of a primitive mesenchymal progenitor cells in the adult murine and human bone marrow, based on the expression of stage-specific embryonic antigen-1 (SSEA-1) and stage-specific embryonic antigen-3/4 respectively (Anjos-Afonso et al. 2007; Gang et al. 2007). These antigens have been characterized as overlapping carbohydrate epitopes on globo- and lacto-series glycolipids (Kannagi et al. 1983; Henderson et al. 2002). Human ES cell lines retain the earlier globo-series pathway and are SSEA-3/4<sup>+</sup> SSEA-1<sup>-</sup> (Henderson et al. 2002), whereas mouse ES cell lines use the lacto-series pathway and are SSEA-3/4<sup>-</sup> SSEA-1<sup>+</sup> (Henderson et al. 2002). With the exception of certain highly specialized cell types, the globo-series ganglioside synthesis pathway has been thought restricted to the pre-implantation embryo and not available to somatic cell types (Kannagi et al. 1983). Although the function of these carbohydrate antigens is still unknown, it is intriguing that in addition to pluripotent ES and EC cells, they are also present on the surface of multipotent BMSCs. Although the evidence associating these markers with a “stemness” state is correlative, it suggests some overlap in specialized metabolic pathways between pluripotent ES cells and multipotent BMSCs (Anjos-Afonso et al. 2007; Gang et al. 2007).

Importantly, two years ago, Sacchetti et al. demonstrated that self-renewing osteoprogenitors isolated from human bone marrow and able to regenerate bone and stroma, and organize a haematopoietic microenvironment *in vivo* are CD146<sup>High</sup> (a melanoma associated cell adhesion molecule), possibly providing a positive selectable marker for BMSCs in fresh tissue (Sacchetti et al. 2007).

## Chapter 2

### **Reaching a balance between self-renewal and differentiation**

Stem cells share the defining characteristics of self-renewal, which maintains or expands the stem-cell pool, and multi-lineage differentiation, which generates and re-generates tissues. These processes are influenced by the convergence of intrinsic cellular signals and extrinsic micro-environmental cues from the surrounding stem-cell niche, but the specific signals involved remain largely unknown (Watt et al. 2000, Figure 4).

Recently, several studies based on genomic array have sought to identify the genetic mechanisms that underlie the stem-cell phenotype. It has been postulated that, although each unique stem cell can be characterized by the expression of a specific set of genes, the defining self-renewal and multi-lineage differentiation characteristics of stem cells are encoded by a shared set of genes that are expressed by all distinct stem-cell populations, and that therefore represents a conserved stem-cell molecular signature (Ivanova et al. 2002; Ramalho-Santos et al. 2002; Fortunel et al. 2003). Several studies have examined the gene-expression pattern of both embryonic and adult stem-cell populations, such as bone marrow stromal cells. In particular, some candidate gene and proteomic approaches have provided interesting data on pathways involved in BMSCs self-renewal (Roche et al. 2006; Song et al. 2006; Jaishankar et al. 2008), however, there are inconsistencies in the resultant lists of ‘stemness’ genes and mechanisms involved in BMSC self-renewal, differentiation and maintenance of the niche are still unknown. In this chapter, I report new advances on self-renewal and regulation of specific lineage differentiation of BMSCs.

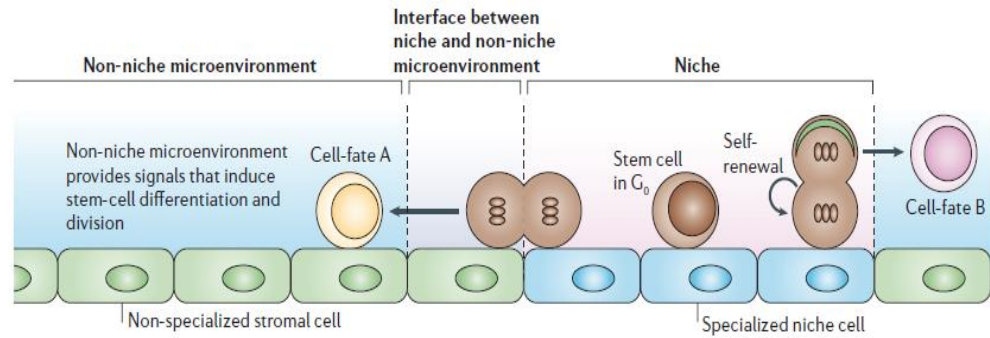


**Figure 4 Bone marrow niche**

*Quiescent stem cells are anchored in the centre of the niche, whereas self-renewing stem cells are located close to the border separating the niche from the non-niche microenvironment. At this interface, niche signals (differentiation and/or division repression) and non-niche microenvironment signals (differentiation and/or division induction) form a signalling centre. The appearance of a stem cell at the niche edge would expose it to proliferative and anti-adhesive signals emanating from the non-niche microenvironment. At the onset of cell division, one daughter cell would transit the interface towards the non-niche microenvironment to initiate differentiation, while the other would remain in the niche as a self-renewing stem cell, thereby achieving asymmetric division by environmental asymmetry. Alternatively, signals from the periphery might induce asymmetric division of a formerly quiescent stem cell by polarization of determinants (right). Attachment of stem cells to niche cells (and possibly signals exchanged between them) would maintain stem-cell fate, while the budding daughter cell would initiate differentiation. Adapted from Wilson A. Nature Immunology Review 2006.*

## 2.1 Niche-External signals

The external signals that control stem cell fate collectively make up the stem cell micro-environment, or niche. A complex interplay of short- and long-range signals between stem cells, their differentiating daughters, and neighbouring cells are involved in the niche maintenance (Figure 4). Soluble factors, cell-cell interaction and cell-extra-cellular matrix interaction seem to contribute to the self-renewal of different type of stem cells (Watt et al. 2000; Moore et al. 2006; Wilson et al. 2006). The most important signals implicated in BMSC ‘stemness’ maintenance are some cytokines such as leukaemia inhibitory factor (LIF, Jiang et al. 2002; Metcalf 2003), fibroblast growth factors (FGFs, Bianchi et al. 2003; Zaragosi et al. 2006; Choi et al. 2008) and mammalian homologues of

*Drosophila wingless* (Wnts, Boland et al. 2004; Etheridge et al. 2004; Kleber et al. 2004; Ling et al. 2008). These factors have drawn particular focus because of their demonstrated role in the self-renewal of other stem cell types, in the maintenance of undifferentiated embryonic mesenchymal tissue, and/or in de-differentiation programs, including tumorigenesis (Figure 5).

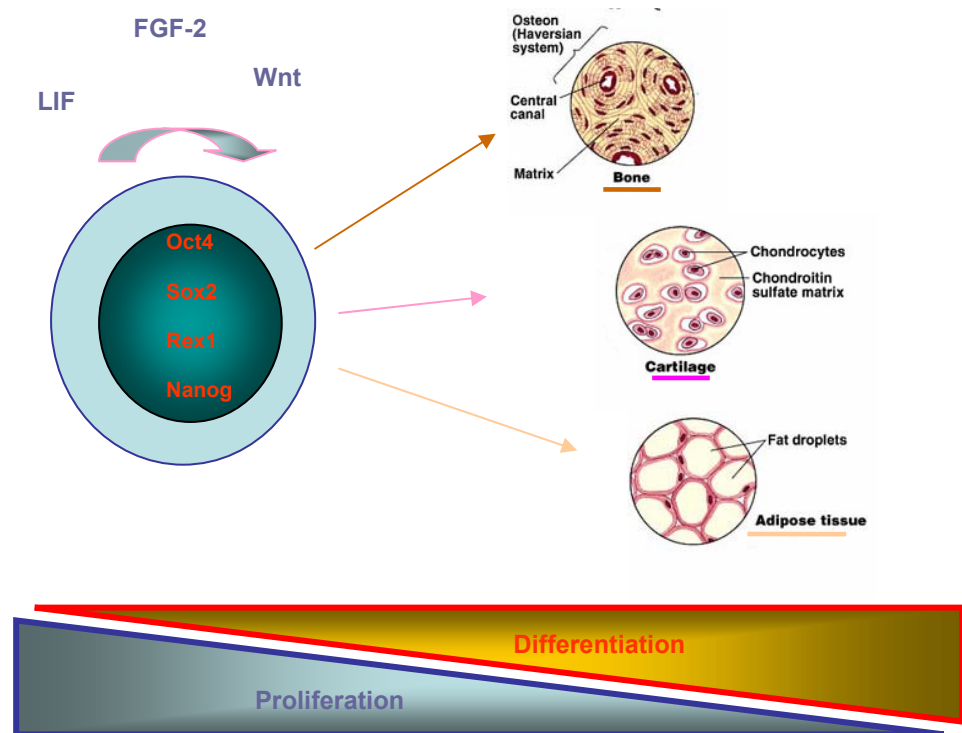


**Figure 5** BMSC self renewal and cytodifferentiation

*In this theoretical model, BMSCs have the capacity to differentiate into all connective tissue cell types, including bone, cartilage and adipose tissue. Furthermore, BMSCs have the potential for self-renewal and proliferation and, under defined environmental cues, can commit to a particular differentiation pathway. The lineage-committed cell progresses through several stages of maturation prior to the onset of terminal differentiation, which is marked by the cessation of proliferative capacity and shift toward synthesis of tissue-specific markers, including components of the extra cellular matrix.*

### **2.1.1 Leukaemia inhibitory factor (LIF)**

LIF, a pleiotropic cytokine, is secreted by BMSCs (Kim et al. 2005) and maintains the stem state of BMSCs (Jiang et al. 2002) and other stem cells (Metcalf 2003; Ying et al. 2003). LIF also has been considered as a cytokine of neuroimmune system with the particular characteristic of stimulation and repression on osteoblast and osteoclast activities (Metcalf 2003) and responsible for blocking osteoblast maturation at late differentiation stages and redirect these cells toward the adipogenic pathway (Falconi et al. 2007; Falconi et al. 2007). These data suggest that the cellular environment and the developmental stage of the target cell influence its differential responses to LIF. Mechanisms of LIF action in BMSC self-renewal are unknown but may involve paracrine crosstalk with neighbouring cells (Metcalf 2003).

### **2.1.2 Fibroblast growth factor 2**

FGF2 maintains the stem state of BMSCs from a variety of species by prolonging their viability in culture and maintaining their differentiation potential at least for 50 population doublings (Bianchi et al. 2003; Choi et al. 2008) and suppressing the cellular senescence (Ito et al. 2007). The underlying mechanism and the target genes of FGF responsible of these effects are not known. It has been proposed that this could be a cell-autonomous mechanism (Zaragosi et al. 2006) and that it could be based on the activation of the ERK1/2 and PI3K-Akt signalling pathways (Choi et al. 2008). Very recent data based on gene expression profiling provided new insights in FGF targets in BMSCs (Ng et al. 2008).

### **2.1.3 Wnt**

Wnt signalling has been implicated in the control over various types of stem cells and may act as a niche factor to maintain stem cells in a self-renewing state (Kleber et al. 2004) . Wnt3a treatment increases adult MSC proliferation and decreases the apoptosis, an effect that is consistent with the mitogenic role of Wnts in haematopoietic stem cells (Reya et al. 2003; Boland et al. 2004).

## **2.2 Niche-Intrinsic signals**

Intrinsic regulators of self-renewal include the proteins responsible for setting up cell divisions, nuclear factors controlling gene expression and chromosomal modifications and telomere length (Watt et al. 2000).

### **2.2.1 Transcription factors**

Embryonic stem (ES) cells maintain pluripotency by a transcriptional program that suppresses differentiation; this property is regulated by a small number of ES cell specific transcription factors such as Nanog, Oct-4 and Sox-2, whose expression is down regulated early during embryogenesis (Boiani et al. 2005). In the last two years several groups have shown the expression of Oct-4, Nanog and Sox2 in BMSCs (Jiang et al. 2002; Anjos-Afonso et al. 2007; Beltrami et al. 2007; Gonzalez et al. 2007; Greco et al. 2007; Kobayashi et al. 2008) and other adult stem cells (Battula et al. 2007; Beltrami et al. 2007; Nadri et al. 2008). Indeed, recent chromatin immunoprecipitation on chromatin immunoprecipitation array (Chip on Chip) studies suggest that some Polycomb chromatin-associated proteins are involved globally in maintaining the repression of differentiation

genes (Boyer et al. 2006). Thus, Polycomb proteins may indirectly maintain Oct-4, Sox-2, and Rex-1 activation in BMSCs.

### 2.2.1.1 Oct4

The *octamer-binding transcription factor 4* gene encodes a nuclear protein (Oct-4, also known as Pou5F1 and Oct3/4) that belongs to a family of transcription factors containing the POU DNA-binding domain and which is expressed in embryonic stem cells and plays a critical role in maintaining pluripotency and self-renewal (Scholer et al. 1990). Deficiency of Oct-4 in ES cells by knock-out or knock-down procedures, abolish both self-renewal and pluripotency and results in differentiation to trophoectoderm lineage (Nichols et al. 1998). Oct-4 has therefore been viewed as being involved in preventing trophectoderm and perhaps somatic-cell differentiation from the inner cell mass, as well as being crucial for maintaining the pluripotent state during embryonic development.

Several authors tried to identify the role of Oct-4 in BMSCs, starting from the expression of this protein in their cultures. Greco et al. demonstrated that Oct-4 provides similar regulatory circuitries in human BMSCs and ESCs and that Oct-4 promote the expression of BMSC-specific genes and regulate BMSCs cell cycle progression (Greco et al. 2007); however very recent papers dispute the role of Oct-4 as stemness marker and its expression in BMSCs. Liedtke et al. raise the issue of six known Oct-4 pseudogenes as a source of confusion in stem cell research (Liedtke et al. 2007; Liedtke et al. 2008). Kotoula et al. demonstrate that the second isoform of hOct-4, hOct-4B, which is related neither to stemness nor pluripotency, can account for much of misinterpretation of experimental data (Kotoula et al. 2008); Cantz T. et al. demonstrated highly methylated regions in Oct-4 promoter of somatic tumor cell lines (Cantz et al. 2008). In addition,

Lengner et al. demonstrated, using a recombination approach to achieve specific inactivation of Oct-4 in bone marrow, that the absence of Oct-4 protein does not interfere with BMSCs self-renewal or differentiation (Lengner et al. 2007).

### **2.2.1.2 Sox-2**

Sox-2 is a member of the HMG-domain DNA-binding-protein family that is implicated in the regulation of transcription and chromatin architecture (Pevny et al. 1997). Sox-2 forms a ternary complex with either Oct-4 or the ubiquitous Oct-1 protein on the enhancer DNA sequences of *Fgf-4*. This allows Sox-2 to participate in the regulation of the inner cell mass and its progeny or derivative cells. Consistent with this role, Sox-2 is expressed in ES cells, but it is also expressed in neural stem cells (Episkopou 2005). When gene targeting has been used to inactivate *Sox2* gene, the primitive ectoderm was defective (Avilion et al. 2003). Very recently the expression of Sox-2 has been reported in BMSCs (Beltrami et al. 2007; Gonzalez et al. 2007; Kobayashi et al. 2008). Go et al., in a gain of function study, observed that Sox-2-expressing BMSCs showed much higher expansion potential than control cells in both high and low serum conditions and higher osteogenic differentiation abilities (Go et al. 2008).

### **2.2.1.3 Rex-1**

The *Rex-1* (*Zfp-42*) gene encodes a zinc finger family transcription factor which is highly expressed in mouse and human embryonic stem cells involved in DNA repair process (Cenkci et al. 2003). A recent papers dispute its role as stem cell marker for ES cells (Masui et al. 2008). Its expression has been reported in BMSCs (Beltrami et al. 2007) and MAPC (Jiang et al. 2002), although it has never correlated with a specific function.

### 2.2.1.4 Nanog

Nanog is a transcription factor expressed in ES cells and is thought to be a key factor in maintaining pluripotency, as, when over expressed, it enhances ES cell self-renewal efficiency to the point of LIF-independence (Chambers et al. 2003; Mitsui et al. 2003). Conversely, deficiency of Nanog in ES cells by knock-out or knock-down procedures, abolish both self-renewal and pluripotency and results in differentiation to extra embryonic endoderm (Mitsui et al. 2003).

Similar to Oct-4, it has been proposed that Nanog might regulate differentiation through the transcriptional repression of genes that promote differentiation, a proposal that was based on the presence of Nanog-binding sites in the control regions of Oct-4, Sox-2 as well as that of Rex1/Zfp42 (Mitsui et al. 2003). Thus negative regulation of Nanog is required to promote differentiation during embryonic development. Transcriptional activator and tumour suppressor p53 binds to the promoter of *Nanog*, thereby enabling p53-dependent suppression of *Nanog* expression (Lin et al. 2005). Loss of p53 results in inefficient Nanog suppression during ES cell differentiation and in a 100-fold increase in susceptibility to testicular teratoma (Lam et al. 2003). Cues or agents that induce DNA damage also down regulate Nanog and this has been shown to maintain genetic stability in ES cells by inducing their differentiation into other cell types.

Very poor data are available about the role of Nanog in adult stem cells, although in the last years many groups have reported Nanog expression in BMSCs (Jiang et al. 2002; Anjos-Afonso et al. 2007; Beltrami et al. 2007; Gonzalez et al. 2007; Greco et al. 2007; Kobayashi et al. 2008) and other adult stem cells (Battula et al. 2007; Beltrami et al. 2007; Nadri et al. 2008). Very recently it has been demonstrated that that Nanog-expressing BMSCs show much higher expansion potential, higher osteogenic differentiation abilities and higher chondrogenic

differentiation abilities (Go et al. 2008; Liu et al. 2008), however the role of Nanog in adult stem cells as well as BMSCs is still disputed.

### **2.2.2 Telomeres length**

A second potential clock mechanism is the telomere length. In somatic cells, telomere length is progressively shortened with each cell division both *in vivo* and *in vitro* due to the inability of the DNA polymerase complex to synthesize the very 5' end of the lagging strand (Harley et al. 1990). It has been suggested that telomeres protect chromosome ends since damaged chromosomes lacking telomeres undergo fusion, rearrangement and translocation. As telomerase activity has been shown to be specifically expressed in immortal cells, cancer, germ cells and embryonic stem cells (Kim et al. 1994), progressive shortening of telomeres could act as a mitotic clock, counting off divisions before senescence.

In BMSC, expression of telomerase is disputed; some studies did not find telomerase activity (Simonsen et al. 2002; Stenderup et al. 2003), but others did (Pittenger et al. 1999; Miura et al. 2006). Such differences may arise from different sensitivity of measurement and differing standards regarding which amount of telomerase activity can be referred to as telomerase-negative.

## **2.3 Differentiation Potential**

The identification of specific signalling networks and 'master' regulatory genes that govern unique BMSC differentiation lineages remains a challenge. Information provided by various studies based on gene expression profiling (Song et al. 2006; Liu et al. 2007; Ng et al. 2008) or RNA interference (Zhao et al. 2007), allowed to draw a model for the regulation of adult stem cells differentiation, based on two continuous and distinct compartments (Figure 6). In

the first compartment (MSC compartment), BMSCs undergo transcriptional modification, generating precursor cells which continue to divide symmetrically, generating more tripotent and bipotent precursor cells. These tripotent and bipotent precursor cells are morphologically similar to the multipotent BMSCs, but differ in their gene transcription repertoire, and therefore, still reside in the stem cell compartment. Gene repression and induction have thought to be the principal mechanism involved in the maintenance of the niche (Quesenberry et al. 2002). Upon stimulation, multipotent, uncommitted BMSCs undergo asymmetric division, giving rise to two daughter cells, one being the exact replica of the mother cell and maintaining multilineage potential, and the other daughter cell becoming a precursor cell, with a restricted developmental program (Quesenberry et al. 2002). At the present, what is not fully understood is the mechanism that governs the transit of uncommitted stem cells to partially committed precursor or progenitor cells, and then to fully differentiated cells (Figure 6).

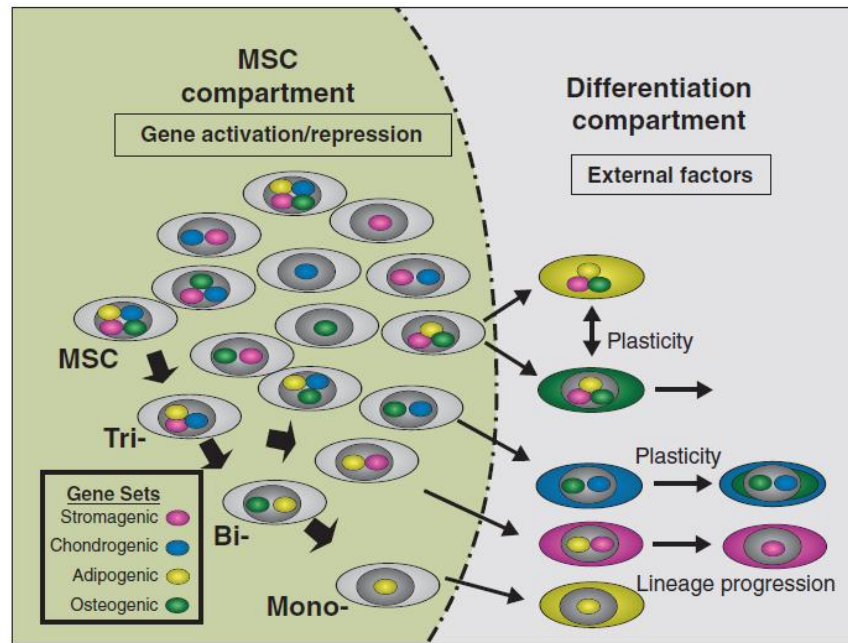


**Figure 6** *The stromal system*

*In the BMSC compartment the stem cells and progenitor cells express different “Gene Set” within a nucleus. This indicates the potential to differentiate in a specific cell type. When they live the niche different external stimuli can induce the differentiation; in this way these cells can acquire the phenotypic expression of the different lineage pathway as showed by the different cytoplasmic colours. Adapted from Dennis J.E. Stem Cells 2002.*

### 2.3.1 Osteogenesis

During osteogenesis, multipotent BMSCs undergo asymmetric division and generate osteoprecursors, which then progress to form osteoprogenitors, pre-osteoblasts, functional osteoblasts and osteocytes. This progression from one differentiation stage to the next is accompanied by the activation and subsequent inactivation of transcription factors, *i.e.*, Cbfa1/Runx2, Msx2, Dlx5, Osx, and expression of bone-related marker genes, *i.e.*, osteopontin, collagen type I, alkaline phosphatase, bone sialoprotein, and osteocalcin (Karsenty et al. 2002; Harada et al. 2003) (Figure 7).

The BMPs pathway has a well known role in promoting osteogenesis (Chen et al. 2004). Other cytokines, such as members of Wnt family have recently shown a

role in osteogenesis (Hartmann 2006), however different members can have dramatically different effects (Boland et al. 2004).

The targets of osteogenic pathways are the two master genes, CbfaI/Runx2 and Osterix. CbfaI/Runx2 is a member of Runt family of transcription factors; it has an essential role in the differentiation of mesenchymal progenitors in osteoblasts in both the endochondral and membranous skeletons. Besides its role in osteogenesis, it is also required for hypertrophic chondrocyte differentiation (Ducy et al. 1997). Osterix is a zinc finger-containing transcription factor that is expressed in osteoblasts of all endochondral and membranous bones. In osterix null mutants no endochondral and no intramembranous bone formation occur. Arrest in osteoblast differentiation occurs at later step than in Runx2/Cbfa I null mice, suggesting that this factor is down stream of CbfaI/Runx2 (Nakashima et al. 2002). It has been proposed that osterix might be a dominant negative regulator of Sox-9 and Sox-5 expression preventing bi-potential progenitors from choosing a chondrocyte differentiation pathway (Nakashima et al. 2002, Figure 7).

### **2.3.2 Chondrogenesis**

Chondrogenic differentiation of BMSCs *in vitro* mimics that of cartilage development *in vivo*. The transcription factor Sox-9 is considered the master gene of chondrogenesis and is responsible for the expression of extra cellular matrix (ECM) genes such as collagen types II and IX, aggrecan, biglycan, decorin, and cartilage oligomeric matrix protein (Goldring et al. 2006, Figure 7). However, the specific signalling pathways that induce the expression of these benchmark chondrogenic genes remain generally unknown. Naturally occurring human mutations and molecular genetic studies have identified several instructive signalling molecules, including various transforming growth factor- $\beta$  (TGF- $\beta$ )

(Massague et al. 2000), bone morphogenetic protein (BMP), growth and differentiation factor (GDF, Chen et al. 2004) and Wnt ligands (Hartmann 2006).

### **2.3.3 Adipogenesis**

The nuclear hormone receptor peroxisome proliferators activated receptor  $\gamma$  (PPAR $\gamma$ ) is a critical adipogenic regulator promoting BMSC adipogenesis while repressing osteogenesis (Rosen et al. 2006) (Figure 7). The binding of PPAR  $\gamma$  to various ligands, including long chain fatty acids and thiazolidinedione compounds, induces the transactivation and transrepression of PPAR $\gamma$ . The bipotent co regulator TAZ was recently discovered to function as a coactivator of Runx2 and as a co repressor of PPAR $\gamma$ , thus promoting osteogenesis while blocking adipogenesis (Hong et al. 2005). A similar role is played by Wnt signalling. As discussed above, some members of Wnt family have recently shown a positive role in osteogenesis (Hartmann 2006); on the other hand suppression of Wnt signalling is required for the cells to undergo adipogenesis (Liu et al. 2004).

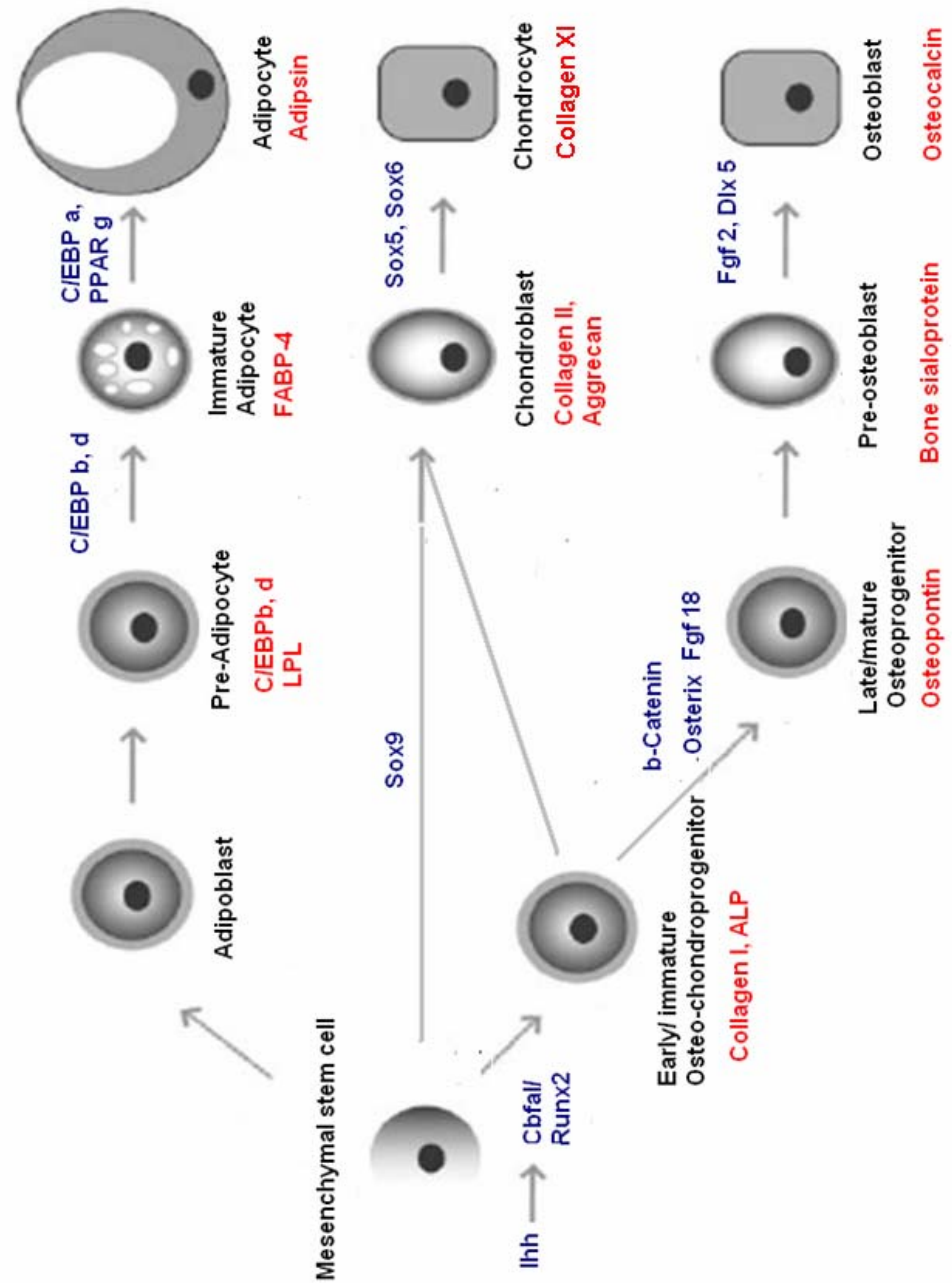


**Figure 7 Molecular regulation of BMSC differentiation**

BMSC is the precursor of osteoblasts, adipocytes and chondroblasts. Expression of specific master genes is essential to drive BMSC towards osteo-, chondro- or adipogenic differentiation. These processes involve different intermediate stages and the expression of different markers.

## Chapter 3

### Senescence and transformation

Most, if not all, human adult cells can undergo 50–60 divisions before they become senescent. This limited replicative capacity is also known as the ‘Hayflick limit’, according to its discoverer Leonard Hayflick (Hayflick 1965) and it is thought to be determined by chromosomal telomere shortening after each cell division. It is well known that cells can escape this process *in vitro* by acquiring mutations in specific genes in a process called transformation. Functional mutations that provide a growth or survival advantage produce positive selection for the mutant stem cell clone, with full fledged cancer resulting from the accumulation of multiple cancer-promoting events. To offset this possibility, stem cells appear to have evolved multiple reinforcing mechanisms that are aimed at maintaining genomic integrity (reviewed by Pelicci et al. 2004 and Sharpless et al. 2004). When mutations occur, despite these error prevention capacities, potent tumor suppressor mechanisms such as senescence and apoptosis are activated to sense damaged stem cells genomes with malignant potential and limit replicative ability of such clones (Figure 8).

Due to the huge number of clinical trials employing BMSCs (Le Blanc et al. 2005; Giordano et al. 2007), a careful consideration about the factors involved in senescence and tumorigenic potential of this population is necessary.

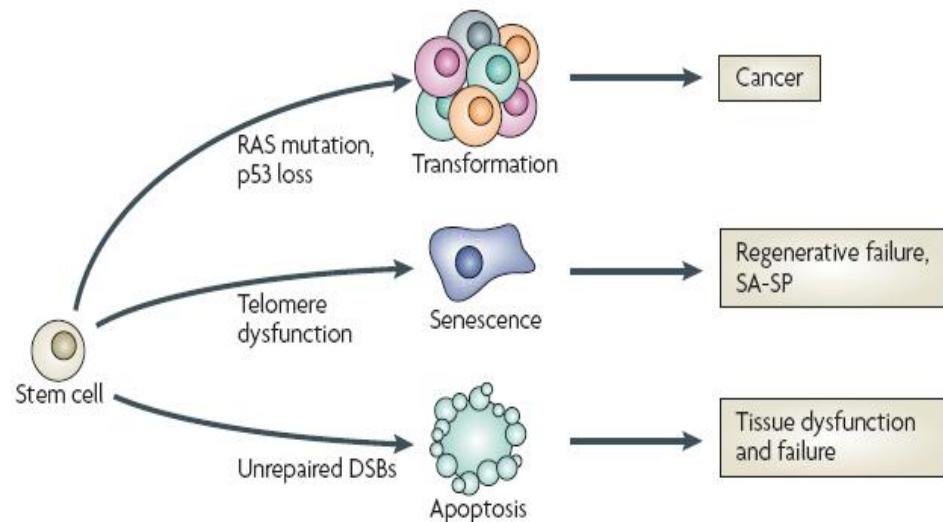


**Figure 8 Fates of damaged stem cells**

A limited number of outcomes appear to be possible for stem cells with heritable DNA damage. Although it is likely that many mutational events do not lead to any alteration of stem-cell function, significant damage is expected to induce apoptosis, senescence, transformation or dysfunction. Examples of DNA lesions associated with each outcome are indicated. Mutations in *RAS* and the tumour-suppressor *p53* are associated with transformation, unrepaired double-strand DNA breaks (DSBs) and telomere dysfunctions induce apoptosis and senescence, respectively. SA-SP, senescence-associated secretory phenotype. Adapted from Sharpless N. *Nature Review Molecular Cell Biology* 2007.

### 3.1 Defining senescence

Senescence, according the definition of Campisi, is “an essentially irreversible arrest of cell division” (Campisi 2000).

The most accredited hypothesis is that accumulation of senescent cells contributes to an ‘aging’ phenotype *in vivo*. In this contest, the process of senescence represents a means to eliminate cells that acquired DNA damage and/or became transformed, that compromise organismal integrity (reviewed by Sharpless et al. 2007). The processes involved in BMSCs senescence are poorly understood. One of the most common observation in a large number of papers is that culture-expanded hBMSC usually stop proliferating before or at 40 population doublings (PD's; at least 60 for mBMSC, see Tropelet al. 2004), at which time the cells lose

spindle-shaped fibroblastic morphology and become bigger and more flattened (Bruder et al. 1997; Stenderup et al. 2003). A phenomenon largely associated with senescence *in vitro* (Hayflick 1965; Dimri et al. 1995). Indeed, several studies reported a dramatic change in differentiation potential during the *in vitro* culture (Digirolamo et al. 1999; Pittenger et al. 1999).

Many kinds of oncogenic or stressful stimuli can induce a senescence response. In the BMSCs field it has been reported that DNA damage (Galderisi et al. 2008), shortening of telomere length (Baxter et al. 2004; Bonab et al. 2006; Guillot et al. 2007) and epigenetic changes to chromatin organizations (Di Bernardo et al. 2008) seems to be the principal inducing factors (Sethe et al. 2006). Indeed, very recently, some micro-array studies have provided new insights in the understanding of molecular pathway involved in BMSC senescence (Ryu et al. 2008; Wagner et al. 2008).

### **3.1.1 DNA damage**

DNA is subjected to spontaneous and extrinsic mutational events on daily basis, and despite a formidable capacity for repair, some damaged DNA appears to evade repair and accumulates over time. Evidences in support of the notion that DNA damage attenuates BMSCs function have been provided by recent studies (Galderisi et al. 2008; Wagner et al. 2008).

Galderisi U. et al. demonstrated that during *in vitro* culture of rat BMSCs, these cells showed an increased growth doubling time, lost telomerase activity and expressed senescence associated beta-galactosidase (SA- $\beta$ -Gal) (Dimri et al. 1995; Galderisi et al. 2008). This phenotype was accompanied by down-regulation of several genes involved in stem cell self-renewal (Nanog, Sox-2, KLF-4 and Bmi1) and DNA repair (especially genes involved in base excision,

nucleotide excision and mismatch repair). These data confirmed the importance of DNA repair in the maintenance of BMSCs genomic integrity, and that activation or response to DNA damage is essential to overcome senescence.

### 3.1.2 Telomere length

One of the mechanisms underlying cell senescence is loss of telomere length. A number of studies have measured telomere length of BMSCs, with varied results. Baxter et al. described in an *in vitro* culture system, a progressive loss of telomere length with each cell division and found that hBMSCs stop dividing when telomere length reaches about 10 kb (Baxter et al. 2004). Several groups documented telomere loss of up to 1.5–2 kb upon passage *in vitro* (Bonab et al. 2006; Guillot et al. 2007).

As mentioned in the Chapter 2, section 2.2.2, expression of telomerase is still disputed in BMSCs. Some studies find no telomerase activity (Simonsen et al. 2002; Stenderup et al. 2003), but in others a certain activity is detected (Pittenger et al. 1999; Miura et al. 2006; Galderisi et al. 2008). In order to understand the role of telomerase activity in BMSCs senescence, several groups have tested whether forced expression of telomerase reverse-transcriptase (TERT) would extend the lifespan of hBMSC.

hTERT-transduced hBMSC have prolonged replicative capacity *in vitro*, as they undergo more than 260 PDs, whereas they retained adipo-, chondro- and osteogenic differentiation potential *in vitro* and osteogenic potential *in vivo* (Shi et al. 2002; Simonsen et al. 2002; Ryu et al. 2008).

According to these studies, the ectopic expression of hTERT can maintain the proliferative and differentiation ability of human BMSC, without altering the karyotype and without providing a tumorigenic potential (Shi et al. 2002;

Simonsen et al. 2002); evidence that is not confirmed by several other studies (Serakinci et al. 2004; Rubio et al. 2005; Miura et al. 2006).

### **3.2 Molecular pathways involved in senescence**

Although diverse stimuli can induce a senescence response, they appear to converge on either or both of two pathways that establish and maintain senescence and growth arrest. This arrest is primarily caused by the expression of cell-cycle inhibitors. Among these, two are often expressed by senescent cells: the cyclin-dependent kinase inhibitors p21<sup>CIP1</sup> and p16<sup>INK4A</sup>. These proteins are key components of tumor suppressor pathways that are governed by p53 and pRB (Campisi et al. 2007; Serrano et al. 2007; Sharpless et al. 2007, Figure 9).

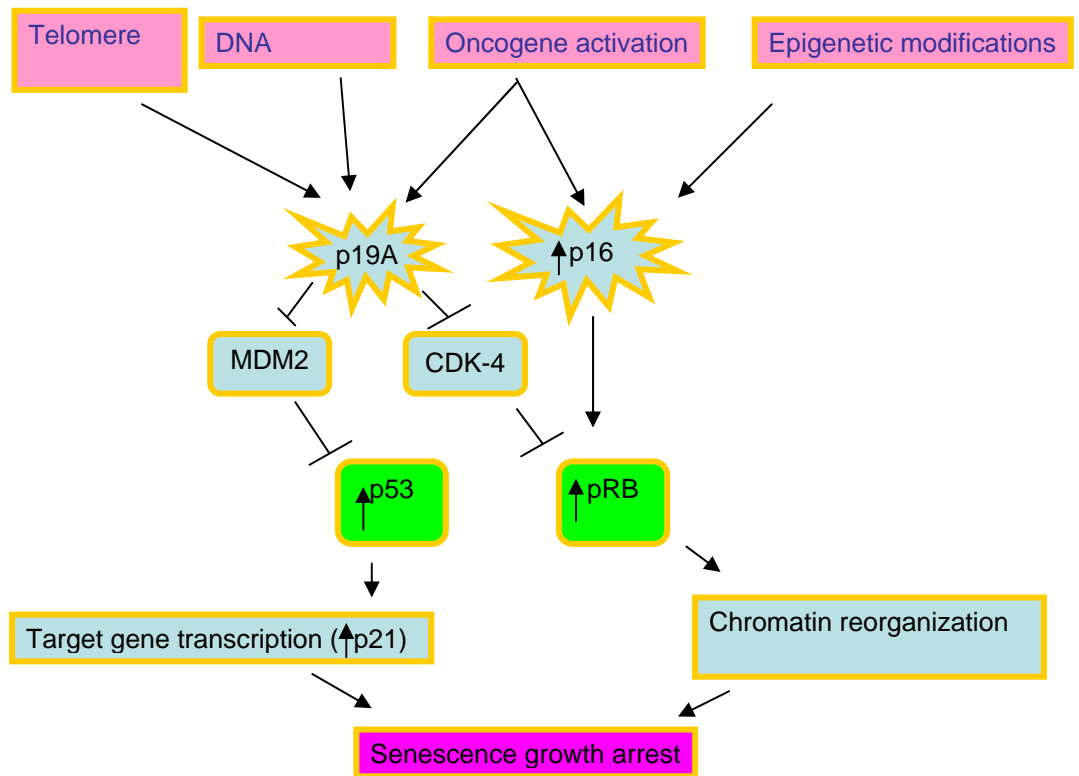


**Figure 9 Roles of p53 and p16RB pathways in senescence response**

*p53* activity is predominantly regulated at the protein level. In the unstressed state, *p53* is rapidly degraded by MDM2; a process which is inhibited by ARF. Also, *p53* can be stabilized by N-terminal serine phosphorylation in response to genotoxic stresses, and this phosphorylation inhibits its interaction with MDM2. *p53* activation potently induces either growth arrest or apoptosis depending on cellular context. The antiproliferative activity of *p53* in part results from *p21* expression, which is a *p53* transcriptional target. *Rb* is inactivated by phosphorylation as a result of the cyclin-dependent kinases CDK4 and CDK6. Hypophosphorylated *Rb* binds E2F and represses proliferation. CDK activity is inhibited by p19ARF.

### 3.2.1 p19ARF/p53 pathway

*p53* is a crucial mediator of cellular responses to DNA damage, including the senescence response (Campisi et al. 2007; Serrano et al. 2007; Sharpless et al. 2007).

In normal cells *p53* is usually inactive, bound to the protein MDM2, which prevents its action and promotes its degradation by acting as ubiquitin ligase. At least in some cells, the induction of senescence by DNA damage, telomere dysfunction, and possibly oncogene over-expression can cause activation of *p53*

through ATM or p19ARF (p14ARF in human cells). p19ARF phosphorylate p53 at sites that are close to or within the MDM2-binding region, blocking the degradation MDM2 dependent and binds directly to and sequesters MDM2, inhibiting the capacity of MDM2 to induce degradation of the p53 tumor suppressor protein. This loss of MDM2 function, in turn, results in the stabilization of p53 and activation of p53-mediated growth arrest or apoptosis (Sherr et al. 2000, Figure 9). Once activated p53 activates expression of several genes including one encoding for p21, that interacts with the G1-S/CDK and S/CDK complexes (molecules important for the G1/S transition in the cell cycle) inhibiting their activity (Campisi et al. 2007; Serrano et al. 2007; Sharpless et al. 2007).

The role of p53 in BMSC senescence is still not clear. Some studies report the up-regulation of p53 during the cellular senescence (Ito et al. 2007; Rubio et al. 2008) and others do not report any significant changes (Galderisi et al. 2008).

### **3.2.2 p16/pRB pathway**

Although the p53 inactivation reverses the senescence arrest in some cells, it fails to do in others (Beausejour et al. 2003).

p16 is a positive regulator of pRB and a tumor suppressor in its on right (Campisi et al. 2007; Serrano et al. 2007; Sharpless et al. 2007).

It is induced by varied stressful stimuli, including over-expression of oncogenes. Some cells spontaneously reduce or silence p16 expression, often by promoter methylation and activate its expression during long-term culture and upon replicative senescence, as reported in hBMSCs by Shibata et al. (Shibata et al. 2007). Thus, the p16 tumor suppression and the pRB pathway provide a formidable barrier to cell proliferation, which cannot be overcome by loss of p53

function. The mechanisms involved in the implementation of senescence by p16/RB pathway are not completely understood, however pRB seems to be involved in a reorganization of chromatin (Narita et al. 2003). Briefly, replicative senescent cells develop dense foci of heterochromatin which coincides with pRB-dependent heterochromatic repression of genes encoding cyclins and other positive cell cycle regulators (Narita et al. 2003).

Up-regulation of p16<sup>INK4A</sup> seems to be the principal mechanism involved in BMSC senescence (Ito et al. 2007; Shibata et al. 2007; Galderisi et al. 2008).

### **3.3 Overcoming the cell crisis: from senescence to spontaneous transformation**

As above described, after 20-40 population doublings *in vitro*, BMSCs enter a senescence phase, which they are able to bypass at a high frequency. These cells then continue to divide until they reach a crisis phase, characterized by generalized chromosome instability that provokes mass apoptosis (Campisi 2000; Sharpless et al. 2004; Serrano et al. 2007; Sharpless et al. 2007). Only some cells are able to escape from this crisis phase spontaneously, but those that do have undergone tumorigenic transformation. This phenomenon has been well described in the studies of Rubio (Rubio et al. 2005; Rubio et al. 2008). In these studies the authors propose a two stage model, immortalization and transformation, in which BMSCs become tumor cell (Figure 10). In the first step the cells bypass the senescence. This phase is accompanied by c-myc over-expression and p16 repression; many DNA repair proteins are subsequently down-regulated, whereas the cells are forced to proliferate. Consequently, the shortening of telomere length provokes the cell crisis phase in which they undergo stringent selection. In the last phase the cells up-regulate many DNA repair proteins, which may be necessary

for crisis bypass. Finally, escape from crisis is associated with telomere stabilization, Rb hyperphosphorylation and p16 deletion that seems to be essential to promote transformation (Sharpless et al. 2004). These essential steps in BMSC transformation have been confirmed by very recent papers (Miura et al. 2006; Li et al. 2007; Tolar et al. 2007; Rubio et al. 2008), leading to the application of “cancer stem cells” hypothesis for BMSCs.

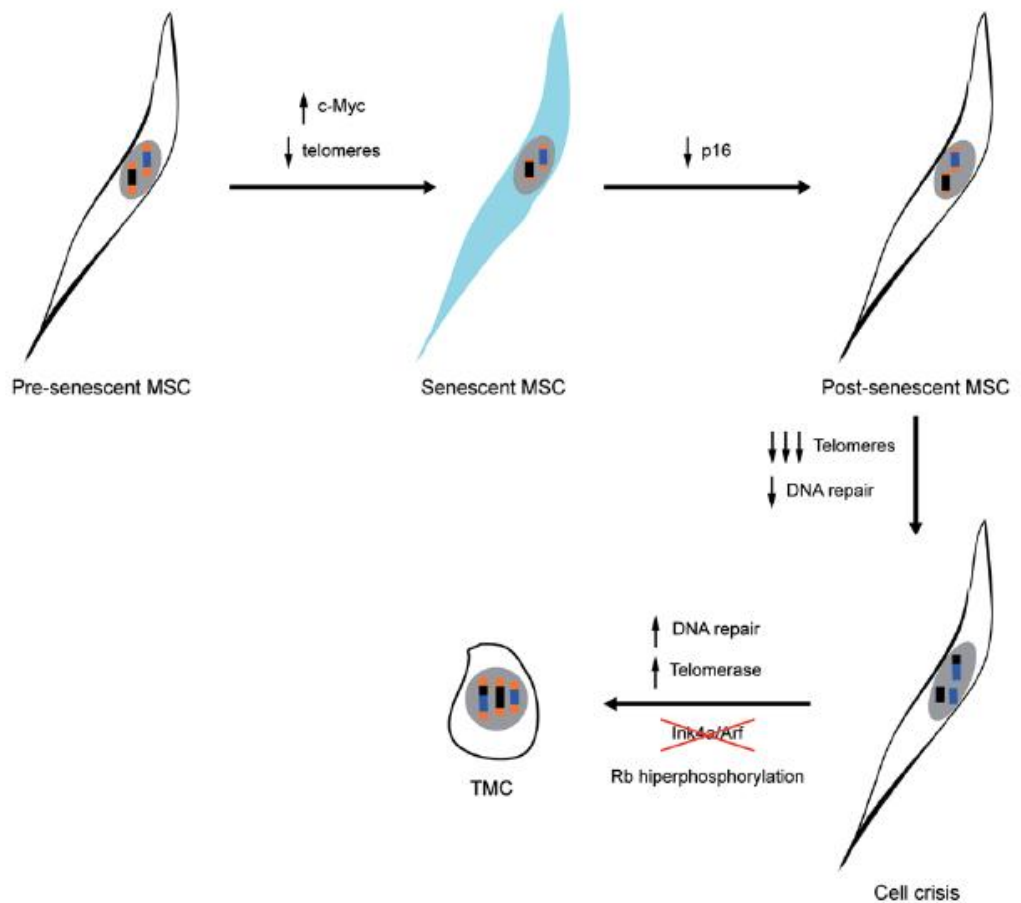


**Figure 10 Model of spontaneous BMSC transformation**

*In the model proposed by Rubio et al published on Plos One in 2008, bypass of senescence is the first step required to lead to transformation. Escape from crisis is associated with telomere stabilization, Rb hyperphosphorylation and p16 deletion that seems to be essential to promote transformation. Black and blue boxes represent chromosomes, orange boxes represent telomeres.*

## **MATERIALS AND METHODS**

### **Chapter 4**

#### **4.1 Mice**

C57BL/6 (H-2K<sup>b</sup>) and nude mice (Foxn1<sup>nu</sup>/Foxn1) were obtained from Harlan Sprague Dawley Inc. All the experiments in this study are performed following all regulations protecting animals used for research purposes, including those of the DL 116/92.

#### **4.2 Cell cultures**

##### **4.2.1 mBMSCs isolation and expansion**

C57BL/6 mice were euthanized with carbon dioxide vapours. Using aseptic technique, skin were peeled from the top of each hind leg and down over the foot. Muscles were removed from legs and femurs and tibias were dislocated, removed and carefully cleaned of adherent soft tissue. Marrows were harvested by flushing bones three times with alpha-modified minimal essential medium ( $\alpha$ -MEM) (Cambrex Bio Science) using a 26 gauge syringe. Cells were centrifuged 10 min at 500 g at room temperature. Supernatant were discarded and cell pellet were suspended in 10 ml of  $\alpha$ -MEM. A little aliquot of cell suspension was diluted 1:1000 with NH<sub>4</sub>Cl (StemCell Technologies) and incubated at 4°C for 15 minutes to lyse erythrocytes. I counted the number of viable cells of this aliquot with Trypan blue (Sigma-Aldrich) in a Burker chamber and then I suspended the cells in  $\alpha$ -MEM supplemented with 10% selected FBS (HyClone), 2 mM L-Glutamine (Gibco, Invitrogen) and 10 U/ml penicillin-10  $\mu$ g/ml streptomycin (Gibco,

Invitrogen) (complete medium) to a final concentration of  $5 \times 10^6$  viable nucleated cells per ml. I initially seeded  $2 \times 10^6$  nucleated cells/cm<sup>2</sup> in complete medium without any supplements in a six -well tissue culture dishes (TPP Techno Plastic Products). After three days I removed the non-adherent cells and waited for a sub-confluent culture. Unfortunately, the cells failed to reach confluence and they formed only a little colony in the centre of the well. I tried to subculture this colony but the cells didn't expand. I decided to change the medium in DMem and IMDM. In both these conditions, I obtained larger colonies: however, when I tried to subculture these colonies, the cells did not expand. When I added 20% bone marrow conditioned medium to the complete medium, as reported by Sun, the cells became confluent in 10-17 days (Sun et al. 2003). At that time they were washed twice with Ca<sup>2+</sup>Mg<sup>2+</sup>- free phosphate buffered saline (PBS, Gibco Invitrogen), detached with accutase (Innovative Cell Technologies) at 37°C for 10 minutes and then suspended in 50% culture supernatant and 50% complete medium with the addition of: a) 20% bone marrow conditioned medium (Sun et al. 2003) (BF mBMSC), b) 20 ng/ml mEGF and 20 ng/ml PDGF-AA (Sigma-Aldrich) after two weeks of culture in condition a (EP mBMSC) c) 20% MS5 conditioned medium (Issaad et al. 1993) (M mBMSC) or d) 20% NIH3T3 conditioned medium (Burroughs et al. 1994) (N mBMSC). The resulting suspensions were split 1:3. 50% of the culture medium was changed every 3-4 days until the cultures became confluent, when they were washed twice with Ca<sup>2+</sup>Mg<sup>2+</sup>- free PBS, detached and split 1:2. At passage 4-5, cultures were transferred to 75 cm<sup>2</sup> flasks or frozen at  $2 \times 10^6$  cell/vial in 10% Dimethyl sulfoxide (DMSO) (Sigma-Aldrich ) and 90% FBS.

Analogous protocol was used to isolate mBMSCs from Balb/c mice (B BMSCs) in the laboratory of Dr Nicole Horwood at Kennedy Institute of Rheumatology,

Imperial College of London. B BMSCs were expanded in Mesencult (StemCell technologies).

#### **4.2.2 Preparation of bone-marrow conditioned medium**

The bone marrow conditioned medium has been prepared following the procedure described in the work of Sun (Sun et al. 2003). Briefly, after flushing the bone marrows out of femur and tibia, fragments from these bones were cultured in  $\alpha$ -MEM supplemented with 20% FBS at 37°C in humidified atmosphere containing 5% CO<sub>2</sub> for three days. Then the incubation medium was collected by centrifugation at 2500 rpm for ten minutes and filtered through a 0.22  $\mu$ m filter.

MS-5 and NIH3T3 cell lines, obtained from DSMZ, were cultured in complete medium at 37°C in humidified atmosphere containing 5% CO<sub>2</sub>. Cells were sub-cultured every three-four days and conditioned media were collected from each cell line, centrifuged at 2.500 rpm for ten minutes and then filtered through a 0.22  $\mu$ m filter.

#### **4.2.3 Culture of cell lines**

MC3T3-E1 sub4, C3H10T1/2, 293 and A549 cell lines were obtained from ATCC (American Type Culture Collection); ATDC5 cell line was obtained from ECACC (European Collection of Cell Culture). MC3T3-E1 sub4 cell line was cultured in IMDM (Sigma- Aldrich) supplemented with 10% selected FBS, 2 mM L-Glutamine, 1 mM sodium pyruvate. For the osteogenic differentiation, cells were plated at  $2 \times 10^4$  cell/cm<sup>2</sup> and cultured in  $\alpha$  MEM supplemented with 10% selected FBS, 2 mM L-Glutamine, 0.05 mM ascorbic acid 2-phosphate (Sigma-Adrich) and 10 mM  $\beta$ -glicerophosphate (Sigma-Adrich), changing the medium every 3 days for 10 days (Wang et al. 1999).

293, A549 and C3H10T1/2 cell lines were cultured in complete medium. For the adipogenic differentiation of C3H10T1/2, the cells were allowed to reach 90% confluence and then cultured in  $\alpha$ -MEM supplemented with 10% selected FBS, 2 mM L-Glutamine,  $10^{-6}$  M dexamethasone (Sigma-Adrich), 5  $\mu$ g/ml insulin (Sigma-Adrich), 0.5  $\mu$ M 3-Isobutyl- 1-methylxanthine (Sigma-Adrich) and 50  $\mu$ M indomethacin (Sigma-Adrich) changing medium every 3-4 days for 14 days (Cho et al. 2004).

ATDC-5 cell line was cultured in DMEM/HamF12 (Sigma-Adrich) supplemented with 5% selected FBS and 2 mM L-Glutamine (Chen et al. 2005). Total RNA from MC3T3-E1, C3H10T1/2 and ATDC-5 was extracted from the cells using TriReagent (Sigma-Adrich) as described below.

#### **4.2.4 Culture of murine embryonic stem (mES) cells**

Mouse ES cell line E14 tg 2A (BayGenomics) was maintained in GMEM (Sigma-Aldrich) supplemented with 10% FBS, 0.1 mM  $\beta$ -mercaptoethanol (Sigma-Aldrich), 1 mM sodium pyruvate (Invitrogen), 1X non essential aminoacids (Invitrogen), 2 mM glutamine, 10 U/ml penicillin-10  $\mu$ g/ml streptomycin and  $10^3$ U/ml leukaemia inhibitory factor (LIF) (Chemicon International) (ES complete medium). ES cells were routinely split every 2 days, and the medium was changed on alternated days. To analyze the expression of LIF in NIH3T3 supernatant, I plated mES cells at 10 cell/cm<sup>2</sup> density in ES complete medium. After 24 hours I changed the medium and maintained cells in ES complete medium (positive control), in ES complete medium without LIF (negative control), in supernatant NIH3T3, supplemented with 10% FBS, 0.1 mM  $\beta$ -mercaptoethanol, 1 mM sodium pyruvate, 1X non essential aminoacids, 2 mM glutamine, 10 U/ml penicillin-10  $\mu$ g/ml streptomycin in absence or presence of blocking anti-LIF

antibody (Chemicon International), according to the manufacture's instructions. The medium was changed every day. After six days we analyzed the formation of alkaline phosphatase positive colonies.

### **4.3 Flow cytometry analysis**

Cells were detached with accutase at 37°C for 10 minutes and suspended in complete medium. The fraction to be analyzed ( $2 \times 10^5$ /tube) was centrifuged, suspended in PBS supplemented with 2% FBS and incubated for 30 minutes at 4°C with a panel of monoclonal antibodies directly coupled with Phycoerythrin (PE) or Fluorescein isothiocyanate (FITC) including Ly-1 (CD5), CD19, Ly-5 (CD45), CD34 (Santa Cruz Biotechnology), Ly-24 (CD44), CD117 (c-kit), CD13, Ly-6A/E (Sca I) and MHC-I (H2-k<sup>b</sup>) (BD Biosciences).

Excess antibodies were removed by washing with PBS. At least 10,000 events were collected and analyzed with FACS Canto II (BD Biosciences).

### **4.4 Cumulative duplication number and doubling time measurement**

Cumulative population doublings were calculated from the initial number of mBMSCs at the first passage and the number of mBMSCs harvested at each of the following passage. This procedure provides a theoretical growth curve that is directly proportional to the cell number (Meirelles Lda et al. 2003).

Doubling time measurement was obtained dividing the number of cells harvested after each passage by number of days in culture.

#### **4.5 Cell cycle analysis**

For each assay,  $2 \times 10^6$  cells were collected, suspended in PBS and fixed in 70% ethanol. After re-hydration with PBS and centrifugation at 500g for five minutes, the cell pellets were incubated with 500  $\mu\text{g/ml}$  propidium iodide solution (Sigma-Aldrich) at the dark for 30 minutes at 37°C. Samples were analyzed by FACS Canto II (BD Biosciences Pharmingen). DNA peaks were analyzed by ModFit LT.

#### **4.6 Senescence associated Beta Galactosidase (SA-B-Gal) staining**

Cells were fixed for 10 minutes with 2% formaldehyde/0.2% glutaraldehyde (Sigma-Adrich). Cells were washed with PBS and then incubated at 37°C for at least two hours with a staining solution (30mM Citric Acid/Phosphate buffer, 5 mM  $\text{K}_4\text{Fe}(\text{CN})_6$ , 5 mM  $\text{K}_3\text{Fe}(\text{CN})_6$ , 150 mM NaCl 2mM  $\text{MgCl}_2$ , 1mg/ml X-gal solution) (all reagents from Sigma-Adrich) (Dimri et al. 1995). Cells were counted in at least 12 fields for each well. The number of senescent cells was calculated by the mean of blue cell number ( $\beta$  galactosidase positive cells) out of three wells.

#### **4.7 Telomeric Repeat Amplification protocol (TRAP) Assay**

Telomerase activity products of mBMSCs were analyzed according the guidelines of TRAPeze ELISA detection kit (Chemicon International). Reaction consists on TRAP extension/amplification followed by results analysis by PAGE and ELISA. Briefly, cells were detached with accutase at 37°C for 10 minutes and suspended in complete medium. The fraction to be analyzed ( $1 \times 10^6$ ) was spun down, washed

in PBS and suspended in 200  $\mu$ l of 1X CHAPS lysis buffer. Determination of protein concentration was obtained by Bradford Assay.

1.5  $\mu$ g of each extract was used in a PCR reaction (incubation at 30°C for 30 minutes, followed by a two-step PCR at 94°C for 30 seconds, 55°C for 30 sec and 72°C 30 sec for 36 cycles). TRAP products were analyzed on a 12% native polyacrylamide gel electrophoresis (PAGE) and, after electrophoresis, the gel was stained with ethidium bromide to visualize the TRAP ladder. As the TRAP products were tagged with biotin and DNP residues, they were also detected by ELISA.

#### **4.8 *In vivo* tumorigenicity: transplantation of mBMSCs into nude mice**

$2 \times 10^6$  mBMSCs were suspended in a 1:1 mixture of PBS and injected subcutaneously in five nude mice (Foxn1<sup>nu</sup>/Foxn1<sup>+</sup>, 6-8 weeks of age from Harlan Sprague Dawley). As a positive tumor cell control, five mice received mES cells subcutaneously ( $2 \times 10^6$  cells/site). The mice that received mES cells were sacrificed 4 weeks post-transplantation, as, at this time, they formed a visible tumor on the neck. The other mice were sacrificed 10 weeks post-transplantation. Sites of injection were analyzed macroscopically and histologically; tissues were dehydrated through ascending concentrations of ethanol, embedded in paraffin and sectioned at 5  $\mu$ m thicknesses. After deparaffinization, sections were stained with hematoxylin and eosin (Bio-Optica).

#### **4.9 Immunofluorescence for Nanog detection**

Cells were fixed in 4% paraformaldehyde and permeabilized with 0.2% TX-100 in 10% normal goat serum /1% BSA (Sigma-Aldrich) in PBS for 15 min at room

temperature. The samples were incubated with primary antibodies anti-Nanog (1:100 dilutions, R&D Systems) and then with an anti-goat IgG conjugated with Alexa Fluor 488 (Molecular Probes). Images were captured with an inverted microscope (DMI4000, Leica Microsystems).

## **4.10 Differentiation Assay**

### **4.10.1 Osteogenic differentiation**

Cells were allowed to grow to 70-90% confluence and then cultured for 3 weeks in  $\alpha$ -MEM supplemented with 10% FBS, 2 mM L-Glutamine, 10 U/ml penicillin - 10  $\mu$ g/ml streptomycin,  $10^{-8}$  M dexamethasone, 0.05 mM ascorbic acid 2-phosphate and 10 mM  $\beta$ -glicerophosphate, changing the medium every 3-4 days (Phinney et al. 1999).

### **4.10.2 Chondrogenic differentiation**

Cells were trypsinized and suspended in DMEM/Ham's F12 medium supplemented with 10% FBS, 2 mM L-Glutamine, 10 U/ml penicillin -10  $\mu$ g/ml streptomycin at a concentration of  $10^7$  cell/ml. A 10  $\mu$ l drop was plated at the centre of well of 24 well-plate. Cells were allowed to adhere for 2-3 h at 37° C and 5% CO<sub>2</sub>, then the culture was flooded with 1 ml medium containing  $\alpha$ -MEM supplemented with 1% FBS, 2mM L-glutamine, 10 U/ml penicillin -10  $\mu$ g/ml streptomycin, 6.25  $\mu$ g/ml insulin, 50 nM ascorbic acid 2-Phosphate, 10 ng/ml TGF- $\beta$ 1 (Sigma-Aldrich) and 12.5  $\mu$ g/ml poly-Lysine (Sigma-Aldrich) very gently to not detach the cells nodules and changing medium every 3-4 days (Sun et al. 2003).

Pellet cultures were used for functional study in chondrogenesis. Briefly,  $2.5 \times 10^5$  BMSCs were placed in a 15 ml polypropylene tube (Corning Costar) and centrifuged. The resulting pellets were cultured at 37°C with 5% CO<sub>2</sub> in 500 µl of chondrogenic media that contained 10 ng/ml TGF-β1,  $10^{-7}$  M dexamethasone, 50 µg/ml ascorbate-2-phosphate, 100 µg/ml sodium pyruvate and 1X ITS+1 (Sigma-Aldrich). The medium was replaced every 3–4 days for 21 days (Mackay et al. 1998).

### **4.10.3 Adipogenic differentiation**

Cells were allowed to grow to 90-95% confluence and then cultured for 2 weeks in  $\alpha$ -MEM supplemented with 10% FBS, 10% Horse Serum (Gibco Invitrogen), 2 mM L-Glutamine, 10 U/ml penicillin-10 µg/ml streptomycin,  $10^{-6}$  M dexamethasone, 5 µg/ml insulin, 0.5 µM 3-Isobutyl- 1-methylxanthine (IBMX ) and 50 µM indomethacin changing medium every 3-4 days (Digirolamo et al. 1999).

## **4.11 Histochemical analysis**

### **4.11.1 Alkaline Phosphatase (ALP) staining and activity assay**

Cells were washed with PBS and fixed in 10% cold Neutral Formalin Buffer (10% formalin, 0.1 M Na<sub>2</sub>HPO<sub>4</sub>, 0.029 M NaH<sub>2</sub>PO<sub>4</sub>.H<sub>2</sub>O) (Sigma-Aldrich) for 15 min. After being rinsed with distilled water, cells were stained with substrate solution [ $2.4 \times 10^{-4}$  M naphthol AS MX-PO<sub>4</sub> (Sigma-Aldrich), 0.4% N,N Dimethylformamide (Sigma-Aldrich), 1.6 µM red violet LB salt (Sigma-Aldrich) in 0.2 M Tris-HCl pH 8.3 (Carlo Erba Reagenti)] for 45 minutes. Excess staining was removed by washing twice with distilled water and then with 2.5% silver

nitrate (Sigma-Aldrich) for 30 min. The cells were washed again with distilled water and examined.

For the determination of ALP activity, cells were washed twice with Tyrode's balanced salt solution (50 mM Tris-HCl pH 7.4, 0.15 M NaCl) and then incubated with 5mM p-nitrophenol phosphate (Sigma-Aldrich) in 50 mM glycine (Sigma-Aldrich), 1mM MgCl<sub>2</sub> pH 10.5 at 37°C for 5-20 minutes. The reaction was stopped adding 3M NaOH each well. Optical density (OD) was measured at 405 nm (Bruder et al. 1997).

#### **4.11.2 Alizarin Red S staining**

Cells were washed with PBS and fixed in 10% formaldehyde for 1 hour; after rinsing with distilled water, they were incubated with 2% alizarin red s (Sigma-Aldrich) pH 4.1 with gentle shaking for 10 minutes. Excess staining was removed by washing twice with PBS (Digirolamo et al. 1999). Dye was extracted by overnight incubation with 4M guanidine-HCl (Sigma-Aldrich) at room temperature. Absorbance at 490 nm of a ten- fold dilution of the resulting supernatant was used for quantitative mineralization determination.

#### **4.11.3 Von Kossa Staining**

Cells were washed with PBS and fixed in 10% formaldehyde for 1 hour; after rinsing with distilled water, they were incubated with 5% Aqueous Silver Nitrate Solution (Sigma-Aldrich) under UV light for 45 minutes. Excess staining was removed by incubation with 5% Sodium Thiosulfate (Sigma-Aldrich) for 1 minute.

#### **4.11.4 Alcian Blue staining**

Cells were fixed with 4% paraformaldehyde for 15 min at room temperature. After rinsing with PBS, they were stained with 1% alcian blue (Sigma-Aldrich) in 0.1 N HCl pH 1.0 (Carlo Erba Reagenti) overnight. Cells were then dried, washed with 0.1 M HCl for 5 minutes to remove excess staining and washed again with distilled water (Denker et al. 1995).

#### **4.11.5 Oil Red O staining**

Cells were washed with PBS and fixed in 10% formaldehyde for 10 minutes. After rinsing with distilled water, they were stained with 0.5% oil red-o working solution prepared by vigorously mixing 3 parts of a stock solution (0.5% Oil Red-O in isopropanol) (Sigma-Aldrich) with 2 parts of water for 5 minutes and filtering through a 0.4  $\mu$ m filter. Excess staining was removed by washing twice with PBS. Cells were then counterstained with hematoxylin for 3 minutes and then washed with distilled water (Digirolamo et al. 1999). Dye was extracted by isopropanol incubation for 15 min at room temperature. Quantitative assessment was obtained by absorbance of a ten-fold dilution of the extracted dye at 550 nm.

#### **4.12 Reverse Transcription Polymerase Chain Reaction (RT-PCR)**

Total RNA was extracted from mBMSCs cultured in control or inductive media at different time points using TriReagent (Sigma-Aldrich), and then treated with DNase I (Ambion). RT-PCR was performed using M-MuLV Reverse Transcriptase (New England BioLabs) according to the manufacturer's instructions. A twenty five-fold dilution of each sample was PCR amplified using

primers and conditions listed in Table 2. Amplified DNA fragments were separated on a 1% agarose gel containing 0.1  $\mu\text{g}/\mu\text{l}$  ethidium bromide and visualized under UV light.

**Table 2: Specific primers for PCR**

Marker	Forward	Reverse	cycle number	size	Ta	Control
<b>Oct3/4</b>	GCAGGAG CACGAGTG GAAAGCA AC	CAAGGC CTCGAA GCGACA GATG	30	269	65	mES
<b>Sox2</b>	CGAGATA AACATGGC AATCAAAT G	AACGTTT GCCTTAA ACAAGA CCAC	30	232	61	mES
<b>Nanog</b>	ATGAAGTG CAAGCGGT GGCAGAA A	CCTGGTG GAGTCA CAGAGT AGTTC	30	464	60	mES
<b>Rex 1</b>	TGACAAA GGGGACG AAGCAAG AG	GCCATC AAAAGG ACACAC AAAG	30	418	62	mES
<b>Cbfa 1/runx2</b>	CCGCACGA CAACCGCA CCAT	CGCTCCG GCCAC AAATCTC	30	289	60	MC3T3
<b>Osterix</b>	CTGGGGA AAGGAGG CACAAAG AAG	GGGTTA AGGGGA GCAAAG TCAGAT	29	496	60	MC3T3
<b>Collagen I</b>	GAAGTCA GCTGCATA CAC	AGGAAG TCCAGG CTGTCC	30	313	50	MC3T3
<b>Osteopontin</b>	TCACCATT CGGATGA GTCTG	ACTTGTG GCTCTGA TGTTC	30	437	50	Differentiated MC3T3
<b>Bone sialo protein</b>	CAAGCGTC ACTGAAGC AGGTG	CATGCCC CTTGTA TAGCTGT ATT	30	296	60	Differentiated MC3T3
<b>Osteocalcin</b>	TCTGCTCA CTCTGCTG AC	GGAGCT GCTGTG ACATCC	30	388	50	Differentiated MC3T3
<b>PPAR <math>\gamma</math>2</b>	GCTGTTAT GGGTGAA ACTCTG	ATAAGG TGGAGA TGCAGG TTC	30	351	54	Differentiated C3H10T1/2
<b>LPL</b>	GAAGGGA AAGGACTC	ATCAGA AGACAT	30	312	54	Differentiated C3H10T1/2

	AGCAG	CAGGCA GG				
<b>FABP-4/aP2</b>	GGGATTTG GTCACCAT CCG	CCAGCTT GTCACC ATCTCG	30	204	54	Differentiated C3H10T1/2
<b>Adipsin</b>	CTGCTGGA CGAGCAGT GG	GATGAC ACTCGG GTATAG ACGC	30	569	54	Differentiated C3H10T1/2
<b>Sox9</b>	ATCGGTGA ACTGAGCA GCGAC	GCCTGCT GCTTCGA CATCCA	30	199	60	ATDC5
<b>Aggrecan</b>	TGGAGCAT GCTAGAAC CCTCG	GCGACA AGAAGA CACCAT GTG	30	324	60	ATDC5
<b>Collagen XI</b>	GGAAAGA TGGGCTAC CAGGACA	GGACGT CCTGGC AAACCA ATTG	30	412	60	ATDC5
<b>Collagen X</b>	GTGAGGTA CAGCCTAC CAGTTTT	CTTTGTG TGCCTTT CAATCG	30	157	50	ATDC5
<b>Actin</b>	GGTCCGA TGCCCTGA GGCTC	ACTTGCG GTGCAC GATGGA GG	26	370	62	
<b>GAPDH</b>	GTATGACT CCACTCAC GGCAA	CTAAGC AGTTGGT GGTGCA G	26	400	60	
<b>LIF</b>	ACCTGTGC CATACGCC AC	CTTCTGG TCCCGG GTGAT	30	275	57	

#### 4.13 Quantitative Real time PCR

Quantitative real time PCR was performed with QuantiFast SYBR Green RT-PCR (Quiagen) according to the manufacturer in a Corbett machine. Briefly, 0.03 µg of total RNA was converted to cDNA and used as template in a quantitative RT-PCR reaction, following these conditions: 10 min at 50°C (reverse transcription), 5min at 95°C (denaturation step), followed by 35 cycles of PCR (95°C for 10 s, 60°C for 30 sec) by using 5 µl of 2x QuantiFast SYBR Green RT-PCR Master Mix, 1 µM forward primer, 1 µM reverse primer and 0.1µl of QuantiFast RT Mix.

The expression of murine GAPDH was used to normalize gene expression levels.

Primers sequence in Table 3.

**Table 3: Specific primers for Real time-PCR**

Marker	Forward	Reverse
<b>Osteocalcin</b>	GACCTCACAGATGCCAAGC C	TTATTGCCCTCCTGCTTGGA
<b>Nanog</b>	TCAGAAGGGCTCAGCACCA	GCGTTCACCAGATAGCCCTG
<b>Sox 2</b>	CTGCAGTACAACTCCATGAC CAG	GGACTTGACCACAGAGCCCAT
<b>Oct4</b>	AACCTTCAGGAGATATGCA AATCG	AACCTTCAGGAGATATGCAAA TCG
<b>p53</b>	CTCTCCCCCGCAAAGAAA AA	CGGAACATCTCGAAGCGTTTA
<b>pRB</b>	ACAACCCAGCAGTGC GTTAT C	ACCAGGTCATCTTCCATCTGT
<b>CCL5</b>	GCTGCTTTGCCTACCTCTCC	TCGAGTGACAAACACGACTGC
<b>CXCL10</b>	CCAAGTGCTGCCGTCATTTT C	GGCTCGCAGGGATGATTTCAA
<b>GAPDH</b>	GTATGACTCCACTCACGGCA AA	TTCCCATTTCTCGGCCTTG
<b>c-myc</b>	GAGCTCCTCGAGCTGTTTGA A	CATCGTCGTGGCTGTCTGC
<b>TERT</b>	GCACTTTGGTTGCCCAATG	GCACGTTTCTCTCGTTGCG

#### 4.14 Cell transfection

##### 4.14.1 Transfection with lipofectamine 2000

Transfection with Lipofectamine 2000 (Invitrogen) was performed following the producer's guidelines. Initially, cells were plated in 96 well- plates at  $5 \times 10^3$  cells/well and allowed to grow overnight to achieve 70%– 80% confluence. Cells were transfected at different DNA: lipofectamine 2000 ratio ranging from 0.07-1.5  $\mu$ l of lipofectamine 2000 and 0.05-0.4  $\mu$ g of DNA. The reagent/DNA mixture was

added to the OptiMem medium (Invitrogen) and the cells incubated for 6 hours, whereupon they were washed once with PBS and changed to standard medium.

#### **4.14.2 Nucleofection Technology**

Nucleofection of mBMSCs was performed according to the optimized protocols provided by the manufacturer (Amaxa Biosystem). Briefly, cells were gently suspended in 100  $\mu$ l of V Solution (Amaxa Biosystem), mixed with DNA plasmid, and pulsed with program U-23. Immediately after, cells were transferred into pre-warmed fresh medium in six-well plates.

#### **4.14.3 Calcium Phosphate transfection**

Transfection of 293 cell line was performed using Profection mammalian system according to the optimized protocols provided by the manufacturer (Promega). Briefly,  $1.6 \times 10^6$  cells were plated in 60 mm dish and allowed to attach overnight. 10  $\mu$ g of DNA were precipitated with 0.3 M Sodium Acetate pH 5.2 and 2.2 V/V of 100% cold ethanol. The day after, DNA was mixed with 0.25 M  $\text{CaCl}_2$  and then added drop wise to HBS solution in a ratio 1:1. The solution was incubated at room temperature for 30 minutes and then added to the cells. After 6 hours the medium was changed.

#### **4.15 Analysis of Green fluorescent protein (GFP) expression**

Analysis of GFP expression in mBMSCs was performed by fluorescence microscopy and flow cytometry.

For visualization of mBMSCs under fluorescence microscopy, GFP positive cells were observed at 10X original magnification with a Zeiss Axiovert 10 inverted microscope equipped with an epifluorescent condenser HBO 100W/2 (lamp excitation range, 450 to 490 nm); micrographs were recorded with a Nikon Coolpix digital image system.

For flow cytometry, cells were detached from culture flasks by incubation with 0.25% Trypsin-EDTA for 5 minutes, recovered by centrifugation, and washed in flow cytometry buffer consisting of 2% BSA and 0.1% sodium azide (Sigma-Aldrich) in PBS. Non specific fluorescence was determined using mBMSCs transfected with no DNA. Samples were analyzed counting 10,000 events on FACS Canto II (BD Biosciences).

#### **4.16 Cell proliferation assay**

$2.5 \times 10^3$  were seeded in each well of a 96 well-plates and cultured for 2, 4 and 7 days in maintenance media. At nominated time-points, cell number was evaluated using CellTiter-Glo Luminescent Cell Viability Assay (Promega).

To determine the effect of Nanog over-expression on mBMSCs proliferation rate,  $1 \times 10^4$  cells were seeded in each well of a six well-plates in triplicate. Cell number was evaluated by counting cells with a hematology analyzer in triplicate at day 3, 6 and 10 days after seeding.

#### **4.17 Construction of expression plasmids**

Some clonings were done in order to generate pCAGGS-NSNS IRES-GFP WPRE, carrying the chicken  $\beta$  actin (CAG) promoter and Citomegalovirus (CMV) enhancer.

As these promoters did not drive the expression of GFP in mBMSCs, I cloned the CMV promoter in place of CAG promoter.

pCAGGS-NSN was generated from the pCAGG vector (Addgene) by insertion of a polylinker *XbaI/NheI/ScaI/NotI/XhoI*. Briefly 5µg of oligos NSN were annealed and ligated with 50 ng of pCAGGS, previously digested with *XbaI* and *XhoI*. Ligation product was transformed in XI-10 gold *Escherichia Coli* cells (Stratagene) and sequence verified. The resulting vector (pCAGGS-NSN) was further modified by insertion of a polylinker *HindIII/Sall/HindIII*, using the same ligation protocol used in the generation of pCAGGS-NSN. The resulting vector was pCAGGS-NSNS.

pIRES-GFP (Applied Biosystem) was modified by insertion of a polylinker *XhoI/NotI/BamHI* using the same ligation protocol used in the generation of pCAGGS-NSN. The resulting vector was pIRES2-GFP-N.

In order to clone IRES2GFP in pCAGGS-NSNS, pIRES2GFP-N- was digested with *NotI* and the insert was cloned in pCAGGS-NSNS, previously treated with *NotI*. Ligation product was transformed in XI-10 gold *Escherichia Coli* cells and sequence verified. The resulting vector was pCAGGS-NSNS-IRESGFP.

WPRE element was amplified from p#277CCLSIN-S-PPT-hPGK-GFP-pre (a gift from Luigi Naldini's lab) using the Pfx Taq DNA polymerase (Invitrogen) and adopting the following PCR conditions: 2 minutes of initial denaturation at 95°C, 3 cycles of 15 s denaturation at 96°C and 30 s annealing at 56°C, followed by 3 s polymerization at 68°C. The 5' region of all the primers contained sequences (underlined letters) recognized by the restriction enzyme *XhoI*, so that the amplification product contained restriction sites near to both ends. Amplicons were directly cloned into the vector pCAGGS-NSN-IRESGFP treated with *XhoI*.

The cloned inserts were transformed into XL10 gold *Escherichia coli* cells and sequence-verified.

CMV promoter was amplified from pCMVGFP (Addgene) by PCR. The 5' region of forward primer contained a sequence (underlined letters) recognized by the restriction enzyme *SpeI*, whereas the reverse primer contained a sequence (underlined letters) recognized by the restriction enzyme *NheI*, so that the amplification product contained restriction sites near to both ends. Amplicons were directly cloned into the vector pCAGGS-NSN-IRESGFP-WPRE treated with *XhoI*. The cloned inserts were transformed into XL10 gold *Escherichia coli* cells and sequence-verified.

Murine Nanog cDNA was obtained from Geneservice and amplified by PCR. The 5' region of all the primers contained sequences (uppercase letters) recognized by the restriction enzyme *NheI*, so that the amplification product contained restriction sites near to both ends. Amplicons were directly cloned into the vector pCMV-IRESGFP-WPRE treated with *XhoI*. The cloned inserts were transformed into XL10 gold *Escherichia coli* cells and sequence-verified to distinguish between pCMVNanogIRES-GFP-WPRE and pCMVantiNanogIRES-GFP-WPRE. Primers are listed in Table 4.

**Table 4 Primers used in molecular clonings**

Oligo name	Forward	Reverse	Ta (°C)
<b>XbaI/NheI/ ScaI/NotI/ XhoI</b>	CTAgAAATTgCTAgCTAg ATCgATAgTACTCgACTTg CggCCgCAATCTAAC	TCgAgTTagATTgCggCCgC AAgTCgAgTACTATCgATC TAgCTAgcAATTT	
<b>HindIII/Sal I/HindIII</b>	AgCTTCggATAgTCgACAA CgTC	AgCTTgACgTTgTCgACTA TCCTA	
<b>XhoI/NotI/ BamHI</b>	TCgAgCgATCCAgCggCCg CAACTgg	gATCCCAgTTgCggCCgCTg gATCgC	
<b>WPRE</b>	gggCTCGAGATCGACAAT CAACCTCTGGAT	gggCTCGAGCAGGCGGGG AGGCGGCC	63
<b>CMV promoter</b>	gggACTAGTTAGTTATTA ATAGTAATCAATTACG	gggGCTAGCCCGCGGGAT CTGACGGTTCACTAAAC	52
<b>Nanog</b>	ggggCTAgCTACCGCGGGC CCGGGATCCATGAGTG	cccgCTAGCGTCGCGGCC GTCATATTTACCTG	66

#### 4.18 Western blot analysis

Cells were collected by centrifugation and cell pellet was suspended in lysis buffer (1mM EDTA, 50 mM Tris-HCl pH 7.5, 70 mM NaCl, 1% Triton, 50 mM NaF) containing 1X proteinase inhibitors (Roche) and incubated on ice for 30 min. Following centrifugation at 16000 g for 15 min at 4°C, the supernatant containing total cell extract was collected and kept at -80°C. Proteins from cell extracts were quantified using Bradford assay.

10 µg of cell extracts were loaded on a 12% polyacrylamide gel and then electrophoretically transferred onto a Hybond-PVDF membrane (GE Healthcare). The membrane was incubated for 1h at room temperature in blocking buffer (TBS-T containing 8% skim milk) to block non specific protein binding and then incubated at 4°C overnight with the primary antibody rabbit anti murine Nanog (CalbioChem) diluted 1:500 in blocking buffer or mouse anti murine GAPDH (Santacruz) diluted 1:100 in blocking buffer. Following four washes with TBS-T, the membrane was incubated for 1 hour with the HPR-conjugated antibody, goat anti rabbit (Dako) diluted (1:3000) in blocking buffer or sheep anti mouse (Ge

Healthcare) 1:5000. Antibody binding was visualized with an ECL Western blotting detection system (GE Healthcare).

#### **4.19 Migration assay**

BMSCs were suspended ( $5 \times 10^4$  cells per ml) in DMEM without FBS. Two hundred  $\mu\text{l}$  ( $1 \times 10^4$  cells) were added to the migration chamber (8- $\mu\text{m}$  pore size) (BD Bioscience). The lower chamber contained 1 ml of DMEM containing 20% FBS. The plates were incubated at 37°C, 5% CO<sub>2</sub> for 12 hours. After incubation, cells suspended in media in the migration chamber were gently removed by flipping out the medium. The cells adhering to the topside of the membrane were removed by scratching with a cotton applicator.

The migration chamber plate was then stained with 1% Crystal violet (Sigma-Aldrich) and the cells analyzed under an inverted microscope. Cells were counted in at least 12 fields for each chamber plate.

#### **4.20 Soft agar assay**

A549, no DNA, GFP and Nanog transfected BMSCs were suspended at density  $10^5$  cell/ 0.5 ml in a solution 1:1 of DMem 2X (Sigma-Aldrich) supplemented with 20% FBS and 0.6% low melting agarose, in order to obtain a final concentration of 0.3%. The suspension was layered as 0.5 ml each well of 6 well-plates, on 0.5% agarose. The cells were fed twice a week and after two weeks they were stained with 1% crystal violet.

#### **4.21 Statistical analysis**

All the experiments were analyzed using two two-way Student's *t*-Test. *p*-values less than 0.05 were considered statistically significant.

## **RESULTS**

### **Chapter 5**

#### **Establishment of mBMSC long term culture and morphologic characterization**

##### **5.1 Background**

BMSC is a cell type better studied and characterized in humans than in mouse and, although in the last few years numerous protocols have been developed to isolate these cells, some problems still remain (Dobson et al. 1999; Phinney et al. 1999; Baddoo et al. 2003; Meirelles Lda et al. 2003; Sun et al. 2003; Peister et al. 2004; Tropel et al. 2004; Wang et al. 2006). The standard method, widely used for the purification of human BMSCs, based on the adherence to plastic substrate does not allow the isolation of homogeneous populations of mBMSCs. Using alternative methods based on immunodepletion (Baddoo et al. 2003) or centrifugation (Dobson et al. 1999; Short et al. 2001; Peister et al. 2004), different populations of mBMSCs have been isolated; however, they expand poorly, probably because of either the loss of relevant cell-cell contacts or the absence of specific cytokines necessary in the early phases of expansion. Moreover, no data are available concerning an exhaustive characterization of the stemness, differentiation potential and acquisition of transformed phenotype of the isolated cells during passages.

Starting from the observation that use of bone fragment-conditioned medium favours BMSCs growth (Sun et al. 2003), I hypothesized that specific conditioned media, obtained from different microenvironments, may contribute to the self-renewal of BMSCs and could be critical in the early phases of mBMSCs

expansion. Therefore I analyzed the effect of supernatants from culture of bone fragments, mouse marrow stroma cell line MS-5, mouse embryonic fibroblast cell line NIH3T3 and a cocktail of epidermal growth factor (EGF) and platelet-derived growth factor (PDGF) on mBMSC expansion.

## **5.2 Isolation of mBMSCs from adult mouse bone marrow**

In this study nine animals have been sacrificed to isolate mBMSCs from bone marrow of tibias and femurs. Different factors resulted to be very important in order to allow the isolation of a homogeneous population of mBMSC without haematopoietic or macrophage contaminants and, as a result, for the establishment of a long term culture.

By the surgical procedure used, the total number of collected marrow nucleated cells was  $1.36 \times 10^7 \pm 3.2 \times 10^6$  per femur and  $8.10 \times 10^6 \pm 1.17 \times 10^6$  per tibia; these results are comparable to StemCell Technology procedure, whose expected cell recovery was  $1 - 2 \times 10^7$  per femur and  $6 \times 10^6$  per tibia.

One of the most important factors to determine the establishment of a long term culture of mBMSC was the density of the starting culture. As mentioned in Chapter 4, section 4.2.1, mBMSCs were seeded at  $2 \times 10^6$  nucleated cells/cm<sup>2</sup> and then allowed to attach to the surface of the plates for three days at which time I removed the non-adherent cells and waited for a sub confluent culture; the cultures underwent an initial lag phase of about 10-17 days during which the colonies were seen to arise from single cells and then they became confluent (Figure 11).

Starting from the observation of published data on mBMSCs (Dobson et al. 1999; Phinney et al. 1999; Baddoo et al. 2003; Meirelles Lda et al. 2003; Sun et al. 2003; Peister et al. 2004; Tropel et al. 2004; Wang et al. 2006), I considered the

composition of the medium used for the isolation and expansion of BMSCs, determining to obtain a long- term culture. For this reason I decided to split our culture in four conditions:

- EP mBMSC: treated for 2 weeks with complete medium supplemented with 20% bone fragments conditioned medium and then with complete medium supplemented with 20 ng/ml mEGF and 20 ng/ml hPDGF BB (Colter et al. 2001; Tropel et al. 2004; Kratchmarova et al. 2005; Figure 11, panel C).
- BF mBMSC: treated for 2 weeks with complete medium supplemented with 20% bone fragments conditioned medium and then with complete medium without this (Sun et al. 2003; Figure 11, panel D).
- M mBMSC: treated with complete medium supplemented with 20% MS5 conditioned medium (Issaad et al. 1993; Figure 11, panel E).
- N mBMSC: treated with complete medium supplemented with 20% NIH3T3 conditioned medium (Burroughs et al. 1994; Figure 11, panel F).

In the conditions described above, initially, the cells were very heterogeneous presenting round, flattened and spindle-shaped cells. The round non adherent cells, the haematopoietic cells, were lost during medium changes; the round adherent cells, which seemed to be macrophage or granulocytic precursors, adhered very strongly to the plate and were not detached easily from the plate, for this reason these cells were lost during the passages (Figure 11).

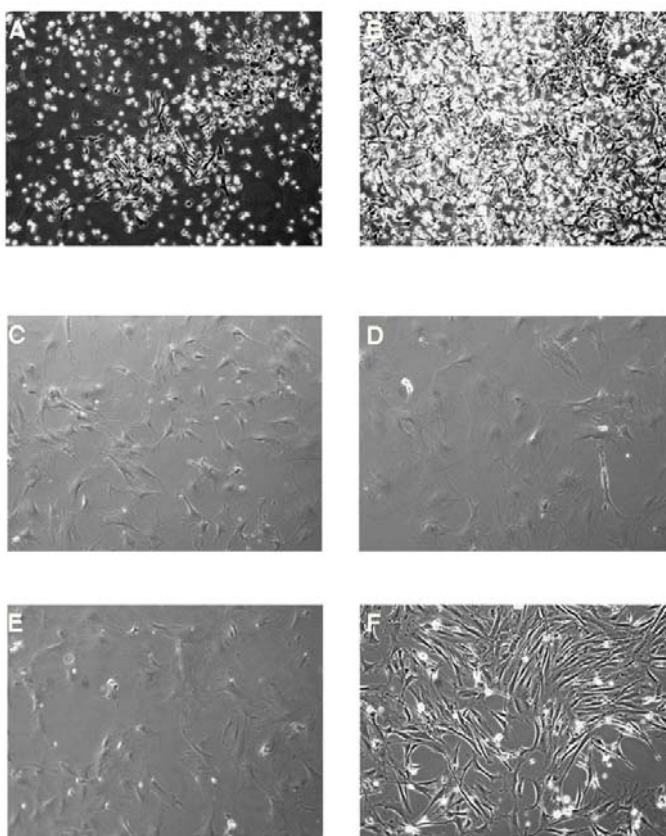


**Figure 11 Morphology of mBMSCs varies according to culture conditions**

*Morphology of BMSCs 72 hours after plating (panel A) and after 10-17 days of culture (panel B). Cells were subdivided and cultured respectively in: complete medium with 20% bone marrow-conditioned medium and, subsequently, in complete medium with 20 ng/ml mEGF and 20 ng/ml PDGF-AA (mBMSC EP, panel C); complete medium with 20% bone marrow conditioned medium (mBMSC BF, panel D); complete medium with 20% MS5 conditioned medium (mBMSC M, panel E) and complete medium with 20% NIH3T3 conditioned medium (mBMSC N, panel F). Magnifications 10X.*

### 5.3 Immunophenotypical characterization

In order to characterize the types of cells present in the different culture conditions, I analyzed a panel of surface antigens by flow cytometry. To avoid the presence of macrophage/granulocytic contamination and to allow the cells to stabilize under the different culture conditions, I analyzed the mBMSCs subpopulations after 10 passages. We observed that mBMSCs in different culture conditions exhibited different morphological features (forward scatter x side scatter) and immunophenotype (Table 5 and Figure 12), however, in all cases the

immunophenotype showed a markers profile strictly compatible with BMSCs (Lai et al. 1998; Deans et al. 2000), without the expression of any haematopoietic cell markers, such as CD45, CD34, CD5, and CD19.

BMSCs from all conditions were positive to Sca I, the hallmark of haematopoietic and mesenchymal progenitor cells (Holmes et al. 2007), and to CD44 which bridges cells to hyaluronan and osteopontin and is involved in niche maintenance (Avigdor et al. 2004). In particular, the EP mBMSCs presented a subset of cells highly positive to CD13, whereas BF and M mBMSCs were negative to H-2k<sup>b</sup>, the major histocompatibility complex of class I, so suggesting a typical feature of very early progenitors known as mMAPC (Jiang et al. 2002).

**Table 5 Variations in culture conditions allow selection of different mesenchymal progenitors.**

Antigen	EP mBMSC	BF mBMSC	M mBMSC	N mBMSC
CD 45	-	-	-	-
CD 34	-	-	-	-
CD 5	-	-	-	-
CD19	-	-	-	-
CD 117 (c-kit)	+	-	-	+
Sca-I	++	+	+	+
CD 44	+++	++	++	+++
CD 13	+	-	+	+
H2-k <sup>b</sup>	+	-	-	+

- indicates that mBMSC type does not express the specific antigen. +, ++ and +++ indicate, a partial overlapping, no overlapping and a big difference between the plot of isotype control and the plot of staining profile, respectively.

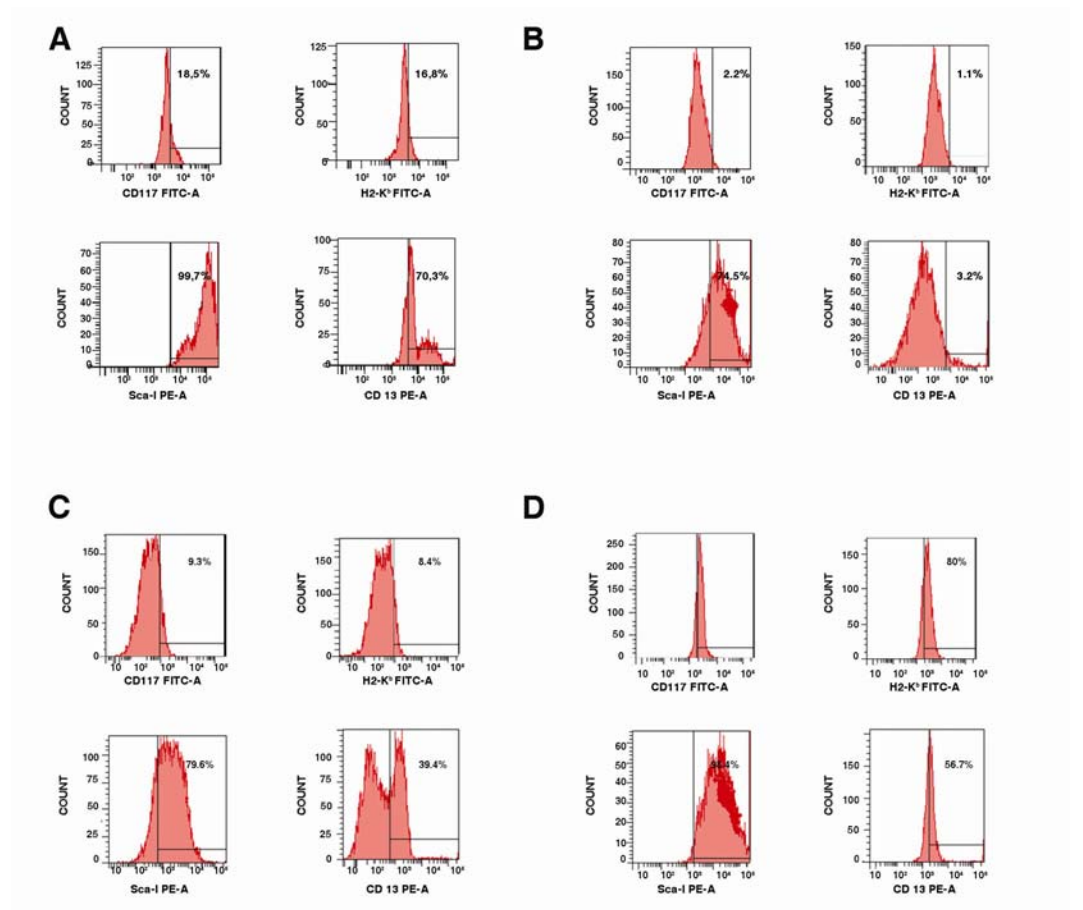


**Figure 12 FACS analysis of mBMSC populations**

Plot shows specific antibody staining profile for CD117, H2-k<sup>b</sup>, ScaI and CD13 (filled histograms). The lines in horizontal and vertical positions indicate the boundaries between isotype control and the specific staining profile (EP, BF, M and N BMSCs panel A, B, C and D, respectively).

### 5.4 Growth kinetic of mBMSCs during 30 passages

I cultured all four BMSC subpopulations for more than 30 passages determining the population doubling potential, progression to senescence and proliferative activity. In order to exclude the acquisition of a tumorigenic potential I analyzed the DNA content of our subcultures, the expression of telomerase and the ability to form tumor in mice under local injection.

### 5.4.1 Cumulative duplication number and doubling measurement

Cumulative population doublings were calculated from the initial number of mBMSCs at the first passage and the number of mBMSCs harvested at each of the following passage (Figure 13). This procedure provides a theoretical growth curve that is directly proportional to the cell number. At the last analyzed passage, the mean cumulative population doublings were 83 for the EP group, 109 for BF, 70 for M and 90 for N, suggesting that progenitors selected in the different conditions have different doublings times. I calculated doubling times and reported in Chapter 4 section 4.4. As expected, small differences were found in their doubling time, which was 58 hours for the EP group, 40 for BF, 57 for M and 44 for N.

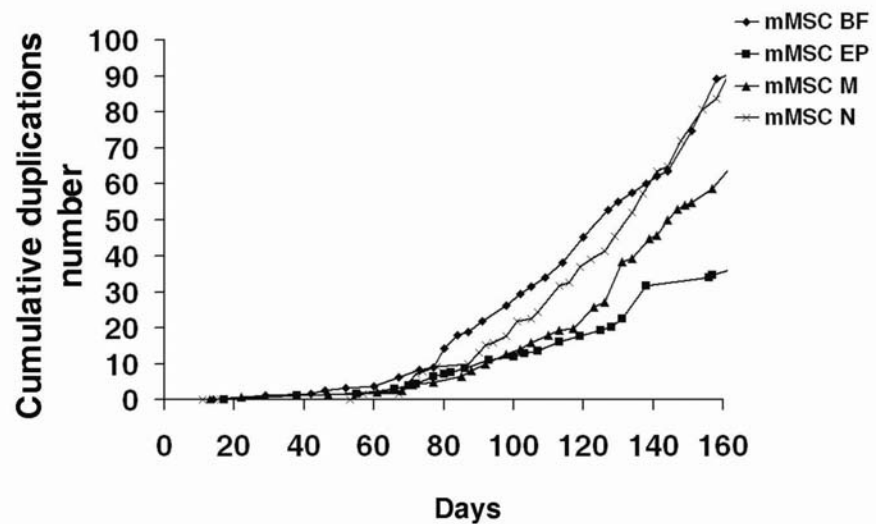


**Figure 13** Growth kinetic of mBMSCs

Cumulative population doublings were calculated from the initial number of mBMSCs at the first detachment from plastic tissue culture and the number of mBMSCs harvested at following passage, as reported in Chapter 4, section 4.4. Different culture conditions are indicated as follows: EP ■, BF ◇, M ▲, N \* mBMSCs.

### **5.4.2 Cell cycle analysis**

I confirmed the growth kinetic data, analyzing the cell cycle (Figure 14). As reported in Chapter 4, section 4.5, cells were detached from the culture dish, fixed, stained for DNA with Propidium Iodide (PI), and analyzed by flow cytometry. All the subcultures were euploid after 10-15 passages, as demonstrated by the same PI intensity among the lymphocytes and the mBMSCs.

A small difference in the percentage of cells in G1, S or G2 phase, was shown according to the differences in doubling time (panel F).

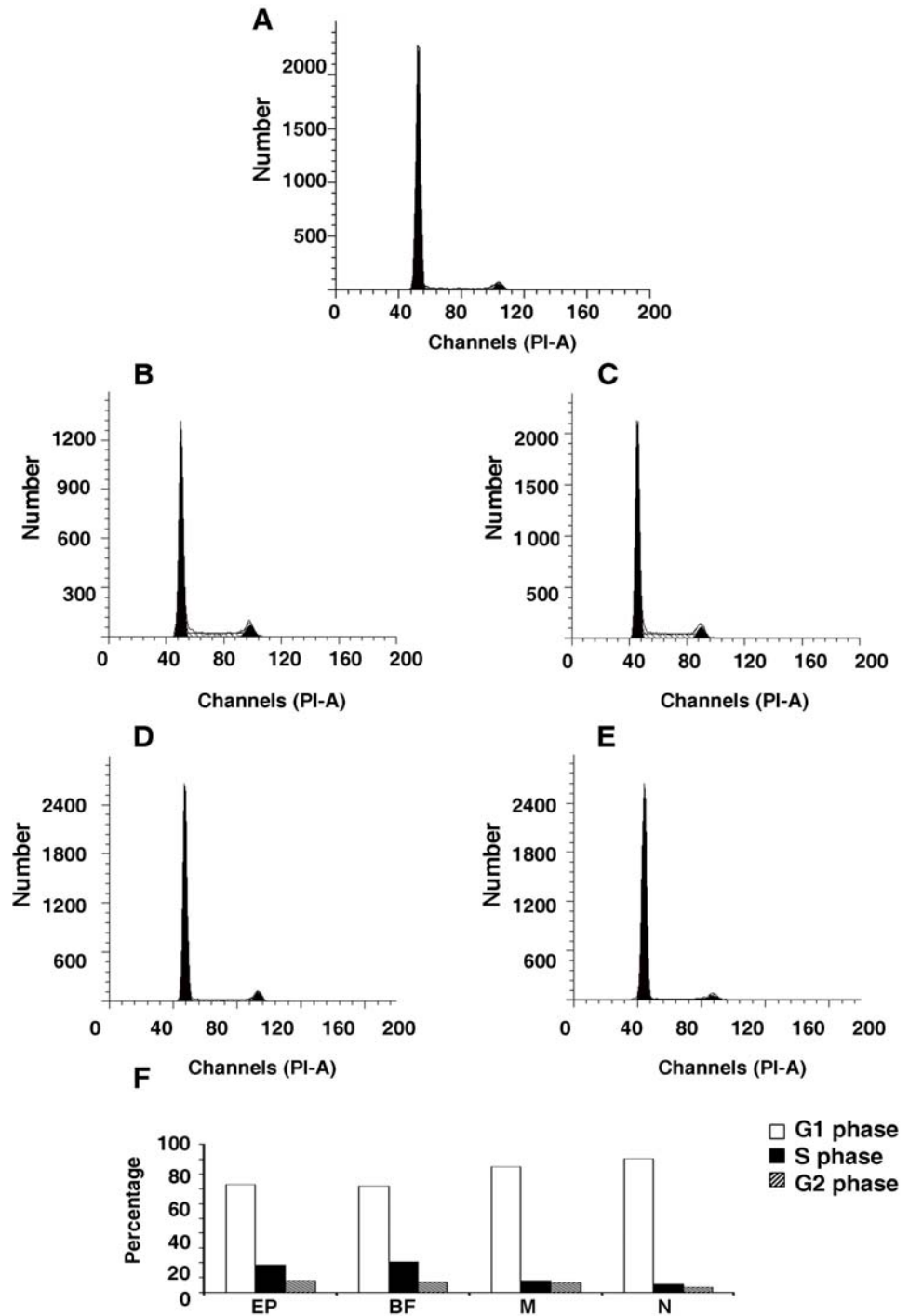


**Figure 14** Cell cycle analysis of mBMSCs

Histograms show DNA content of lymphocytes (panel A), EP (panel B), BF (panel C), M (panel D) and N (panel E) mBMSCs (y-axis, cell count; x-axis, PI intensity). The percentage of cells in G1, S and G2 phase are summarized in panel F.

### 5.4.3 Senescence Associated Beta Galactosidase expression

Senescent cells induce cell growth arrest in the G1 phase and usually this is accompanied in a change in morphology and metabolism. Such an example the cellular enlargement and the expression of senescence associated beta galactosidase (SA-  $\beta$ - Gal) represent two of the most common features of senescent cells (Dimri et al. 1995; Sethe et al. 2006) (Figure 15).

I did not observe any particular changes in cellular morphology during the *in vitro* culture, so, to follow up the appearance of senescence, the cultures were assayed for SA-  $\beta$ - Galactosidase expression.

Number of SA- $\beta$ -Gal positive mBMSCs did not increase during the passages indicating that mBMSCs did not show signs of cellular senescence during *in vitro* culture (Figure 15). These data were very surprising as an increase in the number of senescent cells, assessed by SA-  $\beta$ - Gal staining was reported for human (Ito et al. 2007; Shibata et al. 2007; Ryu et al. 2008; Wagner et al. 2008) and rat BMSCs (Galderisi et al. 2008). As the cellular senescence is one the tumor suppressor functions of normal cells (Sharpless et al. 2007), to further investigate the characteristics of these subcultures and exclude the acquisition of a tumorigenic potential, I analyzed their DNA content, the expression of telomerase and the ability to form tumor in mice under local injection after 30 passages in culture.

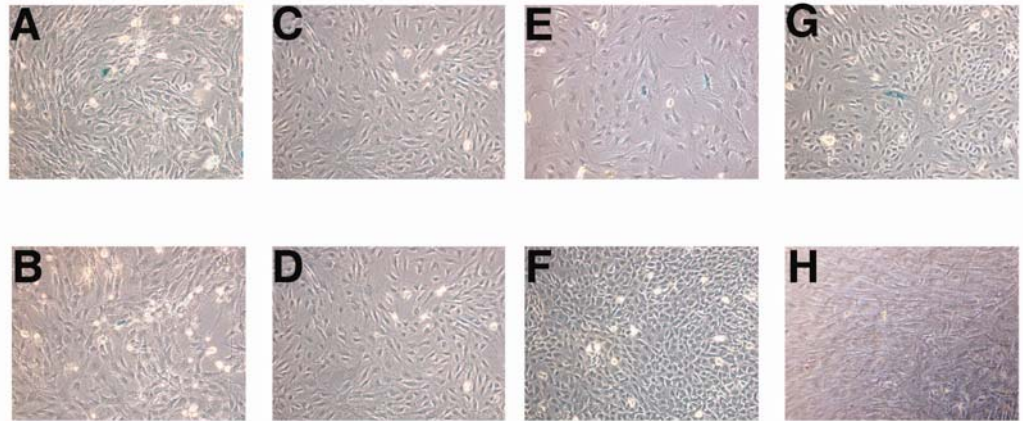


**Figure 15 Senescence Associated Beta Galactosidase (SA-B-Gal) expression in mBMSCs**

*SA- Beta-Gal staining in mBMSC at early passages (EP, BF, M and N mBMSCs panel A, C, E and G respectively) and late passages (EP, BF, M and N panel B, D, F and H respectively. Original magnification 10X).*

#### 5.4.4 Cell cycle analysis at late passages

I repeated the cell cycle and DNA content analysis after 35-40 passages. As reported in Figure 16 and Figure 17, a slight increase in the number of cells in G1 phase and a decrease in S phase were observed for EP and BF mBMSCs. This result confirmed that, in spite of the lack in the increase of SA-  $\beta$ - Gal cells, these cells slow down the progression in the cell cycle over a period of 35-40 passages.

Different results were obtained for M and N BMSCs.

No differences in terms of cells in G1, S or G2 phase were observed between early (10-15) and late (35-40) passages in N BMSCs, suggesting that the NIH3T3 conditioned medium could contain cytokines involved in the suppression of cellular senescence and maintenance. The results obtained for EP, NF and N BMSCs confirm the maintenance of a euploid karyotype over a period of 30 passages.

I observed an aneuploid karyotype in M BMSCs at late passages. As shown in Figure 16, after 35-40 passages this population is made up of two different sub-populations. One of this has a G1 peak, which has the same PI intensity of lymphocytes, confirming the euploid content of DNA of this sub-populations; the other one has a double PI intensity compared to lymphocytes, suggesting a double content of DNA.

Chromosomal alterations in BMSCs are very often associated with the activation of telomerase activity *in vitro* (Serakinci et al. 2004; Rubio et al. 2005; Miura et al. 2006; Rubio et al. 2008) and tumorigenic potential *in vivo* (Serakinci et al. 2004; Rubio et al. 2005; Miura et al. 2006; Zhou et al. 2006; Rubio et al. 2008). For these reasons I analyzed mBMSCs for the expression of telomerase and the ability to form tumor *in vivo*.

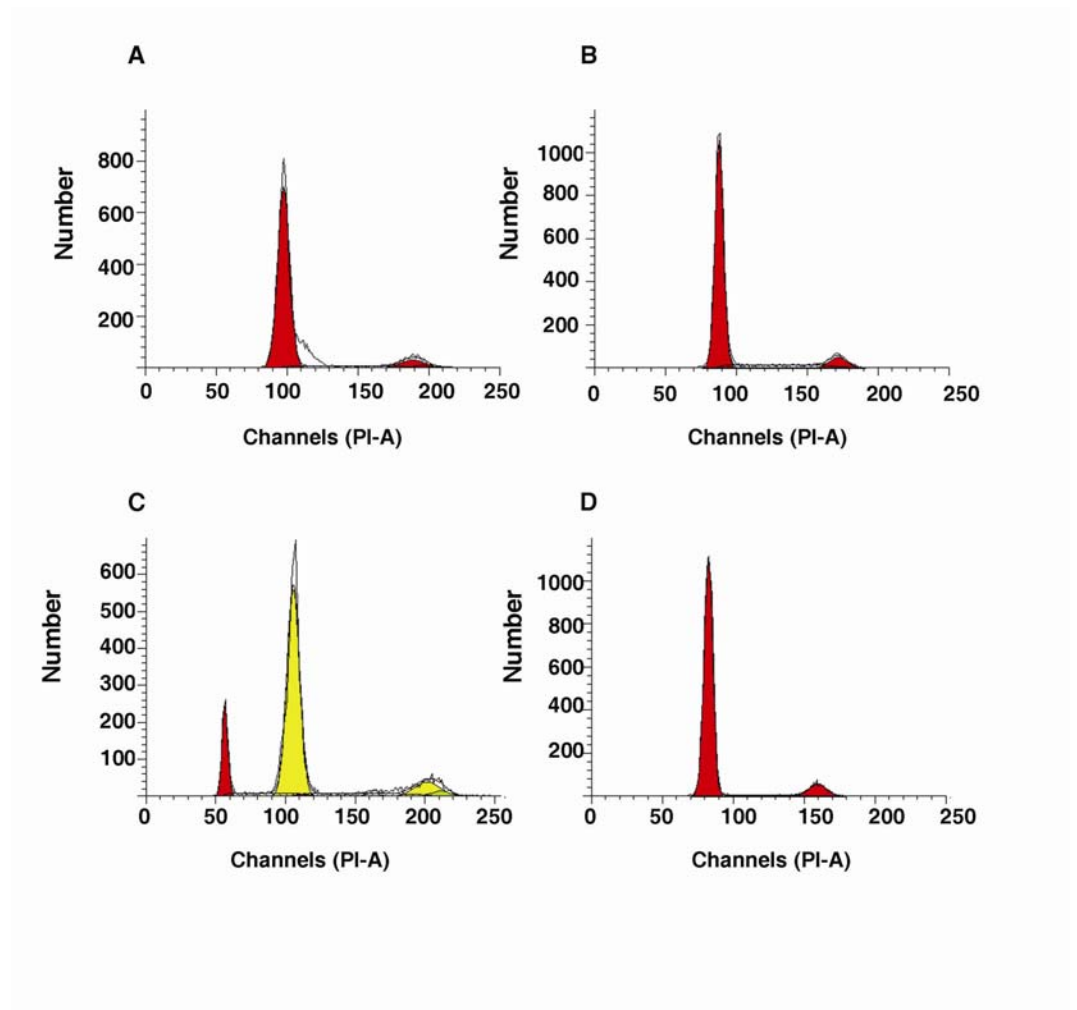


**Figure 16** Cell cycle analysis of mBMSCs after 30 passages in vitro

Histograms show DNA content of EP (panel A), BF (panel B), M (panel C) and N (panel D) mBMSCs (y-axis, cell count; x-axis, PI intensity).

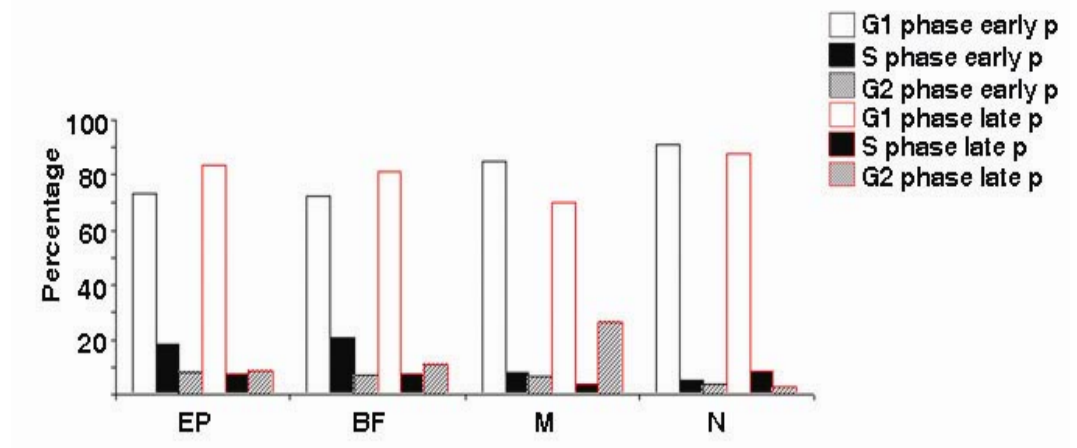


**Figure 17** Cell cycle comparison between mBMSCs at early and late passages

Summary of the percentage of cells in G1, S and G2 phase after early and late passages.

### 5.4.5 Assessment of telomerase activity

In order to verify whether cells growing under these experimental conditions possessed telomerase activity, I measured telomerase activity by a primer extension assay in which telomerase reverse transcriptase (TERT) synthesizes telomeric repeats onto oligonucleotide primers (TRAP assay; Kim et al. 1994; Colter et al. 2000). TRAP products were analyzed on a 12% native polyacrylamide gel electrophoresis (PAGE), and then by ELISA according to manufacturer's instructions (see Chapter 4, section 4.7; Figure 18). As reported in Figure 18 panel A, I did not observe 6-bp periodicity, as in the two positive controls +1 and +2, suggesting that these subcultures did not possess telomerase activity, even at late passages. PCR products were also analyzed by ELISA, confirming the same results (panel B). These findings confirmed that EP, BF and N BMSC subcultures, even without showing dramatic changes in proliferative activity or cellular metabolism, do not activate telomerase expression *in vitro*. The absence of expression of telomerase led me to hypothesize that chromosomal alterations observed in M BMSCs were not transforming events. In order to exclude that these subpopulations contained transformed cells I tested their tumorigenicity *in vivo*.

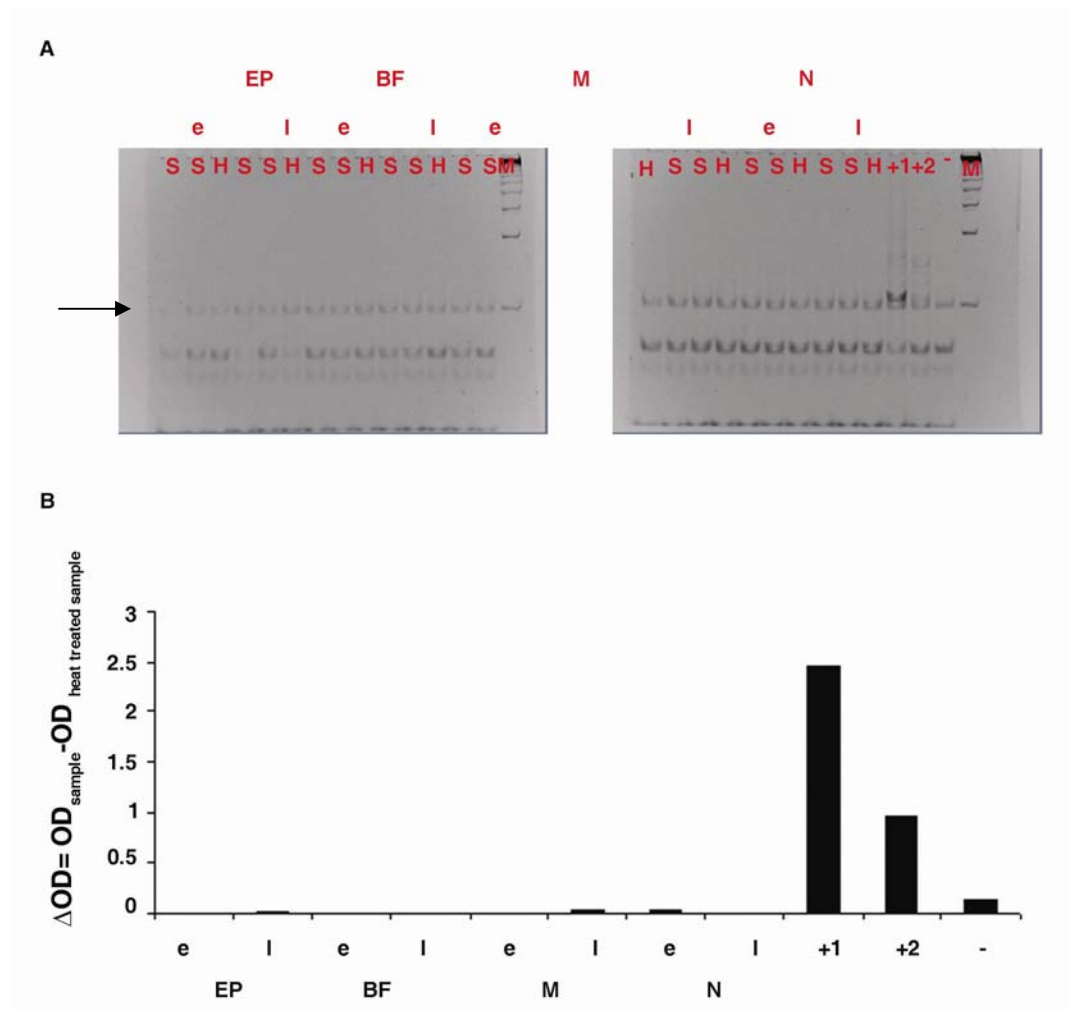


**Figure 18** Telomerase activity assessment in mBMSCs

Polyacrylamide gel electrophoresis of TRAP assay products obtained from mBMSCs at early and late passages (panel A). *e*: early passages BMSCs. *l*: late passages BMSCs. *S*: test extract. *H*: heat-treated test extract. +1: telomerase-positive control, cell extract provided by the Chemicon kit. +2: PCR/ELISA positive control, a synthetic oligonucleotide with 8 telomeric repeats that works as a template of the PCR reaction. -: minus telomerase control, CHAPS lysis buffer. *M*: DNA ladder. Black arrow: TRAP internal control (panel A). ELISA analysis of TRAP products (panel B).

### 5.4.6 Tumorigenicity *in vivo*

I tested *in vivo* tumorigenicity, by subcutaneous injection of  $2 \times 10^6$  mBMSCs in immunodeficient mice. I did not observe any tumor formation, as determined by macroscopic and histological analysis 10 weeks after inoculum ( $n=5$ ; Figure 19), confirming that these sub-populations were essentially free of tumorigenic cells. As a positive for tumor formation control, five mice received at the same site mES

cells ( $2 \times 10^6$  cells/ site). All animals inoculated with mES cells developed large tumors ( $1.28 \pm 0.49$  cm in diameter) at the injected sites within 3-4 weeks (Figure 20).

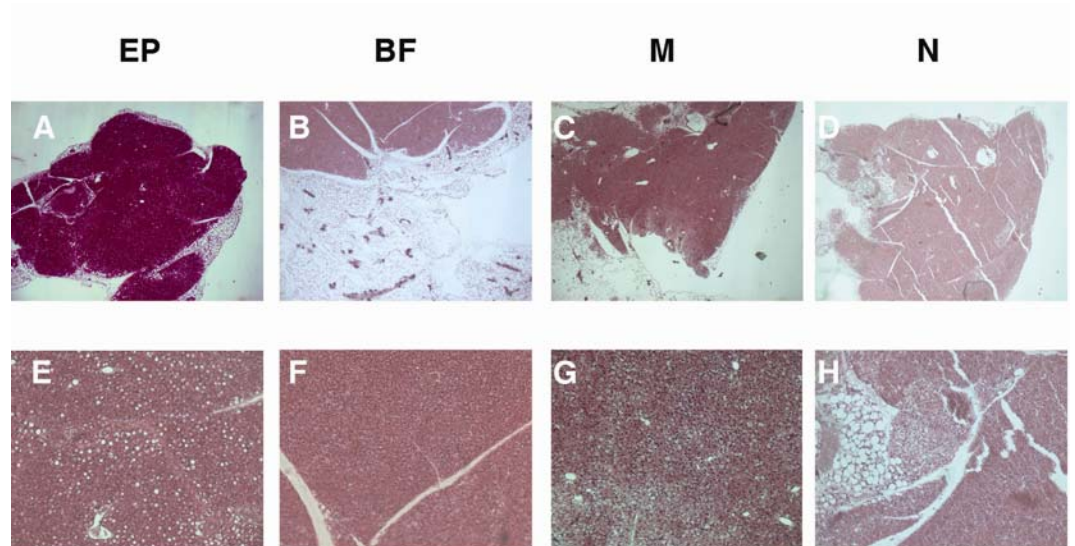


**Figure 19** mBMSCs do not transform in tumorigenic cells

*mBMSCs at 35p showed no tumor formation when transplanted into immunocompromised mice (EP mBMSCs panel A and E, BF mBMSCs panel B and F, M mBMSCs panel C and G, N mBMSCs panel D and H; magnification 2.5X for panel A-D, 10X for panel E-H; hematoxylin and eosin staining).*



**Figure 20** Teratocarcinoma development in mice injected with mES cells

*Mice inoculated with mES cells developed large tumors at the injected sites within 3-4 weeks.*

## 5.5 Stemness expression in mBMSCs

I evaluated whether transcription factors essential for pluripotency and self-renewal in murine embryonic stem (mES) cells, such as Oct 4, Nanog, Sox-2 and Rex-1, were present in mBMSCs and could account for the differences in proliferative ability observed (Boiani et al. 2005).

As mBMSCs are able to spontaneously differentiate along mesenchymal lineages, I analyzed the expression of transcription factors in cells kept in control medium for one and twenty one day. Among the above-mentioned transcription factors only Nanog was expressed in the sub-cultures, as evidenced by RT-PCR, at time 0 and after 21 days of culture in EP mBMSCs, and at time 0 in BF, M and N mBMSCs (Figure 21). Immunofluorescence data confirmed the localization of Nanog in the nucleus of mBMSCs EP ( $71.8\% \pm 16.6\%$ ), BF ( $61\% \pm 20\%$ ), M ( $48.4\% \pm 19.2\%$ ) and N ( $47.9\% \pm 17.5\%$ ) as shown in Figure 22. *t*-Test analysis showed that the differences in percentage of Nanog expressing cells among EP and M BMSCs or EP and N BMSCs are statistically significant (Table 6). Since Nanog is a stemness marker for mES cells and its expression is usually lost as soon as the cells begins to differentiate and lose self-renewal potential (Chambers et al. 2003; Mitsui et al. 2003), I determined its expression also in mBMSCs at high passage number. After 30-40 passages the percentage of Nanog positive cells was reduced for mBMSCs EP ( $71.8\% \pm 16.6\%$  to  $31\% \pm 19.1\%$ ), mBMSCs BF ( $61\% \pm 20\%$  to  $24\% \pm 20\%$ ) and M ( $48.4\% \pm 19.2\%$  to  $28.3\% \pm 22.7\%$ ). On the contrary, the reduction of percentage of Nanog-positive cells was not significant for mBMSCs N ( $47.9\% \pm 17.5\%$  to  $42.6\% \pm 11\%$ ) (Figure 22, panel B). *t*-Test analysis suggests that the differences in Nanog expressing cells, among the four culture conditions used, are significant only in the early phases of expansion and that this percentage reaches the same value after many passages (Table 6).

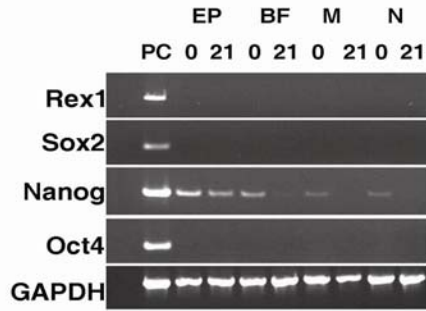


**Figure 21** Stemness factors expression in BMSCs

Expression of stemness markers was analyzed by RT-PCR immediately after cell purification (0) and after 21 days in the different culture conditions. GAPDH as shown as control of RNA quality. PC: positive control, RNA extracted from mES cells.

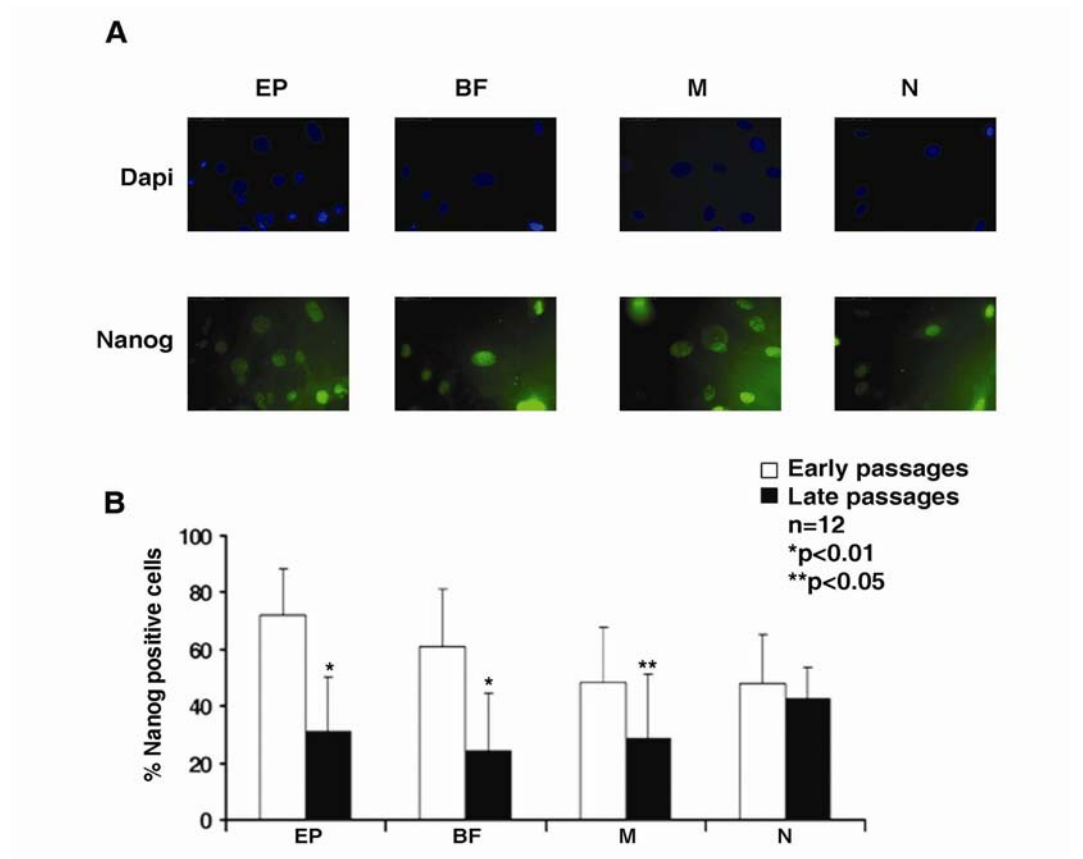


**Figure 22** mBMSCs express Nanog

Expression of Nanog was confirmed in all the subpopulations by immunostaining with an anti-Nanog antibody conjugated with FITC counterstained with DAPI (panel A, magnification 63X). Quantization of the percentage of Nanog positive cells in the different subpopulations at early and late passages (panel B).

**Table 6: Percentage of Nanog expressing BMSCs, *t*-Test result**

<b>Matrix</b>	<b>t-Test result</b>
e.p. EP BMSCs vs e.p. BF BMSCs	p> 0.05
e.p. EP BMSCs vs e.p. M BMSCs	p< 0.005
e.p. EP BMSCs vs e.p. N BMSCs	p< 0.005
e.p. BF BMSCs vs e.p. M BMSCs	p> 0.05
e.p. BF BMSCs vs e.p. N BMSCs	p> 0.05
e.p. M BMSCs vs e.p. N BMSCs	p> 0.05
l.p. EP BMSCs vs l.p. BF BMSCs	p> 0.05
l.p. EP BMSCs vs l.p. M BMSCs	p> 0.05
l.p. EP BMSCs vs l.p. N BMSCs	p> 0.05
l.p. BF BMSCs vs l.p. M BMSCs	p> 0.05
l.p. BF BMSCs vs l.p. N BMSCs	p< 0.05
l.p. M BMSCs vs l.p. N BMSCs	p> 0.05

*e.p.*: early passages; *l.p.*: late passages; *vs*: versus

## 5.6 Differentiation abilities of BMSCs

In order to evaluate whether culture conditions could select subpopulations different not only in the immunophenotype and proliferation ability but also in differentiation potency, I performed osteogenic, chondrogenic and adipogenic differentiation assays.

### 5.6.1 Osteogenesis

mBMSCs were incubated to confluence in their medium and then transferred to osteogenic medium for time indicated as described in Chapter 4, section 4.10.1. In the first time I analyzed alkaline phosphatase (ALP) as an osteoblastic differentiation marker. After 6 days of osteogenic induction, 80% of EP, M and

BF mBMSCs underwent a dramatic change in cellular morphology and were alkaline phosphatase (ALP)-positive (Figure 23). Control cultures in regular growth media expressed a variable and significant background level of ALP-positive staining (Table 7), in agreement with previously described results both in human (Jaiswal et al. 1997) and in murine BMSCs (Fromigue et al. 2008). ALP activity of differentiated cells increased during the first week of induction for EP, BF and M mBMSCs reaching a plateau phase, a phenomenon correlated with the increased extensive mineralization occurred throughout the differentiated cultures (Jaiswal et al. 1997). By contrast, the ALP activity of differentiated N mBMSCs increased during the time, but it did not reach the level of the other subpopulations, suggesting a delay or impairment in osteogenic differentiation (Figure 23).

In order to evaluate the ability of our mesenchymal progenitors to reach osteoblastic terminal differentiation, I analyzed the calcium deposition in the extra cellular matrix after 21 days of differentiation. In the EP, BF, M and N mBMSCs grown in control medium I did not observe detectable calcium deposits throughout all the experiment, as measured by Alizarin Red S staining. By contrast, in BMSCs grown with osteogenic medium I observed a mineralized matrix at day 21 (Figure 24). Alizarin Red S staining confirmed a difference in the osteogenic ability of EP, BF and M compared to N BMSCs. EP, BF and M BMSCs, produce a well mineralized matrix which is distributed uniformly throughout the culture dish. As expected, the mineralization pattern of N mBMSCs was localized to few discrete foci, probably correlated with focal areas of high ALP activity, rather than throughout the culture dish. These data were corroborated by the quantification of mineralization deposits by extraction of bound Alizarin Red S, as reported in Chapter 4, section 4.10.1 (Figure 24, panel

B). These data confirmed a significative difference between calcium content of mBMSC grown in control medium and in differentiation medium.

These results were also corroborated by Von Kossa staining (Figure 25).

To confirm the differentiation status of our subcultures, I analyzed expression of osteoblast-specific markers before and after treatment with the inductive medium by RT-PCR. The results confirmed that the mBMSCs constitutively express some osteoblastic lineage markers, such as Cbfa1/Runx2, Collagen I and osteopontin, as previously described (Tropel et al. 2004). In particular, after osteoinduction EP, BF and M mBMSCs begin to express the well known transcription factor osterix, essential to osteogenic commitment of mBMSCs as well as late osteogenic markers, namely bone sialoprotein and osteocalcin, typically expressed in osteoblasts (Figure 26) (Karsenty et al. 2002). As N mBMSCs do not express bone sialoprotein, even in differentiation medium, I concluded that they are not able to fully differentiate in osteoblasts retaining a pre-osteoblastic-status.

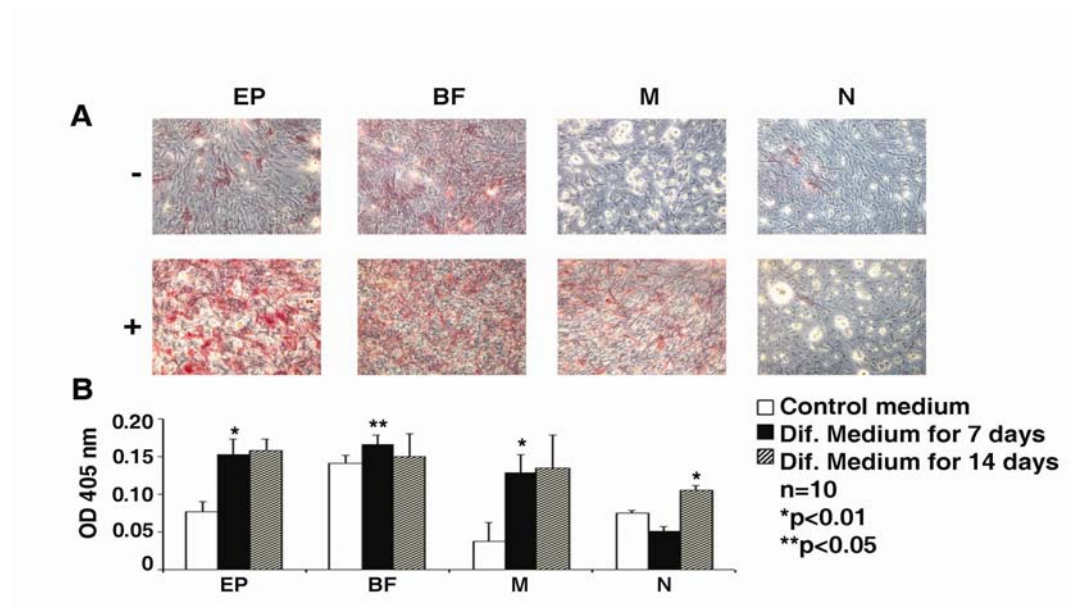


**Figure 23 Osteogenic differentiation of mBMSCs. ALP expression**

ALP staining six days after osteogenic induction (panel A, magnification 10X). ALP activity was determined for each subculture after 7 and 14 days in osteogenic medium (panel B).

**Table 7: Level of ALP activity of BMSCs, ANOVA result**

<b>Matrix</b>	<b>ANOVA result</b>
Control EP BMSCs vs control BF BMSCs	p< 0.001
Diff. 7 days EP BMSCs vs Diff. 7 days BF BMSCs	p> 0.05
Diff. 14 days EP BMSCs vs Diff. 14 days BF BMSCs	p> 0.05
Control EP BMSCs vs control M BMSCs	p< 0.05
Diff. 7 days EP BMSCs vs Diff. 7 days M BMSCs	p> 0.05
Diff. 14 days EP BMSCs vs Diff. 14 days M BMSCs	p> 0.05
Control EP BMSCs vs control N BMSCs	p> 0.05
Diff. 7 days EP BMSCs vs Diff. 7 days N BMSCs	p< 0.001
Diff. 14 days EP BMSCs vs Diff. 14 days N BMSCs	p< 0.01
Control BF BMSCs vs control M BMSCs	p< 0.001
Diff. 7 days BF BMSCs vs Diff. 7 days M BMSCs	p> 0.05
Diff. 14 days BF BMSCs vs Diff. 14 days M BMSCs	p> 0.05
Control BF BMSCs vs control N BMSCs	p< 0.001
Diff. 7 days BF BMSCs vs Diff. 7 days N BMSCs	p< 0.001
Diff. 14 days BF BMSCs vs Diff. 14 days N BMSCs	p< 0.01
Control M BMSCs vs control N BMSCs	p> 0.05
Diff. 7 days M BMSCs vs Diff. 7 days N BMSCs	p< 0.001
Diff. 14 days M BMSCs vs Diff. 14 days N BMSCs	p> 0.05

*Diff. 7 days: Cells kept in osteogenic medium for 7 days*

*Diff. 14 days: Cells kept in osteogenic medium for 14 days*

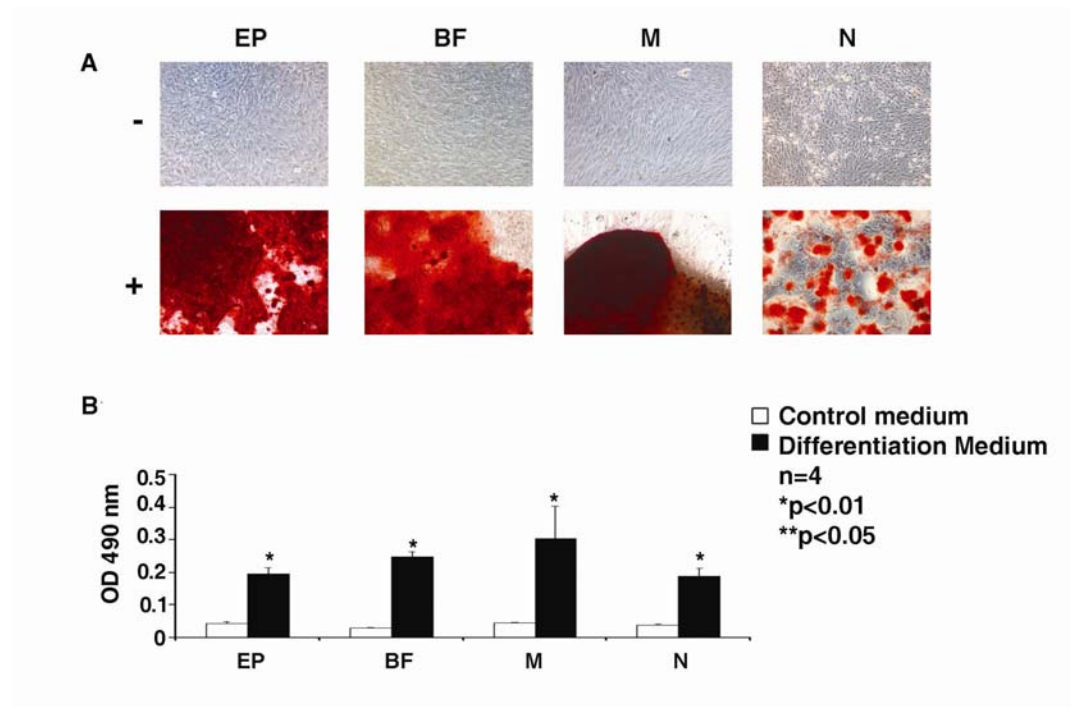


**Figure 24** Osteogenic differentiation of mBMSCs. Bone nodule formation

Alizarin red staining 21 days after induction (panel A, magnification 10X). Calcium deposition was quantified as described in Chapter 4, section 4.11.2 (panel B).

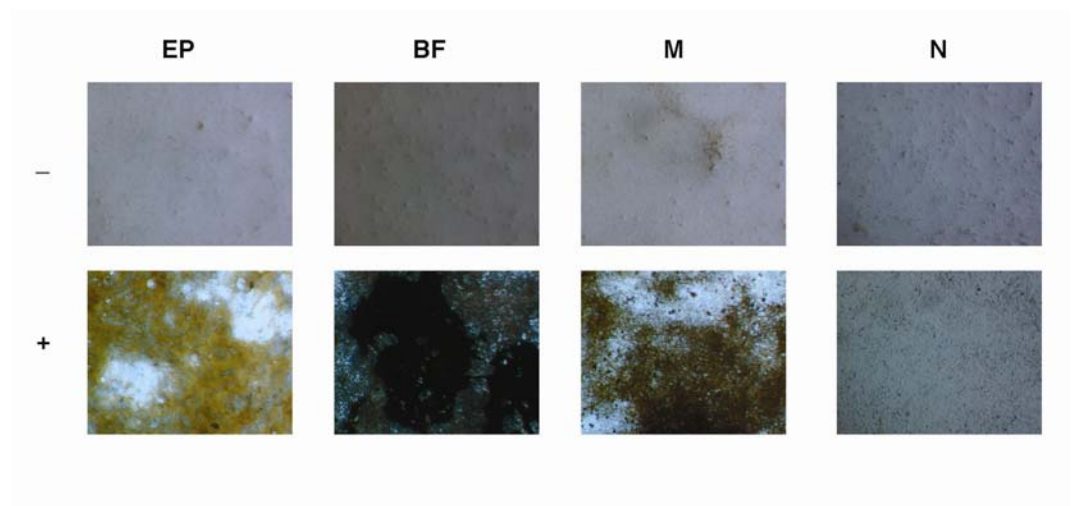


**Figure 25** Osteogenic differentiation of mBMSCs. Von Kossa staining

Von Kossa staining 21 days after induction (magnifications 4X).

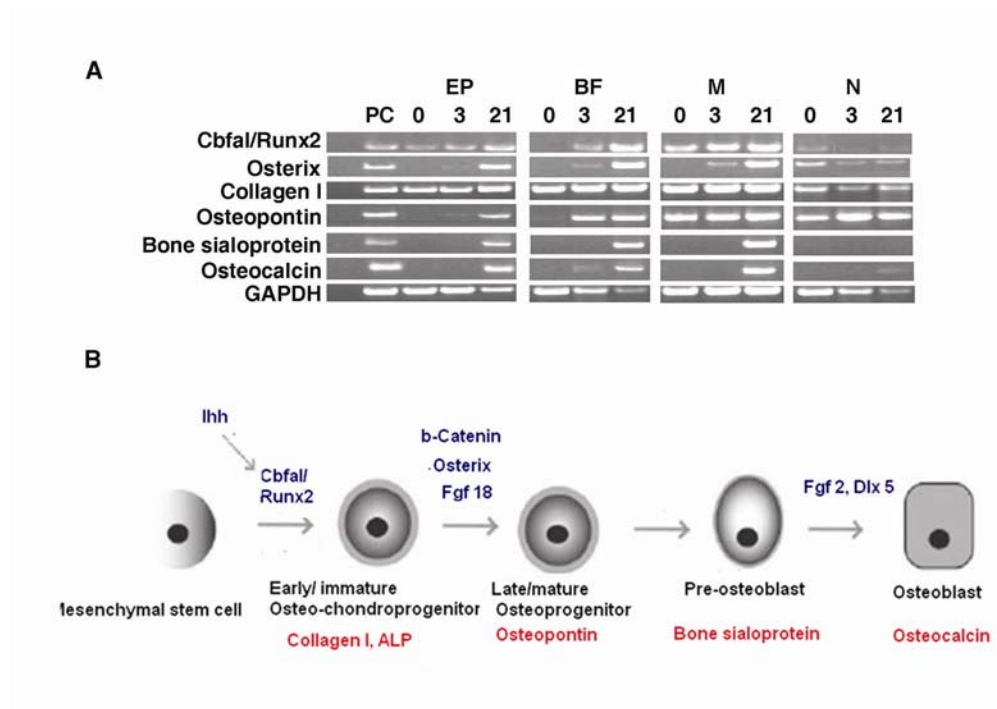


**Figure 26** Expression of osteoblast specific markers

Analysis of the expression of osteoblast-specific markers by RT-PCR (panel A). 0, 3, 21: RNA from cells at day 0 or after 3 or 21 days in induction medium. Pc: positive control. The positive control is the RNA extracted from MC3T3. GAPDH is shown as a control for RNA sample quality. Schematic representation of osteogenic differentiation (panel B).

### 5.6.2 Chondrogenesis

I tested chondrogenic differentiation ability of mBMSC groups using a micro-drop culture technique which mimics the prechondrogenic cellular condensation event that occurs *in vivo* (Denker et al. 1995; Mackay et al. 1998; Sun et al. 2003; Murdoch et al. 2007). Treatment of micro-drop cultures of mBMSC cells with chondrogenic medium resulted in aggregation of the cells into a three-dimensional spherical structure, as observed for EP, BF and M mBMSC groups. For the first 12-24 h of culture, both treated and untreated micro-drop cultures appeared similar; after 72 hr there was a change in shape of the cells on the outer edge of the micro-drop culture. These cells acquired a more elongated/bipolar shape compared to their untreated counterparts. Then the cells just inside the periphery of the micro-drop culture piled upon each other to form a ridge-like structure that

was attached on one side to the dish. After twenty one days these spheroids accumulated sulphated proteoglycans as shown by Alcian Blue staining (Figure 27). Different results were obtained for N mBMSC group; when I treated these cells with chondrogenic medium in micro-drop cultures, I did not observe spheroids formation but only a contraction of the remainder of the micro-drop culture into an opaque sheet of cells that was significantly smaller in diameter than the original culture, and detached from the surface of the dish except for the centre of the sheet-like structure, which remained attached and was positive to Alcian Blue; this data suggested that these cells have a delay or impairment in chondrogenic differentiation.

Pellet cultures (Mackay et al. 1998) were used to obtain the RNA for the analysis of the expression of chondrogenic-specific markers before and after treatment with the inductive medium by RT-PCR (Figure 28). RT-PCR results confirmed that all analyzed mBMSC progenitors constitutively express Sox-9, as previously described (Mackay et al. 1998; Murdoch et al. 2007; Figure 29). Following induction, BF and M mBMSCs began to express aggrecan and collagen XI, confirming a differentiation in chondroblasts. During the last phase of cartilage development, differentiating cells begin to express the collagen X, which is the only known hypertrophic chondrocyte-specific molecular marker. The appearance of this marker is accompanied to the peak of CbfaI/Runx 2 which, as occurs *in vivo*, appears at day 3 in a proliferation phase and after 14 days in a hypertrophic state (Ducy et al. 1997). Only EP and M mBMSCs were able to differentiate in hypertrophic chondrocyte as they express mRNA of collagen X and CbfaI/Runx2 after 21 days of differentiation. I was able to observe the expression of Sox9 and Collagen XI in N mBMSCs at time-point 0, in cells grown in monolayer, but not after three or twenty-one days in micro-pellet culture. As reported by Murdoch

there is a reduction in Collagen I and Sox9 expression from monolayer at time-point 0 and micro-pellet at time-point 3, but these markers normally increase throughout the three weeks of differentiation (Murdoch et al. 2007). As N mBMSCs do not express any marker, even in differentiation medium, I concluded that they do not differentiate in chondroblasts, confirming my initial hypothesis, above discussed.

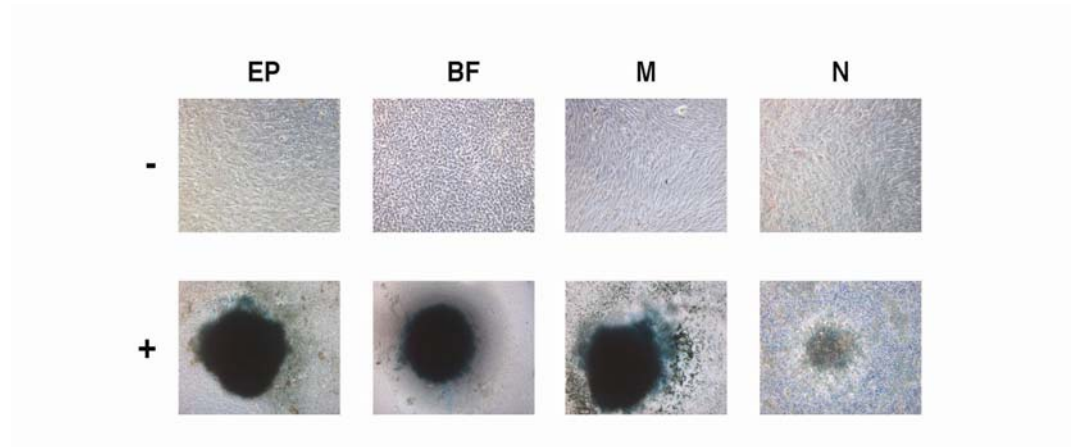


**Figure 27 Chondrogenic differentiation of mBMSCs micro-drops**

*Alcian blue staining of micro-drops cultures of mBMSCs (magnification 10X).*

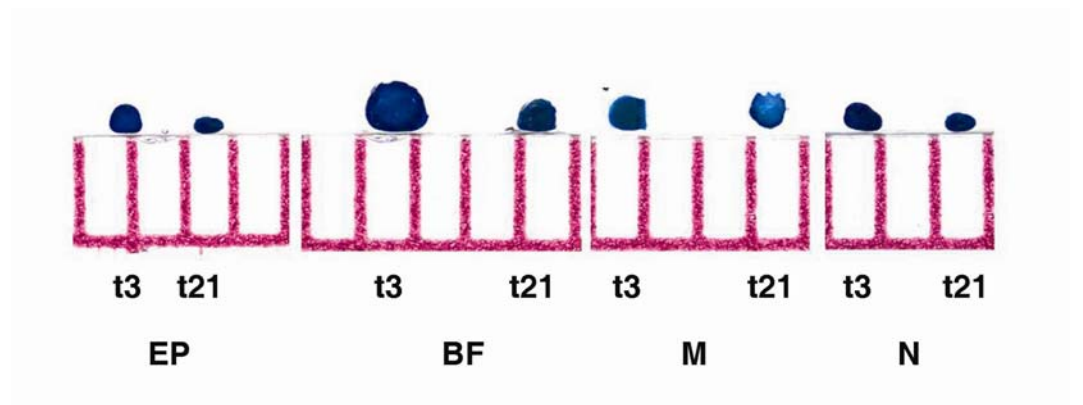


**Figure 28 Chondrogenic differentiation of mBMSCs micro-pellet**

*Alcian blue staining of micro pellet cultures of mBMSCs.*

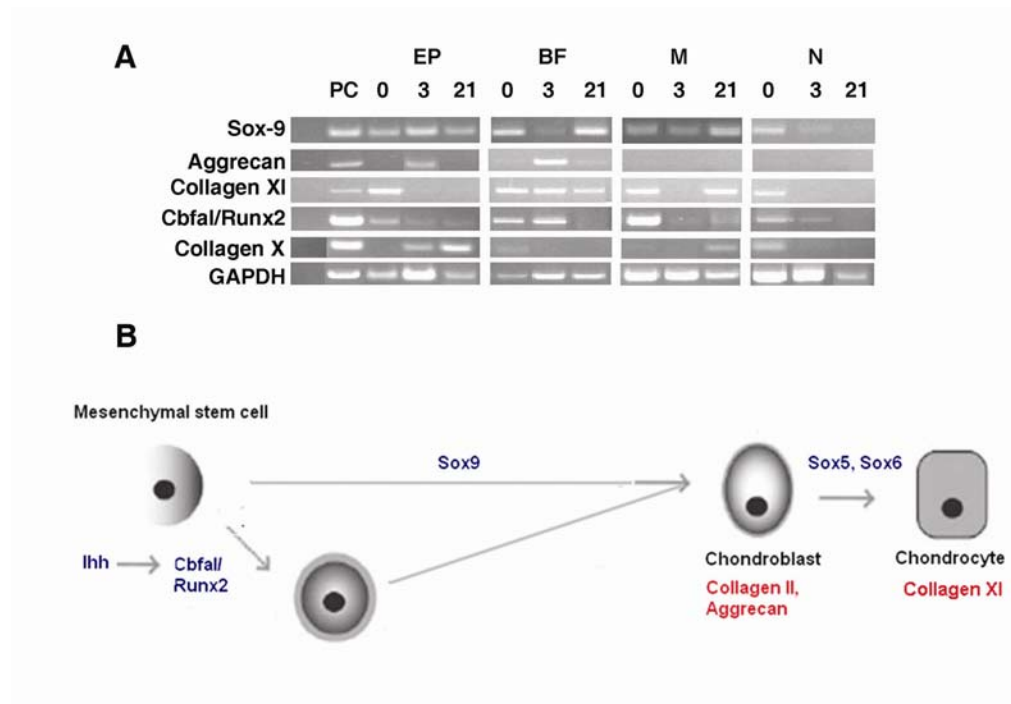


**Figure 29 Expression of chondrogenic markers**

Expression of chondrocyte-specific markers by RT-PCR (panel A). 0: RNA from monolayer cells at day 0. 3, 21: RNA from micro pellets after 3 or 21 days in induction medium. Pc: positive control. The positive control is the RNA extracted from ATDC5. GAPDH is shown as a control for RNA sample quality. Schematic representation of chondrogenic differentiation (panel B).

### 5.6.3 Adipogenesis

I induced adipogenic differentiation in mBMSCs subpopulations, according to the protocol described in Chapter 4, section 4.10.3 (Reyes et al. 2001). After fourteen days of induction the cells were fixed and stained with Oil Red O (Figure 30). N mBMSCs underwent a dramatic change in cellular morphology from spindle shaped to polygonal which was accompanied by a significant lipid droplets accumulation detectable just after 3-4 days of induction as shown by Oil Red O staining and confirmed by quantification of bound oil red (panel B). Conversely, EP, BF and M mBMSC subpopulations treated with adipogenic medium accumulated very few and small lipid droplets, even after 14 days of induction. To further confirm these data, I determined the expression of adipogenic specific markers before and after treatment with the inductive medium by RT-PCR. These

data suggest that BF and M mBMSCs are able to become immature adipocytes, as they express lipoprotein lipase (LPL) and fatty acid binding protein-4 (FABP-4) after 14 days of induction (Figure 31). N mBMSCs express early adipogenic markers also before induction, suggesting that these cells are pre-adipocytes. Upon stimulation they can differentiate readily in adipocytes, as they express the transcription factor PPAR $\gamma$ 2, essential to adipogenic commitment of mBMSCs and adipisin, a late adipogenic marker (Rosen et al. 2006), just three days after treatment with induction medium.

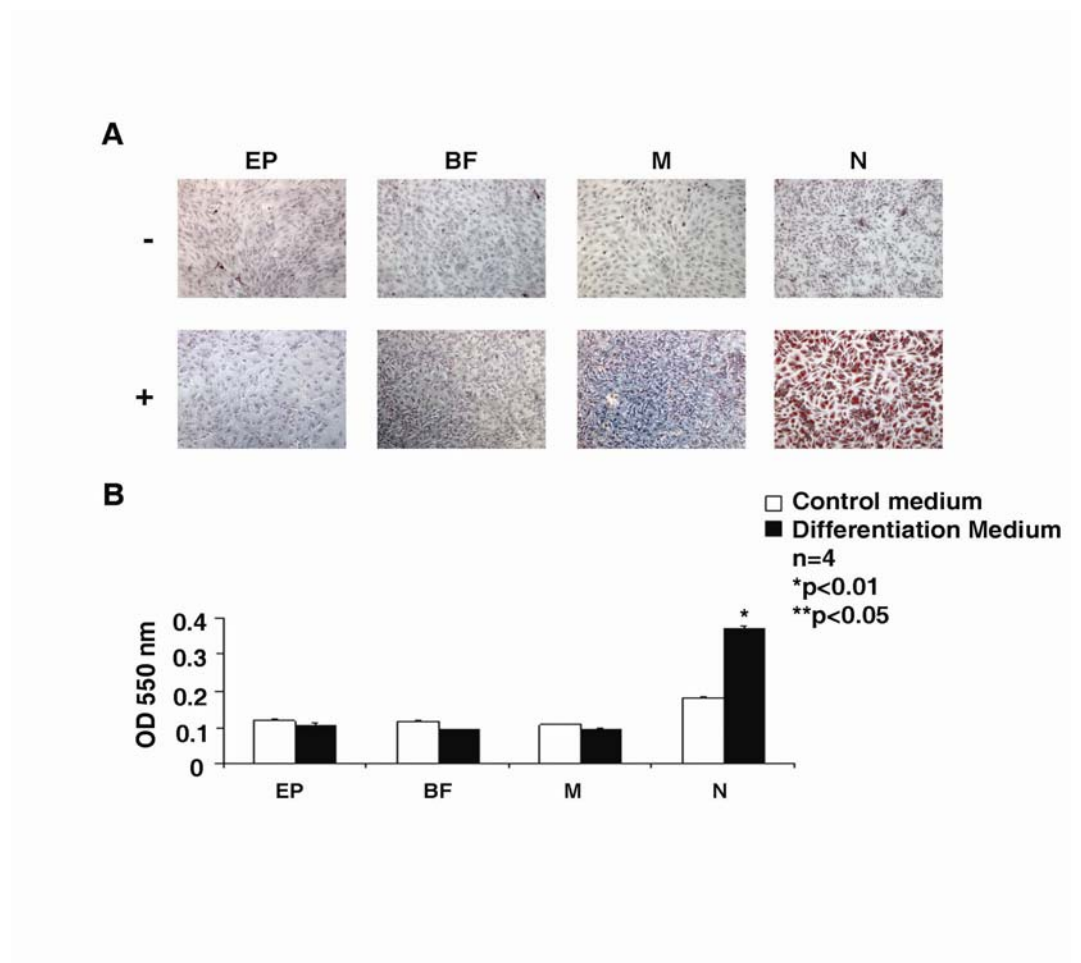


**Figure 30** Adipogenic differentiation of mBMSCs

Oil Red O staining of mBMSCs (panel A, magnification 10X). Lipid accumulation was quantified as described in Chapter 4, section 4.11.5 (panel B).

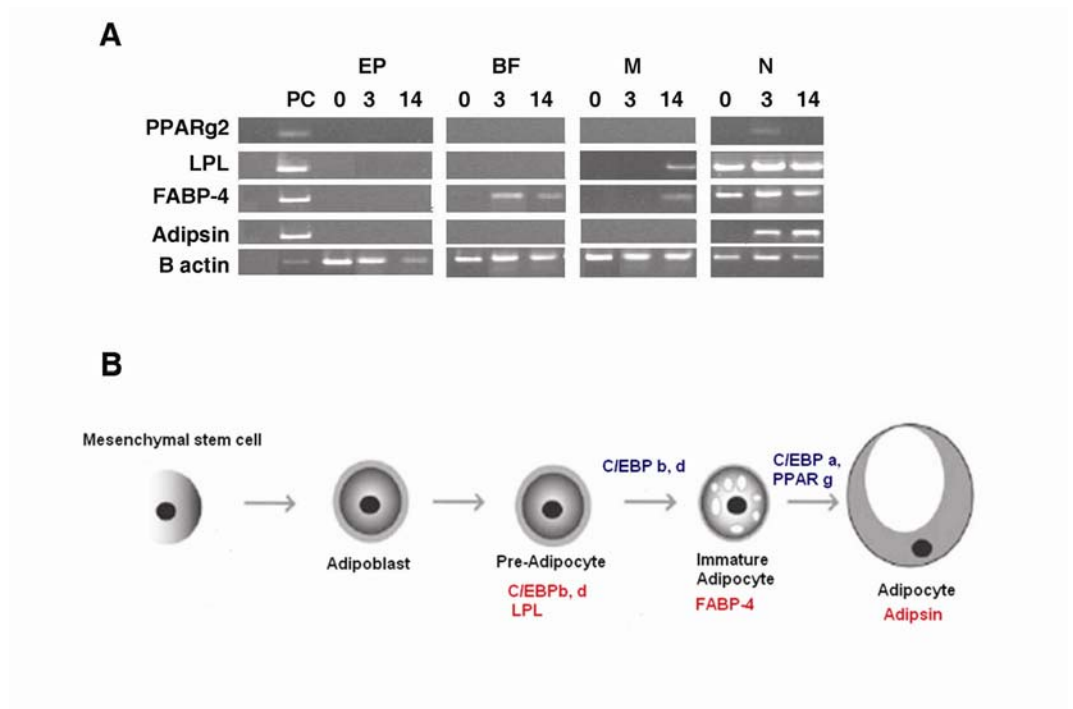


**Figure 31** Expression of adipogenic specific markers

Expression of adipocyte-specific markers was analyzed by RT-PCR (panel A). 0, 3, 14: RNA from cells at day 0 or after 3 or 14 days in induction medium. Pc: positive control. The positive control is the RNA extracted from C3H10T1/2. B actin is shown as a control for RNA sample quality. Schematic representation of adipogenic differentiation (panel B).

## 5.7 Switching the N BMSC cells into standard growth medium does not rescue their osteogenic potential

Using NIH3T3 conditioned medium, I obtained cells that showed impairment in osteogenic and chondrogenic differentiation, whereas retaining a very high adipogenic potential during passages. I hypothesized that this could be the result of NIH3T3 conditioned medium exposition. Therefore, in order to address this behaviour, I switched the N BMSC cells into standard growth medium for ten passages, a condition identified as N\*BMSCs. I induced osteogenic differentiation of N BMSCs and N\*BMSCs and I evaluated bone nodule formation and expression of osteoblast specific markers after 21 days. A slight increase in bone nodule formation was observed in N\*BMSCs (Figure 32), whereas by RT-PCR I did not observe a dramatic change in the expression of osteogenic specific

markers (Figure 33). In order to better analyze if switching the N BMSC cells into standard growth medium rescue their osteogenic potential, I evaluated by Real-time PCR expression of osteocalcin, which is the only known specific osteogenic marker (Ducy et al. 1996; Karsenty et al. 2002; Figure 34). No statistically significant difference was observed in levels of osteocalcin mRNA between N and N\* BMSCs, suggesting that this treatment is not sufficient to recover the osteogenic potential of these cells.

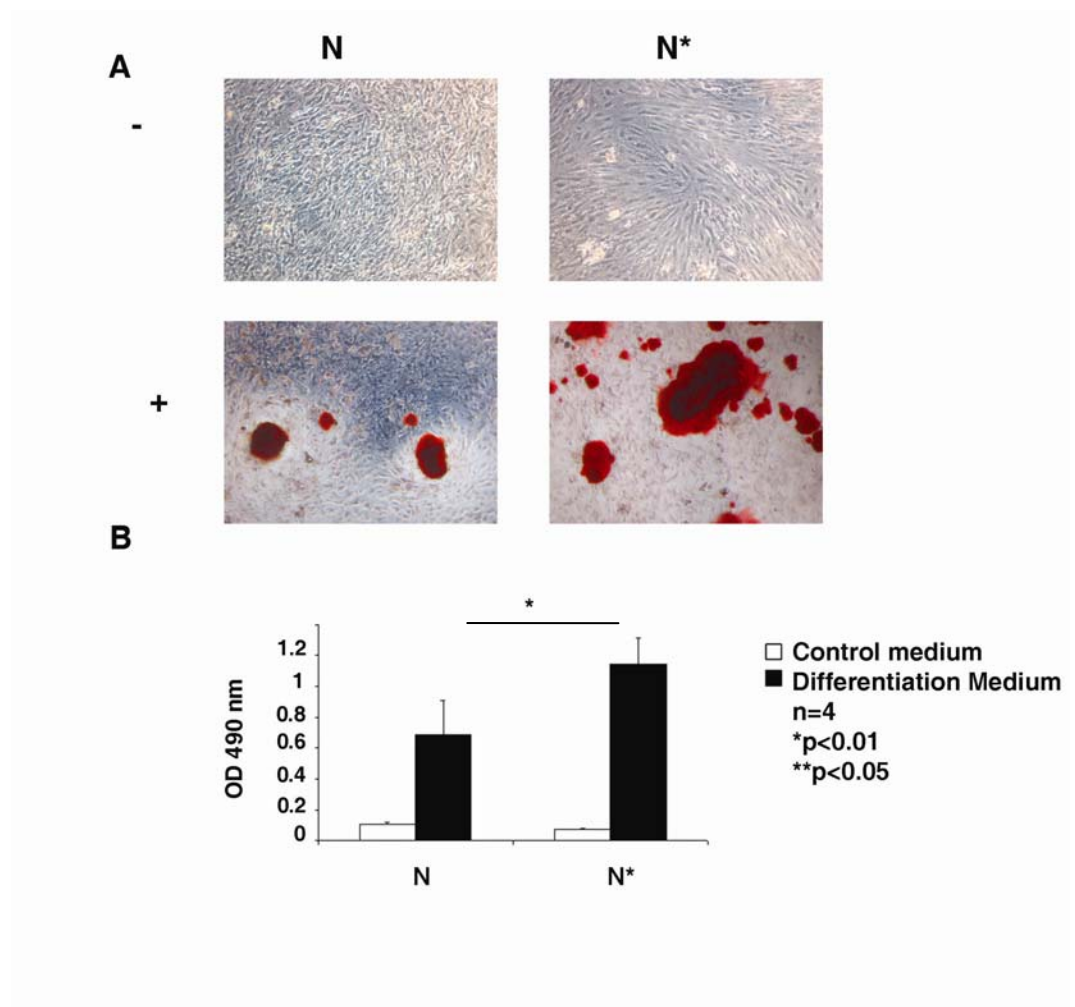


**Figure 32** Osteogenic differentiation of N\*BMSCs

*Alizarin red S staining of BMSCs (panel A, magnification 10X). Calcium deposition was quantified as described in Chapter 4, section 4.11.2 (panel B).*

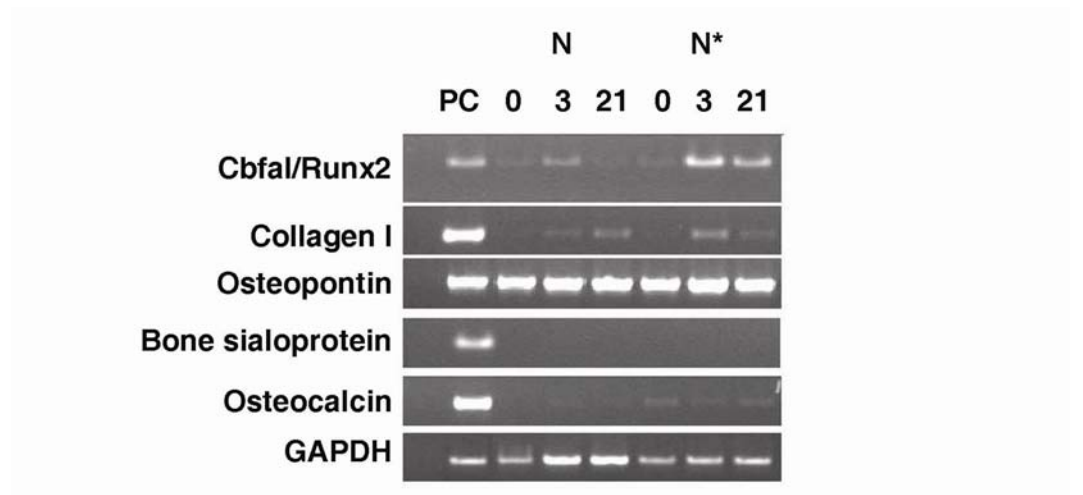


**Figure 33 Expression of osteogenic specific markers in N and N\* BMSCs**

Analysis of the expression of osteogenic-specific markers by RT-PCR. 0, 3, 21: RNA from cells at day 0 or after 3 or 21 days in induction medium. Pc: positive control. The positive control is the RNA extracted from MC3T3. GAPDH is shown as a control for RNA sample quality.

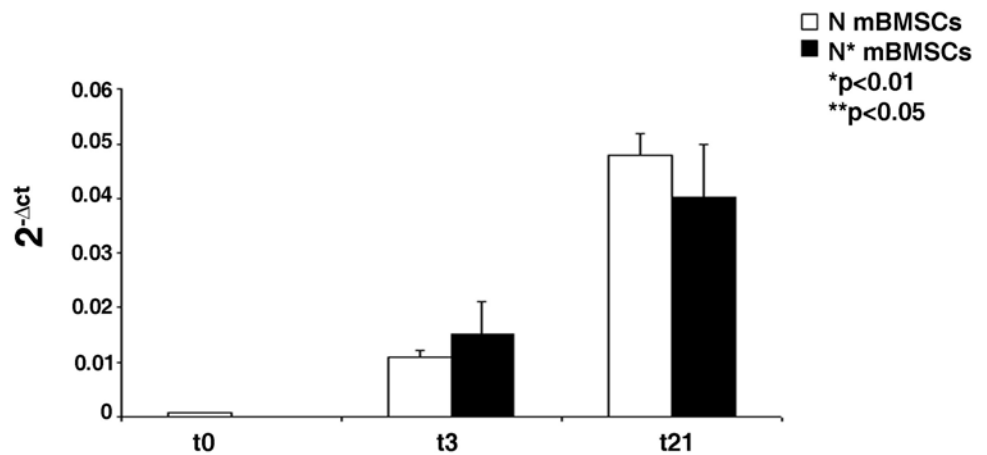


**Figure 34 Osteocalcin expression in N and N\* BMSCs**

Real Time-PCR analysis. mRNA levels were normalized with respect to GAPDH, chosen as an internal control. 0, 3, 21: RNA from cells at day 0 or after 3 or 21 days in induction medium. Pc: positive control. Histograms show mean expression values ( $\pm$  SD, n=3; \* p < 0.05; \*\* p < 0.01).

## **5.8 Expression of leukaemia inhibitory factor (LIF) in NIH3T3**

Switching N BMSCs to standard medium did not produce any significant recovery of osteogenic potential leading to the conclusion that this effect was not reversible. In the attempt to identify cytokines possibly responsible for this behaviour, I focused my attention on LIF (Metcalf 2003).

It has been recently observed that LIF is responsible for blocking osteoblast maturation at late differentiation stages and redirect these cells toward the adipogenic pathway (Falconi et al. 2007; Falconi et al. 2007); I therefore analyzed LIF expression in NIH3T3 and MS-5 cell lines by RT-PCR to evaluate whether this cytokine was expressed and could constitute a potential determinant for the observed effect on differentiation ability. RT-PCR data demonstrated that LIF was expressed only in NIH3T3 cells (Figure 35). In order to verify the capacity of NIH3T3 to secrete bioactive LIF, I tested the capacity of NIH3T3 supernatant to support maintenance of undifferentiated state of pluripotent mES cells, as it is well known that it requires the presence of LIF or LIF-related factors (Ying et al. 2003). Therefore, I plated mES cells in NIH3T3 supernatant supplemented with serum and after 6 days I determined the number of ALP- positive colonies, distinguishing among undifferentiated (ALP- positive), partially differentiated (ALP expression localized to a few discrete cells forming a colony) and differentiated colonies (ALP- negative) as ALP is a well known marker of undifferentiated mES cells (O'Connor et al. 2008). As shown in Figure 36, NIH3T3 conditioned medium supported the maintenance of undifferentiated state of mES cells. On the other hand, addition of an antagonist of LIF completely blocked this effect, supporting the production of bioactive LIF from NIH3T3 cells.

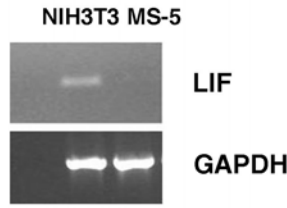


**Figure 35 Expression of LIF in NIH3T3**

*LIF expression in NIH3T3 was determined by RT-PCR analysis. GAPDH is shown as a control for RNA sample quality.*

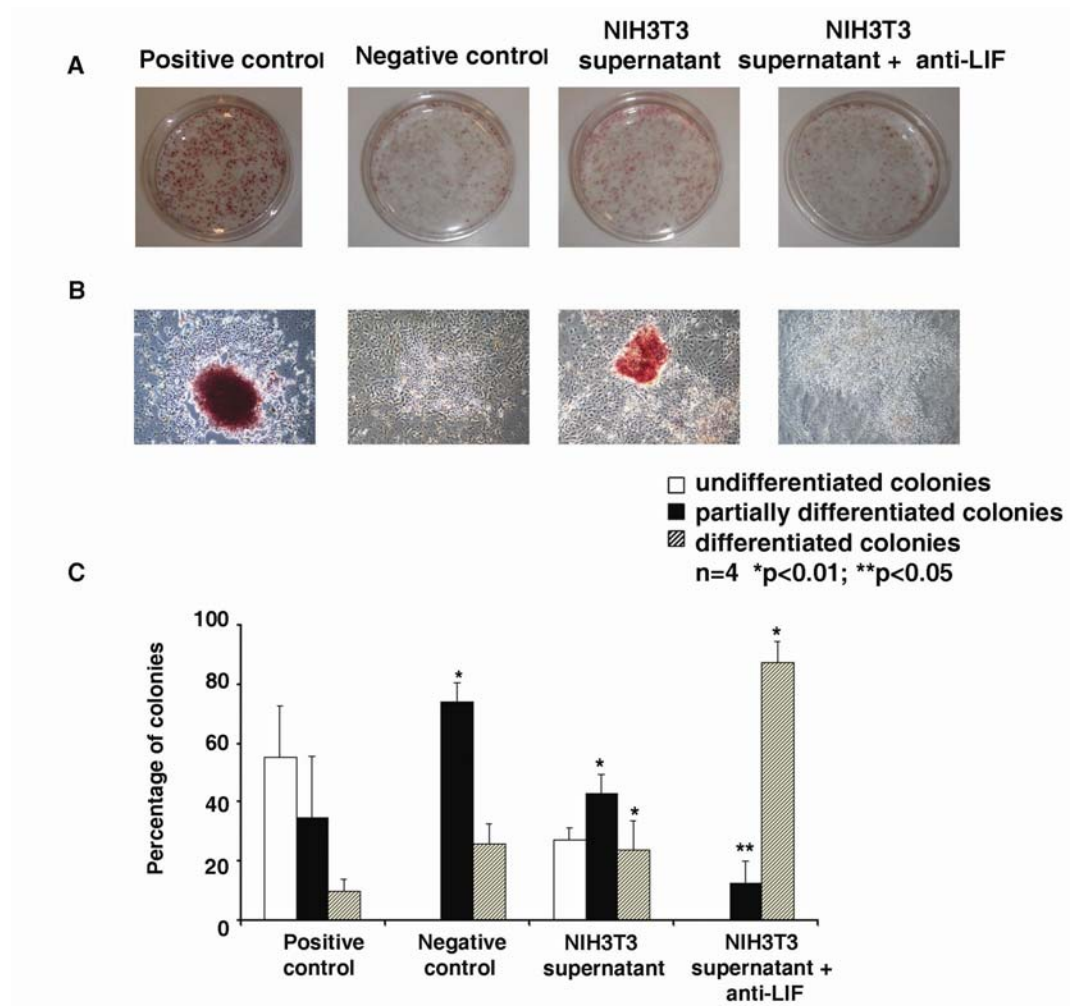


**Figure 36 NIH3T3 secrete bioactive LIF**

*ALP staining of mES cells (panel A, magnification 10X). Quantization of ALP-positive colonies (panel C). Positive control: cells maintained in ES complete medium. Negative control: cells maintained in ES complete medium without LIF.*

## Chapter 6

# Efficient non viral transfection of mBMSCs using Nucleofection technology

### 6.1 Background

Adult primary cells are, in general, difficult to transfect with DNA and BMSCs are no exception. Traditional techniques that give high transfection efficiencies throughout a range of cell lines are unable to transfer foreign DNA into BMSCs. Importantly, for *in vitro* analysis of BMSCs, the introduction of DNA has to be mediated by a technique that does not affect proliferation and differentiation.

The use of cationic lipids complexed to DNA has been widely used for transfection assays in a range of cell lines and also in mES cells. Lipofectamine 2000 has proved useful for plasmid DNA delivering in BMSCs (Hoelters et al. 2005) and is the best reagent to transfect shRNA and siRNA in BMSCs and in mES cells (Parisi et al. 2008). In order to establish a quick and reliable transfection protocol for mBMSCs, I initially tested lipofectamine 2000 from Invitrogen and nucleofection buffer solution V from Amaxa.

### 6.2 Testing BMSCs transfection efficiency with Lipofectamine 2000

To test whether mBMSCs could be transfected with Lipofectamine2000, I started with a set-up experiment in 96 well-plates, following the manufacturer's instructions. Cells were seeded at 80% confluence the day before manipulation, and then transfected with pCMV-GFP plasmid at different DNA/lipofectamine

2000 ratio, ranging from 0.075-1.5  $\mu\text{l}$  of lipofectamine 2000 and 0.05-0.4  $\mu\text{g}$  of DNA. I observed a weak GFP signal in some of the wells, which I scaled-up in 6 well-plates. After 24 h, the cells were monitored for, GFP expression, viability and changes in phenotype as compared to non transfected cells.

Notably, transfection efficiency was very low and there was a significant change in morphology in transfected cells; not only the cells were bigger, containing visible vesicles in the cytoplasm, but there was also extensive cell death when compared to non transfected controls, as determined by a significant number of floating dead cells in the culture media (Figure 37). This adverse affect prompted me to examine other transfection protocols.

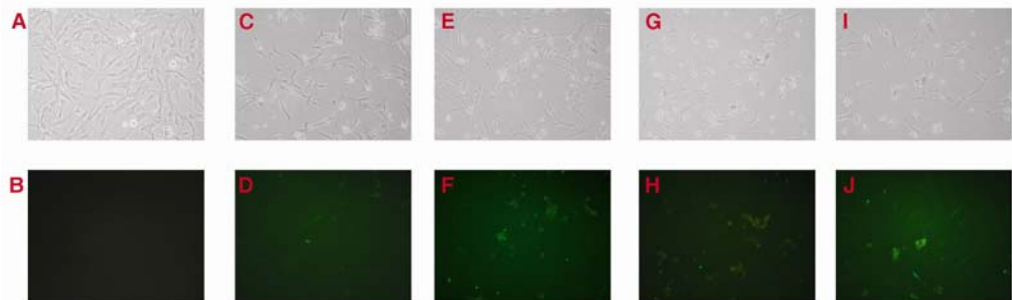


**Figure 37** *Transfection efficiency with lipofectamine 2000*

*mBMSCs were transfected with pCMV-GFP/lipofectamine at different ratio. After 24 hours the phenotype was analyzed and compared to non transfected cells (panel A and B). Ratio 1:6 (7.8  $\mu\text{g}$  DNA and 46  $\mu\text{l}$  lipofectamine 2000) in panel C and D. Ratio 1:5 (9.3  $\mu\text{g}$  DNA and 46  $\mu\text{l}$  lipofectamine 2000) in panel E and F. Ratio 1:4 (12.5  $\mu\text{g}$  DNA and 46  $\mu\text{l}$  lipofectamine 2000) in panel G and H. Ratio 1:3 (9.3  $\mu\text{g}$  DNA and 32.3  $\mu\text{l}$  lipofectamine 2000) in panel I and L. Panel A, C, E, G, I, original magnification 10X, phase contrast microscopy. Panel B, D, F, H, L, original magnification 10X, fluorescence microscopy.*

### **6.3 Testing BMSC transfection efficiency by using nucleofection technology**

The Nucleofector Technology is a new non viral transfection method, based on electroporation, specially designed for primary cells and hard to transfect cell lines, such as BMSCs (Lakshmipathy et al. 2004; Aluigi et al. 2006). I tested the efficacy of this method in mBMSCs transfection following the optimized protocol provided by the manufacturer. To this end I used  $5 \times 10^5$  cells and 2  $\mu\text{g}$  of pCMVGFP plasmid and the pulsing program U-23, specifically indicated for high transfection efficiency. As shown in Figure 38, 24 hours after nucleofection, GFP positive cells represented more than 40% of transfected mBMSCs, with no significant amount of cell debris or dead cells. Furthermore, significantly more GFP-positive cells were observed with optimized protocols, increasing the number of cells and the amount of DNA. Using  $1 \times 10^6$  cells and 8  $\mu\text{g}$  of pCMVGFP plasmid, 52.39% of cells resulted GFP positive (Figure 39) with a mean cell viability of 97.3% and an overall recovery of  $120\% \pm 30\%$  for cell treated with no DNA and  $88.4\% \pm 15.2\%$  for cell treated with pCMV-GFP (n=5). These results can be considered extremely satisfactory compared to those obtained in BMSCs with lipofectamine 2000 (Hoelters et al. 2005) or standard electroporation (Helledie et al. 2008).

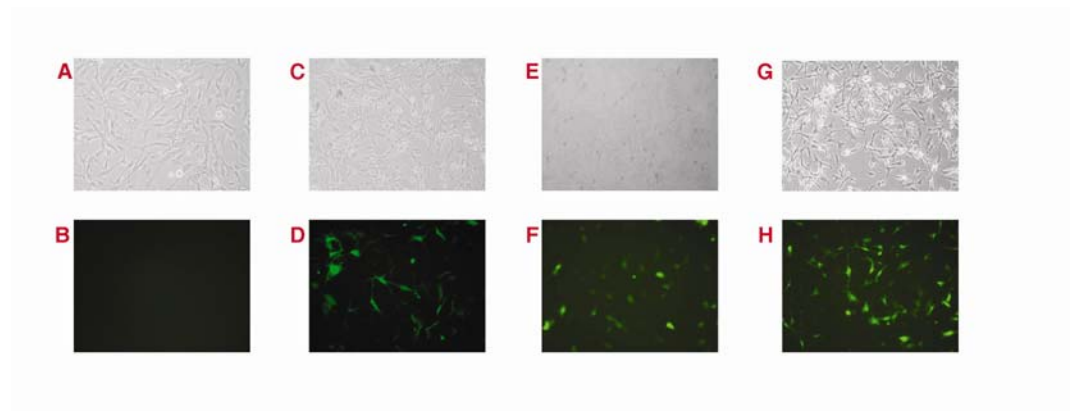


**Figure 38** *Transfection efficiency with nucleofection technology. Fluorescence Microscopy*

*mBMSCs were pulsed with U-23 program in the presence of different amount of pCMV-GFP. After 24 hours phenotype was analyzed and compared to non transfected cells (panel A and B).  $5 \times 10^5$  cells and  $2 \mu\text{g}$  DNA in panel C and D.  $1 \times 10^6$  cells and  $4 \mu\text{g}$  DNA in panel E and F.  $1 \times 10^6$  cells and  $8 \mu\text{g}$  DNA in panel G and H. Panel A, C, E and G, original magnification 10X, phase contrast microscopy. Panel B, D, F and H, original magnification 10X, fluorescence microscopy.*

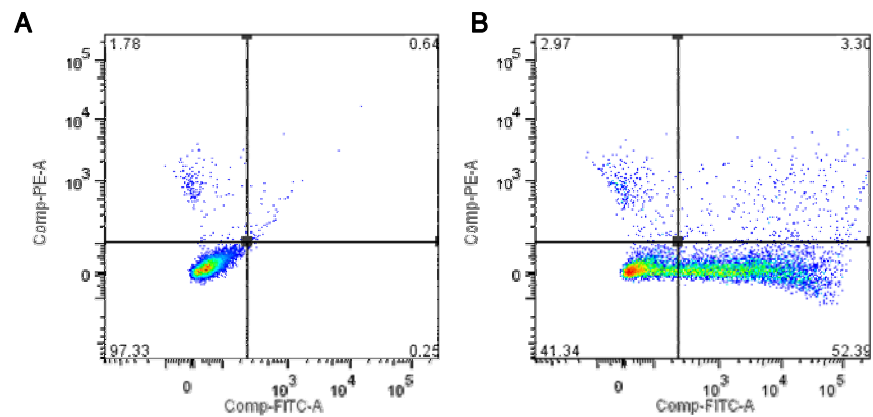


**Figure 39** *Transfection efficiency with nucleofection technology. FACS analysis*

*Flow cytometry analysis of non transfected cells (panel A) and GFP transfected cells (panel B).*

## 6.4 Time course analysis of GFP expression in nucleofected mBMSCs

To assess the stability of the nucleofection-based transfection, I performed a time course analysis over a period of one week. In accordance with the transient nature of plasmid-based transfection, GFP levels in mBMSCs declined over time. Afterward, although GFP expression decreased due to the dilution of the plasmid in culture, the percentage of GFP positive cells was still as high after one week (Figure 40), according to the hypothesis that as the DNA is delivered into the nucleus and is not retained in the cytoplasm after the transfection, it could be less subjected to degradation (Hamm et al. 2002).

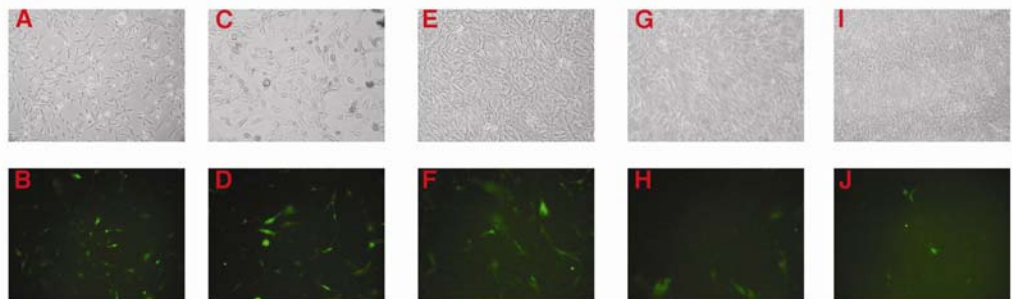


**Figure 40** Time course analysis of GFP expression

*1x10<sup>6</sup> mBMSCs were pulsed with U-23 program in the presence of 8  $\mu$ g pCMV-GFP. GFP expression was analyzed after 1 (panel A and B), 2 (panel C and D), 3 (panel E and F), 4 (panel G and H) and 5 (panel I and L) days after transfection. Original magnification 10X, panel A, C, E, G, I phase contrast microscopy; panel B, D, F, H and L, fluorescence microscopy.*

## 6.5 Effect of nucleofection on cell proliferation

In order to test whether nucleofected mBMSCs maintain their phenotype after transfection, I considered the effect on cell proliferation and senescence.

Twenty-four hours after transfection, mBMSCs were seeded at 2500 cells each well of a 96-well plates, and after 2 days, cell numbers in nucleofected, non transfected and mock (no DNA) transfected cells were determined from three wells of each culture, as described in Chapter 4, section 4.15. Notably, nucleofected cells yielded similar cell growth rates compared to both controls, indicating that nucleofection technology does not impair cell proliferation (Figure 41).

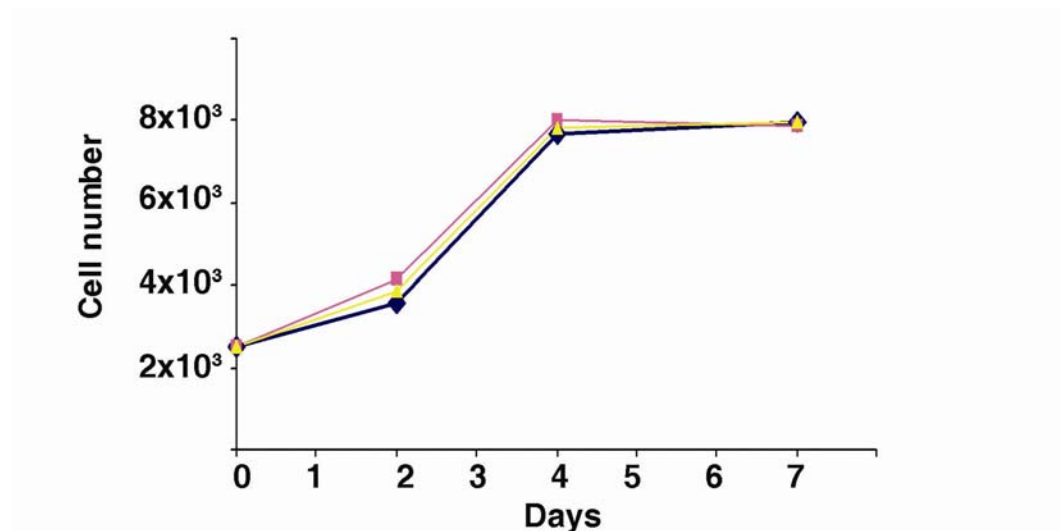


**Figure 41 Nucleofection does not affect cell proliferation**

Cell number was evaluated using CellTiter-Glo Luminescent Cell Viability Assay from Promega. Blue line: non nucleofected mBMSCs; pink line: mBMSCs nucleofected with no DNA; yellow line: mBMSCs nucleofected with pCMV-GFP.

## 6.6 Effect of nucleofection on cellular senescence

I evaluated the number of senescent cells in nucleofected cells compared to non transfected and mock (no DNA) transfected cells. Twenty-four hours after transfection, mBMSCs were seeded at  $10^4$  cells/cm<sup>2</sup> in six-well plates, and after 3 days, the cultures were assayed for SA-  $\beta$ - Galactosidase expression, as described in Chapter 4, section 4.6. Importantly, nucleofected cells gave similar results in terms of SA-  $\beta$ - Galactosidase positive cells compared to both controls (t-Test between untransfected and mock,  $p=0.18$ ; t-Test between untransfected and pCMVGFP,  $p=0.28$ ; t-Test between mock and pCMVGFP,  $p=0.53$ ) indicating that nucleofection technology does not induce cellular senescence (Figure 42).

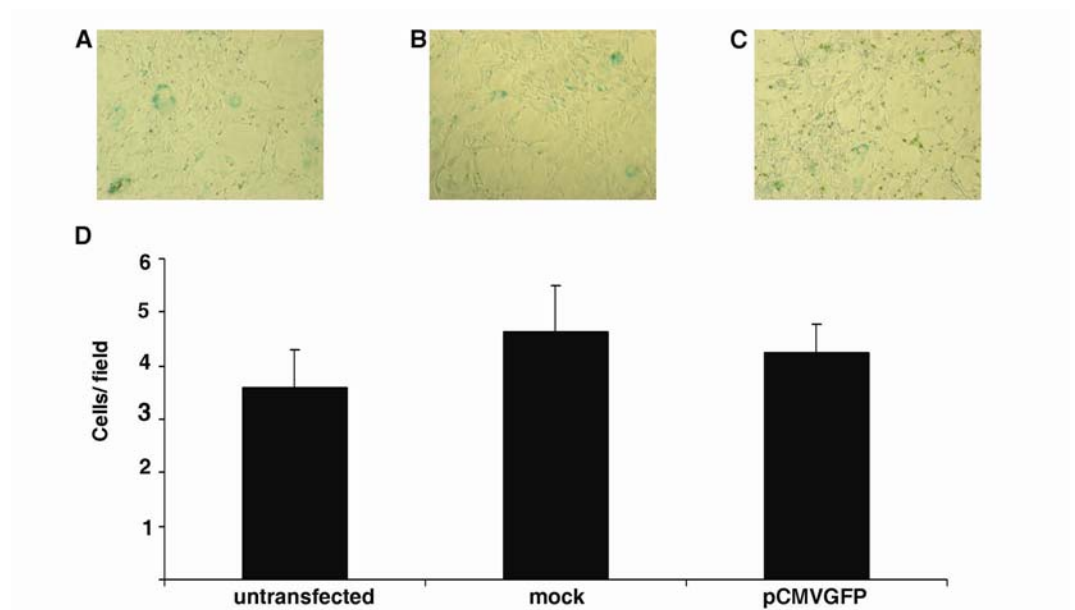


**Figure 42** Nucleofection does not induce cellular senescence

*B-gal-staining in mBMSC untransfected (panel A), transfected with no DNA (panel B) or with pCMVGFP (panel C) (original magnification 10x). Quantization of the number of SA-Beta-Gal positive cells (panel D).*

## 6.7 Effect of nucleofection on cell migration

I assessed whether nucleofection affect cell migration. The motility of BMSCs was examined in a migration chamber in which the migrating cells in the insert chamber went through the poles on the membrane. The cells landing in the lower chamber or attaching on the other side of the membrane were stained and quantified by counting several fields. The results showed that nucleofection does not impair cell migration (t-Test between untransfected and mock,  $p=0.35$ ; t-Test between untransfected and pCMVGFP,  $p=0.76$ ; t-Test between mock and pCMVGFP  $p=0.80$ ; Figure 43).

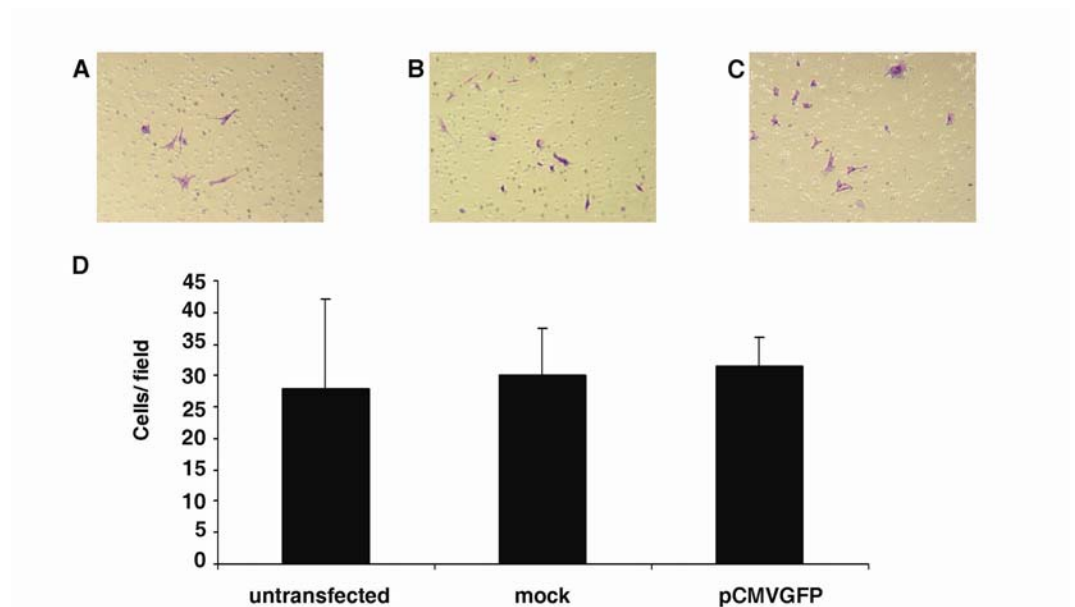


**Figure 43** Nucleofection does not affect cell migration

*Crystal violet staining of chamber slides of untransfected mBMSC (panel A), transfected with no DNA (panel B) or with pCMVGFP (panel C) (original magnification 10x). Quantization of the number of migrated cells (panel D).*

## Chapter 7

# Effect of Nanog over-expression and down-regulation in mBMSCs

### 7.1 Background

ES cells maintain pluripotency by a transcriptional program that suppresses differentiation; this property is regulated by a small number of ES cell specific transcription factors such as Nanog, Oct-4 and Sox-2, whose expression is down regulated early during embryogenesis (Boiani et al. 2005).

Very recent papers showed the expression of Oct-4, Nanog and Sox2 in BMSCs (Jiang et al. 2002; Anjos-Afonso et al. 2007; Beltrami et al. 2007; Gonzalez et al. 2007; Greco et al. 2007; Kobayashi et al. 2008).

Although the role of Nanog, Oct4 and Sox2 in adult tissue stem cells remains unclear, it has been expected that it may be possible to use them to enhance the self-renewal of tissue stem cells, as it has recently been reported that pluripotent stem cells can be directly generated from mouse fibroblasts by the introduction of concomitant four transcription factors, Sox2, Oct4, KLF-4 and c-myc (Takahashi et al. 2006); Nanog is not one of the four genes, however, its functional importance is evident from the fact that up regulation of the Nanog gene seemed to be critical for reprogramming the cell (Okita et al. 2007). Very poor data are available about the role of Nanog in BMSCs. Studies of Go et al. and Liu et al. showed an effect of Nanog on proliferation and osteogenic and chondrogenic abilities (Go et al. 2008; Liu et al. 2008), however, nobody of them tested the effect of Nanog in the balance between senescence, apoptosis and tumorigenesis

and in cell migration. The last part of this study was dedicated to start a project aimed to dissect the role of Nanog in these phenomena in collaboration with the group of Dr Nicole Horwood at the Kennedy Institute of Rheumatology, Imperial College of London.

## **7.2 Stemness factors expression in B BMSCs**

For these studies, I used primary bone marrow stromal cells isolated from Balb/c mice (B mBMSCs) in the laboratory of Dr Nicole Horwood. Recent unpublished data from this laboratory confirm an immunophenotype compatible with mBMSCs (Lai et al. 1998; Deans et al. 2000) and tri-lineage differentiation potential (Pittenger et al. 1999). I evaluated the expression of Oct-4, Nanog and Sox-2, as well as done in my previous preparation of mBMSCs. As evidenced by real time-PCR, Nanog is highly expressed in B mBMSCs, whereas the expression of Sox-2 was ten times lower than Nanog and Oct4 was undetectable (Figure 44). These data are consistent with the previous results, obtained in EP, BF, M and N BMSCs and several published papers (Jiang et al. 2002; Anjos-Afonso et al. 2007; Beltrami et al. 2007; Gonzalez et al. 2007; Greco et al. 2007; Galderisi et al. 2008; Kobayashi et al. 2008).

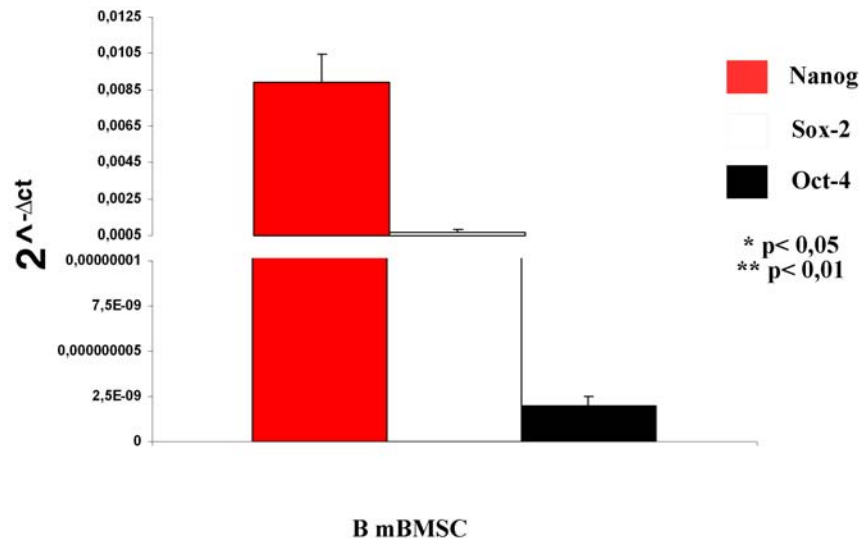


**Figure 44** Stemness factor expression in B BMSCs

*Real Time-PCR analysis. mRNA levels were normalized with respect to GAPDH, chosen as an internal control. Histograms show mean expression values ( $\pm$  SD,  $n=3$ ; \*  $p < 0.05$ ; \*\*  $p < 0.01$ ).*

### 7.3 Transient over- expression and down-regulation of Nanog

In order to obtain a transient over-expression or down-regulation of Nanog in BMSCs, I cloned the murine Nanog cDNA in sense and antisense direction in expression vectors carrying a CMV promoter and an IRES-GFP-WPRE sequence, so that expression of the construct would have been easily detectable during the cell culture. IRES sequence, the internal ribosome entry site, allows for translation initiation in the middle of a mRNA sequence as part of the greater process of protein synthesis. Usually, in eukaryotes, translation can only be initiated at the 5' end of the mRNA molecule, since 5' cap recognition is required for the assembly of the initiation complex. However, when an IRES segment is located between two open reading frames (ORFs) in a eukaryotic mRNA molecule, it can drive translation of the downstream protein coding region independently of the 5'-cap structure bound to the 5' end of the mRNA molecule. In such a setup both

proteins are produced in the cell. The first reporter protein located in the first cistron is synthesized by the cap-dependent initiation approach while translation initiation of the second protein is directed by the IRES segment located in the intercistronic spacer region between the two reporter protein coding regions (Pelletier et al. 1988). The WPRE, woodchuck hepatitis virus post-transcriptional regulatory element, is a sequence which facilitates nucleocytoplasmic transport of RNA and therefore stimulates cDNA expression (Higashimoto et al. 2007).

### **7.3.1 Over-expression of Nanog in 293 cell line**

In order to test the efficacy of the vector carrying Nanog cDNA, I initially transfected 293 cell line, using calcium-phosphate method, as described in Chapter 4, section 4.14.3. As shown in Figure 45, 48 hours after nucleofection, GFP positive cells represented more than 70% of pCMVIREGFP-WPRE and pCMVNanogIRES-GFP-WPRE transfected 293.

Western Blot analysis confirms that Nanog protein is expressed at high levels in Nanog over-expressing cells, while is not expressed in untreated or pCMV-IRESGFP-WPRE treated cells (Figure 46).

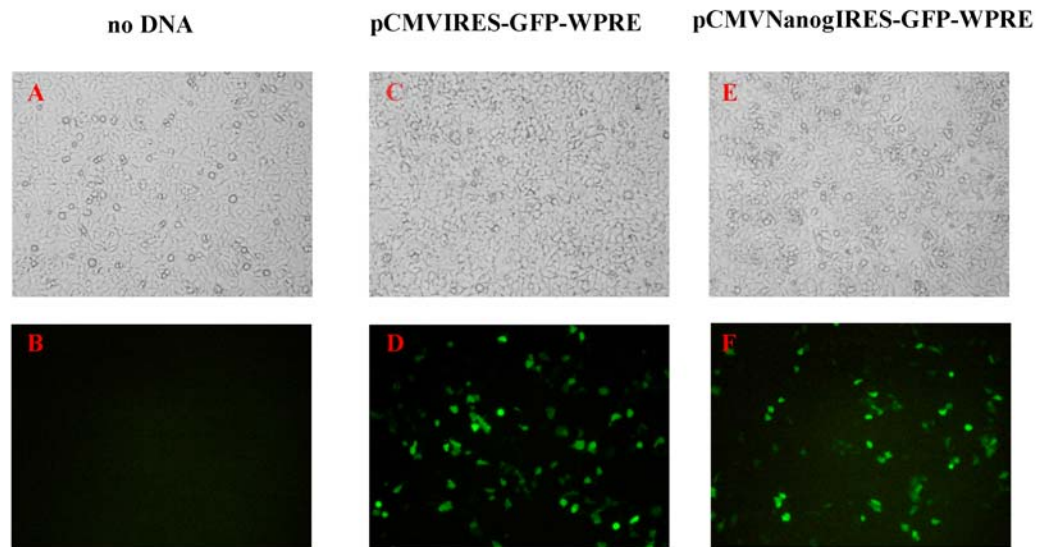


**Figure 45** GFP expression in 293 transfected with Nanog vector

293 cells were transfected with no DNA (panel A and B), 10  $\mu$ g pCMVIREs-GFP-WPRE (panel C and D) or pCMVNanogIREs-GFP-WPRE (panel E and F). GFP expression was analyzed after 24 hr. (original magnification 10X; panel A, C and E phase contrast microscopy; panel B, D and F fluorescence microscopy).

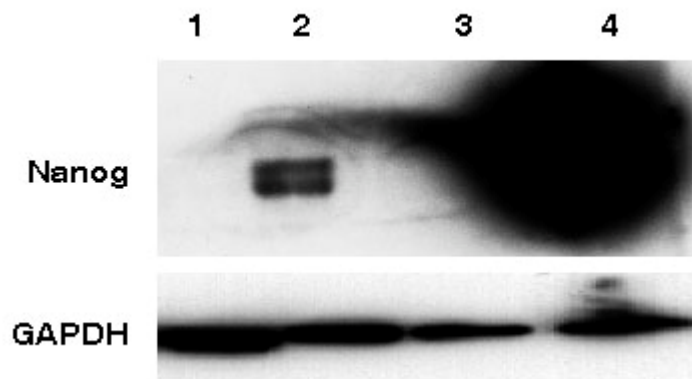


**Figure 46** Nanog expression in 293 transfected with Nanog vector

Western blot analysis of Nanog in 293. 1, 293; 2, mES; 3 293 transfected with pCMVIREs-GFP-WPRE; 4 293 transfected with pCMVNanogIREs-GFP-WPRE. The protein levels were normalized with respect to GAPDH, which was chosen as an internal control.

### 7.3.2 Down-regulation of Nanog in 293 cell line

In order to test the efficacy of the vector expressing antisense sequence of Nanog to interfere with the expression of Nanog, I transfected this vector in 293 cell line, using calcium-phosphate method, as described in Chapter 4, section 4.13.3. As shown in Figure 47, 24 hours after transfection of pCMVIREs-GFP-WPRE, GFP positive cells represented more than 70%; a significant less number of GFP positive cells were observed in 293 transfected with pCMVantiNanogIREs-GFP-WPRE transfected.

293 cells do not express Nanog. So, in order to test the efficacy of the antisense to down regulate the expression of Nanog, I co-transfected pCMVNanogIREs-GFP-WPRE and pCMVantiNanogIREs-GFP-WPRE at different ratio (Figure 48).

Western Blot analysis confirms that antisense of Nanog is able to reduce the expression of Nanog protein to less than 25% when cotransfected with Nanog at ratio 1.1. Increasing ratios reduce Nanog protein to level undetectable by western blot (Figure 49).

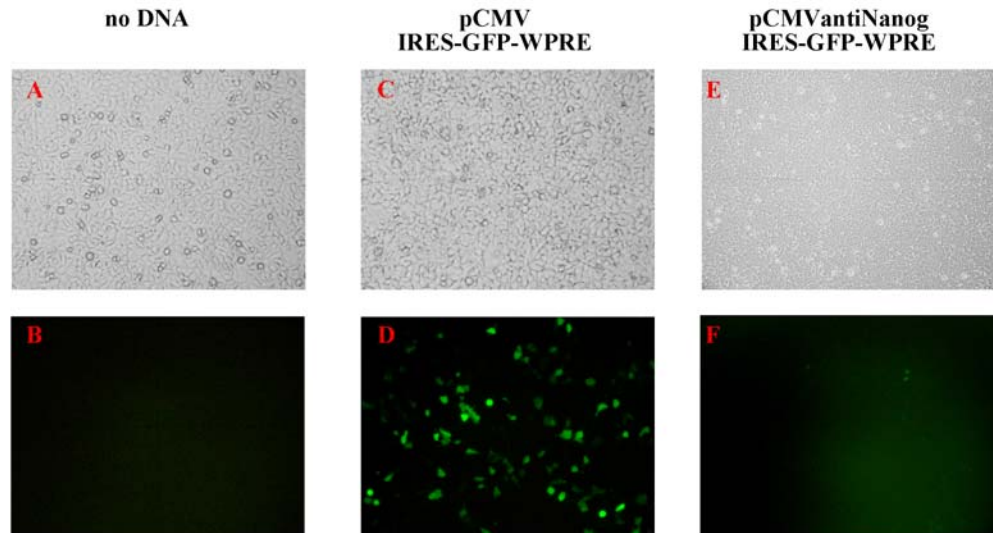


**Figure 47** *GFP expression in 293 transfected with antiNanog vector*

293 cells were transfected with no DNA (panel A and B), 10  $\mu$ g pCMV IRES-GFP-WPRE (panel C and D) or pCMV antiNanog IRES-GFP-WPRE (panel E and F). GFP expression was analyzed after 24 hr (original magnification 10x; panel A, C and E phase contrast microscopy; panel B, D and F fluorescence microscopy).

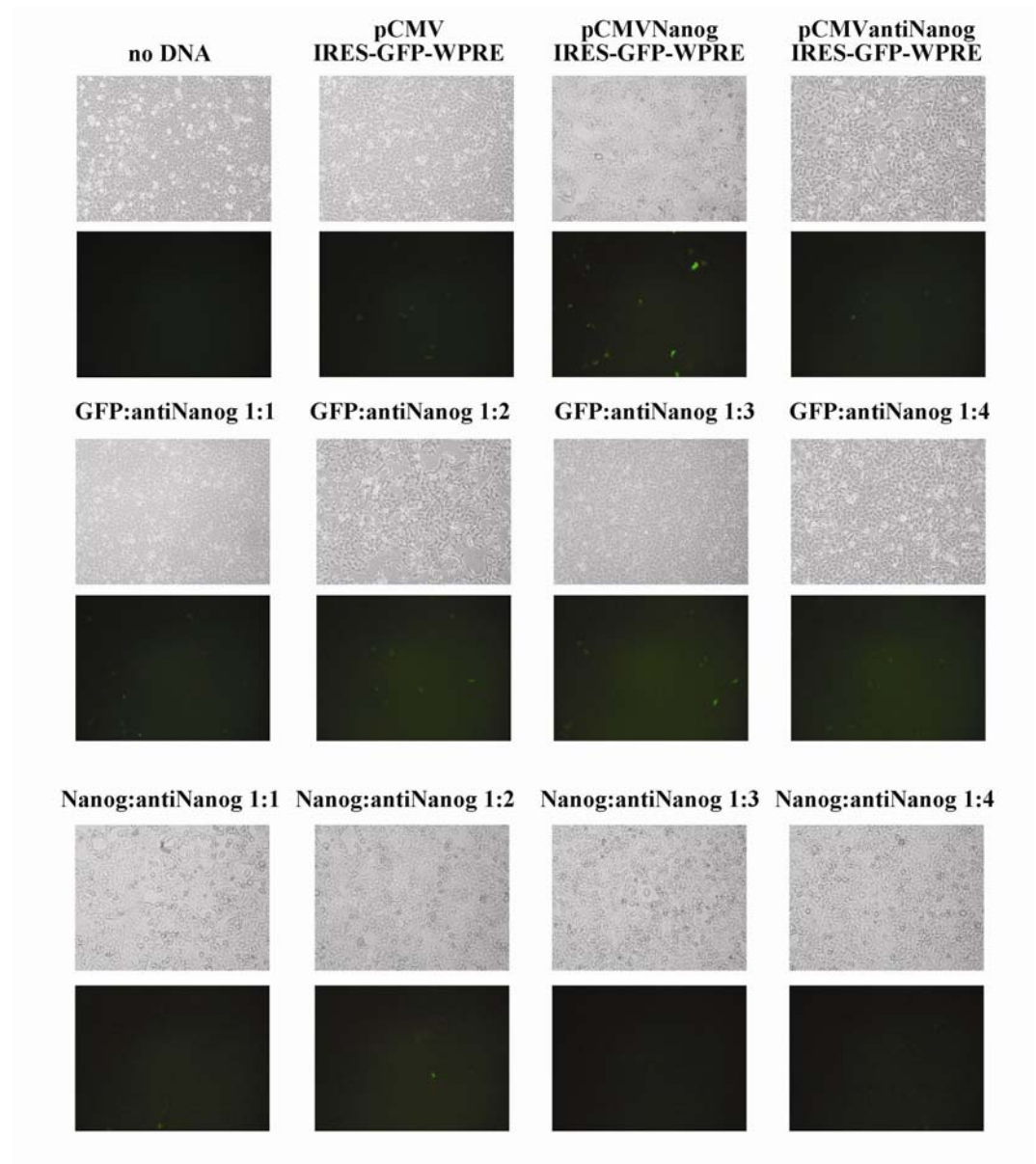


**Figure 48** *GFP expression in 293 co-transfected with Nanog and antiNanog vectors*

*GFP expression was analyzed after 24 hr (original magnification 10x; upper panels phase contrast microscopy; lower panels fluorescence microscopy).*

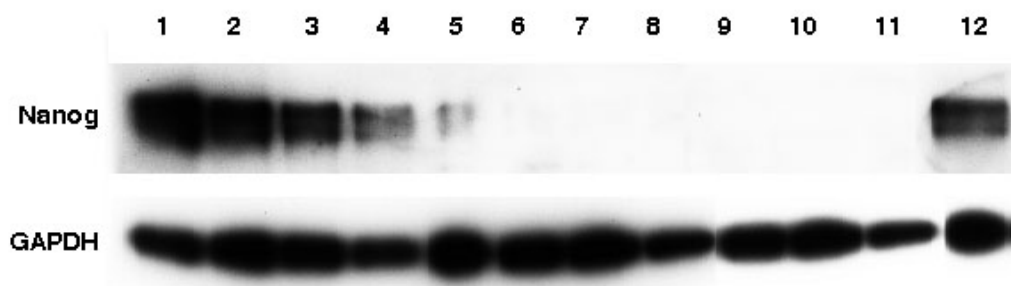


**Figure 49** Down- regulation in Nanog expression in 293 co-transfected with Nanog and antiNanog vectors

Western blot analysis of Nanog in 293. 1, 293 transfected with pCMVNanogIRES-GFP-WPRE; 2, 75% sample 1; 3, 50% sample 1; 4 25% sample 1; 5, 293 co-transfected with pCMVNanogIRES-GFP-WPRE and pCMVantiNanogIRES-GFP-WPRE ratio 1.1; 6, 293 co-transfected with pCMVNanogIRES-GFP-WPRE and pCMVantiNanogIRES-GFP-WPRE ratio 1.2; 7, 293 co-transfected with pCMVNanogIRES-GFP-WPRE and pCMVantiNanogIRES-GFP-WPRE ratio 1.3; 8, 293 co-transfected with pCMVNanogIRES-GFP-WPRE and pCMVantiNanogIRES-GFP-WPRE ratio 1.4; 9, 293; 10, 293 transfected with pCMVIREs-GFP-WPRE; 11, 293 transfected with pCMVantiNanogIRES-GFP-WPRE; 12, mES cells. The protein levels were normalized with respect to GAPDH, which was chosen as an internal control.

### 7.3.3 Transfection efficiency, cell viability and cell recovery in mBMSCs nucleofected with pCMVNanogIRES-GFP-WPRE and pCMVantiNanogIRES-GFP-WPRE

I transfected the vectors described above in B BMSCs, using the optimized nucleofection protocol described in the Chapter 4, section 4.14.2 and discussed in Chapter 6. As shown in Figure 50, 24 hours after nucleofection, GFP positive cells represented more than 70% of pCMV-GFP transfected mBMSCs; lower percentages of GFP positive cells were observed in cell nucleofected with pCMVIREs-GFP-WPRE, pCMVNanogIRES-GFP-WPRE and pCMVNanogIRES-GFP-WPRE. This difference in GFP expression was due to the presence of IRES element: as discussed above, in these constructs Nanog expression is driven by CMV promoter and protein is synthesized by the cap-

dependent initiation approach while, translation initiation of the GFP protein is directed by the IRES segment located in the intercistronic spacer region between the two protein coding regions, so the efficiency is lower (Pelletier et al. 1988; Go et al. 2008).

The transfected cells were also analyzed by fluorescence activated cell sorter (FACS) in order to quantify the results in terms of efficiency, viability and cell recovery.

The flow cytometry analysis verified that nucleofection of pCMVIREs-GFP-WPRE resulted in 32.2% GFP positive cells, while the percentage of GFP positive cells obtained with nucleofection of pCMVNanogIRES-GFP-WPRE and pCMVantiNanogIRES-GFP-WPRE was 38,36% and 3,95%, respectively, confirming the results obtained with fluorescence microscopy (Figure 51).

I observed a mean cell viability of 93.4%, 87.15%, 83.89 % and 90.72% for cell treated with no DNA, pCMVIREs-GFP-WPRE, pCMVNanog-IRES-GFP-WPRE or pCMVantiNanogIRES-GFP-WPRE respectively, confirming no particular difference in toxicity of different vectors (Figure 51).

Cell recovery was  $120\% \pm 30\%$ ,  $88.4\% \pm 15.2\%$ ,  $73.8\% \pm 9.49\%$  and  $61\% \pm 13.45\%$ , for cell treated with no DNA, pCMVIREs-GFP-WPRE, pCMVNanog-IRES-GFP-WPRE or pCMVantiNanogIRES-GFP-WPRE respectively. T-Test analysis confirm that the difference between no DNA and pCMVIREs-GFP-WPRE, no DNA and pCMVNanogIRES-GFP-WPRE and pCMVIREs-GFP-WPRE and pCMVNanogIRES-GFP-WPRE were not statistically significant ( $p=0.072$ ;  $p=0.052$ ;  $p=0.10$ ); whereas the difference between no DNA and pCMVantiNanogIRES-GFP-WPRE, and between pCMVIREs-GFP-WPRE and pCMVantiNanogIRES-GFP-WPRE were statistically significant ( $p=0.021$ ;  $p=0.042$ ).

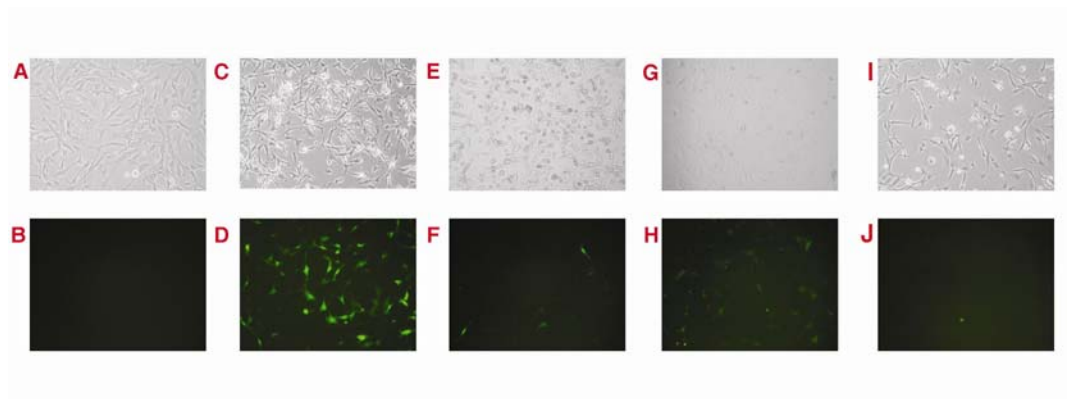


**Figure 50** GFP expression in B BMSCs nucleofected with pCMVIRESGFP-WPRE vector. Fluorescence microscopy analysis

$1 \times 10^6$  mBMSCs were pulsed with U-23 program in the presence of no DNA (panel A and B), 8  $\mu$ g pCMV-GFP (panel C and D), pCMVIRESGFP-WPRE (panel E and F), pCMVNanogIRES-GFP-WPRE (panel G and H) pCMVantiNanogIRES-GFP-WPRE (panel I and J) original magnification 10X; panel A, C, E, G and I phase contrast microscopy; panel B, D, F, H and J fluorescence microscopy).

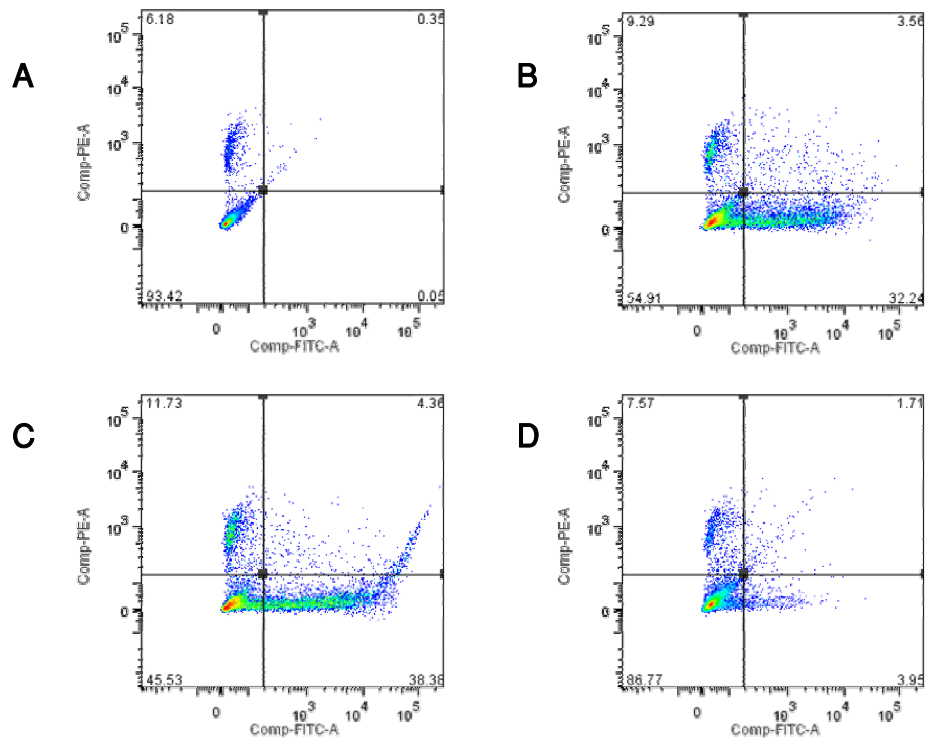


**Figure 51** GFP expression in cell nucleofected with pCMVIRESGFP-WPRE vector. FACS analysis

Flow cytometry analysis of BMSCs transfected with no DNA (panel A), pCMVIRESGFP-WPRE (panel B), pCMVNanogIRES-GFP-WPRE (panel C), pCMVantiNanogIRES-GFP-WPRE (panel D).

### 7.3.4 Over-expression of Nanog in mBMSCs

In order to confirm that the nucleofection with pCMVNanogIRES-GFP-WPRE allows over expression of Nanog in B mBMSCs, I analyzed the expression of Nanog by Real time-PCR and Western Blot analysis.

As showed in Figure 52, over expression of Nanog driven by CMV promoter leads to an increase in Nanog mRNA of 50 times, compared to mBMSCs treated with pCMVIREs-GFP-WPRE ( $p=6.23E-07$ ), confirming the efficacy of the vector in driving Nanog expression in BMSCs.

Western Blot analysis confirms that Nanog protein is expressed at high levels in Nanog over-expressing cells (Figure 53). I did not detect Nanog protein in control B mBMSCs by western blot analysis, even when I loaded 10-50  $\mu\text{g}$  of proteins as also showed by several papers (Greco et al. 2007; Go et al. 2008; Liu et al. 2008).

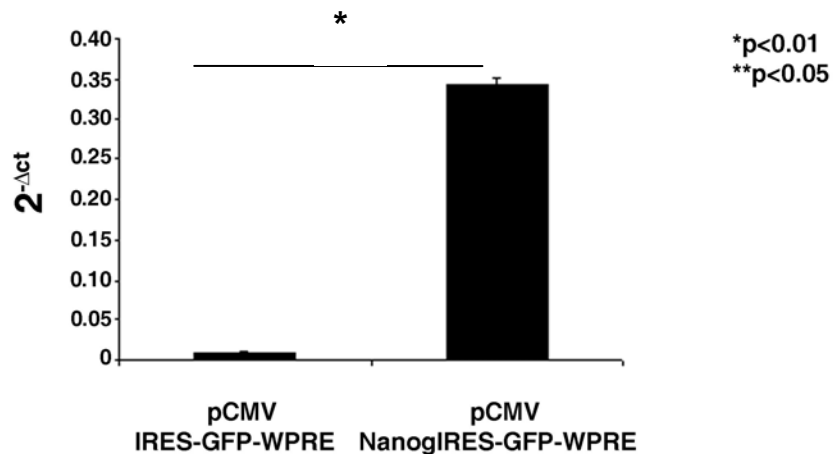


**Figure 52 Nanog expression in BMSCs nucleofected with Nanog vector. Real time PCR**

*mRNA levels were normalized with respect to GAPDH, chosen as an internal control. The histogram shows the mean expression values expressed as  $2^{-\Delta ct}$  ( $\pm$  SD,  $n=3$ ). (\*  $p < 0.05$ ; \*\*  $p < 0.01$ ).*

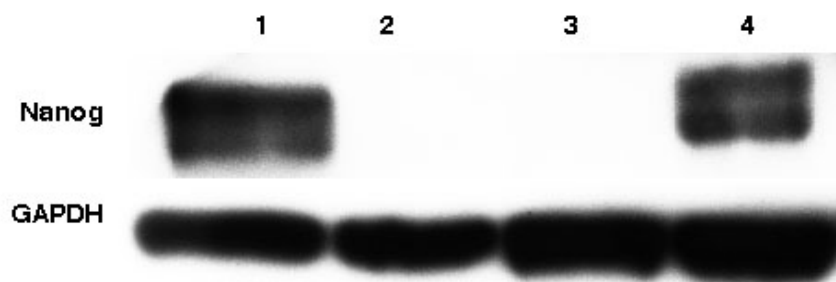


**Figure 53** *Nanog* expression in BMSCs nucleofected with *Nanog* vector. Western-blot

Western blot analysis of *Nanog* in *B mBMSCs*. 1, *mES*; 2, *B mBMSCs*; 3 *B mBMSCs* nucleofected with *pCMVIREES-GFP-WPRE*; 4 *B mBMSCs* nucleofected with *pCMVNanogIRES-GFP-WPRE*. The protein levels were normalized with respect to *GAPDH*, which was chosen as an internal control.

#### **7.4 Effect of over-expression and down-regulation of *Nanog* in *mBMSCs***

I assessed whether over- expression or down- regulation of *Nanog* affect cell migration. The motility of *BMSCs* was examined in a migration chamber in which the migrating cells in the insert chamber went through the poles on the membrane. The cells landing in the lower chamber or attaching on the other side of the membrane were stained and quantified by counting several fields. The results show that *Nanog* does not affect cell migration (Figure 43;  $p=0.35$  t-Test between untransfected and mock;  $p=0.76$  t-Test between untransfected and *pCMVGFP*;  $p=0.80$  t-Test between mock and *pCMVGFP*), whereas down regulation of *Nanog* enhances cell migration in a significant way.

In order to rationalise the effect of down- regulation of *Nanog* in *BMSCs* migration, I analyzed by real- time PCR expression of *CCL5* and *CXCL10*, two cytokines involved in *BMSC* migration (Honczarenko et al. 2006; Chamberlain et al. 2008; Lazennec et al. 2008). Real- time PCR data confirm that down- regulation of *Nanog* in *BMSCs* stimulates expression of these cytokines (t- Test

between pCMVIRE5-GFP-WPRE and pCMVantiNanogIRES-GFP-WPRE ( $p=0.01377$  for CCL5;  $p=0.022$  for CXCL10), whereas Nanog over expression does not affect expression of these genes (t- Test between pCMVIRE5-GFP-WPRE and pCMVNanogIRES-GFP-WPRE  $p=0.258$  for CCL5;  $p=0.320$  for CXCL10).

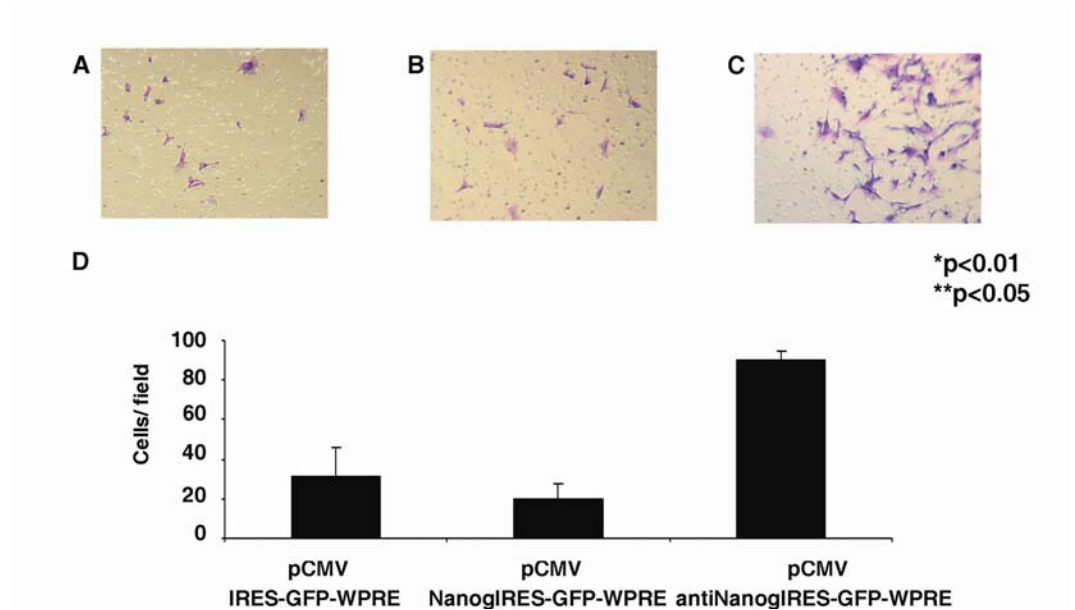


**Figure 54** Effect of over expression or down regulation of Nanog on cell migration

Crystal violet staining of chamber slides of mBMSC transfected with pCMVIRE5-GFP-WPRE (panel A), transfected with pCMVNanogIRES-GFP-WPRE (panel B) or with pCMVantiNanogIRES-GFP-WPRE (panel C) (original magnification 10X). Quantization of the number of migrated cells (panel D).

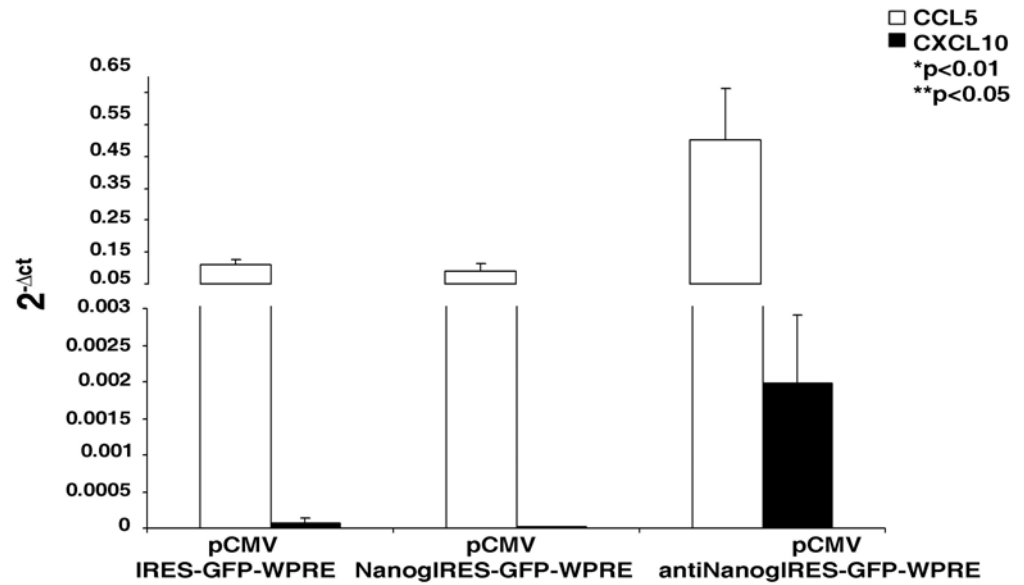


**Figure 55 CCL5 and CXCL10 expression in BMSCs**

mRNA levels were normalized with respect to GAPDH, chosen as an internal control. The histogram shows the mean expression values expressed as  $2^{-\Delta\Delta ct}$  ( $\pm SD$ ,  $n=3$ ) (\*  $p < 0.05$ ; \*\*  $p < 0.01$ ).

## **DISCUSSION**

### **Chapter 8**

In the present study, I have provided a characterization of four mBMSC subpopulations enriched through distinct culture conditions and showing different immunophenotype, self-renewal ability and differentiation potential.

In the recent years, BMSCs have generated a great deal of interest as potential source of cells for therapy as several papers have suggested a function in tissue repair by migration-differentiation (Bianco et al. 2001; Jiang et al. 2002; Anjos-Afonso et al. 2004; Kawada et al. 2004; Lemoli et al. 2005), by fusion (Ferrari et al. 1998; Wagers et al. 2004), by provision of a stromal support network (Caplan et al. 2006; Schenk et al. 2007) or mediated by their immunosuppressive abilities (Aggarwal et al. 2005; Le Blanc et al. 2005; Uccelli et al. 2008). Indeed, involvement of BMSCs has been demonstrated in the regeneration of a number of organs and tissues including bone (Lieberman et al. 1998; Olmsted et al. 2001; Gafni et al. 2004), skin (Fu et al. 2009), liver (Khurana et al. 2007), kidney (Choi et al. 2008), muscle (Ferrari et al. 1998; Gussoni et al. 1999; Ferrari et al. 2001) and infarcted myocardium (Orlic et al. 2001).

These observations, together with the possibility to obtain these cells from biopsies, escaping the ethical issue concerning embryonic stem cells, make them one of the most promising therapeutic tools of this century (for a review of clinical trials employing BMSCs see Le Blanc et al. 2005; Giordano et al. 2007 and [www.clinicaltrial.gov](http://www.clinicaltrial.gov)).

Nevertheless, the ability to move forward their use in therapy is impeded by the inability to definitively identify and characterize this population in a simple

mammalian model, such as the mouse and also by the lack of information regarding their biology, their *in vivo* role and factors involved in senescence and tumorigenic potential. BMSC, in fact is a cell type better studied and characterized in humans than in mouse and, although in the last few years numerous protocols have been developed to isolate these cells, some problems still remain (Baddoo et al. 2003; Meirelles Lda et al. 2003; Sun et al. 2003; Peister et al. 2004; Tropel et al. 2004; Wang et al. 2006) most of the published papers lack optimization of culture conditions to obtain a high number of specific progenitors, maintaining the same characteristic for many passages without acquisition of tumorigenic potential (Serakinci et al. 2004; Rubio et al. 2005; Miura et al. 2006; Li et al. 2007; Tolar et al. 2007; Rubio et al. 2008).

## **8.1 Culture expansion of mBMSCs from C57bl/6 mouse bone marrow**

In this work I described a protocol to isolate BMSCs from C57bl/6 mice, as this strain is frequently used to prepare transgenic mice. The yield in CFU-F obtained from C57bl/6 mice has already been reported to be very low compared to other strains such as Balb/c, FVB/N and DBA (Phinney et al. 1999; Peister et al. 2004). When I tried to isolate and expand mBMSC from C57Bl/6 mice using complete medium without any supplements, the few adherent cells obtained after the incubation period were not able to proliferate even when I sub-cultured them in another plate. Starting from the observation that use of bone fragment-conditioned medium favors BMSCs growth (Sun et al. 2003), I devised the conditions that selected the subpopulations described as BF and EP. As it is well known that mBMSCs expand very poorly (Baddoo et al. 2003; Meirelles Lda et al. 2003; Sun

et al. 2003; Peister et al. 2004; Tropel et al. 2004; Wang et al. 2006), after 2 weeks of culture, I cultured a part of these cells, named EP mBMSCs, in complete medium supplemented with EGF and PDGF-AA (Colter et al. 2001; Tropel et al. 2004; Kratchmarova et al. 2005); on the other hand, I maintained BF mBMSCs in complete medium with no additional components. Surprisingly, in spite of the above cited considerations, I observed an expansion of BF mBMSCs. These results led us to hypothesize that a specific bone marrow derived microenvironment could be responsible for the selection and maintenance of mesenchymal progenitors. I therefore decided to evaluate whether conditioned media obtained from MS-5 (Issaad et al. 1993) and NIH3T3 cell lines (Burroughs et al. 1994) could mimic the properties of bone marrow microenvironment. To this aim, I grew MS-5 and NIH3T3 in the same medium (see Chapter 4, section 4.2.2) in order to minimize any difference between the conditioned media harvested from these cell lines, that differ only in the molecules secreted from each individual line. Using the above-mentioned conditioned media I was able to efficiently culture mBMSC. I therefore hypothesized that one of the main determinant for a successful isolation and expansion of mouse mesenchymal progenitors were the growth supplement adopted for the isolation and expansion. Immunophenotypical characterization of BMSC subpopulations showed in each case profiles compatible with BMSCs (Lai et al. 1998; Deans et al. 2000). Interestingly, I observed differences in CD117, CD13 and H2-k<sup>b</sup> expression (Table 5). All cultures were positive to Sca I, the hallmark of hematopoietic and mesenchymal progenitor cells (Holmes et al. 2007) and CD44 which bridges the cells to hyaluronan and osteopontin (Avigdor et al. 2004) and is involved in BMSC- T-cell interaction (Aggarwal et al. 2005; Uccelli et al. 2007; Uccelli et al. 2008) (Figure 12).

Some papers have reported Sca I expression typical of haematopoietic stem cells (HSC) (Holmes et al. 2007) and higher in BMSCs from C57Bl/6 compared to Balb/c mice (Peister et al. 2004). As this antigen is trypsin sensitive (Meirelles Lda et al. 2003), this variability could be also associated to the type of treatment used to detach the cells. As also suggested by Mereilles (Meirelles Lda et al. 2003) our data confirm that usage of accutase from Stemcell technology allows us to avoid the cleavage of this antigen from cell surface.

EP mBMSCs showed two populations regarding CD13 expression (Figure 12); as mentioned in Chapter 4, section 4.2.1, EP mBMSCs were treated with EGF and PDGF, so it is likely that these cytokines contributed to this phenotype, as they expanded subpopulations of mBMSC which expressed EGF and PDGF receptors (Satomura et al. 1998; Colter et al. 2000; Colter et al. 2001).

BF and M mBMSCs were negative to H-2k<sup>b</sup>, the major histocompatibility complex of class I, so suggesting a typical feature of very early progenitors known as mMAPC (Jiang et al. 2002).

After an initial lag phase of about 10-17 days (Figure 11), these cells started to proliferate showing different growth kinetics (Figure 12). Cell cycle analysis confirmed a small difference in the percentage of cells in G1, S or G2 phase among the four groups, according to the differences in doubling time (Figure 13, Figure 14).

One of the most common observation in a large number of papers is that culture-expanded hBMSC usually stop proliferating before or at 40 population doublings (PD's) (at least 60 for mBMSCs (Tropel et al. 2004)), at which time the cells lose spindle-shaped fibroblastic morphology, become bigger and more flattened and accumulate SA- $\beta$ -Gal in cytoplasm (Bruder et al. 1997; Stenderup et al. 2003; Ito et al. 2007; Shibata et al. 2007; Ryu et al. 2008; Wagner et al. 2008). A

phenomenon largely associated with senescence *in vitro* (Hayflick 1965; Dimri et al. 1995; Sethe et al. 2006). In contrast to these studies, during the observation period (30 passages) I did not observe any signs of cellular senescence such as absence of mitotic activity (Figure 13, Figure 14) accumulation of cellular debris or increase in expression of SA- $\beta$ - galactosidase (Figure 15). These data were very surprising as an increase in the number of senescent cells, assessed by SA-  $\beta$ - Gal staining was reported both for human (Ito et al. 2007; Shibata et al. 2007; Ryu et al. 2008; Wagner et al. 2008) and rat BMSCs (Galderisi et al. 2008). As the cellular senescence is one the tumor suppressor functions of normal cells (Sharpless et al. 2007), to further investigate the characteristics of these subcultures and exclude the acquisition of a tumorigenic potential, I analyzed their DNA content, the expression of telomerase and the ability to form tumor in mice after 30 passages in culture.

Analysis of cell cycle after 30 passages showed a slight increase in the number of cells in G1 phase and a decrease in S phase for EP and BF mBMSCs (Figure 16, Figure 17). No differences in terms of cells in G1, S or G2 phase were observed between early (10-15) and late (35-40) passages in N BMSCs, suggesting that the NIH3T3 conditioned medium could contain cytokines involved in the suppression of cellular senescence and maintenance. One of this could be FGF-2. It has been already shown that NIH3T3 express FGF- 2 (Quarto et al. 2005). This cytokine has been considered one of the most important mitogens for human (Bianchi et al. 2003; Choi et al. 2008) and murine BMSCs (Sun et al. 2003) because it is able to maintain the cells in an immature state during *in vitro* expansion; recently Ito et al. have also demonstrated that FGF-2 is able to suppress the cellular senescence through down-regulation of TGF- $\beta$ 2 (Ito et al. 2007).

Considering the results obtained for EP, BF and N BMSCs jointly, they confirm the maintenance of a euploid karyotype over a period of 30 passages. Different results were obtained with M BMSCs, which showed an aneuploid karyotype at late passages (Figure 16).

Chromosomal alterations in BMSCs are very often associated with the activation of telomerase activity *in vitro* (Serakinci et al. 2004; Rubio et al. 2005; Miura et al. 2006; Rubio et al. 2008) and tumorigenic potential *in vivo* (Serakinci et al. 2004; Rubio et al. 2005; Miura et al. 2006; Zhou et al. 2006; Rubio et al. 2008). For these reason I decided to analyze expression of telomerase in mBMSCs and their ability to form tumor *in vivo*.

Telomerase activity has been found in almost all human tumors but not in normal cells (Kim et al. 1994) and maintenance of telomere stability is required for bypassing senescence and for the long-term proliferation of the cells. Indeed, ectopic expression of hTERT can immortalize hBMSCs, maintaining their proliferative and differentiation ability (Shi et al. 2002; Simonsen et al. 2002) and, in conjunction with additional events usually implying an oncogene deregulation such as KRAS (Serakinci et al. 2004) and c-myc, (Rubio et al. 2005; Miura et al. 2006; Zhou et al. 2006; Tolar et al. 2007; Rubio et al. 2008), produce cell transformation (Serakinci et al. 2004; Rubio et al. 2005; Miura et al. 2006).

TRAP assay did not show any significant telomerase expression in BMSCs (Figure 18) in accordance to some published papers (Simonsen et al. 2002; Stenderup et al. 2003). This finding confirms that BMSCs, even without showing dramatic changes in proliferative activity or cellular metabolism after 20 passages *in vitro*, do not activate telomerase expression.

In order to exclude that these subpopulations contained transformed cells I tested their tumorigenicity *in vivo*. When mBMSCs were subcutaneously injected in

nude mice, no animals developed a tumour within 2 months, demonstrating that these BMSCs were free of transformed or tumorigenic cells.

## **8.2 Culture condition select mBMSCs with different differentiation potential**

As for the differentiation potential, in two of the four conditions, BF and M, cells showed tri-potential differentiation ability, giving rise to osteoblasts, chondrocytes and pre-adipocytes, whereas EP cells lost adipogenic potential, probably during the first passages (Digirolamo et al. 1999). Interestingly, we observed that the ability to differentiate in pre-adipocytes was typical of BF and M BMSCs, which are negative to the major histocompatibility complex of class I (H2-k<sup>b</sup>), a typical characteristic of mMAPCs (Jiang et al. 2002). Moreover, the ability to differentiate in hypertrophic chondrocytes was typical of EP and M BMSCs, which showed lower expansion profiles than the other subpopulations (Figure 13). We speculate that this data could be partially due to the effect of EGF on these cells. The EGF, added directly to EP BMSCs and contained in MS-5 conditioned medium (Issaad et al. 1993) could act not only as mitogen in mesenchymal proliferation (Tropel et al. 2004), but also as a stimulator of osteogenic differentiation (Kratchmarova et al. 2005). This effect could account for the high chondrogenic-osteogenic potential of these cells.

On the other hand, using NIH3T3 conditioned medium, I obtained cells that showed impairment in osteogenic and chondrogenic differentiation, whereas retaining a very high adipogenic potential during passages. We hypothesized that this could be the result of NIH3T3 conditioned medium exposition. Therefore, in order to address this behavior, I switched the N BMSC cells into standard growth

medium for ten passages. I was not able to appreciate any significant recovery of osteogenic potential (Figure 32, Figure 33), which leads to the conclusion that this effect was not reversible. In the attempt to identify cytokines possibly responsible for this behaviour, we focused our attention on LIF (Falconi et al. 2007). It has been recently observed that LIF is responsible for blocking osteoblast maturation at late differentiation stages and redirecting these cells toward the adipogenic pathway (Falconi et al. 2007; Falconi et al. 2007) I speculate that in N BMSC model, LIF could suppress the osteoblast maturation at late differentiation stages (Falconi et al. 2007; Falconi et al. 2007), contributing to the selection of adipogenic progenitors from bone marrow by stimulating the expression of proteins involved in PPAR $\gamma$  expression such as C/EBP $\beta$  and C/EBP $\delta$  (Hogan et al. 2005; Falconi et al. 2007).

RT-PCR data confirmed that the mBMSCs constitutively express some osteoblastic lineage markers such as CbfaI/Runx2, Collagen I and osteopontin (Figure 26) and chondrogenic markers such as Sox-9 and Collagen XI (Figure 29). Expression of these lineage markers in undifferentiated cells is not surprising (Mackay et al. 1998; Karsenty et al. 2002; Tropel et al. 2004; Goldring et al. 2006; Rosen et al. 2006; Murdoch et al. 2007) and could be explained by two different hypotheses. In a classical model of differentiation, there could be a spontaneous and continuous generation of lineage restricted progenitors from stem cells (Dennis et al. 2002) (Figure 6, MSC compartment). Gene-lineage repression could be the common regulatory mechanism of mesenchymal lineage differentiation, so, according to this model, expression of the master regulatory genes Cbfa I/Runx2, C/EBP $\alpha$  and PPAR $\gamma$ 2 or Sox 9 could be not sufficient to induce, respectively, osteogenic, adipogenic and chondrogenic differentiation of mBMSCs; factors of one lineage repress factors of the other lineages, thereby

maintaining the undifferentiated state (Hong et al. 2005). However, under appropriate conditions, the balance can be tipped leading to a cascade that promotes one cell fate while repressing other possible fates. Alternatively, these results could be explained by “the chiaroscuro model” described by Quesenberry et al. (Quesenberry et al. 2002) on available data concerning haematopoietic stem cell physiology. In this model, (Figure 6, differentiation compartment), cells from a wide stem cell compartment oscillate between different states of differentiation competencies. Consequently, a cell may express lineage-specific genes (similarly to a unipotent progenitor) and its progeny may present a stem cell phenotype. This model underlies great cell plasticity, which is a major BMSC property (Wagers et al. 2004; Lemoli et al. 2005). As an example, bone marrow adipocytes can dedifferentiate and re-differentiate towards adipocytic or osteoblastic pathways (Park et al. 1999).

### **8.3 BMSCs express the homeodomain gene Nanog**

A very interesting feature of all the BMSC subpopulations isolated was the expression of a well-known marker of undifferentiated embryonic stem cells, Nanog (Chambers et al. 2003; Mitsui et al. 2003; Boiani et al. 2005) (Figure 21Figure 22).

Initially I analyzed Nanog expression by RT-PCR: at day 0 Nanog is expressed in all the BMSC groups. At day 21 I observed the expression of Nanog only in EP BMSCs. As BMSCs are able to spontaneously differentiate along mesenchymal lineages during the time in culture, I believe that at day 21 BF, M and N mBMSCs differentiate and lose expression of a stemness marker such as Nanog. The maintenance of the expression of Nanog in EP mBMSC at day 21 can be due to culture conditions used to expand these cells. As reported in Chapter 4, section

4.2.1, EP mBMSCs were treated with EGF and PDGF. Very recently, a link between PDGF and Nanog expression was elucidated: PDGF induces phosphorylation of p68 that binds to  $\beta$  catenin, allowing its nuclear localization; in this way it can up-regulate the expression of Nanog (He 2006; Yang et al. 2006; Takao et al. 2007). Immunofluorescence data confirm the nuclear localization of Nanog in BMSCs (Figure 22).

Although the role of Nanog in adult tissue stem cells remains unclear, it is possible that it enhances self-renewal of tissue stem cells. In the last two years, many papers have shown that the introduction of the transcription factors, Sox2, Oct4, KLF-4 and c-myc, into adult somatic cells resulted in the generation of induced pluripotent stem cells (iPS) (Takahashi et al. 2006). These results have suggested that the over-expression of these genes in BMSCs can improve the quality of these cells, in terms of stemness, or promote their proliferation. The homeodomain gene Nanog is not one of the four genes, however, its functional importance was evident by the fact that up regulation of the Nanog gene is critical for reprogramming the cell (Okita et al. 2007).

Several groups (Anjos-Afonso et al. 2007; Battula et al. 2007; Beltrami et al. 2007) have demonstrated expression of Nanog in BMSCs; however its role in these cells is still unknown. Very recent studies of Go et al. and Liu et al. have shown an effect of Nanog on proliferation and osteogenic and chondrogenic abilities (Go et al. 2008; Liu et al. 2008), however, nobody of them tested the effect of Nanog in cell migration and in the balance between senescence, apoptosis and tumorigenesis.

During a six-month period as visitor in the lab of Dr Nicole Horwood I constructed and tested in BMSCs the efficacy of vectors expressing Nanog sense

and antisense to employ in experiments of Nanog over- expression and down-regulation in BMSCs.

As strategy to mediate expression of Nanog in BMSCs, I used a non viral transfection method, the nucleofection technology of Amaxa System, which has been already used in BMSC transfection (Lakshmipathy et al. 2004; Aluigi et al. 2006). After 24 hours from transfection 52.39% of cells resulted GFP positive with mean cell viability of 97.3% and an overall recovery of  $120\% \pm 30\%$  for cells treated with no DNA and  $88.4\% \pm 15.2\%$  for cell treated with pCMV-GFP (Figure 39). These results are very satisfying compared to other transfection methods. Cell survival was reported to be less than 50%, 35-40% and 40% with lipofectamine 2000 (Hoelters et al. 2005), electroporation (Helledie et al. 2008) or nucleofection (Aluigi et al. 2006) respectively, whereas, with the same methods, transfection efficiency, measured as GFP positive cells, was reported to be 50%, 30% and 28%. Time course analysis confirms that GFP levels declined over time, according to the transient nature of plasmid-based transfection. Afterward, the introduction of DNA in BMSCs did not affect proliferation (Figure 41), senescence (Figure 42) and migration (Figure 43) and the percentage of GFP positive cells was still as high after one week (Figure 40), according to the hypothesis that as the DNA is delivered into the nucleus and is not retained in the cytoplasm after the transfection, it could be less subjected to degradation (Hamm et al. 2002). These results allowed me to perform some experiments which required just a transient over expression or down regulation of Nanog.

Preliminary data suggest that down-regulation of Nanog enhances migration ability (Figure 54), and induces an increase in the expression of CCL5 (Rantes) and CXCL10 (IP10, interferon  $\gamma$  inducible protein-10)

(

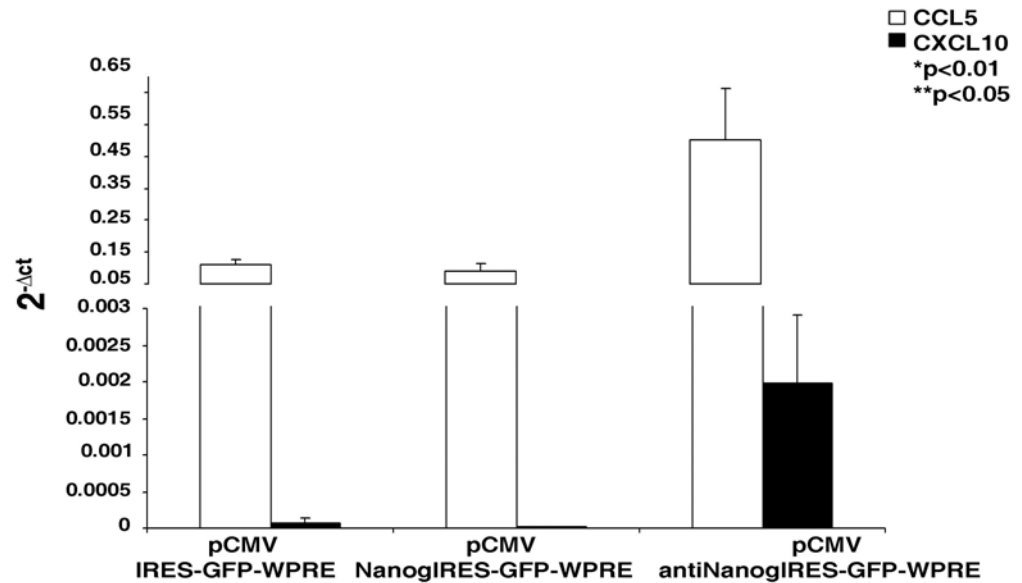
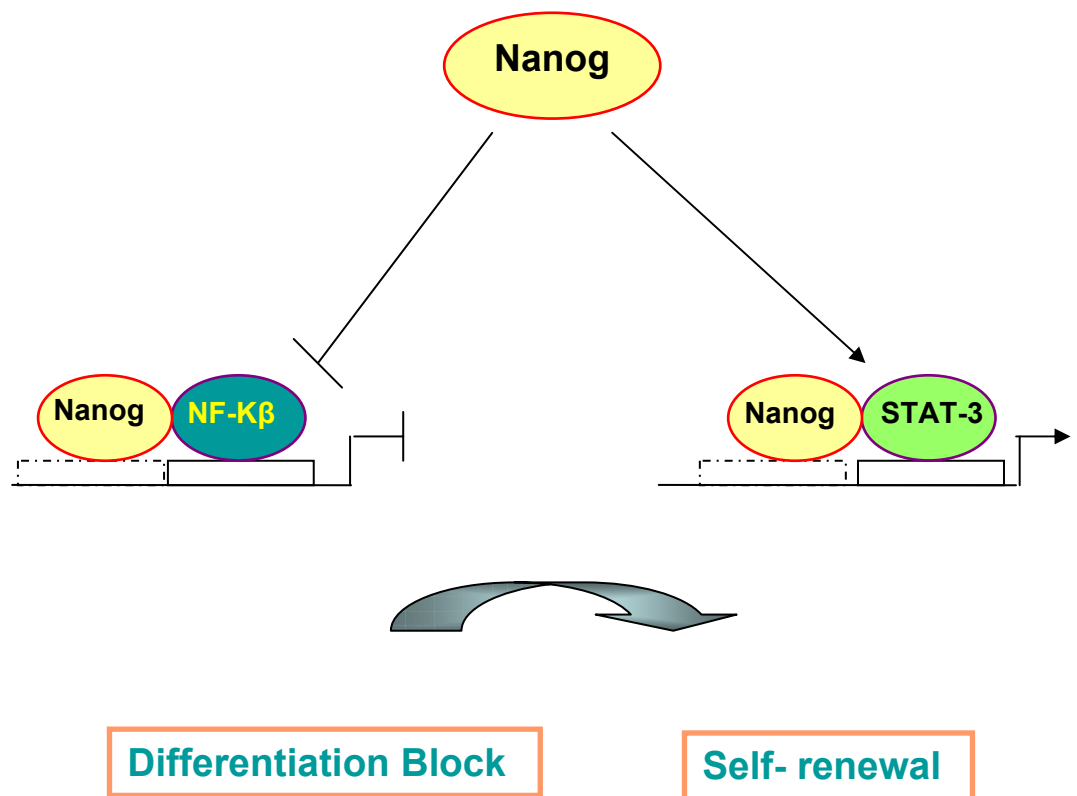


Figure 55), which have been reported to enhance motility, invasion and metastasis of breast cancer cells (Karnoub et al. 2007) and to have a potent thymus-dependent antitumoral effect (Luster et al. 1993). Very recent micro-array data gave some insights in specific Nanog target genes in BMSCs (Liu et al. 2008). According to these data, Nanog over expression induces 1.5 fold increase in CCL5 expression (Liu et al. 2008), in contrast with my results. Notably, CCL5 and CXCL10 have also shown to be direct targets inhibited by STAT-3 (McLoughlin et al. 2005) and activated by NF- $\kappa$ B (Yang et al. 2007); Nanog has been shown to be able to cooperate with NF- $\kappa$ B and STAT-3 by protein– protein interaction (Narayanan et al. 1993; Pan et al. 2005; Torres et al. 2008). So we hypothesize that the effect of Nanog on CCL5 and CXCL10 could be indirect and mediated by STAT3 or NF- $\kappa$ B (Figure 56).

On the other hand, over-expression of Nanog does not affect cell proliferation (Figure 58) or reduce the number of senescent cells (Figure 59), however Nanog over-expressing cells show a decrease in p53 expression, a well known tumor-suppressor gene (Campisi et al. 2007; Serrano et al. 2007; Sharpless et al. 2007) (Figure 60) and acquire the ability to grow in soft agar (Figure 61), an *in vitro* hallmark of tumorigenic cells (Freedman et al. 1974).

Several papers have elucidated expression of Nanog in different tumors, such as germ cell tumors, (Hart et al. 2005) breast tumors (Ezeh et al. 2005) and bone sarcomas, (Gibbs et al. 2005) leading to the identification of tumor-stem-like cells expressing the key molecular machinery of embryonic stem cells. Indeed other two papers suggest a potential oncogenic role for Nanog in NIH3T3 and HSCs (Piestun et al. 2006; Tanaka et al. 2007).



**Figure 56 Model of interaction among Nanog, STAT3 and NF-Kb**

*Interaction of Nanog with STAT-3 can activate this molecule in its activity as activator or repressor of specific target genes. Interaction of Nanog with NF-Kβ has a negative effect on the activity of this protein, which repress genes involved in ES self-renewal.*

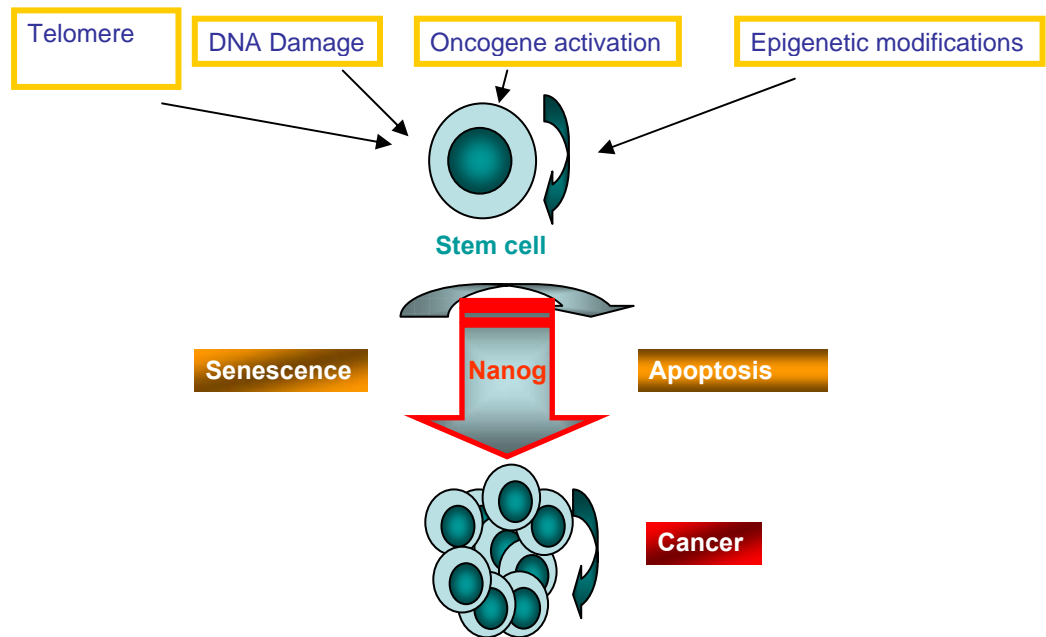


**Figure 57 "Cancer stem cell hypothesis" for BMSCs**

Normal signalling influences the proliferation and renewal of stem cells (dark blue) during development of a variety of tissues. Different stressful stimuli such as telomere shortening, DNA damage, oncogene activation and epigenetic modifications can induce senescence or apoptosis. Uncontrolled signalling (dark blue arrow) can lead to constitutive renewal in spite of accumulated DNA damage, leading to aberrant expansion of the stem cell pool. These changes can, in turn, lead to formation of cancerous tissues.

## 8.4 Conclusions and Future Perspectives

The work described reports the isolation and the enrichment of specific progenitors from C57bl/6 mice bone marrow using cytokines, bone marrow derived fragment, MS5 and NIH3T3 conditioned medium. These data suggest that the use of appropriate conditioned media can determine the obtainment of a large number of desired cells for large scale transplantations or cell therapies. In the

near future the identification of growth factors regulating the survival rate, the self-renewal, the lineage differentiation will be crucial for the understanding of BMSCs biology and for their safe application in clinical settings. In the attempt to analyze potential factors involved in BMSC self-renewal I focused my attention on the homeodomain gene Nanog. Preliminary data concerning Nanog down regulation and over expression show a potential role for Nanog in migration and tumorigenesis. Data obtained by the transient transfection system of Amaxa did not allow me to observe a significant change in proliferative abilities of the cells, as already shown by Go et al. and Liu et al. (Go et al. 2008; Liu et al. 2008), or in the number of senescent cells. Transgene expression declined over time and transfection efficiency did not reach 100%. We plan to use lentiviruses in order to obtain a long-lasting expression and high infection efficiency in BMSCs (Zhang et al. 2002; Zhang et al. 2004; Ricks et al. 2008). I have already cloned Nanog cDNA in sense and antisense orientation in a vector containing the backbone of a self-inactivating lentiviral vector (Zhang et al. 2002; Zhang et al. 2004; Ricks et al. 2008). Lentivirus work will allow us to better investigate the effects of Nanog in BMSCs both *in vitro* than *in vivo*, unravelling the role of Nanog in the balance between apoptosis, senescence and tumorigenesis (Figure 57). This work is vital for our understanding of how levels of Nanog affect BMSC properties as these cells are being widely used in clinical trials for the treatment of GVHD, myocardial infarction and cartilage degeneration (Giordano et al. 2007).

## **Appendix**

### **Chapter 9**

#### **Effect of Nanog over-expression on BMSC tumorigenesis**

##### **9.1 Effect of Nanog over expression on cell proliferation**

I tested the proliferation of BMSCs over expressing Nanog compared to mock (no DNA) and pCMVIRE5-GFP-WPRE transfected cells. Twenty-four hours after transfection, mBMSCs were seeded at  $1 \times 10^4$  cells each well of a 6 well- plates and after 3, 6 and 10 days, cell numbers were determined from three wells of each culture, as described in Chapter 4, section 4.16. No effects were observed during the time course. The results indicated that Nanog over expressing cells have no advantage in cell proliferation compared to cells transfected with no DNA or with the mock vector (Figure 58).

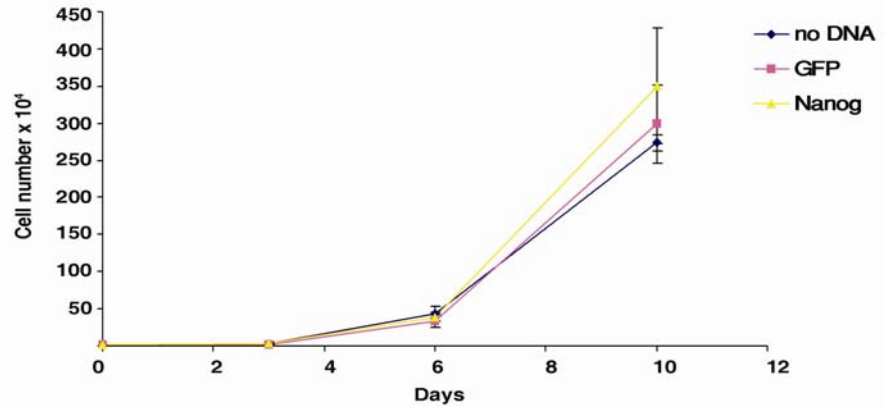


**Figure 58 Growth kinetic of BMSCs over expressing Nanog**

Cell number was evaluated by counting cells with a hematometer in triplicates. Blue line: mBMSCs nucleofected with no DNA; pink line: mBMSCs nucleofected with pCMVIRESGFP-WPRE; yellow line: mBMSCs nucleofected with pCMVNanogIRES-GFP-WPRE.

## 9.2 Effect of Nanog over-expression on cellular senescence

I evaluated the effect of over expression of Nanog on cellular senescence. Twenty-four hours after transfection, mBMSCs were seeded at  $10^4$  cell/cm<sup>2</sup> in six-well plates, and after 3 days, the cultures were assayed for SA- $\beta$ -Galactosidase expression, as described in Chapter 4, section 4.6. As shown in Figure 59, Nanog over expressing cells gave similar results in terms of SA- $\beta$ -Galactosidase positive cells compared to both controls (cells transfected with no DNA and pCMVIRESGFP-WPRE), indicating that the over expression of Nanog does not have an effect on cellular senescence.

In order to better analyze the behaviour of Nanog over expressing cells I analyzed by real time PCR expression of p53 and pRB, which are the principal mediators of senescence and apoptosis (Campisi et al. 2007; Serrano et al. 2007; Sharpless et al. 2007). Real time data show a statistically significant slight reduction in p53 expression of BMSCs over expressing Nanog ( $p=0.0008$ ), whereas pRB is not affected ( $p=0.304$ ) (Figure 60).

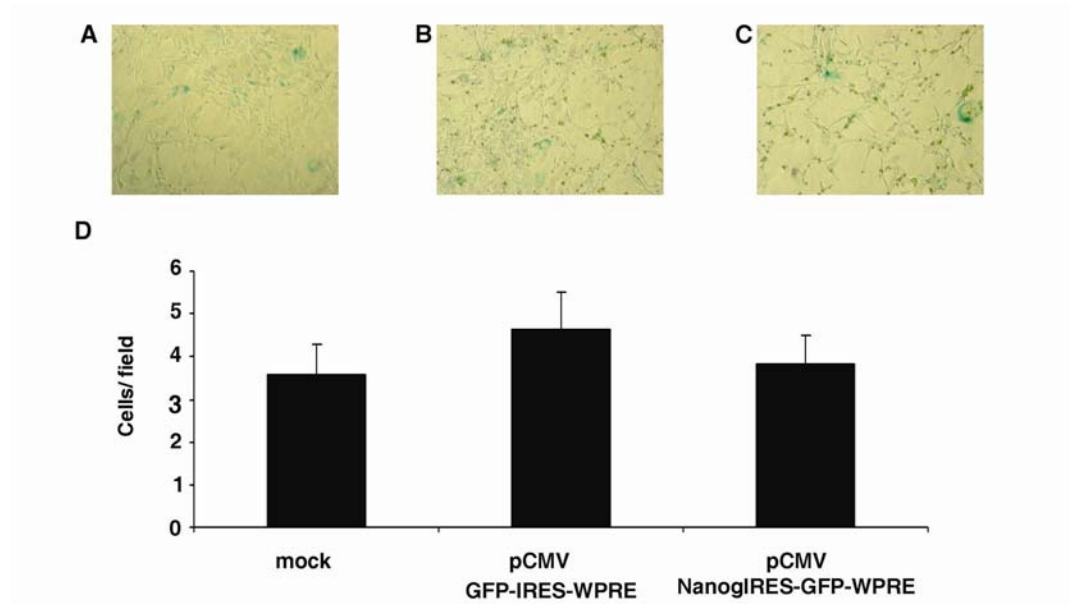


**Figure 59 Effect of over expression of Nanog on cellular senescence**

*B gal staining of BMSCs transfected with no DNA (panel A) pCMV-IRES-GFP-WPRE BMSCs (panel B) and pCMV-Nanog-IRES-GFP-WPRE (panel C). Original magnifications 10X. Quantization of  $\beta$  gal positive cells (panel D).*

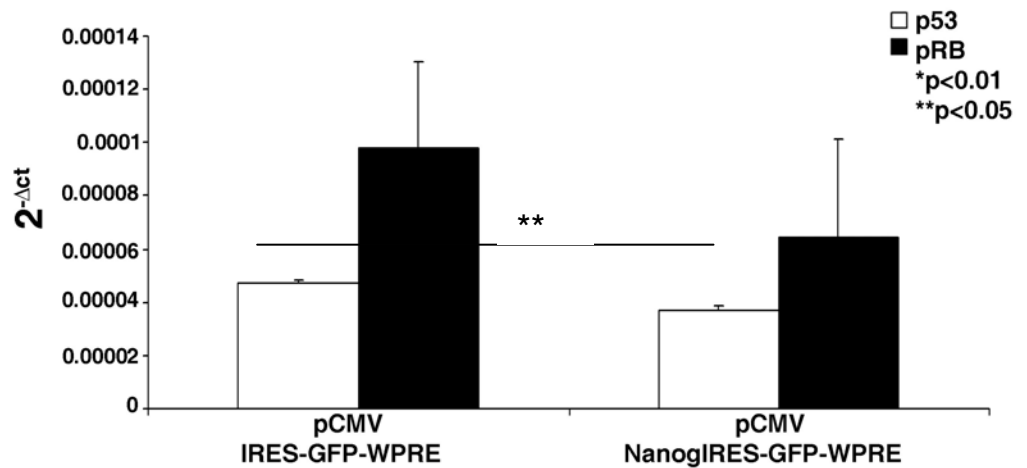


**Figure 60 Nanog effect on p53 and pRB expression**

*Real Time-PCR analysis. mRNA levels were normalized with respect to GAPDH, chosen as an internal control. Histograms show mean expression values ( $\pm$  SD, n=3; \* p < 0.05; \*\* p < 0.01).*

### **9.3 Effect of Nanog over-expression on acquisition of tumorigenic ability**

p53 is a well known tumor suppressor and a crucial mediator of cellular responses to DNA damage, including the senescence response (Campisi et al. 2007; Serrano et al. 2007; Sharpless et al. 2007). A reduction in p53 level could be extremely dangerous for cells, because it can provide the cells with the ability to escape from senescence and apoptosis, leading to a tumorigenic transformation (Pelicci 2004; Sharpless et al. 2004; Rubio et al. 2005; Rubio et al. 2008). For this reason I decide to investigate the effect of Nanog over expression on BMSCs tumorigenesis. As readout of acquisition of tumorigenic ability, I assessed colony formation in soft agar (Freedman et al. 1974). A549, lung adenocarcinoma cell line was used as positive control (Sithanandam et al. 2005). A549 cells, Nanog over expressing BMSCs, mock (no DNA) and pCMVIRE5-GFP-WPRE transfected BMSCs were suspended in medium containing 0.3% low melting agarose at a density of  $10^5$  cells/dish and layered on medium containing 0.5% agarose. After two weeks I analyzed the number of colonies. As expected A549 cells formed a huge number of big colonies, whereas no colony formation was observed in mock (no DNA) and pCMVIRE5-GFP-WPRE transfected BMSCS (Figure 61). Notably, over-expression of Nanog in BMSCs induced acquisition of ability to grow in soft agar (Figure 61). This result confirms the hypothesis that Nanog could transform BMSCs.

Nanog is able to up-regulate expression of Sox2 and Oct4 in ES cells (Boiani et al. 2005). Aberrant expression of these pluripotency-associated genes has been shown to be closely associated with aggressive cancer progression (Ezeh et al. 2005; Gibbs et al. 2005; Bourguignon et al. 2008). I decided to investigate

expression of these genes in Nanog over expressing cells by Real time PCR. As shown in figure there is no significant increase in Oct4 ( $p= 0.102$ ) and Sox2 ( $p= 0.078$ ) mRNA in response to Nanog over expression (Figure 62), leading to the hypothesis that these promoters could be no accessible to Nanog in BMSCs.

To further analyze the potential tumorigenic role of Nanog in BMSCs, I analyzed by real time PCR expression of two genes commonly associated with BMSCs tumorigenicity such as c-myc (Rubio et al. 2005; Miura et al. 2006; Zhou et al. 2006; Tolar et al. 2007; Rubio et al. 2008) and TERT (Kim et al. 1994; Serakinci et al. 2004; Rubio et al. 2005; Miura et al. 2006; Serakinci et al. 2006). Real time data show no difference in the expression of c-myc ( $p= 0.054$ ) and TERT ( $p=0.067$ ) in control and Nanog over expressing cells (Figure 62).

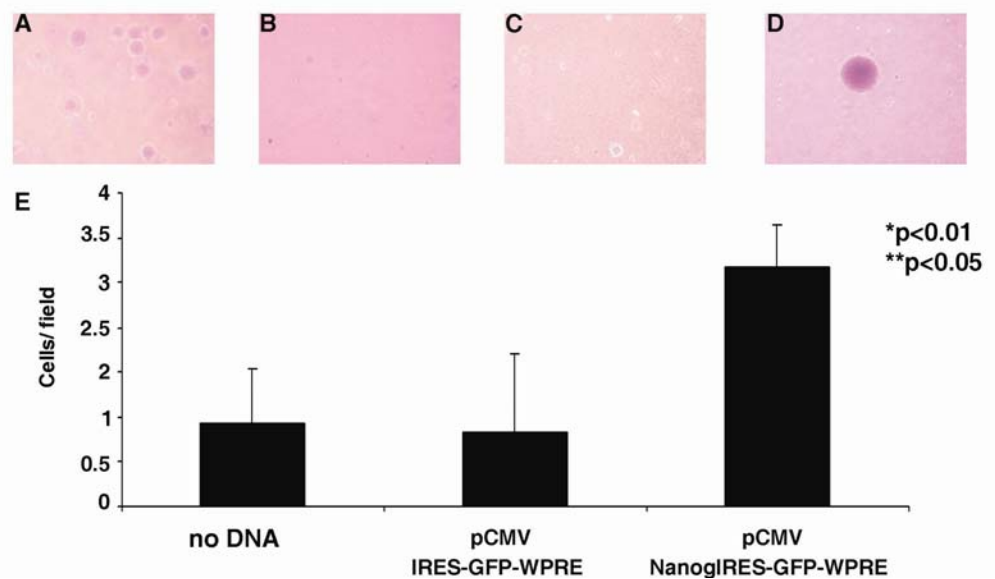


**Figure 61 Anchorage independent-growth of BMSCs over-expressing Nanog**

Crystal violet staining of BMSCs transfected with no DNA (panel A), pCMV IRES-GFP-WPRE (panel B) and pCMV Nanog IRES-GFP-WPRE (panel C). Quantification of colonies (panel E; \*  $p < 0.05$ ; \*\*  $p < 0.01$ ).

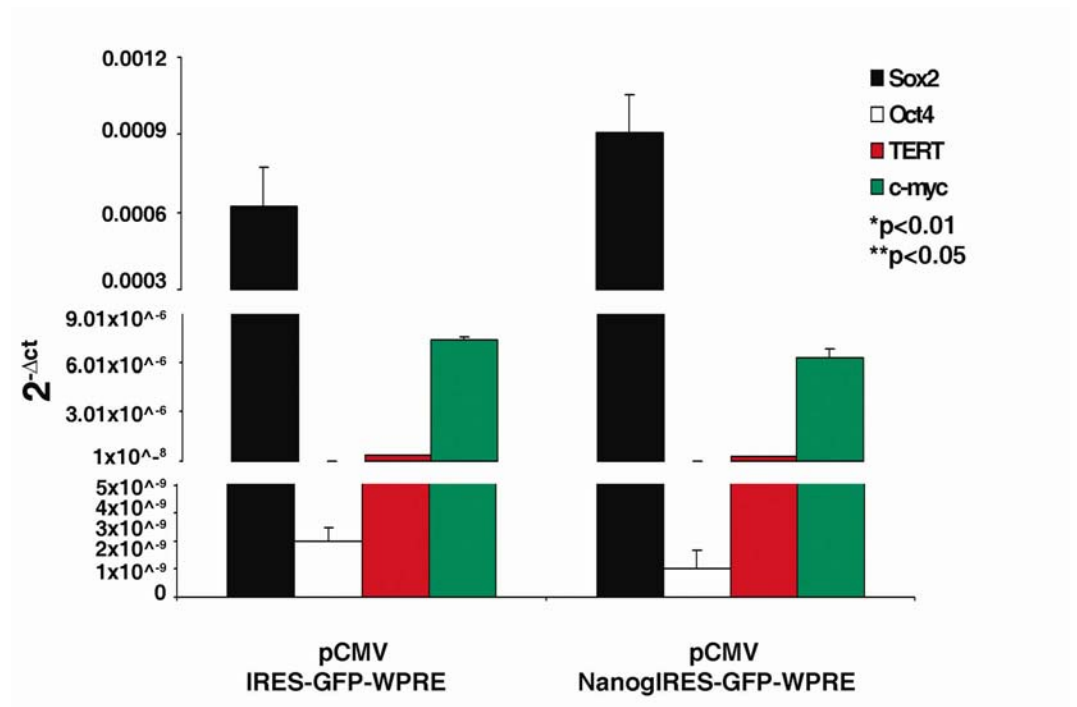


**Figure 62 Expression of Sox-2, Oct4, c-myc and TERT in BMSCs**

Real Time-PCR analysis. mRNA levels were normalized with respect to GAPDH, chosen as an internal control. Histograms show mean expression values ( $\pm$  SD,  $n=3$ ; \*  $p < 0.05$ ; \*\*  $p < 0.01$ ).

## **ACKNOWLEDGMENTS**

*Ringrazio i professori, ricercatori, segretarie, dottorandi, studenti e tutti i colleghi e gli amici che in questi anni mi sono stati vicini, lasciandomi ognuno un piccolo pezzo di loro stessi. Non potrò mai dimenticare i pomeriggi passati ad analizzare dati, sollevando quel criticismo che mi è sempre stato fedele compagno di vita; e tutte le volte che, invece, mi avete spinto a non fossilizzarmi nella ricerca di risposte definitive e a guardare con più serenità a quello che stavo facendo e ai risultati ottenuti. Non potrò mai ringraziare a sufficienza le persone che mi hanno ascoltato in tutti i momenti in cui ero triste e demoralizzata.*

*Ringrazio mia madre grazie alla quale ho appreso l'autonomia, il senso di responsabilità, e che mi ha dato l'esempio migliore per capire che non bisogna cedere mai, ma rialzarsi da ogni caduta, anche quella che sembri ti paralizzi al suolo. E le mie sorelle?*

*Si, vanno ringraziate per i loro vani tentativi di mantenere un po' di silenzio in casa quando avevo bisogno di concentrarmi nello studio.*

*Un grazie speciale va a Carlo, che ha avuto lo stomaco di leggere una tesi intera di dottorato, così tanto lontana dalla sua preparazione professionale.*

*Ma il grazie più sentito va a tutte quelle persone che con la loro superficialità, con il loro infantilismo, con la loro mancanza di rispetto per il lavoro e le responsabilità, hanno scosso la mia coscienza e mi hanno indicato, in maniera inequivocabile, qual è la direzione che non voglio prendere e quale persona non voglio diventare.*

## **REFERENCES**

- Aggarwal, S. and M. F. Pittenger (2005). "Human mesenchymal stem cells modulate allogeneic immune cell responses." Blood **105**(4): 1815-22.
- Aluigi, M., M. Fogli, et al. (2006). "Nucleofection is an efficient nonviral transfection technique for human bone marrow-derived mesenchymal stem cells." Stem Cells **24**(2): 454-61.
- Anjos-Afonso, F. and D. Bonnet (2007). "Nonhematopoietic/endothelial SSEA-1+ cells define the most primitive progenitors in the adult murine bone marrow mesenchymal compartment." Blood **109**(3): 1298-306.
- Anjos-Afonso, F., E. K. Siapati, et al. (2004). "In vivo contribution of murine mesenchymal stem cells into multiple cell-types under minimal damage conditions." J Cell Sci **117**(Pt 23): 5655-64.
- Avigdor, A., P. Goichberg, et al. (2004). "CD44 and hyaluronic acid cooperate with SDF-1 in the trafficking of human CD34+ stem/progenitor cells to bone marrow." Blood **103**(8): 2981-9.
- Avilion, A. A., S. K. Nicolis, et al. (2003). "Multipotent cell lineages in early mouse development depend on SOX2 function." Genes Dev **17**(1): 126-40.
- Baddoo, M., K. Hill, et al. (2003). "Characterization of mesenchymal stem cells isolated from murine bone marrow by negative selection." J Cell Biochem **89**(6): 1235-49.
- Battula, V. L., P. M. Bareiss, et al. (2007). "Human placenta and bone marrow derived MSC cultured in serum-free, b-FGF-containing medium express cell surface frizzled-9 and SSEA-4 and give rise to multilineage differentiation." Differentiation **75**(4): 279-91.

- Baxter, M. A., R. F. Wynn, et al. (2004). "Study of telomere length reveals rapid aging of human marrow stromal cells following in vitro expansion." Stem Cells **22**(5): 675-82.
- Beausejour, C. M., A. Krtolica, et al. (2003). "Reversal of human cellular senescence: roles of the p53 and p16 pathways." EMBO J **22**(16): 4212-22.
- Beltrami, A. P., D. Cesselli, et al. (2007). "Multipotent cells can be generated in vitro from several adult human organs (heart, liver, and bone marrow)." Blood **110**(9): 3438-46.
- Bianchi, G., A. Banfi, et al. (2003). "Ex vivo enrichment of mesenchymal cell progenitors by fibroblast growth factor 2." Exp Cell Res **287**(1): 98-105.
- Bianco, P., M. Riminucci, et al. (2001). "Bone marrow stromal stem cells: nature, biology, and potential applications." Stem Cells **19**(3): 180-92.
- Boiani, M. and H. R. Scholer (2005). "Regulatory networks in embryo-derived pluripotent stem cells." Nat Rev Mol Cell Biol **6**(11): 872-84.
- Boland, G. M., G. Perkins, et al. (2004). "Wnt 3a promotes proliferation and suppresses osteogenic differentiation of adult human mesenchymal stem cells." J Cell Biochem **93**(6): 1210-30.
- Bonab, M. M., K. Alimoghaddam, et al. (2006). "Aging of mesenchymal stem cell in vitro." BMC Cell Biol **7**: 14.
- Bourguignon, L. Y., K. Peyrollier, et al. (2008). "Hyaluronan-CD44 interaction activates stem cell marker Nanog, Stat-3-mediated MDR1 gene expression, and ankyrin-regulated multidrug efflux in breast and ovarian tumor cells." J Biol Chem **283**(25): 17635-51.
- Boyer, L. A., K. Plath, et al. (2006). "Polycomb complexes repress developmental regulators in murine embryonic stem cells." Nature **441**(7091): 349-53.

- Bruder, S. P., N. Jaiswal, et al. (1997). "Growth kinetics, self-renewal, and the osteogenic potential of purified human mesenchymal stem cells during extensive subcultivation and following cryopreservation." J Cell Biochem **64**(2): 278-94.
- Burroughs, J., P. Gupta, et al. (1994). "Diffusible factors from the murine cell line M2-10B4 support human in vitro hematopoiesis." Exp Hematol **22**(11): 1095-101.
- Campisi, J. (2000). "Cancer, aging and cellular senescence." In Vivo **14**(1): 183-8.
- Campisi, J. and F. d'Adda di Fagagna (2007). "Cellular senescence: when bad things happen to good cells." Nat Rev Mol Cell Biol **8**(9): 729-40.
- Cantz, T., G. Key, et al. (2008). "Absence of OCT4 expression in somatic tumor cell lines." Stem Cells **26**(3): 692-7.
- Caplan, A. I. (1991). "Mesenchymal stem cells." J Orthop Res **9**(5): 641-50.
- Caplan, A. I. and J. E. Dennis (2006). "Mesenchymal stem cells as trophic mediators." J Cell Biochem **98**(5): 1076-84.
- Castro-Malaspina, H., R. E. Gay, et al. (1980). "Characterization of human bone marrow fibroblast colony-forming cells (CFU-F) and their progeny." Blood **56**(2): 289-301.
- Cenkci, B., J. L. Petersen, et al. (2003). "REX1, a novel gene required for DNA repair." J Biol Chem **278**(25): 22574-7.
- Chamberlain, G., K. Wright, et al. (2008). "Murine mesenchymal stem cells exhibit a restricted repertoire of functional chemokine receptors: comparison with human." PLoS ONE **3**(8): e2934.
- Chambers, I., D. Colby, et al. (2003). "Functional expression cloning of Nanog, a pluripotency sustaining factor in embryonic stem cells." Cell **113**(5): 643-55.

- Chen, D., M. Zhao, et al. (2004). "Bone morphogenetic proteins." Growth Factors **22**(4): 233-41.
- Chen, L., T. Fink, et al. (2005). "Quantitative transcriptional profiling of ATDC5 mouse progenitor cells during chondrogenesis." Differentiation **73**(7): 350-63.
- Cho, Y. C. and C. R. Jefcoate (2004). "PPARgamma1 synthesis and adipogenesis in C3H10T1/2 cells depends on S-phase progression, but does not require mitotic clonal expansion." J Cell Biochem **91**(2): 336-53.
- Choi, S., M. Park, et al. (2008). "The role of mesenchymal stem cells in the functional improvement of the chronic renal failure." Stem Cells Dev.
- Choi, S. C., S. J. Kim, et al. (2008). "Fibroblast growth factor-2 and -4 promote the proliferation of bone marrow mesenchymal stem cells by the activation of the PI3K-Akt and ERK1/2 signaling pathways." Stem Cells Dev **17**(4): 725-36.
- Colter, D. C., R. Class, et al. (2000). "Rapid expansion of recycling stem cells in cultures of plastic-adherent cells from human bone marrow." Proc Natl Acad Sci U S A **97**(7): 3213-8.
- Colter, D. C., I. Sekiya, et al. (2001). "Identification of a subpopulation of rapidly self-renewing and multipotential adult stem cells in colonies of human marrow stromal cells." Proc Natl Acad Sci U S A **98**(14): 7841-5.
- D'Ippolito, G., S. Diabira, et al. (2004). "Marrow-isolated adult multilineage inducible (MIAMI) cells, a unique population of postnatal young and old human cells with extensive expansion and differentiation potential." J Cell Sci **117**(Pt 14): 2971-81.
- Deans, R. J. and A. B. Moseley (2000). "Mesenchymal stem cells: biology and potential clinical uses." Exp Hematol **28**(8): 875-84.

- Denker, A. E., S. B. Nicoll, et al. (1995). "Formation of cartilage-like spheroids by micromass cultures of murine C3H10T1/2 cells upon treatment with transforming growth factor-beta 1." Differentiation **59**(1): 25-34.
- Dennis, J. E. and P. Charbord (2002). "Origin and differentiation of human and murine stroma." Stem Cells **20**(3): 205-14.
- Di Bernardo, G., T. Squillaro, et al. (2008). "Histone Deacetylase inhibitors promote apoptosis and senescence in human mesenchymal stem cells." Stem Cells Dev.
- Digirolamo, C. M., D. Stokes, et al. (1999). "Propagation and senescence of human marrow stromal cells in culture: a simple colony-forming assay identifies samples with the greatest potential to propagate and differentiate." Br J Haematol **107**(2): 275-81.
- Dimri, G. P., X. Lee, et al. (1995). "A biomarker that identifies senescent human cells in culture and in aging skin in vivo." Proc Natl Acad Sci U S A **92**(20): 9363-7.
- Dobson, K. R., L. Reading, et al. (1999). "Centrifugal isolation of bone marrow from bone: an improved method for the recovery and quantitation of bone marrow osteoprogenitor cells from rat tibiae and femurae." Calcif Tissue Int **65**(5): 411-3.
- Ducy, P., C. Desbois, et al. (1996). "Increased bone formation in osteocalcin-deficient mice." Nature **382**(6590): 448-52.
- Ducy, P., R. Zhang, et al. (1997). "Osf2/Cbfa1: a transcriptional activator of osteoblast differentiation." Cell **89**(5): 747-54.
- Episkopou, V. (2005). "SOX2 functions in adult neural stem cells." Trends Neurosci **28**(5): 219-21.

- Etheridge, S. L., G. J. Spencer, et al. (2004). "Expression profiling and functional analysis of wnt signaling mechanisms in mesenchymal stem cells." Stem Cells **22**(5): 849-60.
- Ezeh, U. I., P. J. Turek, et al. (2005). "Human embryonic stem cell genes OCT4, NANOG, STELLAR, and GDF3 are expressed in both seminoma and breast carcinoma." Cancer **104**(10): 2255-65.
- Falconi, D. and J. E. Aubin (2007). "LIF Inhibits Osteoblast Differentiation at Least in Part By Regulation of HAS2 and Its Product Hyaluronan." J Bone Miner Res.
- Falconi, D., K. Oizumi, et al. (2007). "Leukemia inhibitory factor influences the fate choice of mesenchymal progenitor cells." Stem Cells **25**(2): 305-12.
- Ferrari, G., G. Cusella-De Angelis, et al. (1998). "Muscle regeneration by bone marrow-derived myogenic progenitors." Science **279**(5356): 1528-30.
- Ferrari, G., A. Stornaiuolo, et al. (2001). "Failure to correct murine muscular dystrophy." Nature **411**(6841): 1014-5.
- Fortunel, N. O., H. H. Otu, et al. (2003). "Comment on " 'Stemness': transcriptional profiling of embryonic and adult stem cells" and "a stem cell molecular signature"." Science **302**(5644): 393; author reply 393.
- Freedman, V. H. and S. I. Shin (1974). "Cellular tumorigenicity in nude mice: correlation with cell growth in semi-solid medium." Cell **3**(4): 355-9.
- Friedenstein, A. J., R. K. Chailakhjan, et al. (1970). "The development of fibroblast colonies in monolayer cultures of guinea-pig bone marrow and spleen cells." Cell Tissue Kinet **3**(4): 393-403.
- Friedenstein, A. J., N. W. Latzinik, et al. (1982). "Marrow microenvironment transfer by heterotopic transplantation of freshly isolated and cultured cells in porous sponges." Exp Hematol **10**(2): 217-27.

- Friedenstein, A. J., S. Piatetzky, II, et al. (1966). "Osteogenesis in transplants of bone marrow cells." J Embryol Exp Morphol **16**(3): 381-90.
- Fromigue, O., Z. Hamidouche, et al. (2008). "Distinct osteoblastic differentiation potential of murine fetal liver and bone marrow stroma-derived mesenchymal stem cells." J Cell Biochem **104**(2): 620-8.
- Fu, X. and H. Li (2009). "Mesenchymal stem cells and skin wound repair and regeneration: possibilities and questions." Cell Tissue Res **335**(2): 317-21.
- Fukuchi, Y., H. Nakajima, et al. (2004). "Human placenta-derived cells have mesenchymal stem/progenitor cell potential." Stem Cells **22**(5): 649-58.
- Gafni, Y., G. Turgeman, et al. (2004). "Stem cells as vehicles for orthopedic gene therapy." Gene Ther **11**(4): 417-26.
- Galderisi, U., H. Helmbold, et al. (2008). "In vitro senescence of rat mesenchymal stem cells is accompanied by downregulation of stemness-related and DNA damage repair genes." Stem Cells Dev.
- Gang, E. J., D. Bosnakovski, et al. (2007). "SSEA-4 identifies mesenchymal stem cells from bone marrow." Blood **109**(4): 1743-51.
- Gang, E. J., S. H. Hong, et al. (2004). "In vitro mesengenic potential of human umbilical cord blood-derived mesenchymal stem cells." Biochem Biophys Res Commun **321**(1): 102-8.
- Gibbs, C. P., V. G. Kukekov, et al. (2005). "Stem-like cells in bone sarcomas: implications for tumorigenesis." Neoplasia **7**(11): 967-76.
- Giordano, A., U. Galderisi, et al. (2007). "From the laboratory bench to the patient's bedside: an update on clinical trials with mesenchymal stem cells." J Cell Physiol **211**(1): 27-35.

- Go, M. J., C. Takenaka, et al. (2008). "Forced expression of Sox2 or Nanog in human bone marrow derived mesenchymal stem cells maintains their expansion and differentiation capabilities." Exp Cell Res **314**(5): 1147-54.
- Goldring, M. B., K. Tsuchimochi, et al. (2006). "The control of chondrogenesis." J Cell Biochem **97**(1): 33-44.
- Gonzalez, R., C. B. Maki, et al. (2007). "Pluripotent marker expression and differentiation of human second trimester Mesenchymal Stem Cells." Biochem Biophys Res Commun **362**(2): 491-7.
- Greco, S. J., K. Liu, et al. (2007). "Functional similarities among genes regulated by OCT4 in human mesenchymal and embryonic stem cells." Stem Cells **25**(12): 3143-54.
- Gronthos, S., S. E. Graves, et al. (1994). "The STRO-1+ fraction of adult human bone marrow contains the osteogenic precursors." Blood **84**(12): 4164-73.
- Guillot, P. V., C. Gotherstrom, et al. (2007). "Human first-trimester fetal MSC express pluripotency markers and grow faster and have longer telomeres than adult MSC." Stem Cells **25**(3): 646-54.
- Gussoni, E., Y. Soneoka, et al. (1999). "Dystrophin expression in the mdx mouse restored by stem cell transplantation." Nature **401**(6751): 390-4.
- Hamm, A., N. Krott, et al. (2002). "Efficient transfection method for primary cells." Tissue Eng **8**(2): 235-45.
- Harada, S. and G. A. Rodan (2003). "Control of osteoblast function and regulation of bone mass." Nature **423**(6937): 349-55.
- Harley, C. B., A. B. Futcher, et al. (1990). "Telomeres shorten during ageing of human fibroblasts." Nature **345**(6274): 458-60.
- Hart, A. H., L. Hartley, et al. (2005). "The pluripotency homeobox gene NANOG is expressed in human germ cell tumors." Cancer **104**(10): 2092-8.

- Hartmann, C. (2006). "A Wnt canon orchestrating osteoblastogenesis." Trends Cell Biol **16**(3): 151-8.
- Hayflick, L. (1965). "The Limited in Vitro Lifetime of Human Diploid Cell Strains." Exp Cell Res **37**: 614-36.
- Haynesworth, S. E., M. A. Baber, et al. (1992). "Cell surface antigens on human marrow-derived mesenchymal cells are detected by monoclonal antibodies." Bone **13**(1): 69-80.
- He, Q., C. Wan, et al. (2007). "Concise review: multipotent mesenchymal stromal cells in blood." Stem Cells **25**(1): 69-77.
- He, X. (2006). "Unwinding a path to nuclear beta-catenin." Cell **127**(1): 40-2.
- Helledie, T., V. Nurcombe, et al. (2008). "A simple and reliable electroporation method for human bone marrow mesenchymal stem cells." Stem Cells Dev **17**(4): 837-48.
- Henderson, J. K., J. S. Draper, et al. (2002). "Preimplantation human embryos and embryonic stem cells show comparable expression of stage-specific embryonic antigens." Stem Cells **20**(4): 329-37.
- Higashimoto, T., F. Urbinati, et al. (2007). "The woodchuck hepatitis virus post-transcriptional regulatory element reduces readthrough transcription from retroviral vectors." Gene Ther **14**(17): 1298-304.
- Hoelters, J., M. Ciccarella, et al. (2005). "Nonviral genetic modification mediates effective transgene expression and functional RNA interference in human mesenchymal stem cells." J Gene Med **7**(6): 718-28.
- Hogan, J. C. and J. M. Stephens (2005). "Effects of leukemia inhibitory factor on 3T3-L1 adipocytes." J Endocrinol **185**(3): 485-96.
- Holmes, C. and W. L. Stanford (2007). "Concise review: stem cell antigen-1: expression, function, and enigma." Stem Cells **25**(6): 1339-47.

- Honczarenko, M., Y. Le, et al. (2006). "Human bone marrow stromal cells express a distinct set of biologically functional chemokine receptors." Stem Cells **24**(4): 1030-41.
- Hong, J. H., E. S. Hwang, et al. (2005). "TAZ, a transcriptional modulator of mesenchymal stem cell differentiation." Science **309**(5737): 1074-8.
- Issaad, C., L. Croisille, et al. (1993). "A murine stromal cell line allows the proliferation of very primitive human CD34<sup>++</sup>/CD38<sup>-</sup> progenitor cells in long-term cultures and semisolid assays." Blood **81**(11): 2916-24.
- Ito, T., R. Sawada, et al. (2007). "FGF-2 suppresses cellular senescence of human mesenchymal stem cells by down-regulation of TGF-beta2." Biochem Biophys Res Commun **359**(1): 108-14.
- Ivanova, N. B., J. T. Dimos, et al. (2002). "A stem cell molecular signature." Science **298**(5593): 601-4.
- Jaishankar, A., M. Barthelery, et al. (2008). "Human Embryonic and Mesenchymal Stem Cells Express Different Nuclear Proteomes." Stem Cells Dev.
- Jaiswal, N., S. E. Haynesworth, et al. (1997). "Osteogenic differentiation of purified, culture-expanded human mesenchymal stem cells in vitro." J Cell Biochem **64**(2): 295-312.
- Jiang, Y., B. N. Jahagirdar, et al. (2002). "Pluripotency of mesenchymal stem cells derived from adult marrow." Nature **418**(6893): 41-9.
- Kannagi, R., N. A. Cochran, et al. (1983). "Stage-specific embryonic antigens (SSEA-3 and -4) are epitopes of a unique globo-series ganglioside isolated from human teratocarcinoma cells." EMBO J **2**(12): 2355-61.

- Karnoub, A. E., A. B. Dash, et al. (2007). "Mesenchymal stem cells within tumour stroma promote breast cancer metastasis." Nature **449**(7162): 557-63.
- Karsenty, G. and E. F. Wagner (2002). "Reaching a genetic and molecular understanding of skeletal development." Dev Cell **2**(4): 389-406.
- Kawada, H., J. Fujita, et al. (2004). "Nonhematopoietic mesenchymal stem cells can be mobilized and differentiate into cardiomyocytes after myocardial infarction." Blood **104**(12): 3581-7.
- Khurana, S. and A. Mukhopadhyay (2007). "Characterization of the potential subpopulation of bone marrow cells involved in the repair of injured liver tissue." Stem Cells **25**(6): 1439-47.
- Kim, D. H., K. H. Yoo, et al. (2005). "Gene expression profile of cytokine and growth factor during differentiation of bone marrow-derived mesenchymal stem cell." Cytokine **31**(2): 119-26.
- Kim, N. W., M. A. Piatyszek, et al. (1994). "Specific association of human telomerase activity with immortal cells and cancer." Science **266**(5193): 2011-5.
- Kleber, M. and L. Sommer (2004). "Wnt signaling and the regulation of stem cell function." Curr Opin Cell Biol **16**(6): 681-7.
- Kobayashi, M., T. Yakuwa, et al. (2008). "Multilineage potential of side population cells from human amnion mesenchymal layer." Cell Transplant **17**(3): 291-301.
- Kogler, G., S. Sensken, et al. (2006). "Comparative generation and characterization of pluripotent unrestricted somatic stem cells with mesenchymal stem cells from human cord blood." Exp Hematol **34**(11): 1589-95.

- Kotoula, V., S. I. Papamichos, et al. (2008). "Revisiting OCT4 expression in peripheral blood mononuclear cells." Stem Cells **26**(1): 290-1.
- Kratchmarova, I., B. Blagoev, et al. (2005). "Mechanism of divergent growth factor effects in mesenchymal stem cell differentiation." Science **308**(5727): 1472-7.
- Kuznetsov, S. A., A. J. Friedenstein, et al. (1997). "Factors required for bone marrow stromal fibroblast colony formation in vitro." Br J Haematol **97**(3): 561-70.
- Lai, L., N. Alaverdi, et al. (1998). "Mouse cell surface antigens: nomenclature and immunophenotyping." J Immunol **160**(8): 3861-8.
- Lakshmipathy, U., B. Pelacho, et al. (2004). "Efficient transfection of embryonic and adult stem cells." Stem Cells **22**(4): 531-43.
- Lam, M. Y. and J. H. Nadeau (2003). "Genetic control of susceptibility to spontaneous testicular germ cell tumors in mice." APMIS **111**(1): 184-90; discussion 191.
- Lazennec, G. and C. Jorgensen (2008). "Concise review: adult multipotent stromal cells and cancer: risk or benefit?" Stem Cells **26**(6): 1387-94.
- Le Blanc, K. and M. Pittenger (2005). "Mesenchymal stem cells: progress toward promise." Cytotherapy **7**(1): 36-45.
- Lemoli, R. M., F. Bertolini, et al. (2005). "Stem cell plasticity: time for a reappraisal?" Haematologica **90**(3): 360-81.
- Lengner, C. J., F. D. Camargo, et al. (2007). "Oct4 expression is not required for mouse somatic stem cell self-renewal." Cell Stem Cell **1**(4): 403-15.
- Li, H., X. Fan, et al. (2007). "Spontaneous expression of embryonic factors and p53 point mutations in aged mesenchymal stem cells: a model of age-related tumorigenesis in mice." Cancer Res **67**(22): 10889-98.

- Lieberman, J. R., L. Q. Le, et al. (1998). "Regional gene therapy with a BMP-2-producing murine stromal cell line induces heterotopic and orthotopic bone formation in rodents." J Orthop Res **16**(3): 330-9.
- Liedtke, S., J. Enczmann, et al. (2007). "Oct4 and its pseudogenes confuse stem cell research." Cell Stem Cell **1**(4): 364-6.
- Liedtke, S., M. Stephan, et al. (2008). "Oct4 expression revisited: potential pitfalls for data misinterpretation in stem cell research." Biol Chem **389**(7): 845-50.
- Lin, T., C. Chao, et al. (2005). "p53 induces differentiation of mouse embryonic stem cells by suppressing Nanog expression." Nat Cell Biol **7**(2): 165-71.
- Ling, L., V. Nurcombe, et al. (2008). "Wnt signaling controls the fate of mesenchymal stem cells." Gene.
- Liu, J. and S. R. Farmer (2004). "Regulating the balance between peroxisome proliferator-activated receptor gamma and beta-catenin signaling during adipogenesis. A glycogen synthase kinase 3beta phosphorylation-defective mutant of beta-catenin inhibits expression of a subset of adipogenic genes." J Biol Chem **279**(43): 45020-7.
- Liu, T. M., M. Martina, et al. (2007). "Identification of common pathways mediating differentiation of bone marrow- and adipose tissue-derived human mesenchymal stem cells into three mesenchymal lineages." Stem Cells **25**(3): 750-60.
- Liu, T. M., Y. N. Wu, et al. (2008). "Effects of Ectopic Nanog and Oct4 Overexpression on Mesenchymal Stem Cells." Stem Cells Dev.
- Luster, A. D. and P. Leder (1993). "IP-10, a -C-X-C- chemokine, elicits a potent thymus-dependent antitumor response in vivo." J Exp Med **178**(3): 1057-65.

- Mackay, A. M., S. C. Beck, et al. (1998). "Chondrogenic differentiation of cultured human mesenchymal stem cells from marrow." Tissue Eng **4**(4): 415-28.
- Massague, J., S. W. Blain, et al. (2000). "TGFbeta signaling in growth control, cancer, and heritable disorders." Cell **103**(2): 295-309.
- Masui, S., S. Ohtsuka, et al. (2008). "Rex1/Zfp42 is dispensable for pluripotency in mouse ES cells." BMC Dev Biol **8**: 45.
- McLoughlin, R. M., B. J. Jenkins, et al. (2005). "IL-6 trans-signaling via STAT3 directs T cell infiltration in acute inflammation." Proc Natl Acad Sci U S A **102**(27): 9589-94.
- Meirelles Lda, S. and N. B. Nardi (2003). "Murine marrow-derived mesenchymal stem cell: isolation, in vitro expansion, and characterization." Br J Haematol **123**(4): 702-11.
- Metcalf, D. (2003). "The unsolved enigmas of leukemia inhibitory factor." Stem Cells **21**(1): 5-14.
- Mitsui, K., Y. Tokuzawa, et al. (2003). "The homeoprotein Nanog is required for maintenance of pluripotency in mouse epiblast and ES cells." Cell **113**(5): 631-42.
- Miura, M., Y. Miura, et al. (2006). "Accumulated chromosomal instability in murine bone marrow mesenchymal stem cells leads to malignant transformation." Stem Cells **24**(4): 1095-103.
- Moore, K. A. and I. R. Lemischka (2006). "Stem cells and their niches." Science **311**(5769): 1880-5.
- Murdoch, A. D., L. M. Grady, et al. (2007). "Chondrogenic differentiation of human bone marrow stem cells in transwell cultures: generation of scaffold-free cartilage." Stem Cells **25**(11): 2786-96.

- Nadri, S., M. Soleimani, et al. (2008). "Multipotent mesenchymal stem cells from adult human eye conjunctiva stromal cells." Differentiation **76**(3): 223-31.
- Nakashima, K., X. Zhou, et al. (2002). "The novel zinc finger-containing transcription factor osterix is required for osteoblast differentiation and bone formation." Cell **108**(1): 17-29.
- Narayanan, R., K. A. Higgins, et al. (1993). "Evidence for differential functions of the p50 and p65 subunits of NF-kappa B with a cell adhesion model." Mol Cell Biol **13**(6): 3802-10.
- Narita, M., S. Nunez, et al. (2003). "Rb-mediated heterochromatin formation and silencing of E2F target genes during cellular senescence." Cell **113**(6): 703-16.
- Ng, F., S. Boucher, et al. (2008). "PDGF, TGF-beta, and FGF signaling is important for differentiation and growth of mesenchymal stem cells (MSCs): transcriptional profiling can identify markers and signaling pathways important in differentiation of MSCs into adipogenic, chondrogenic, and osteogenic lineages." Blood **112**(2): 295-307.
- Nichols, J., B. Zevnik, et al. (1998). "Formation of pluripotent stem cells in the mammalian embryo depends on the POU transcription factor Oct4." Cell **95**(3): 379-91.
- O'Connor, M. D., M. D. Kardel, et al. (2008). "Alkaline phosphatase-positive colony formation is a sensitive, specific, and quantitative indicator of undifferentiated human embryonic stem cells." Stem Cells **26**(5): 1109-16.
- Okita, K., T. Ichisaka, et al. (2007). "Generation of germline-competent induced pluripotent stem cells." Nature **448**(7151): 313-7.
- Olmsted, E. A., J. S. Blum, et al. (2001). "Adenovirus-mediated BMP2 expression in human bone marrow stromal cells." J Cell Biochem **82**(1): 11-21.

- Orlic, D., J. Kajstura, et al. (2001). "Bone marrow cells regenerate infarcted myocardium." Nature **410**(6829): 701-5.
- Owen, M. (1988). "Marrow stromal stem cells." J Cell Sci Suppl **10**: 63-76.
- Pan, G. and D. Pei (2005). "The stem cell pluripotency factor NANOG activates transcription with two unusually potent subdomains at its C terminus." J Biol Chem **280**(2): 1401-7.
- Parisi, S., F. Passaro, et al. (2008). "Klf5 is involved in self-renewal of mouse embryonic stem cells." J Cell Sci **121**(Pt 16): 2629-34.
- Park, S. R., R. O. Oreffo, et al. (1999). "Interconversion potential of cloned human marrow adipocytes in vitro." Bone **24**(6): 549-54.
- Peister, A., J. A. Mellad, et al. (2004). "Adult stem cells from bone marrow (MSCs) isolated from different strains of inbred mice vary in surface epitopes, rates of proliferation, and differentiation potential." Blood **103**(5): 1662-8.
- Pelicci, P. G. (2004). "Do tumor-suppressive mechanisms contribute to organism aging by inducing stem cell senescence?" J Clin Invest **113**(1): 4-7.
- Pelletier, J. and N. Sonenberg (1988). "Internal initiation of translation of eukaryotic mRNA directed by a sequence derived from poliovirus RNA." Nature **334**(6180): 320-5.
- Pevny, L. H. and R. Lovell-Badge (1997). "Sox genes find their feet." Curr Opin Genet Dev **7**(3): 338-44.
- Phinney, D. G., G. Kopen, et al. (1999). "Plastic adherent stromal cells from the bone marrow of commonly used strains of inbred mice: variations in yield, growth, and differentiation." J Cell Biochem **72**(4): 570-85.

- Piestun, D., B. S. Kochupurakkal, et al. (2006). "Nanog transforms NIH3T3 cells and targets cell-type restricted genes." Biochem Biophys Res Commun **343**(1): 279-85.
- Pittenger, M. F., A. M. Mackay, et al. (1999). "Multilineage potential of adult human mesenchymal stem cells." Science **284**(5411): 143-7.
- Prockop, D. J. (1997). "Marrow stromal cells as stem cells for nonhematopoietic tissues." Science **276**(5309): 71-4.
- Quarto, N., K. D. Fong, et al. (2005). "Gene profiling of cells expressing different FGF-2 forms." Gene **356**: 49-68.
- Quesenberry, P. J., G. A. Colvin, et al. (2002). "The chiaroscuro stem cell: a unified stem cell theory." Blood **100**(13): 4266-71.
- Quirici, N., D. Soligo, et al. (2002). "Isolation of bone marrow mesenchymal stem cells by anti-nerve growth factor receptor antibodies." Exp Hematol **30**(7): 783-91.
- Ramalho-Santos, M., S. Yoon, et al. (2002). "'Stemness': transcriptional profiling of embryonic and adult stem cells." Science **298**(5593): 597-600.
- Reya, T., A. W. Duncan, et al. (2003). "A role for Wnt signalling in self-renewal of haematopoietic stem cells." Nature **423**(6938): 409-14.
- Reyes, M., T. Lund, et al. (2001). "Purification and ex vivo expansion of postnatal human marrow mesodermal progenitor cells." Blood **98**(9): 2615-25.
- Ricks, D. M., R. Kutner, et al. (2008). "Optimized lentiviral transduction of mouse bone marrow-derived mesenchymal stem cells." Stem Cells Dev **17**(3): 441-50.
- Roche, S., M. Provansal, et al. (2006). "Proteomics of primary mesenchymal stem cells." Regen Med **1**(4): 511-7.

- Rocheffort, G. Y., B. Delorme, et al. (2006). "Multipotential mesenchymal stem cells are mobilized into peripheral blood by hypoxia." Stem Cells **24**(10): 2202-8.
- Rosen, E. D. and O. A. MacDougald (2006). "Adipocyte differentiation from the inside out." Nat Rev Mol Cell Biol **7**(12): 885-96.
- Rubio, D., J. Garcia-Castro, et al. (2005). "Spontaneous human adult stem cell transformation." Cancer Res **65**(8): 3035-9.
- Rubio, D., S. Garcia, et al. (2008). "Molecular characterization of spontaneous mesenchymal stem cell transformation." PLoS ONE **3**(1): e1398.
- Ryu, E., S. Hong, et al. (2008). "Identification of senescence-associated genes in human bone marrow mesenchymal stem cells." Biochem Biophys Res Commun **371**(3): 431-6.
- Sacchetti, B., A. Funari, et al. (2007). "Self-renewing osteoprogenitors in bone marrow sinusoids can organize a hematopoietic microenvironment." Cell **131**(2): 324-36.
- Satomura, K., A. R. Derubeis, et al. (1998). "Receptor tyrosine kinase expression in human bone marrow stromal cells." J Cell Physiol **177**(3): 426-38.
- Schaffler, A. and C. Buchler (2007). "Concise review: adipose tissue-derived stromal cells--basic and clinical implications for novel cell-based therapies." Stem Cells **25**(4): 818-27.
- Schenk, S., N. Mal, et al. (2007). "Monocyte chemotactic protein-3 is a myocardial mesenchymal stem cell homing factor." Stem Cells **25**(1): 245-51.
- Scholer, H. R., S. Ruppert, et al. (1990). "New type of POU domain in germ line-specific protein Oct-4." Nature **344**(6265): 435-9.

- Serakinci, N., P. Guldberg, et al. (2004). "Adult human mesenchymal stem cell as a target for neoplastic transformation." Oncogene **23**(29): 5095-8.
- Serakinci, N., S. F. Hoare, et al. (2006). "Telomerase promoter reprogramming and interaction with general transcription factors in the human mesenchymal stem cell." Regen Med **1**(1): 125-31.
- Serrano, M. and M. A. Blasco (2007). "Cancer and ageing: convergent and divergent mechanisms." Nat Rev Mol Cell Biol **8**(9): 715-22.
- Sethe, S., A. Scutt, et al. (2006). "Aging of mesenchymal stem cells." Ageing Res Rev **5**(1): 91-116.
- Sharpless, N. E. and R. A. DePinho (2004). "Telomeres, stem cells, senescence, and cancer." J Clin Invest **113**(2): 160-8.
- Sharpless, N. E. and R. A. DePinho (2007). "How stem cells age and why this makes us grow old." Nat Rev Mol Cell Biol **8**(9): 703-13.
- Sherr, C. J. and J. D. Weber (2000). "The ARF/p53 pathway." Curr Opin Genet Dev **10**(1): 94-9.
- Shi, S., S. Gronthos, et al. (2002). "Bone formation by human postnatal bone marrow stromal stem cells is enhanced by telomerase expression." Nat Biotechnol **20**(6): 587-91.
- Shibata, K. R., T. Aoyama, et al. (2007). "Expression of the p16INK4A gene is associated closely with senescence of human mesenchymal stem cells and is potentially silenced by DNA methylation during in vitro expansion." Stem Cells **25**(9): 2371-82.
- Short, B., N. Brouard, et al. (2001). "Prospective isolation of stromal progenitor cells from mouse BM." Cytotherapy **3**(5): 407-8.

- Simmons, P. J. and B. Torok-Storb (1991). "Identification of stromal cell precursors in human bone marrow by a novel monoclonal antibody, STRO-1." Blood **78**(1): 55-62.
- Simonsen, J. L., C. Rosada, et al. (2002). "Telomerase expression extends the proliferative life-span and maintains the osteogenic potential of human bone marrow stromal cells." Nat Biotechnol **20**(6): 592-6.
- Sithanandam, G., L. W. Fornwald, et al. (2005). "Inactivation of ErbB3 by siRNA promotes apoptosis and attenuates growth and invasiveness of human lung adenocarcinoma cell line A549." Oncogene **24**(11): 1847-59.
- Song, L., N. E. Webb, et al. (2006). "Identification and functional analysis of candidate genes regulating mesenchymal stem cell self-renewal and multipotency." Stem Cells **24**(7): 1707-18.
- Stenderup, K., J. Justesen, et al. (2003). "Aging is associated with decreased maximal life span and accelerated senescence of bone marrow stromal cells." Bone **33**(6): 919-26.
- Sun, S., Z. Guo, et al. (2003). "Isolation of mouse marrow mesenchymal progenitors by a novel and reliable method." Stem Cells **21**(5): 527-35.
- Takahashi, K. and S. Yamanaka (2006). "Induction of pluripotent stem cells from mouse embryonic and adult fibroblast cultures by defined factors." Cell **126**(4): 663-76.
- Takao, Y., T. Yokota, et al. (2007). "Beta-catenin up-regulates Nanog expression through interaction with Oct-3/4 in embryonic stem cells." Biochem Biophys Res Commun **353**(3): 699-705.
- Tanaka, Y., T. Era, et al. (2007). "Forced expression of Nanog in hematopoietic stem cells results in a gammadeltaT-cell disorder." Blood **110**(1): 107-15.

- Thomson, T. M., W. J. Rettig, et al. (1988). "Expression of human nerve growth factor receptor on cells derived from all three germ layers." Exp Cell Res **174**(2): 533-9.
- Tolar, J., A. J. Nauta, et al. (2007). "Sarcoma derived from cultured mesenchymal stem cells." Stem Cells **25**(2): 371-9.
- Torres, J. and F. M. Watt (2008). "Nanog maintains pluripotency of mouse embryonic stem cells by inhibiting NFkappaB and cooperating with Stat3." Nat Cell Biol **10**(2): 194-201.
- Tropel, P., D. Noel, et al. (2004). "Isolation and characterisation of mesenchymal stem cells from adult mouse bone marrow." Exp Cell Res **295**(2): 395-406.
- Uccelli, A., L. Moretta, et al. (2008). "Mesenchymal stem cells in health and disease." Nat Rev Immunol **8**(9): 726-36.
- Uccelli, A., V. Pistoia, et al. (2007). "Mesenchymal stem cells: a new strategy for immunosuppression?" Trends Immunol **28**(5): 219-26.
- Wagers, A. J. and I. L. Weissman (2004). "Plasticity of adult stem cells." Cell **116**(5): 639-48.
- Wagner, W., P. Horn, et al. (2008). "Replicative senescence of mesenchymal stem cells: a continuous and organized process." PLoS ONE **3**(5): e2213.
- Wang, D., K. Christensen, et al. (1999). "Isolation and characterization of MC3T3-E1 preosteoblast subclones with distinct in vitro and in vivo differentiation/mineralization potential." J Bone Miner Res **14**(6): 893-903.
- Wang, Z., J. Song, et al. (2006). "Ablation of proliferating marrow with 5-fluorouracil allows partial purification of mesenchymal stem cells." Stem Cells **24**(6): 1573-82.

- Watt, F. M. and B. L. Hogan (2000). "Out of Eden: stem cells and their niches." Science **287**(5457): 1427-30.
- Wilson, A. and A. Trumpp (2006). "Bone-marrow haematopoietic-stem-cell niches." Nat Rev Immunol **6**(2): 93-106.
- Yang, J., X. Liao, et al. (2007). "Unphosphorylated STAT3 accumulates in response to IL-6 and activates transcription by binding to NFkappaB." Genes Dev **21**(11): 1396-408.
- Yang, L., C. Lin, et al. (2006). "P68 RNA helicase mediates PDGF-induced epithelial mesenchymal transition by displacing Axin from beta-catenin." Cell **127**(1): 139-55.
- Ying, Q. L., J. Nichols, et al. (2003). "BMP induction of Id proteins suppresses differentiation and sustains embryonic stem cell self-renewal in collaboration with STAT3." Cell **115**(3): 281-92.
- Zaragosi, L. E., G. Ailhaud, et al. (2006). "Autocrine fibroblast growth factor 2 signaling is critical for self-renewal of human multipotent adipose-derived stem cells." Stem Cells **24**(11): 2412-9.
- Zhang, X. Y., V. F. La Russa, et al. (2002). "Lentiviral vectors for sustained transgene expression in human bone marrow-derived stromal cells." Mol Ther **5**(5 Pt 1): 555-65.
- Zhang, X. Y., V. F. La Russa, et al. (2004). "Transduction of bone-marrow-derived mesenchymal stem cells by using lentivirus vectors pseudotyped with modified RD114 envelope glycoproteins." J Virol **78**(3): 1219-29.
- Zhao, Y. and S. Ding (2007). "A high-throughput siRNA library screen identifies osteogenic suppressors in human mesenchymal stem cells." Proc Natl Acad Sci U S A **104**(23): 9673-8.

Zhou, Y. F., M. Bosch-Marce, et al. (2006). "Spontaneous transformation of cultured mouse bone marrow-derived stromal cells." Cancer Res **66**(22): 10849-54.

Zuk, P. A., M. Zhu, et al. (2001). "Multilineage cells from human adipose tissue: implications for cell-based therapies." Tissue Eng **7**(2): 211-28.

# Culture Conditions Allow Selection of Different Mesenchymal Progenitors from Adult Mouse Bone Marrow

Maria Teresa Esposito, B.Sc.,<sup>1,2</sup> Rosa Di Noto, B.Sc.,<sup>1,3</sup> Peppino Mirabelli, Ph.D.,<sup>1,3</sup> Marisa Gorrese, B.Sc.,<sup>1,3</sup> Silvia Parisi, Ph.D.,<sup>1,2</sup> Donatella Montanaro, B.Sc.,<sup>1</sup> Luigi Del Vecchio, M.D.,<sup>1,3</sup> and Lucio Pastore, M.D., Ph.D.<sup>1,2,3</sup>

The use of adult stem cells in tissue engineering approaches will benefit from the establishment of culture conditions that allow the expansion and maintenance of cells with stem cell-like activity and high differentiation potential. In the field of adult stem cells, bone marrow stromal cells (BMSCs) are promising candidates. In the present study, we define, for the first time, conditions for optimizing the yields of cultures enriched for specific progenitors of bone marrow. Using four distinct culture conditions, supernatants from culture of bone fragments, marrow stroma cell line MS-5, embryonic fibroblast cell line NIH3T3, and a cocktail of epidermal growth factor (EGF) and platelet-derived growth factor (PDGF), we isolated four different sub-populations of murine BMSCs (mBMSCs). These cells express a well-known marker of undifferentiated embryonic stem cells (Nanog) and show interesting features in immunophenotype, self-renewal ability, and differentiation potency. In particular, using NIH3T3 conditioned medium, we obtained cells that showed impairment in osteogenic and chondrogenic differentiation while retaining high adipogenic potential during passages. Our results indicate that the choice of the medium used for isolation and expansion of mBMSCs is important for enriching the culture of desired specific progenitors.

## Introduction

**T**HE USE OF bone marrow stromal cells (BMSCs) for applications such as tissue engineering and gene therapy is one of the major challenges of regenerative medicine. The ability to move forward the use of these cells in therapy depends on the setting up of mammalian models, necessary to evaluate pre-clinical efficacy and standardize procedures. In particular, characterization of murine BMSCs (mBMSCs) is a major breakthrough that can benefit from numerous established genetic models of human diseases now available in this organism.<sup>1-3</sup>

However, the BMSC is a cell type better studied and characterized in humans than in mice, and although in the last few years, numerous protocols have been developed to isolate these cells, some problems remain.<sup>4-11</sup> The standard method, widely used for the purification of human BMSCs, based on adherence to plastic substrate, does not allow the isolation of homogeneous populations of mBMSCs. Using alternative methods based on immunodepletion<sup>6</sup> or centrifugation,<sup>4,9,12</sup> different populations of mBMSCs have been isolated; however, they expand poorly, probably because of the loss of relevant cell-cell contacts or the absence of specific cytokines

necessary in the early phases of expansion. Moreover, no data are available concerning an exhaustive characterization of the stemness, differentiation potential, and acquisition of transformed phenotype of the isolated cells during passages.

Starting from the observation that use of bone fragment-conditioned medium favors BMSC growth,<sup>8</sup> we hypothesized that specific conditioned media, obtained from different microenvironments, might contribute to the self-renewal of BMSCs and could be critical in the early phases of mBMSC expansion. Therefore, the aim of this work was to compare supernatants from cultures of bone fragments, mouse marrow stroma cell line MS-5, mouse embryonic fibroblast cell line NIH3T3, and a cocktail of epidermal growth factor (EGF) and platelet-derived growth factor (PDGF) to identify culture conditions that would enable us to expand and maintain BMSCs with stem cell-like activity and high differentiation potential, also at late passages.

## Materials and Methods

### Mice

C57BL/6 (H-2K<sup>b</sup>) and nude (Foxn1<sup>nu</sup>/Foxn1) mice were obtained from Harlan Sprague Dawley, Inc., Indianapolis,

<sup>1</sup>CEINGE Biotecnologie Avanzate s.c.a r. l., Naples, Italy.

<sup>2</sup>European School of Molecular Medicine, SEMM, Naples, Italy.

<sup>3</sup>Department of Biochemistry e Medical Biotechnology, University of Naples "Federico II", Naples, Italy.

Indiana. All of the experiments in this study were performed following all regulations protecting animals used for research purposes, including those of the DL 116/92.

#### *mBMSC isolation and expansion*

C57Bl/6 mice were euthanized with carbon dioxide vapors. The cells were isolated as described by Mereilles *et al.*<sup>7</sup>

We initially seeded  $2 \times 10^6$  nucleated cells/cm<sup>2</sup> in complete medium (alpha minimum essential medium ( $\alpha$ -MEM; Cambrex Bio Science Verviers, Verviers, Belgium) with 10% selected fetal bovine serum (FBS) (HyClone, Logan, Utah), 2 mM L-glutamine (Gibco, Invitrogen, San Giuliano Milanese (Mi), Italy) and 10 U/mL penicillin–10  $\mu$ g/mL streptomycin (Gibco, Invitrogen) without any supplements. After 3 days, we removed the nonadherent cells and waited for a subconfluent culture. Unfortunately, the cells failed to reach confluence and formed a single small colony. We tried to subculture this colony, but the cells did not expand in this condition. We then decided to start with another culture, using Dulbecco's modified Eagle medium (DMEM), and Iscove's modified Dulbecco's medium (IMDM). In both conditions, we obtained larger colonies, although when we tried to subculture these colonies, the cells were not able to expand. After these unsuccessful attempts, we decided to add 20% bone marrow-conditioned medium to the complete medium, as reported by Sun *et al.*, and the cells became confluent in 10 to 17 days.<sup>8</sup> At that time, they were washed twice with Ca<sup>2+</sup>Mg<sup>2+</sup>-free phosphate buffered saline (PBS) (Gibco, Invitrogen), detached with Accutase (Innovative Cell Technologies, San Diego, California) at 37°C for 10 min and then suspended in 50% culture supernatant and 50% complete medium with the addition of (a) 20% bone marrow-conditioned medium<sup>8</sup> (BF mBMSC), (b) 20 ng/mL murine EGF and 20 ng/mL PDGF-AA (Sigma-Aldrich, Milano, Italy) after 2 weeks of culture in condition (a) (EP mBMSC), (c) 20% MS5-conditioned medium<sup>13</sup> (M mBMSC), or (d) 20% NIH3T3 conditioned medium<sup>14</sup> (N mBMSC). The resulting suspensions were split 1:3. Half of the culture medium was changed every 3 to 4 days until the cultures became confluent, at which point they were washed twice with Ca<sup>2+</sup>Mg<sup>2+</sup>-free PBS, detached, and split 1:2.

#### *Preparation of bone marrow-conditioned medium*

The bone marrow-conditioned medium has been prepared following the procedure described in Sun *et al.*<sup>8</sup> Briefly, after flushing the bone marrow out of femurs and tibiae, fragments from these bones were cultured in  $\alpha$ -MEM (Cambrex Bio Science) supplemented with 20% selected FBS (HyClone) at 37°C in humidified atmosphere containing 5% carbon dioxide (CO<sub>2</sub>) for 3 days. Then the incubation medium was collected using centrifugation at 2500 rpm for 10 min and filtered through a 0.22- $\mu$ m filter.

MS-5 and NIH3T3 cell lines, obtained from DSMZ (Braunschweig, Germany), were cultured in  $\alpha$ -MEM (Cambrex Bio Science) supplemented with 10% selected FBS (HyClone), 2 mM L-Glutamine (Gibco, Invitrogen), and 10 U/mL penicillin–10  $\mu$ g/mL streptomycin (Gibco, Invitrogen) at 37°C in humidified atmosphere containing 5% CO<sub>2</sub>. Cells were subcultured every 3 to 4 days, and conditioned media were collected from each cell line, centrifuged at 2500 rpm for 10 min, and filtered through a 0.22- $\mu$ m filter.

#### *Flow cytometry analysis*

mBMSCs were analyzed using flow cytometry with FACS Canto II (BD Biosciences, Buccinasco (Mi), Italy). Monoclonal antibodies directly coupled with phycoerythrin or fluorescein isothiocyanate including Ly-1 (CD5), CD19, Ly-5 (CD45), and CD34 were obtained from Santa Cruz Biotechnology, and monoclonal antibodies against Ly-24 (CD44), CD117 (c-kit), CD13, Ly-6A/E (Sca 1), and MHC-I (H2-k<sup>b</sup>) were obtained from BD Biosciences.

#### *In vivo tumorigenicity: transplantation of mBMSCs into nude mice*

mBMSCs ( $2 \times 10^6$ ) were resuspended in a 1:1 mixture of PBS and injected subcutaneously into five nude mice (Foxn1<sup>nu</sup>/Foxn1<sup>+</sup>, 6 to 8 weeks of age from Harlan Sprague Dawley). As a positive control for tumors induction, five mice subcutaneously received murine embryonic stem cells E14 tg2A (Bay Genomics, San Francisco, California) at a concentration of  $2 \times 10^6$  cells per site. The mice that received murine embryonic stem cells (mESCs) were sacrificed 4 weeks post-transplantation, because at that time, they had formed a visible tumor in the injection site. The mice treated with the different BMSC subpopulations were sacrificed 10 weeks post-transplantation. Sites of injection were analyzed macroscopically and histologically using hematoxylin and eosin staining.

#### *Immunofluorescence for Nanog detection*

Cells were fixed in 4% paraformaldehyde and permeabilized with 0.2% TX-100 in 10% normal goat serum/1% bovine serum albumin (Sigma-Aldrich) in PBS for 15 min at room temperature. The samples were incubated with primary antibody goat anti-murine Nanog (1:100 dilution, R&D Systems, Minneapolis, USA) and then with an anti-goat immunoglobulin G conjugated with Alexa Fluor 488 (Molecular Probes, Eugene, Oregon). Images were captured using an inverted microscope (DMI4000, Leica Microsystems, Milano, Italy).

#### *Differentiation assays*

For osteogenic and adipogenic differentiations, cells were allowed to grow to 70% to 90% confluence and then cultured in osteogenic<sup>5</sup> or adipogenic<sup>15</sup> medium for 3 and 2 weeks, respectively. Cells were induced to chondrogenic differentiation using the micro-drops and micro-pellet techniques as described.<sup>8,16</sup>

#### *Reverse transcription polymerase chain reaction*

Total RNA was extracted from mBMSCs cultured in control or inductive media at different time points using TriReagent (Sigma-Aldrich) and then treated with DNase I (Ambion, Monza, Italy). Reverse transcription polymerase chain reaction (RT-PCR) was performed using M-MuLV Reverse Transcriptase (New England BioLabs, Beverly, Massachusetts). A 25-fold dilution of each sample was PCR amplified using primers and conditions listed in the supplementary materials (Supplemental Table S1, available online at [www.liebertonline.com/ten](http://www.liebertonline.com/ten)). Amplified DNA fragments were separated on a 1% agarose gel containing 0.1  $\mu$ g/ $\mu$ L ethidium bromide and visualized under ultraviolet light.

*Alizarin red S staining*

Cells were washed with PBS and fixed in 10% formaldehyde (Sigma-Aldrich) for 1 h; after rinsing with distilled water, they were incubated with 2% alizarin red S (Sigma-Aldrich) at pH 4.1 with gentle agitation for 10 min. After removal of excess staining using PBS, presence of mineralization was examined as described previously.<sup>17</sup> After visual examination, the mineralized depot-bound dye was extracted using overnight incubation with 4 M guanidine-hydrochloric acid (Sigma-Aldrich) at room temperature. Absorbance at 490 nm of a 10-times dilution of the resulting supernatant was used for quantitative calcium determination.

*Alcian blue staining*

Cells were fixed with 4% paraformaldehyde (Sigma-Aldrich) for 15 min at room temperature. After being rinsed with PBS, cells were stained with 1% Alcian blue (Sigma-Aldrich) in 0.1 N HCl at pH 1.0 (Carlo Erba Reagenti, Milano, Italy) overnight. Cells were then dried, washed with 0.1 M HCl for 5 min to remove excess staining, and then washed with distilled water.<sup>18</sup>

*Oil red-O staining*

Cells were washed with PBS and fixed in 10% formaldehyde for 10 min. After being rinsed with distilled water, they were stained with 0.5% Oil red-o working solution prepared by vigorously mixing three parts of a stock solution (0.5% Oil red-O in isopropanol) (Sigma-Aldrich) with two parts of water for 5 min and filtering through a 0.4- $\mu$ m filter. Excess staining was removed using PBS. Cells were then counterstained with hematoxylin (Bio-Optica, Milano, Italy) for 3 min and then washed with distilled water.<sup>17</sup> After visual examination, the lipid-bound dye was extracted using isopropanol incubation for 15 min at room temperature. Quantitative assessment was obtained by measuring absorbance of a ten-times dilution of the extracted dye at 550 nm.

*Alkaline phosphatase staining*

Briefly, the cells were washed with PBS and fixed in 10% cold neutral formalin buffer (10% formalin, 0.1 M Na<sub>2</sub>HPO<sub>4</sub>, 0.029 M NaH<sub>2</sub>PO<sub>4</sub>·H<sub>2</sub>O) (Sigma-Aldrich) for 15 min. After being rinsed with distilled water, cells were stained with substrate solution [ $2.4 \times 10^{-4}$  M naphthol AS MX-PO<sub>4</sub>

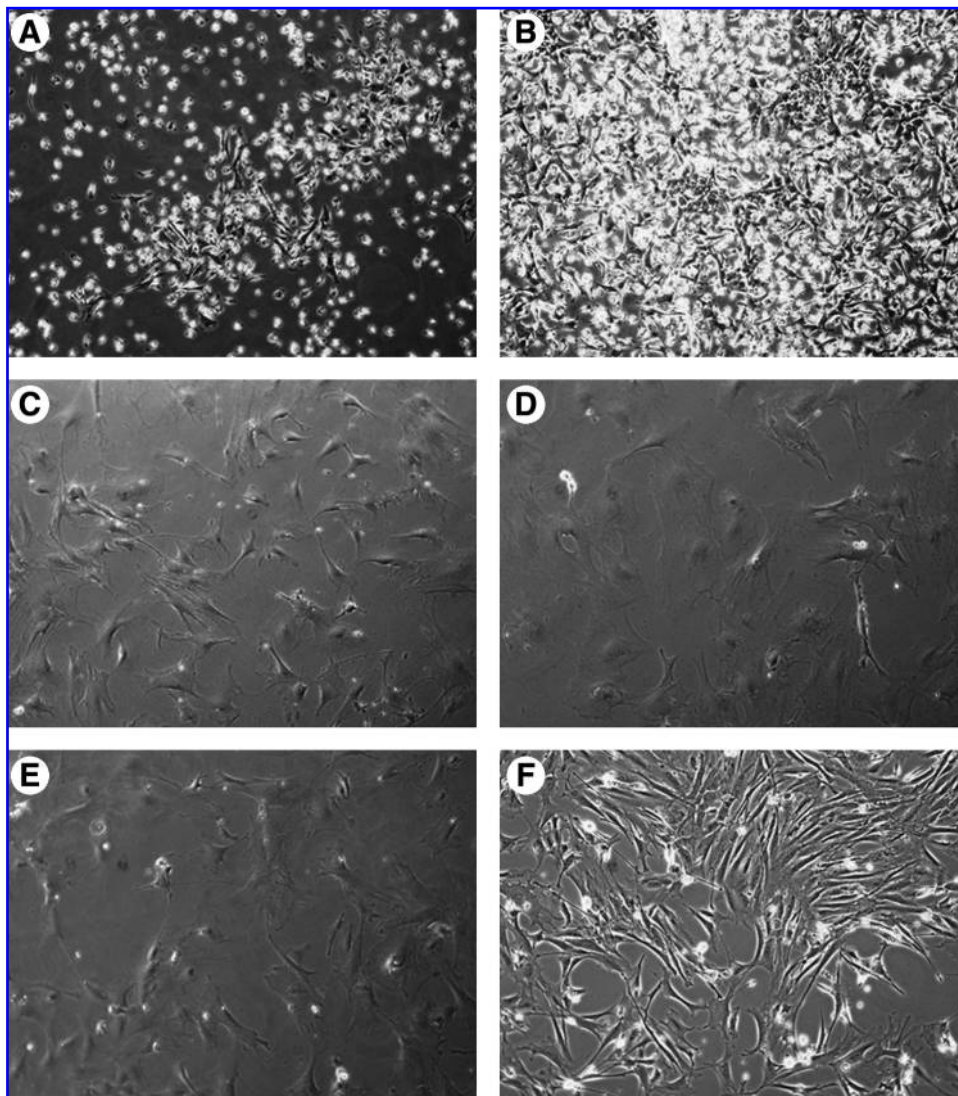


**FIG 1.** Morphology of murine bone marrow stromal cells (mBMSCs) varies according to culture condition. Morphology of BMSCs 72 h after plating (A) and after 10 to 17 days of culture (B). Cells were subdivided and cultured in complete medium with 20% bone marrow-conditioned medium and, subsequently, in complete medium with 20 ng/mL murine epidermal growth factor and 20 ng/mL Lof platelet-derived growth factor-AA (mBMSC EP, C); complete medium with 20% bone marrow-conditioned medium (mBMSC BF, D); complete medium with 20% MS5-conditioned medium (mBMSC M, E), and complete medium with 20% NIH3T3-conditioned medium (mBMSC N, F). Magnification 10 $\times$ .

TABLE 1. VARIATIONS IN CULTURE CONDITIONS ALLOW SELECTION OF DIFFERENT MESENCHYMAL PROGENITORS

Antigen	20 ng/mL Murine Epidermal Growth Factor and 20 ng/mL Platelet-Derived Growth Factor-AA	20% Bone Marrow-Conditioned Medium	20% MS5-Conditioned Medium	20% NIH3T3-Conditioned Medium
CD 45	–	–	–	–
CD 34	–	–	–	–
CD 5	–	–	–	–
CD19	–	–	–	–
CD 117 (c-kit)	+	–	–	+
Sca-I	++	+	+	+
CD 44	+++	++	++	+++
CD 13	+	–	+	+
H2-k <sup>b</sup>	+	–	–	+

– indicates that murine bone marrow stromal cell type does not express the specific antigen. +, ++, and +++ indicate a partial overlapping, no overlapping, and a large difference between the plot of isotype control and the plot of staining profile, respectively.

(Sigma-Aldrich), 0.4% N,N dimethylformamide (Sigma-Aldrich), 1.6  $\mu$ M red violet LB salt (Sigma-Aldrich) in 0.2M Tris-HCl pH 8.3 (Carlo Erba Reagenti)] for 45 min. Excess staining was removed by washing twice with distilled water and then with 2.5% silver nitrate (Sigma-Aldrich) for 30 min. Excess silver nitrate staining was removed with distilled water.

#### Alkaline phosphatase assay

Determination of the activity of alkaline phosphatase (ALP) was performed as previously described.<sup>19</sup> Briefly, the cells were washed twice with Tyrode's balanced salt solution (50mM Tris-HCl pH 7.4, 0.15M sodium chloride) and then incubated with 5mM p-nitrophenylphosphate (Sigma-Aldrich) in 50 mM glycine (Sigma-Aldrich), 1mM magnesium chloride (Carlo Erba Reagenti) pH 10.5 at 37°C for 5 to 20 min. The reaction was stopped by adding 3M sodium hydroxide to each well. Optical density (OD) was measured at 405 nm.

#### Culture of mESCs

mESC line E14 tg 2A (BayGenomics) was maintained in Glasgow Minimum Essential Medium (GMEM) (Sigma-Aldrich) supplemented with 10% fetal bovine serum (HyClone), 0.1mM  $\beta$ -mercaptoethanol (Sigma-Aldrich), 1mM sodium pyruvate (Invitrogen), 1 $\times$  non essential amino acids (Invitrogen), 2mM glutamine (Invitrogen), 10 U/mL penicillin–10  $\mu$ g/mL streptomycin (Gibco, Invitrogen), and 10<sup>3</sup> U/mL leukemia inhibitory factor (LIF) (Chemicon International, Vimodrone (MI), Italy) (ES complete medium). ESCs were routinely split every 2 days, and the medium was changed on alternate days. To analyze the expression of LIF in NIH3T3 supernatant, we plated mESCs at 10 cells/cm<sup>2</sup> in ES complete medium. After 24 h, we changed the medium and maintained cells in ES complete medium (positive control); in ES complete medium without LIF (negative control); and in supernatant NIH3T3 supplemented with 10% fetal bovine serum, 0.1mM  $\beta$ -mercaptoethanol, 1mM sodium pyruvate, 1 $\times$  non essential amino acids, 2mM glutamine, and 10 U/mL penicillin–10  $\mu$ g/mL streptomycin in the absence or presence of blocking anti-LIF antibody (Chemicon International), according to the manufacture's instructions. The medium was changed every day. After 6 days, we analyzed the formation of ALP-positive colonies.

#### Culture of MC3T3, C3H10T1/2, and ATDC5 cell lines

MC3T3-E1 sub4 and C3H10T1/2 cell lines were obtained from American Type Culture Collection (Sesto San Giovanni, Milano, Italy) ATDC5 cell line were obtained from European Collection of Cell Culture (Milano, Italy). MC3T3-E1 sub4 cell line was cultured in IMDM (Sigma-Aldrich) supplemented with 10% selected FBS, 2mM L-glutamine, and 1mM sodium pyruvate at 37°C in a humidified atmosphere containing 5% CO<sub>2</sub>. For osteogenic differentiation, cells were plated at 2 $\times$ 10<sup>4</sup> cell/cm<sup>2</sup> and cultured in  $\alpha$ -MEM supplemented with 10% selected FBS, 2mM L-glutamine, 0.05mM ascorbic acid 2-phosphate, and 10mM  $\beta$ -glycerophosphate, and the medium was changed every 3 days for 10 days.<sup>20</sup>

C3H10T1/2 cell line was cultured in  $\alpha$ -MEM supplemented with 10% selected FBS and 2mM L-glutamine at 37°C in a humidified atmosphere containing 5% CO<sub>2</sub>. For adipogenic differentiation, cells were allowed to reach 90% confluence and then cultured in  $\alpha$ -MEM supplemented with 10% selected FBS, 2mM L-glutamine, 10<sup>-6</sup> M dexamethasone, 5  $\mu$ g/mL insulin, 0.5  $\mu$ M 3-isobutyl-1-methylxanthine, and 50  $\mu$ M indomethacin, and the medium was changed every 3 to 4 days for 14 days.<sup>21</sup>

ATDC-5 cell line was cultured in DMEM/HamF12 supplemented with 5% selected FBS and 2mM L-glutamine at 37°C in a humidified atmosphere containing 5% CO<sub>2</sub>.<sup>22</sup> Total RNA from MC3T3-E1, C3H10T1/2, and ATDC-5 was extracted from the cells using TriReagent as described above.

#### Statistical analysis

All the experiments were analyzed using two-way Student *t*-Test. *P*-values less than 0.05 were considered statistically significant.

## Results

#### Mesenchymal progenitors

Our initial cultures were heterogeneous, presenting round, flattened, or spindle-shaped morphologies, and underwent an initial lag phase of approximately 10 to 17 days (Fig. 1A, B); then the colonies started to proliferate, became confluent, and were split in four different conditions, as reported in Materials and Methods (Fig. 1C–F).

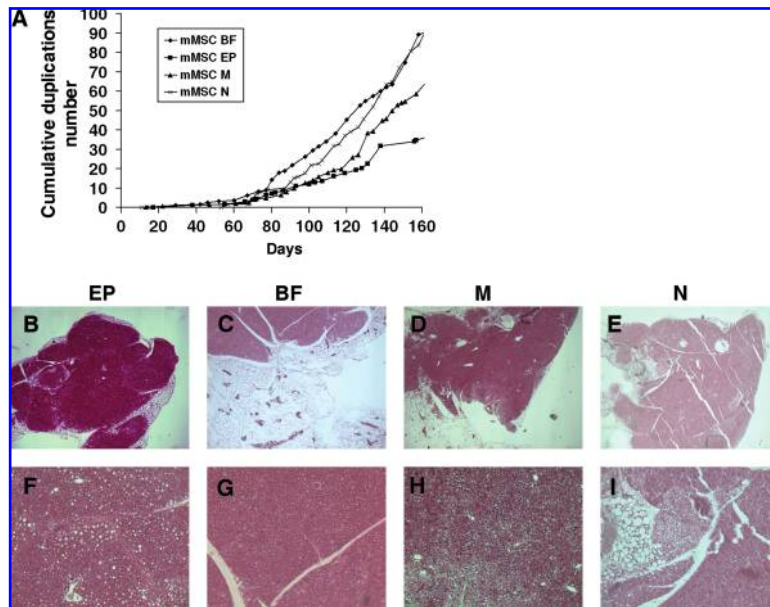


**FIG 2.** Selected mesenchymal progenitors exhibit different self-renewal characteristics. Cumulative population doublings were calculated from the initial number of mBMSCs at the first detachment from plastic tissue culture and the number of mBMSCs harvested at the following passage. This procedure was repeated for each passage, providing a theoretical growth curve that is directly proportional to the cell number. Different culture conditions are indicated as follows: ■ EP, ◇ BF, ▲ M, and \* N mBMSCs (A). All the described subpopulations after 35 passages showed no tumor formation when transplanted into immunocompromised mice (EP mBMSCs **B** and **F**, BF mBMSCs **C** and **G**, M mBMSCs **D** and **H**, N mBMSCs **E** and **I**; magnification 2.5× for **B-E**, 10× for **F-I**; hematoxylin and eosin staining).

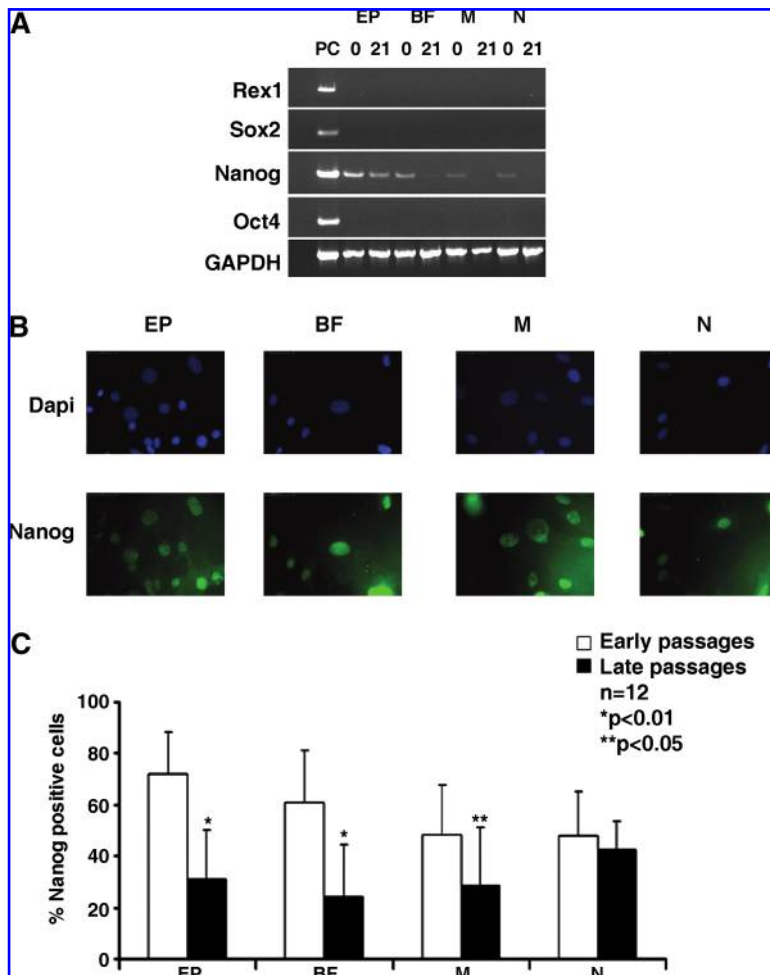


**FIG 3.** Mesenchymal progenitors express Nanog. Expression of stemness markers was analyzed using reverse transcription polymerase chain reaction (RT-PCR) immediately after cell purification (0) and after 21 days in the different culture conditions (A). Expression of Nanog was confirmed in all the subpopulations using immunostaining with an anti-Nanog antibody conjugated with fluorescein isothiocyanate counterstained with 4',6-diamidino-2-phenylindole (B, magnification 63×) and quantified as percentage of Nanog-positive cells at early and late passages (C).

After 5 to 10 passages, we analyzed the four mBMSC subpopulations using flow cytometry (Table 1). In all cases, the immunophenotype showed a marker profile strictly compatible with BMSCs,<sup>23</sup> without the expression of any hematopoietic cell markers, such as CD45, CD34, CD5, and CD19. In addition, although the EP mBMSCs presented a subset of cells highly positive to CD13, the BF and M mBMSC subpopulations were negative to the major histocompatibility complex of class I (H2-k<sup>b</sup>), suggesting a typical feature of early multipotent bone marrow progenitors known as multipotent adult progenitor cells (MAPCs).<sup>24</sup>

#### *Mesenchymal progenitors exhibit different self-renewal abilities*

We were able to subculture all four BMSC subpopulations for more than 30 passages without observing any signs of cellular senescence such as absence of mitotic activity, accumulation of cellular debris, total degeneration of the culture or aneuploidy, as evidenced by the diploid DNA content of our subcultures (data not shown). So to evaluate self-renewal ability of the different isolated progenitors, we determined their doubling time that resulted 58 h for the EP, 40 h for the BF, 57 h for the M, and 44 h for the N groups, as confirmed also according to cell cycle analysis (data not shown). These data accounted for the different numbers of cumulative duplication numbers reached after 30 passages. As reported in Figure 2A, cumulative duplication numbers were 83, 109, 70, and 90 for the EP, BF, M and N groups, respectively.

To exclude that our subpopulations contained transformed cells with abnormal proliferative characteristics, we first cultured them without serum. In these conditions, the cells showed signs of cellular senescence and died in few days (data not shown). Subsequently, we tested their tumorigenicity *in vivo* in immunodeficient mice, by subcutaneous injection of  $2 \times 10^6$  mBMSCs, for each subpopulation. We did not observe any tumor formation, as determined by macroscopic and histological analysis 10 weeks after inoculum ( $n = 5$ ; Fig 2B-I), confirming that our subpopulations were essentially free of tumorigenic cells. As a positive control for tumor formation, five mice received mESCs ( $2 \times 10^6$  cells/site) at the same site. All animals inoculated with mESCs developed large tumors ( $1,28 \pm 0,49$  cm in diameter) at the injected sites within 3 to 4 weeks (data not shown).

We then evaluated whether transcription factors essential for pluripotency and self-renewal in mESCs, such as Oct 4, Nanog, Sox-2, and Rex-1, were present in our progenitors and could account for the differences in proliferative ability observed. Of the above-mentioned transcription factors, only Nanog was expressed in our sub-cultures, as evidenced by RT-PCR, at time 0 and after 21 days of culture in EP mBMSCs and at time 0 in BF, M, and N mBMSCs (Fig. 3A). Immunofluorescence data confirmed the localization of Nanog in the nucleus of mBMSCs EP ( $71.8\% \pm 16.6\%$ ), BF ( $61.0\% \pm 20.0\%$ ), M ( $48.4\% \pm 19.2\%$ ) and N ( $47.9\% \pm 17.5\%$ ), as shown in Figure 3B. *T*-test analysis showed that the differences in percentage of Nanog expressing cells between EP and M BMSCs or EP and N BMSCs were statistically significant (Supplemental Table S2, available online at [www.liebertonline.com/ten](http://www.liebertonline.com/ten)). Because Nanog is a stemness marker for mESCs, and its expression is usually lost as soon as

the cells begin to differentiate and lose self-renewal potential,<sup>25</sup> we determined its expression also in mBMSCs at high passage number. After 30 to 40 passages, the percentage of Nanog-positive cells was reduced for mBMSCs EP ( $71.8\% \pm 16.6\%$  to  $31.0\% \pm 19.1\%$ ), mBMSCs BF ( $61.0\% \pm 20.0\%$  to  $24.0\% \pm 20.0\%$ ) and M ( $48.4\% \pm 19.2\%$  to  $28.3\% \pm 22.7\%$ ). On the contrary, the reduction in percentage of Nanog-positive cells was not significant for mBMSCs N ( $47.9\% \pm 17.5\%$  to  $42.6\% \pm 11.0\%$ ) (Fig. 3C). *T*-test analysis suggested that the differences in Nanog-expressing cells between the four culture conditions used were significant only in the early phases of expansion and that this percentage reached the same value after a high number of passages (Table S2).

#### *Differentiation abilities of mesenchymal progenitors*

To further characterize the isolated subpopulations, we evaluated their differentiation potency, performing osteogenic, chondrogenic, and adipogenic differentiation assays.

#### *Osteogenesis*

After 6 days of osteogenic induction, 80% of EP, M, and BF mBMSCs underwent a dramatic change in cellular morphology and were ALP-positive (Fig. 4A). Control cultures in regular growth media expressed a variable and significant background level of ALP-positive staining (Supplemental Table S3, available online at [www.liebertonline.com/ten](http://www.liebertonline.com/ten)), in agreement with previously described results in human<sup>26</sup> and murine BMSCs.<sup>27</sup> In fact, in the conditions studied, EP and BF subpopulations seemed to express ALP at time 0, suggesting that several osteogenic patterns might already be active. ALP activity of differentiated cells increased during the first week of induction for EP, BF, and M mBMSCs (Fig. 4B), reaching a plateau phase, a phenomenon correlated with the increased extensive mineralization that occurred throughout the differentiated cultures.<sup>26</sup> On the other hand, the ALP activity of differentiated N mBMSCs increased during the time, but it did not reach the level of the other subpopulations, suggesting a delay or an impairment in osteogenic differentiation (Fig. 4B). Alizarin red S staining confirmed that EP, BF, and M subpopulations, grown with osteogenic medium for 21 days, produce a well-mineralized matrix (Fig. 4C). As expected, the mineralization pattern of N mBMSCs was localized to a few discrete foci, rather than throughout the culture dish, as reported for EP, BF, and M mBMSCs (Fig. 4C). The extraction of bound Alizarin red S allowed us to quantify mineralization deposits elaborated from the cells (Fig. 4D).

To confirm the differentiation status of our subcultures, we analyzed expression of osteoblast-specific markers using RT-PCR. Our results confirmed that the mBMSCs constitutively express some osteoblastic lineage markers, such as core-binding factor alpha 1/runt-related transcription factor 2 (Cbfa 1/Runx2), collagen I, and osteopontin, as previously described.<sup>10</sup> In particular, after osteoinduction, EP, BF, and M mBMSCs begin to express the well-known transcription factor osterix, which is essential to osteogenic commitment of mBMSCs, as well as late osteogenic markers, namely bone sialoprotein and osteocalcin, typically expressed in osteoblasts (Fig. 4E).<sup>28</sup> Because N mBMSCs do not express bone sialoprotein, even in differentiation medium, we concluded that they are not able to fully differentiate in osteoblasts retaining a pre-osteoblastic status.

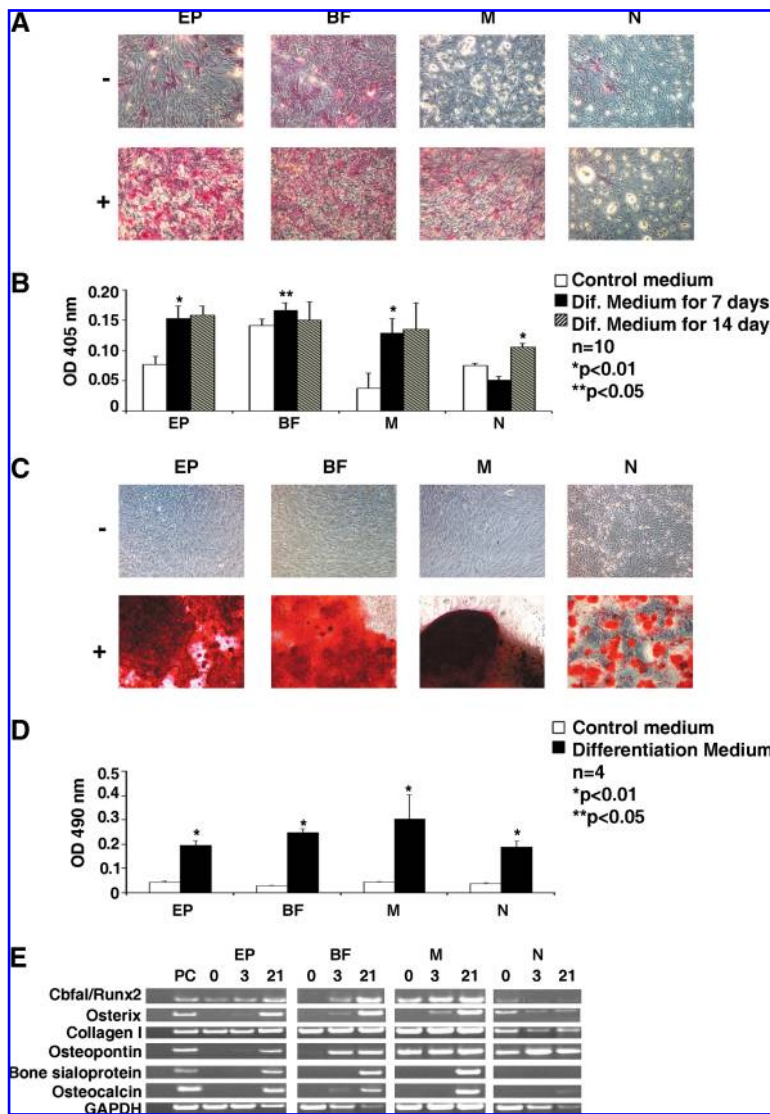


**FIG 4.** Osteogenic differentiation of mBMSC subpopulations. Alkaline phosphatase (ALP) staining was performed 6 days after osteogenic induction (A, magnification 10 $\times$ ). ALP activity was determined for each subculture. The ALP activity of differentiated cells increased during the first week of induction for EP, BF, and M mBMSCs, reaching a plateau after 6 days; a slight increase in ALP-positive cells was observed in the N subpopulation during the entire period of induction (B). Alizarin red S staining was performed 21 days after induction. EP, BF, and M BMSCs exhibit calcium deposition in the extracellular matrix; a lower level of calcium deposition was observed for the subpopulation N (C, magnification 10 $\times$ ). Calcium deposition was quantified as described in Materials and Methods (D). Expression of osteoblast-specific markers was determined using RT-PCR (E) at 0, 3, and 21 days after induction. Pc, a positive control constituted by RNA extracted from MC3T3. Glycerinaldehyde 3 phosphate dehydrogenase (GAPDH) is shown as a control for RNA sample quality.

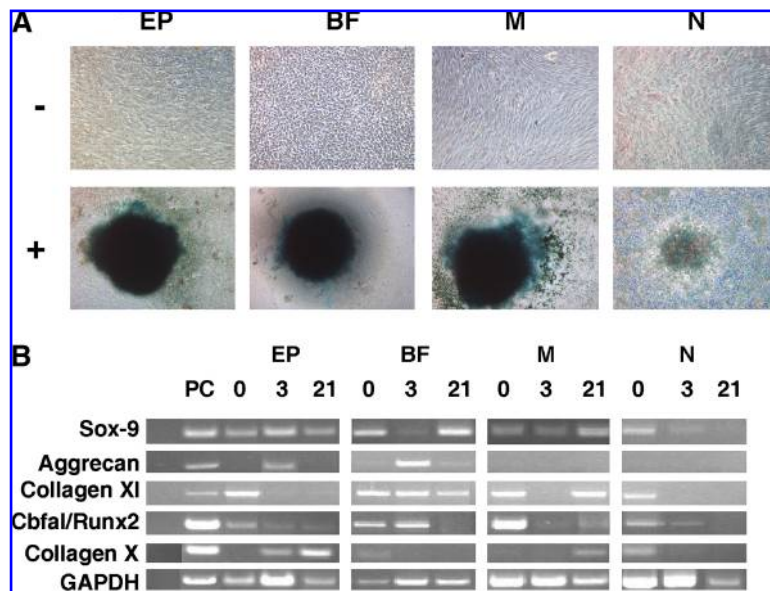


**FIG 5.** Chondrogenic differentiation of mBMSC subpopulations. Micromass cultures of the different mBMSC subpopulations were treated with control or chondrogenic medium. All of the cultures were fixed after 21 days and stained with Alcian blue (A, magnification 10 $\times$ ). Expression of chondrocyte-specific markers was determined using RT-PCR (B). RNA was extracted from cells induced in monolayer at day 0 and from micropellets after 3 or 21 days in induction medium. Pc, positive control constituted by RNA extracted from ATDC5 cells. GAPDH is shown as a control for RNA sample quality.

### Chondrogenesis

Treatment of micro-mass cultures of EP, BF, and M mBMSCs with chondrogenic medium resulted in aggregation of the cells into a three-dimensional spherical structure that accumulated sulphated proteoglycans, as shown using Alcian blue staining (Fig. 5A).<sup>16,18,29</sup> When we treated N mBMSCs with chondrogenic medium in micro-mass cultures, we did not observe spheroid formation but only a contraction of the micro-mass culture into an opaque sheet of cells smaller in diameter than the original culture, and weakly positive to Alcian blue (Fig. 5A); these data suggested to us that these cells have a delay or impairment in chondrogenic differentiation.

To corroborate this hypothesis, we analyzed the expression of specific markers using RT-PCR in our four subpopulations. The results confirmed that all analyzed mBMSC progenitors constitutively express Sox-9.<sup>16,29</sup> After induction, BF and M mBMSCs began to express aggrecan and collagen XI, confirming a differentiation in chondroblasts. Only EP and M mBMSCs were able to differentiate in hypertrophic chondrocyte because they express mRNA of collagen X and Cbfa 1/Runx2 after 21 days of differentiation (Fig. 5B).<sup>30</sup> We were able to observe the expression of Sox9 and collagen XI in N mBMSCs at time-point 0 in cells grown in monolayer, but not after 3 or 21 days in micropellet culture. As reported by Murdoch *et al.*, there is a reduction in collagen I and Sox9 expression from monolayer at time-point 0 and micropellet at time-point 3, but these markers normally increase throughout the 3 weeks of differentiation.<sup>29</sup> Because N mBMSCs do not express any marker, even in differentiation medium, we concluded that they do not differentiate in chondroblasts, confirming our initial hypothesis, discussed above.

### Adipogenesis

After adipo-induction, we observed full adipogenic differentiation only in N mBMSCs, with small lipid droplets detectable after 3 to 4 days of induction as shown using Oil red O staining and confirmed using quantification of bound Oil red (Fig. 6A, B). Conversely, EP, BF, and M mBMSC subpopulations treated with adipogenic medium did not accumulate lipid droplets, even after 14 days of induction (Fig. 5A, B). To further corroborate these data, we determined the expression of adipogenic-specific markers using RT-PCR. Our data suggest that BF and M mBMSCs are able to become immature adipocytes, because they express lipoprotein lipase and fatty acid binding protein-4 after 14 days of induction (Fig. 6C). N mBMSCs also express early adipogenic markers before induction, suggesting that these cells are pre-adipocytes. Upon stimulation, they can differentiate readily into adipocytes, because they express the transcription factor peroxisome proliferator-activated receptor gamma 2, essential to adipogenic commitment of mBMSCs and adiponin, a late adipogenic marker,<sup>31</sup> just 3 days after treatment with induction medium (Fig. 6C).

### Expression of LIF in NIH3T3-conditioned medium

We hypothesized that the different results, in terms of adipogenic differentiation abilities, were due to the composition of the medium used for isolation and expansion of

mBMSCs. It has been recently observed that LIF is responsible for blocking osteoblast maturation at late differentiation stages and redirecting these cells toward the adipogenic pathway;<sup>32,33</sup> we therefore analyzed LIF expression in NIH3T3 and MS-5 cell lines using RT-PCR, demonstrating that LIF was expressed only in NIH3T3 cells (Fig. 7A). To further investigate the ability of NIH3T3 to secrete bioactive LIF, we tested whether NIH3T3 supernatant could support maintenance of the undifferentiated state of mESCs, because it is well known that the maintenance of the undifferentiated state of mESCs requires the presence of LIF or LIF-related factors.<sup>34</sup> Therefore, we plated mESCs in NIH3T3 supernatant supplemented with serum, and after 6 days we determined the number of ALP-positive colonies, because ALP is a well-known marker of undifferentiated mESCs.<sup>35</sup> As shown in Figure 7B–D, NIH3T3-conditioned medium supported the maintenance of the undifferentiated state of mESCs. On the other hand, addition of an antagonist of LIF completely blocked this effect, supporting the production of bioactive LIF from NIH3T3 cells.

### Discussion

In the present study, we have provided a characterization of four mBMSC subpopulations enriched through distinct culture conditions and showing different immunophenotypes, self-renewal abilities, and differentiation potentials.

In the recent years, BMSCs have generated a great deal of interest as a potential source of cells for therapy because of their interesting differentiation, trophic, and immunosuppressive abilities.<sup>3,36–38</sup> Nevertheless, the inability to definitively identify and characterize this population in a simple mammalian model, such as the mouse, impeded the ability to move their use forward in therapy. mBMSCs have been partially characterized,<sup>4–11</sup> and although some studies have been done to demonstrate their *in vivo* contribution<sup>24,39</sup> or the *in vivo* potential for tissue regeneration and gene delivery,<sup>1–3</sup> most of them lacked optimization of culture conditions to obtain a high number of specific progenitors, maintaining the same characteristic for many passages without acquisition of tumorigenic potential.<sup>40</sup>

We tried to obtain mMSCs using complete medium without any supplements. However, the few adherent cells obtained after the incubation period were not able to proliferate even when we sub-cultured them in another plate. Starting from the observation that use of bone fragment-conditioned medium favors BMSC growth,<sup>8</sup> we devised the conditions that selected the subpopulations described as BF and EP. Because it is well known that mBMSCs expand poorly,<sup>4–11</sup> after 2 weeks of culture, we cultured a part of these cells (EP mBMSCs) in complete medium supplemented with EGF and PDGF-AA,<sup>10,41,42</sup> whereas we maintained BF mBMSCs in complete medium with no additional components. Surprisingly, in spite of the above-cited considerations, we observed an expansion of BF mBMSCs. These results led us to hypothesize that a specific bone marrow-derived microenvironment could be responsible for the selection and maintenance of mesenchymal progenitors. We therefore decided to evaluate whether conditioned media obtained from MS-5<sup>13</sup> and NIH3T3 cell lines<sup>14</sup> could mimic the properties of the bone marrow microenvironment. With this aim, we grew MS-5 and NIH3T3 cells in the same medium (see Materials and

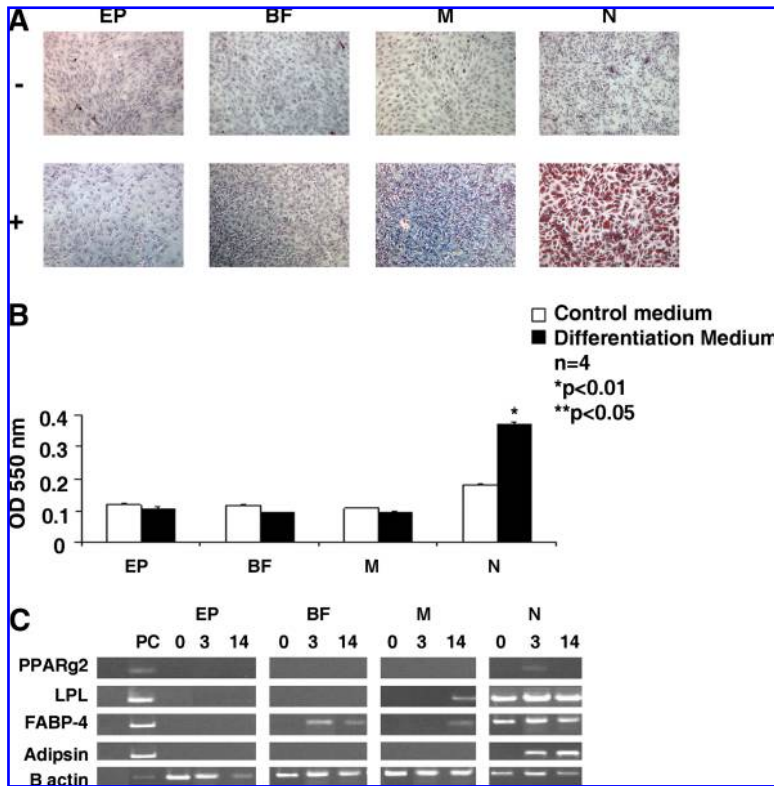


**FIG 6.** Adipogenic differentiation of mBMSC subpopulations. The different BMSC subpopulations were incubated in adipogenic medium as described in Materials and Methods. Fourteen days after induction, the cells were fixed and stained with Oil red O. The N mBMSC subpopulation underwent a dramatic change in cellular morphology from spindle-shaped to polygonal, which was accompanied by a significant lipid accumulation; to the contrary, EP, BF, and M mBMSC subpopulations showed absence of lipid droplets (A, magnification 10 $\times$ ). Lipid accumulation was also quantified as described in Materials and Methods (B). Expression of adipocyte-specific markers was analyzed using RT-PCR (C) from RNA extracted at day 0 or after 3 or 14 days in induction medium. P<sub>c</sub>, positive control constituted by RNA extracted from C3H10T1/2 cells. B-actin is shown as a control for RNA sample quality.

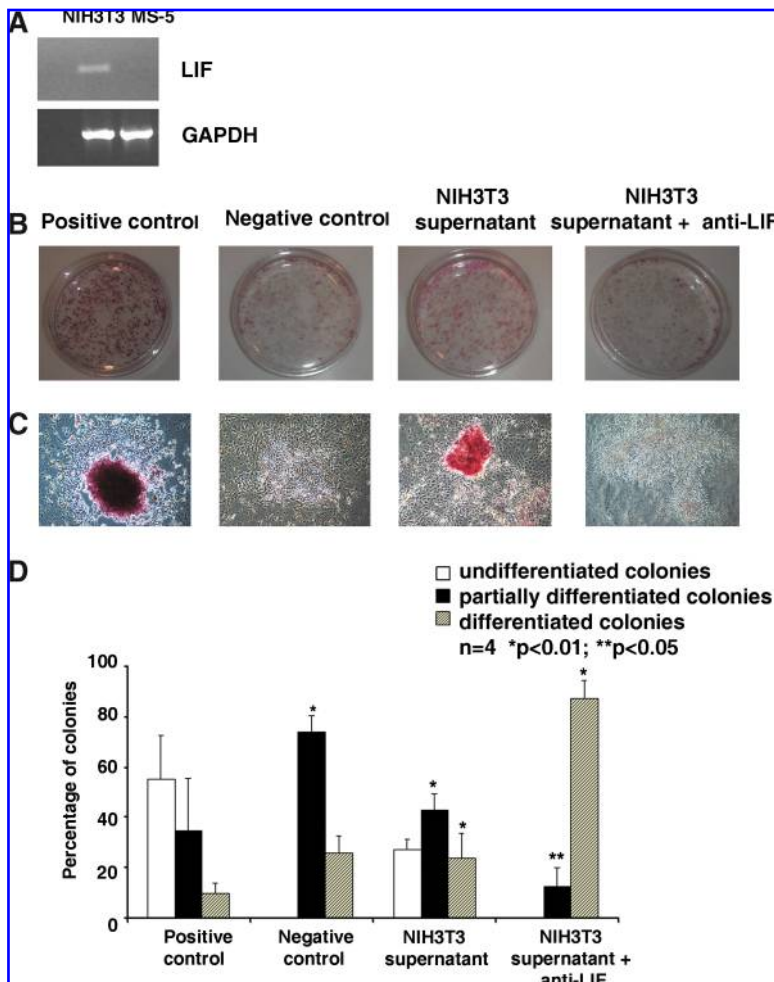


**FIG 7.** NIH3T3 cells secrete bioactive leukemia inhibitory factor (LIF). LIF expression in NIH3T3 cells was determined using RT-PCR analysis (A). GAPDH is shown as a control for RNA sample quality. ALP staining of murine embryonic stem cells (mESCs) plated in NIH3T3 supernatant in the absence or presence of blocking anti-LIF antibody (B and C at 10 $\times$  magnification). We distinguished between undifferentiated (ALP-positive), partially differentiated (ALP-negative) colonies. ALP-positive colonies were also quantified (D). The positive control in all the experiments was constituted by cells maintained in ES complete medium, whereas as negative control, we used cells maintained in ES complete medium without LIF.

Methods) to minimize any difference between the conditioned media harvested from these cell lines, which differ only in the molecules secreted from each individual line. Using the above-mentioned conditioned media, we were able to efficiently culture mBMSCs. We therefore hypothesized that one of the main determinants of successful isolation and expansion of mouse mesenchymal progenitors was the growth supplement used for isolation and expansion.

Immunophenotypical characterization of our four BMSC subpopulations showed in each case profiles compatible with BMSCs. We observed differences in CD117, CD13, and H2-k<sup>b</sup> expression (Table 1). Moreover, these progenitors have different growth kinetics, and after an initial lag phase of approximately 10 to 17 days, they started to proliferate, after 30 passages reaching different numbers of cumulative duplications (Fig. 2A).

An interesting feature of all of the BMSC subpopulations isolated was the expression of a well-known marker of undifferentiated embryonic stem cells: Nanog (Fig. 3).

Although the role of Nanog in adult tissue stem cells remains unclear, it is possible that it enhances self-renewal of tissue stem cells. In a recent paper, Go *et al.*, observed that Nanog-over-expressing human BMSCs showed much higher expansion potential and osteogenic differentiation abilities than control cells.<sup>43</sup> So it is possible to argue that the expression of Nanog, strictly correlated to proliferation ability, could play a key role in quality of specific markers for the selection of BMSC progenitors to employ in cell therapy protocols.

About the differentiation potential, in two of the four conditions (BF and M), cells showed tri-potential differentiation ability, giving rise to osteoblasts, chondrocytes, and pre-adipocytes, whereas EP cells lost adipogenic potential, probably during the first passages.<sup>17</sup> We observed that the ability to differentiate in pre-adipocytes was typical of BF and M BMSCs, which are negative to H2-k<sup>b</sup>, a typical characteristic of mMAPCs.<sup>24</sup> Moreover, the ability to differentiate in hypertrophic chondrocytes was typical of EP and M BMSCs, which showed lower expansion profiles than the other subpopulations. We speculate that this could be partially due to the effect of EGF on these cells. The EGF, added directly to EP BMSCs and contained in MS-5-conditioned medium,<sup>13</sup> could act not only as mitogen in mesenchymal proliferation,<sup>10</sup> but also as a stimulator of osteogenic differentiation.<sup>42</sup> This effect could account for the high chondrogenic and osteogenic potential of these cells.

On the other hand, using NIH3T3-conditioned medium, we obtained cells that showed impairment in osteogenic and chondrogenic differentiation while retaining a high adipogenic potential during passages. We hypothesized that this could be the result of NIH3T3-conditioned medium exposition. Therefore, with the aim of addressing this behavior, we switched the N BMSCs into standard growth medium for 10 passages. We were not able to appreciate any significant recovery of osteogenic potential (data not shown), leading to the conclusion that this effect was not reversible. In the attempt to identify cytokines possibly responsible for this behavior, we focused our attention on LIF.<sup>32</sup> It has been recently observed that LIF is responsible for blocking osteoblast maturation at late differentiation stages and redirecting these cells toward the adipogenic pathway.<sup>32,33</sup> We speculate that, in our N BMSCs model, LIF could suppress

the osteoblast maturation at late differentiation stages<sup>32,33</sup> contributing to selection of adipogenic progenitors from bone marrow.<sup>32,44,45</sup>

Our differentiation data, which include tissue-specific staining and RT-PCR results, are aimed only at confirming the differentiation process, based on the presence or the absence of markers;<sup>16,28,29,31</sup> analysis of the kinetics of the process may produce further indications on the effect of specific factors on BMSCs and may constitute object of future research.

To our knowledge, this is the first article that reports the enrichment of specific progenitors from murine bone marrow using MS5- and NIH3T3-conditioned medium. Our data suggest that the use of appropriate conditioned media can determine the obtainment of a large number of desired cells for large-scale transplantations or cell therapies. In the near future, we believe that the identification of growth factors regulating survival rate, self-renewal, and lineage differentiation will be crucial for the understanding of MSC biology and for their application in clinical settings.

### Acknowledgments

This work was partially supported by a grant L.R.5 from Regione Campania. MTE, RDN, PM, and SP were involved in progenitor cultures and characterization; MG and LDV in cytofluorimetric assessment; DM in histological characterization; and LP in project coordination.

### Disclosure Statement

No competing financial interests exist.

### References

- Ferrari, G., Cusella-De Angelis, G., Coletta, M., Paolucci, E., Stornaiuolo, A., Cossu, G., Mavilio, F. Muscle regeneration by bone marrow-derived myogenic progenitors. *Science* **279**, 1528, 1998.
- Lieberman, J.R., Daluiski, A., Stevenson, S., Wu, L., McAllister, P., Lee, Y.P., Kabo, J.M., Finerman, G.A., Berk, A.J., Witte, O.N. The effect of regional gene therapy with bone morphogenetic protein-2-producing bone-marrow cells on the repair of segmental femoral defects in rats. *J Bone Joint Surg Am* **81**, 905, 1999.
- Orlic, D., Kajstura, J., Chimenti, S., Jakoniuk, I., Anderson, S.M., Li, B., Pickel, J., McKay, R., Nadal-Ginard, B., Bodine, D.M., Leri, A., Anversa, P. Bone marrow cells regenerate infarcted myocardium. *Nature* **410**, 701, 2001.
- Dobson, K.R., Reading, L., Haberey, M., Marine, X., Scutt, A. Centrifugal isolation of bone marrow from bone: an improved method for the recovery and quantitation of bone marrow osteoprogenitor cells from rat tibiae and femur. *Calcif Tissue Int* **65**, 411, 1999.
- Phinney, D.G., Kopen, G., Isaacson, R.L., Prockop, D.J. Plastic adherent stromal cells from the bone marrow of commonly used strains of inbred mice: variations in yield, growth, and differentiation. *J Cell Biochem* **72**, 570, 1999.
- Baddoo, M., Hill, K., Wilkinson, R., Gaupp, D., Hughes, C., Kopen, G.C., Phinney, D.G. Characterization of mesenchymal stem cells isolated from murine bone marrow by negative selection. *J Cell Biochem* **89**, 1235, 2003.
- Meirelles Lda, S., Nardi, N.B. Murine marrow-derived mesenchymal stem cell: isolation, *in vitro* expansion, and characterization. *Br J Haematol* **123**, 702, 2003.

8. Sun, S., Guo, Z., Xiao, X., Liu, B., Liu, X., Tang, P.H., Mao, N. Isolation of mouse marrow mesenchymal progenitors by a novel and reliable method. *Stem Cells* **21**, 527, 2003.
9. Peister, A., Mellad, J.A., Larson, B.L., Hall, B.M., Gibson, L.F., Prockop, D.J. Adult stem cells from bone marrow (MSCs) isolated from different strains of inbred mice vary in surface epitopes, rates of proliferation, and differentiation potential. *Blood* **103**, 1662, 2004.
10. Tropel, P., Noel, D., Platet, N., Legrand, P., Benabid, A.L., Berger, F. Isolation and characterisation of mesenchymal stem cells from adult mouse bone marrow. *Exp Cell Res* **295**, 395, 2004.
11. Wang, Z., Song, J., Taichman, R.S., Krebsbach, P.H. Ablation of proliferating marrow with 5-fluorouracil allows partial purification of mesenchymal stem cells. *Stem Cells* **24**, 1573, 2006.
12. Short, B., Brouard, N., Driessen, R., Simmons, P.J. Prospective isolation of stromal progenitor cells from mouse BM. *Cytherapy* **3**, 407, 2001.
13. Issaad, C., Croisille, L., Katz, A., Vainchenker, W., Coulombel, L. A murine stromal cell line allows the proliferation of very primitive human CD34<sup>+</sup>/CD38<sup>-</sup> progenitor cells in long-term cultures and semisolid assays. *Blood* **81**, 2916, 1993.
14. Burroughs, J., Gupta, P., Blazar, B.R., Verfaillie, C.M. Diffusible factors from the murine cell line M2-10B4 support human *in vitro* hematopoiesis. *Exp Hematol* **22**, 1095, 1994.
15. Reyes, M., Lund, T., Lenvik, T., Aguiar, R., Koodie, L., Verfaillie, C.M. Purification and *ex vivo* expansion of post-natal human marrow mesodermal progenitor cells. *Blood* **98**, 2615, 2001.
16. Mackay, A.M., Beck, S.C., Murphy, J.M., Barry, F.P., Chichester, C.O., Pittenger, M.F. Chondrogenic differentiation of cultured human mesenchymal stem cells from marrow. *Tissue Eng* **4**, 415, 1998.
17. Digirolamo, C.M., Stokes, D., Colter, D., Phinney, D.G., Class, R., Prockop, D.J. Propagation and senescence of human marrow stromal cells in culture: a simple colony-forming assay identifies samples with the greatest potential to propagate and differentiate. *Br J Haematol* **107**, 275, 1999.
18. Denker, A.E., Nicoll, S.B., Tuan, R.S. Formation of cartilage-like spheroids by micromass cultures of murine C3H10T1/2 cells upon treatment with transforming growth factor-beta 1. *Differentiation* **59**, 25, 1995.
19. Bruder, S.P., Jaiswal, N., Haynesworth, S.E. Growth kinetics, self-renewal, and the osteogenic potential of purified human mesenchymal stem cells during extensive subcultivation and following cryopreservation. *J Cell Biochem* **64**, 278, 1997.
20. Wang, D., Christensen, K., Chawla, K., Xiao, G., Krebsbach, P.H., Franceschi, R.T. Isolation and characterization of MC3T3-E1 preosteoblast subclones with distinct *in vitro* and *in vivo* differentiation/mineralization potential. *J Bone Miner Res* **14**, 893, 1999.
21. Cho, Y.C., Jefcoate, C.R. PPARgamma1 synthesis and adipogenesis in C3H10T1/2 cells depends on S-phase progression, but does not require mitotic clonal expansion. *J Cell Biochem* **91**, 336, 2004.
22. Chen, L., Fink, T., Zhang, X.Y., Ebbesen, P., Zachar, V. Quantitative transcriptional profiling of ATDC5 mouse progenitor cells during chondrogenesis. *Differentiation* **73**, 350, 2005.
23. Deans, R.J., Moseley, A.B. Mesenchymal stem cells: biology and potential clinical uses. *Exp Hematol* **28**, 875, 2000.
24. Jiang, Y., Jahagirdar, B.N., Reinhardt, R.L., Schwartz, R.E., Keene, C.D., Ortiz-Gonzalez, X.R., Reyes, M., Lenvik, T., Lund, T., Blackstad, M., Du, J., Aldrich, S., Lisberg, A., Low, W.C., Largaespada, D.A., Verfaillie, C.M. Pluripotency of mesenchymal stem cells derived from adult marrow. *Nature* **418**, 41, 2002.
25. Chambers, I., Colby, D., Robertson, M., Nichols, J., Lee, S., Tweedie, S., Smith, A. Functional expression cloning of Nanog, a pluripotency sustaining factor in embryonic stem cells. *Cell* **113**, 643, 2003.
26. Jaiswal, N., Haynesworth, S.E., Caplan, A.I., Bruder, S.P. Osteogenic differentiation of purified, culture-expanded human mesenchymal stem cells *in vitro*. *J Cell Biochem* **64**, 295, 1997.
27. Fromiguet, O., Hamidouche, Z., Chateauvieux, S., Charbord, P., Marie, P.J. Distinct osteoblastic differentiation potential of murine fetal liver and bone marrow stroma-derived mesenchymal stem cells. *J Cell Biochem* **104**, 620, 2008.
28. Karsenty, G., Wagner, E.F. Reaching a genetic and molecular understanding of skeletal development. *Dev Cell* **2**, 389, 2002.
29. Murdoch, A.D., Grady, L.M., Ablett, M.P., Katopodi, T., Meadows, R.S., Hardingham, T.E. Chondrogenic differentiation of human bone marrow stem cells in transwell cultures: generation of scaffold-free cartilage. *Stem Cells* **25**, 2786, 2007.
30. Ducy, P., Zhang, R., Geoffroy, V., Ridall, A.L., Karsenty, G. Osf2/Cbfa1: a transcriptional activator of osteoblast differentiation. *Cell* **89**, 747, 1997.
31. Rosen, E.D., MacDougald, O.A. Adipocyte differentiation from the inside out. *Nat Rev Mol Cell Biol* **7**, 885, 2006.
32. Falconi, D., Oizumi, K., Aubin, J.E. Leukemia inhibitory factor influences the fate choice of mesenchymal progenitor cells. *Stem Cells* **25**, 305, 2007.
33. Falconi, D., Aubin, J.E. LIF inhibits osteoblast differentiation at least in part by regulation of HAS2 and its product hyaluronan. *J Bone Miner Res* **22**, 1289, 2007.
34. Ying, Q.L., Nichols, J., Chambers, I., Smith, A. BMP induction of Id proteins suppresses differentiation and sustains embryonic stem cell self-renewal in collaboration with STAT3. *Cell* **115**, 281, 2003.
35. Satomura, K., Derubeis, A.R., Fedarko, N.S., Ibaraki-O'Connor, K., Kuznetsov, S.A., Rowe, D.W., Young, M.F., Gheron Robey, P. Receptor tyrosine kinase expression in human bone marrow stromal cells. *J Cell Physiol* **177**, 426, 1998.
36. Pittenger, M.F., Mackay, A.M., Beck, S.C., Jaiswal, R.K., Douglas, R., Mosca, J.D., Moorman, M.A., Simonetti, D.W., Craig, S., Marshak, D.R. Multilineage potential of adult human mesenchymal stem cells. *Science* **284**, 143, 1999.
37. Caplan, A.I., Dennis, J.E. Mesenchymal stem cells as trophic mediators. *J Cell Biochem* **98**, 1076, 2006.
38. Aggarwal, S., Pittenger, M.F. Human mesenchymal stem cells modulate allogeneic immune cell responses. *Blood* **105**, 1815, 2005.
39. Anjos-Afonso, F., Siapati, E.K., Bonnet, D. *In vivo* contribution of murine mesenchymal stem cells into multiple cell-types under minimal damage conditions. *J Cell Sci* **117**, 5655, 2004.
40. Miura, M., Miura, Y., Padilla-Nash, H.M., Molinolo, A.A., Fu, B., Patel, V., Seo, B.M., Sonoyama, W., Zheng, J.J., Baker, C.C., Chen, W., Ried, T., Shi, S. Accumulated chromosomal instability in murine bone marrow mesenchymal stem cells leads to malignant transformation. *Stem Cells* **24**, 1095, 2006.
41. Colter, D.C., Sekiya, I., Prockop, D.J. Identification of a subpopulation of rapidly self-renewing and multipotential adult stem cells in colonies of human marrow stromal cells. *Proc Natl Acad Sci U S A* **98**, 7841, 2001.

42. Kratchmarova, I., Blagoev, B., Haack-Sorensen, M., Kassem, M., Mann, M. Mechanism of divergent growth factor effects in mesenchymal stem cell differentiation. *Science* **308**, 1472, 2005.
43. Go, M.J., Takenaka, C., Ohgushi, H. Forced expression of Sox2 or Nanog in human bone marrow derived mesenchymal stem cells maintains their expansion and differentiation capabilities. *Exp Cell Res* **314**, 1147, 2008.
44. Hogan, J.C., Stephens, J.M. Effects of leukemia inhibitory factor on 3T3-L1 adipocytes. *J Endocrinol* **185**, 485, 2005.
45. Aubert, J., Dessolin, S., Belmonte, N., Li, M., McKenzie, F.R., Staccini, L., Villageois, P., Barhanin, B., Vernallis, A., Smith, A.G., Ailhaud, G., Dani, C. Leukemia inhibitory factor and its receptor promote adipocyte differentiation via the mitogen-activated protein kinase cascade. *J Biol Chem* **274**, 24965, 1999.

Address reprint requests to:

*Lucio Pastore, M.D., Ph.D.*

*Professor of Clinical Biochemistry and Molecular Biology*

*Dip. Biochimica e Biotecnologie Mediche,*

*Università degli Studi di Napoli "Federico II", and*

*CEINGE Biotecnologie Avanzate*

*Via Comunale Margherita n. 482*

*80145 Napoli*

*Italy*

*E-mail: pastore@ceinge.unina.it*

*Received: September 15, 2008*

*Accepted: January 20, 2009*

*Online Publication Date: March 17, 2009*